

<b>1. FY05 PROGRESS FOR PEP-II BY JOHN SEEMAN, MICHAEL SULLIVAN, AND ULI WIENANDS ...2</b>	
<b>2. FY05 PROGRESS IN BABAR AT PEP-II BY DAVID MACFARLANE AND BILL WISNIEWSKI.....10</b>	
<b>3. FY05 PROGRESS IN THE PARTICLE ASTROPHYSICS PROGRAM BY STEVEN KAHN .....30</b>	
GLAST.....	31
LSST.....	34
SNAP.....	36
OTHER ACTIVITIES.....	36
<b>4. FY05 PROGRESS: EXPERIMENT E158: A PRECISION MEASUREMENT OF THE WEAK MIXING ANGLE IN MØLLER SCATTERING BY KRISHNA KUMAR AND MIKE WOODS .....37</b>	
<b>5. FY2005 SELF-APPRAISAL FOR DOE: ILC DEPARTMENT AND NLCTA.....38</b>	
<b>5.1. THE ILC DEPARTMENT AT SLAC.....</b>	<b>38</b>
5.1. a. SLAC ILC Department Organization.....	40
5.1. b. ILC GDE Activities.....	40
5.1. c. Reviews and Meetings.....	41
5.1. d. Collaborations.....	42
5.1. e. Safety.....	43
<b>5.2. X-BAND RF R&amp;D.....</b>	<b>43</b>
5.2.a. Accelerator Structures.....	44
5.2.b. Pulse Compression.....	44
5.2.c. X-band rf Stations.....	45
<b>5.3. L-BAND RF.....</b>	<b>45</b>
5.3.a. Modulator.....	46
5.3.b. Klystrons.....	46
5.3.c. Rf Distribution.....	47
5.3.d. Coupler.....	47
5.3.e. L-band Normal-conducting Accelerator Structures.....	48
5.3.f. L-band Test Station.....	48
<b>5.4. ILC ACCELERATOR DESIGN AND R&amp;D.....</b>	<b>49</b>
5.4.a. Electron Source.....	49
5.4.b. Positron Source.....	49
5.4.c. Damping Rings.....	50
5.4.d. Main linacs.....	51
5.4.e. Beam Delivery System.....	52
5.4.f. End Station A Test Facility for Prototypes of Beam Diagnostics and IR Design.....	52
5.4.g. Diagnostics and Controls.....	53
5.4.h. Operations and Availability.....	54
5.4.i. Civil Design.....	54
<b>5.5. NLCTA OPERATIONS.....</b>	<b>55</b>
5.5.a. NLCTA Operations.....	55
5.5.b. NLCTA Schedule.....	55
5.5.c. NLCTA Safety.....	56
<b>5.6. LHC ACCELERATOR RESEARCH PROGRAM (LARP) COLLIMATORS.....</b>	<b>56</b>
<b>6.A. ADVANCED ACCELERATOR RESEARCH DEPARTMENT-A BY RONALD RUTH.....57</b>	
<b>6.B. FY05 PROGRESS: ACCELERATOR RESEARCH DEPARTMENT B (ARDB) BY ROBERT SIEMANN .....82</b>	
<b>7. FY05 PROGRESS IN ADVANCED COMPUTATIONS RESEARCH BY KWOK KO .....86</b>	
<b>8. FY05 HIGH POLARIZATION ELECTRON SOURCE/ACCELERATOR MATERIALS DEVELOPMENT BY BOB KIRBY AND TAKASHI MARUYAMA .....94</b>	
<b>9. FY05 PROGRESS IN FRACTIONAL CHARGE PARTICLE RESEARCH (MARTIN PERL).....97</b>	
<b>10. FY05 PROGRESS IN THE TEST EXPERIMENT PROGRAM (COORDINATED BY ROGER ERICSSON) .....97</b>	
<b>11. FY05 PROGRESS FOR THE EXO DOUBLE-BETA-DECAY R&amp;D PROGRAM BY PETER ROWSON .....101</b>	
<b>12. FY05 PROGRESS IN THEORETICAL PHYSICS BY MICHAEL PESKIN.....104</b>	

**13. FY05 PROGRESS IN THE KLYSTRON DEPARTMENT BY GEORGE CARYOTKIS .....107**

**14. FY05 SCIENCE & TECHNOLOGY PROGRESS IN THE RADIATION PROTECTION DEPARTMENT BY SAYED ROKNI .....109**

**15. FY05 PROGRESS IN SSRL OPERATIONS BY PIRO PIANETTA .....110**

**16. SCIENCE EDUCATION BY MIKE WOODS .....169**

**17. FY05 DOE ASSESSMENT: SCIENTIFIC AND TECHNICAL INFORMATION MANAGEMENT BY PAT KREITZ.....172**

**FY05 ACCOMPLISHMENTS .....174**

**FY06 PLANS .....174**

**18. FOURTH GENERATION SOURCE DEVELOPMENT – THE LINAC COHERENT LIGHT SOURCE PROJECT BY MARK REICHANADTER.....175**

**PROJECT AUTHORIZATION MILESTONES .....175**

**ENVIRONMENT, SAFETY AND HEALTH .....175**

**MANAGEMENT .....176**

**SCIENTIFIC/TECHNICAL .....176**

**FY05 PROGRESS IN LINAC COHERENT LIGHT SOURCE .....179**

## 1. FY05 PROGRESS FOR PEP-II by John Seeman, Michael Sullivan, and Uli Wienands

**General statements:** PEP-II is a particle beam accelerator which collides 1732 bunches of electrons with 1732 bunches of positrons in two counter-circulating storage rings to produce continuous luminosity to make B mesons in the BaBar physics detector. It is called a B-Factory. Each bunch contains about 100 billion particles. Each bunch collides on every turn around the accelerator or about 136,300 times per second.

Construction and installation of PEP-II was completed within budget in early July 1998. First collisions were observed in late July 1998 that was two months ahead of the final PEP-II DOE construction milestone. The BaBar detector was installed in May 1999. PEP-II has been delivering luminosity to BaBar nearly continuously over the past six years. PEP-II exceeded its design luminosity ( $3 \times 10^{33} \text{ cm}^{-2}\text{s}^{-1}$ ) in October 2000 by achieving  $3.30 \times 10^{33} \text{ cm}^{-2}\text{s}^{-1}$ . Through steady progress, PEP-II exceeded twice its design luminosity in May 2003 and well over three times its design luminosity in early October 2005 reaching  $1.0 \times 10^{34} \text{ cm}^{-2}\text{s}^{-1}$ . The peak integrated luminosity per day has reached  $728 \text{ pb}^{-1}$  which is 5.6 times the design of  $130 \text{ pb}^{-1}$  per day.

**October 2004 installation:** October 2004 was an installation period for PEP-II where many new components were installed or upgraded. The original vacuum chambers (arcs and straights) were designed to handle twice the LER current and four times the HER current. However, to reach these higher currents the interaction region vacuum chambers need upgrading. Similarly, space was left to add many rf stations, as needed, to increase the current and hence the luminosity of the ring. Several specific hardware upgrades were done in the fall of 2004 ending in October to allow increased luminosity. The bunch-by-bunch feedback systems were strengthened to accommodate the higher beam currents. New longitudinal feedback amplifiers and two new “Frascati style” longitudinal feedback kickers were installed in the LER to improve feedback reliability at higher beam currents. A new large steel shielding wall was installed at the forward end of the BaBar detector, shielding the forward muon chambers from lost particles in PEP-II. A fourth LER rf station was installed to increase the LER current capability from 2.7 to 3.6 A. A ninth HER rf station was installed to increase its current capability to 1.8 A. A new synchrotron-light beam size monitor for the LER was installed to improve the resolution of the vertical beam size measurement to aid in luminosity optimization as very small vertical emittances are needed to get more luminosity from the accelerator. The electrodes of the transverse bunch-by-bunch feedbacks in the LER were changed to molybdenum from aluminum to improve their high temperature capabilities. Cooling fans were added to all the HER expansion bellows to allow higher currents. All the quadrupoles in both rings were realigned to improve the errors in roll leading to beam x-y coupling. Several Nonevaporable Getter (NEG) pumps were removed from LER interaction region vacuum chambers which were being heated by beam Higher Order Modes (HOMs). Finally, the interaction region support tube inside BaBar associated with the PEP-II collider must be chilled to support the increased beam current. The chiller was upgraded in early FY2005 to support increased currents.

**Directed Off:** November 2004 through March 2005 was a “directed accelerator off” time period for laboratory-wide investigation, review, and remediation of safety concerns and revalidation of all systems and procedures. Many safety and operational documents were upgraded during that

time. Some of the documents include Accelerator Department Operations Directives, PEP-II and Linac Restart Validation plan, Tunnel Access Procedures, Operations Personnel safety training, Work Authorization Procedures, and Lock and Tag Procedures for working near electromagnets in the accelerator tunnels.

**PEP-II Operation:** PEP-II collider operation (Run 5a) started in April 2005. Run 5a for PEP-II and BaBar operated from mid-April 2005 to October 10, 2005, during which  $58.73 \text{ fb}^{-1}$  of data on the Upsilon 4S resonance were delivered to BaBar.

The luminosity increases over the past six months have come from several factors. Reducing  $\beta y^*$ s from 11 to about 10 mm increased the luminosity by about 10%. The bunch spacing has been changed from the By-2 (a bunch every second rf bucket) with minigaps to a full By-2 without minigaps. This configuration has only one gap of about 14 missing bunches which is used for the abort gap. This By-2 spacing has some (anticipated) parasitic crossing effects but the adverse affects were measured to be below a few percent in the luminosity, consistent with our beam-beam computer simulations. The new bunch spacing allowed more bunches to be collided which also allowed the beam currents to be increased with constant bunch current. The higher beam currents with the new rf stations are now about 2995 mA in the LER and 1745 mA in the HER. Both of these currents are world records. The betatron tunes were optimized near the half integer reducing the effects of the beam-beam interaction. The optical magnet lattice has been improved by reducing “beta” errors around the rings which should allow even higher beam-beam tune shifts.

Trickle injection was a great improvement for PEP-II in FY2004 and continued to improve in FY2005. An example of a good day with trickle injection is shown in Figure 1 below. A collaboration between the PEP-II accelerator staff and the BaBar detector operators has worked for several years to make the injection losses small. In FY2004, PEP-II and BaBar have reduced the backgrounds to an acceptable level to allow BaBar to take data with continuous injection. Trickle injection for positrons uses about six injection pulses per second from the linac, resulting in the positron current being stable to about 0.1% and BaBar getting better than 99% of the data. The HER injection of electrons is about 3 Hz. The SLAC linac was designed to allow up to 40 injected positron pulses and also 40 electron pulses each second in any order, although fewer pulses are in fact actually needed. Thus, PEP-II has true trickle injection with very steady currents and steady luminosity. The overall improvement in efficiency jumped to just over 40% in FY2005 with both rings. The PEP-II and BABAR groups are all very pleased with this improvement. All data taking is with continuous injection.

There was an unfortunate power outage in May 2005 when an offsite tree belonging to a neighbor fell onto the SLAC main power lines and kept the laboratory cold for three days. The linac and PEP-II accelerator took about a week to recover.

**Performance Summary:** The beam run in the FY2005 achieved several milestones for the PEP-II program. PEP-II exceeded 3.3 times its design luminosity this year (October 2005) by achieving  $1.003 \times 10^{34} \text{ cm}^{-2}\text{s}^{-1}$ . These luminosity levels correspond to giving BaBar over 1 million new particle physics events every day! This very high luminosity was reached using 1732 bunches with 2940 mA of positrons and 1740 mA of electrons; record beam currents. The

vertical and horizontal beam sizes at the interaction region were about 4.0 by 125 microns, respectively. Furthermore, PEP-II delivered  $728 \text{ pb}^{-1}$  to BaBar in one day in October 2005. This rate is 5.6 times the design delivered luminosity per day of  $130 \text{ pb}^{-1}/\text{day}$ . Thus, the luminosity delivery efficiency is excellent. From April 2005 to October 10, 2005, PEP-II has delivered  $58.73 \text{ fb}^{-1}$ , which is a very sizable data sample by itself. Overall, from May 1999 to October 10, 2005, PEP-II has delivered over  $314.8 \text{ fb}^{-1}$  to BaBar.

The achievements of FY2005 for PEP-II can be seen in the eight figures below. Figure 1 shows a good day with trickle injection, stable beam currents and steady luminosity. Figure 2 shows the peak luminosity in each month since starting of PEP-II with BaBar in May of 1999. Note that the PEP-II luminosity passed  $1 \times 10^{34}/\text{cm}^2/\text{s}$  on October 9, 2005. Figure 3 shows the weekly integrated luminosity in Run 5a from April 2005 to October 2005. The last week reached  $3950 \text{ pb}^{-1}$ . The plot, Figure 4, shows the total integrated luminosity with time over Run 5A indicating a total of  $58.73 \text{ fb}^{-1}$  over the six-month period. The next plot, Figure 5, shows the total integrated luminosity since May 1999 indicating that PEP-II has delivered to BaBar over  $314.8 \text{ fb}^{-1}$ . Figure 6 shows the daily integrated luminosity average in each month. The month of October 2005 was our best average month to date. Table I shows the operational records of PEP-II, highlighting our peak luminosity of over  $1 \times 10^{34}/\text{cm}^2/\text{s}$ . Table II and Figure 7 show our integrated luminosity and run time statistics for the four fiscal quarters of FY2005.

**PEP-II installation in October 2005:** PEP-II entered a shut-down period October 10, 2005, to perform safety-related activities in the tunnels and to install new hardware for increasing the luminosity. There are about a dozen projects associated with increased luminosity. A new HER Q5L vacuum chamber in the interaction region will be replaced to improve the HER vacuum pressure with beam current and BaBar backgrounds. A LER collimator will be installed downstream of the interaction point also to improve backgrounds. A beam spoiler will be installed upstream of the LER abort dump to protect the vacuum window from cracking from high peak currents. The electrical feed-throughs on the transverse feedback kickers will be replaced. Several new beam position monitor (BPM) units will be tried in the LER leading to a more extensive change later next year. A HER vacuum transition chamber will be changed with a higher power unit. The rf systems for both rings will be upgraded with several small changes meant to improve the mean time to failure. Several of the NEG vacuum pumps in the LER interaction region overheat with beam current. These NEG pumps will be removed and replaced with HOM power absorbers. A HOM absorber will also be placed in the HER luminosity chamber. A higher-power expansion bellows will be installed near a vacuum gate valve in PEP-II Region 4 which is in a higher HOM power region. All of the tasks will be completed during the October 2005 shut down. The restart of PEP-II is anticipated for November 14, 2005.

**PEP-II DOE Performance Measure:** The DOE HEP integrated luminosity measure for FY2005 for PEP-II was  $50 \text{ fb}^{-1}$ . The actual integrated luminosity delivered by PEP-II in FY 2005 was  $53.5 \text{ fb}^{-1}$  which meets the goal.

**PEP-II Performance in FY2005 Shown Graphically**

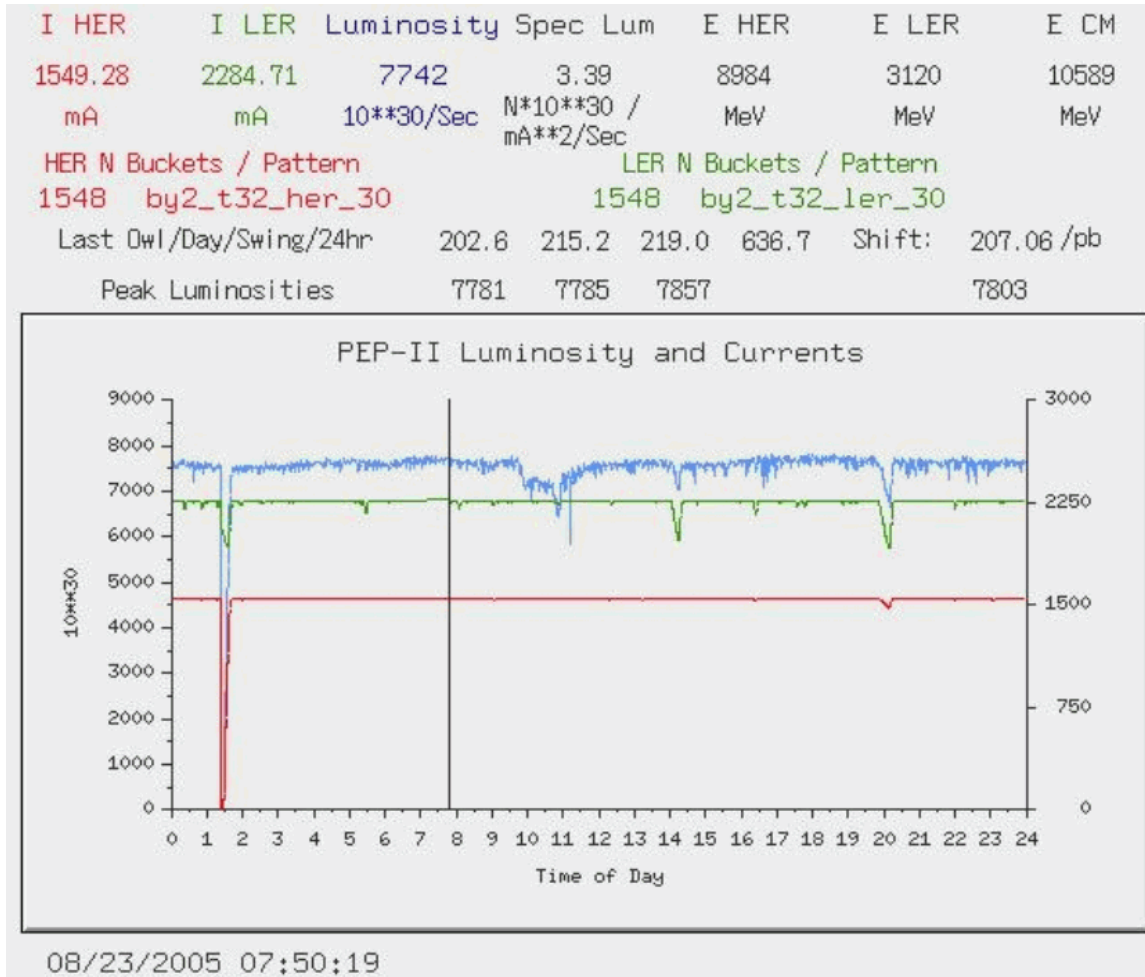


Figure 1: PEP-II beam currents and luminosity for 24 hours showing the stability of continuous (trickle) injection.

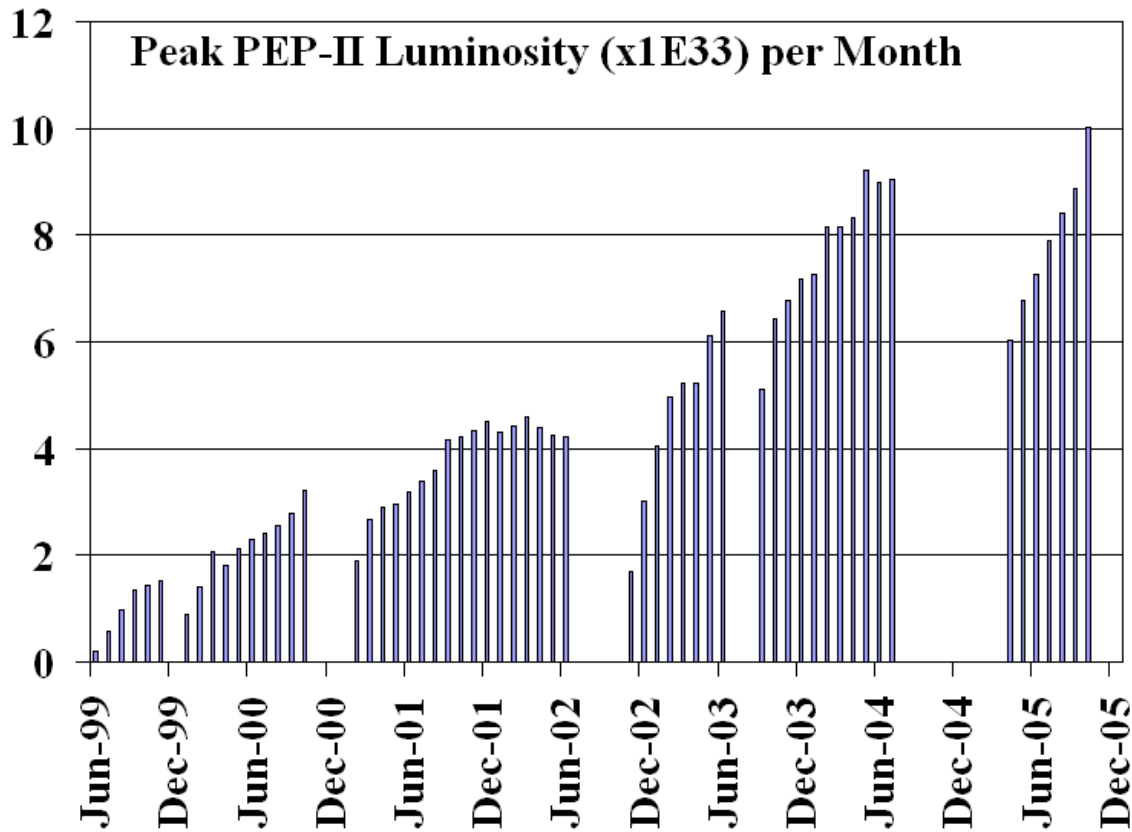


Figure 2: PEP-II peak luminosity in each month since May 1999.

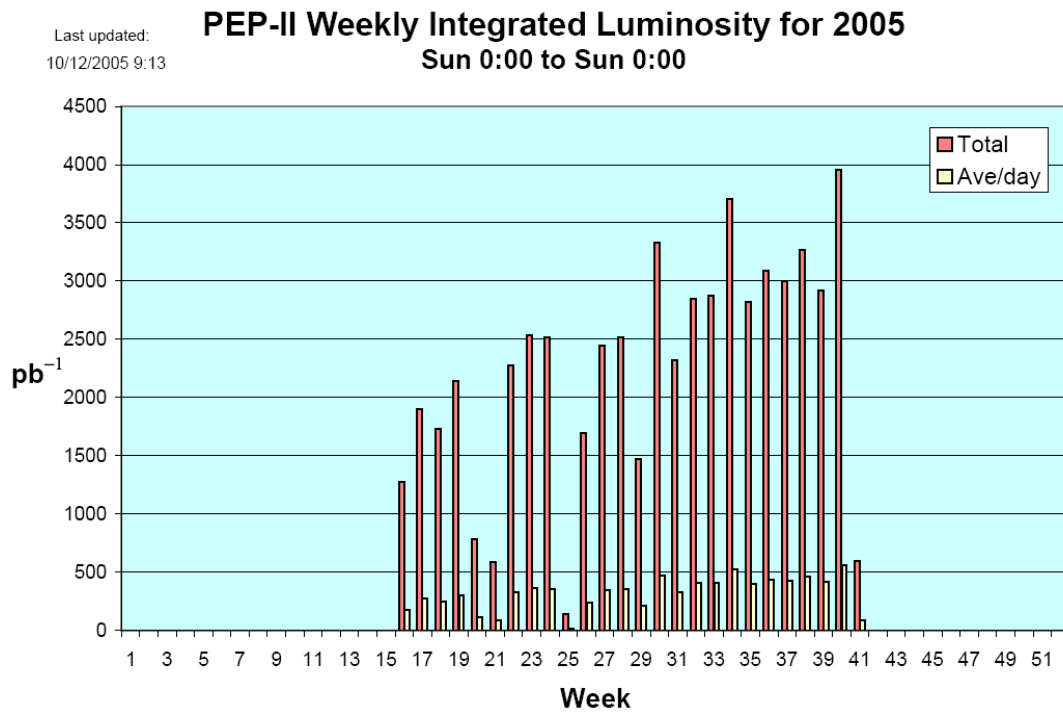


Figure 3: PEP-II integrated luminosity per week showing steady improvement.

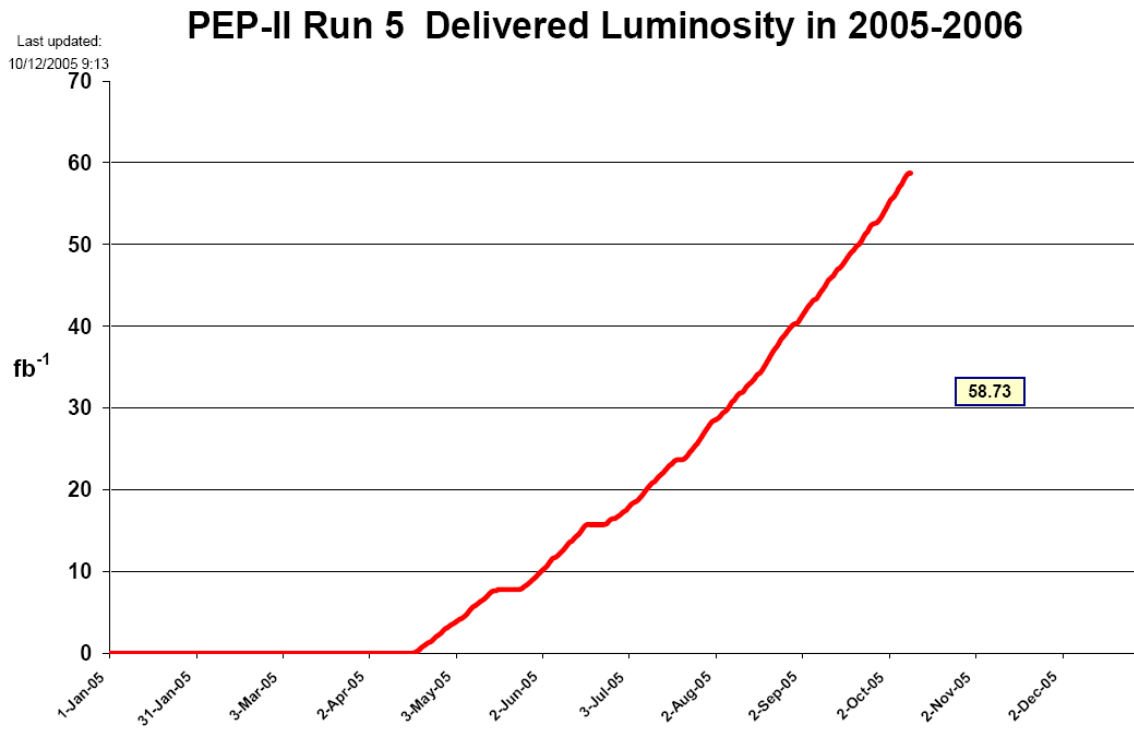


Figure 4: PEP-II accumulated integrated luminosity during FY 2005.

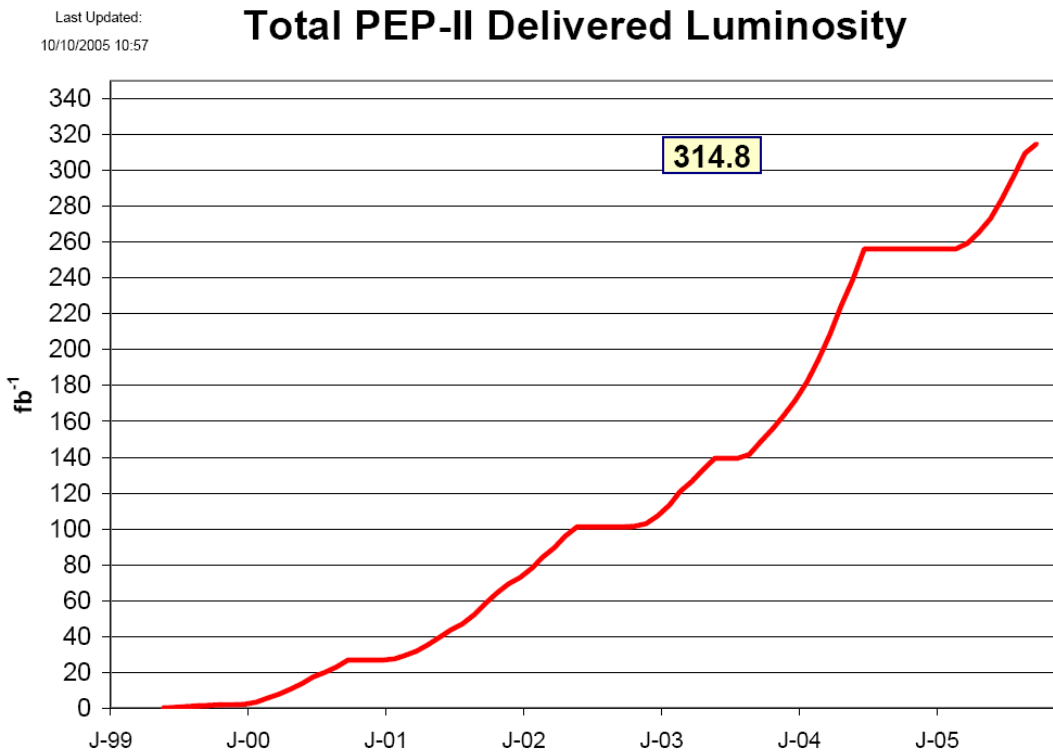


Figure 5: PEP-II accumulated integrated luminosity since May 1999.



Last Updated:  
10/10/2005 10:57

# PEP-II Daily Average for each Month

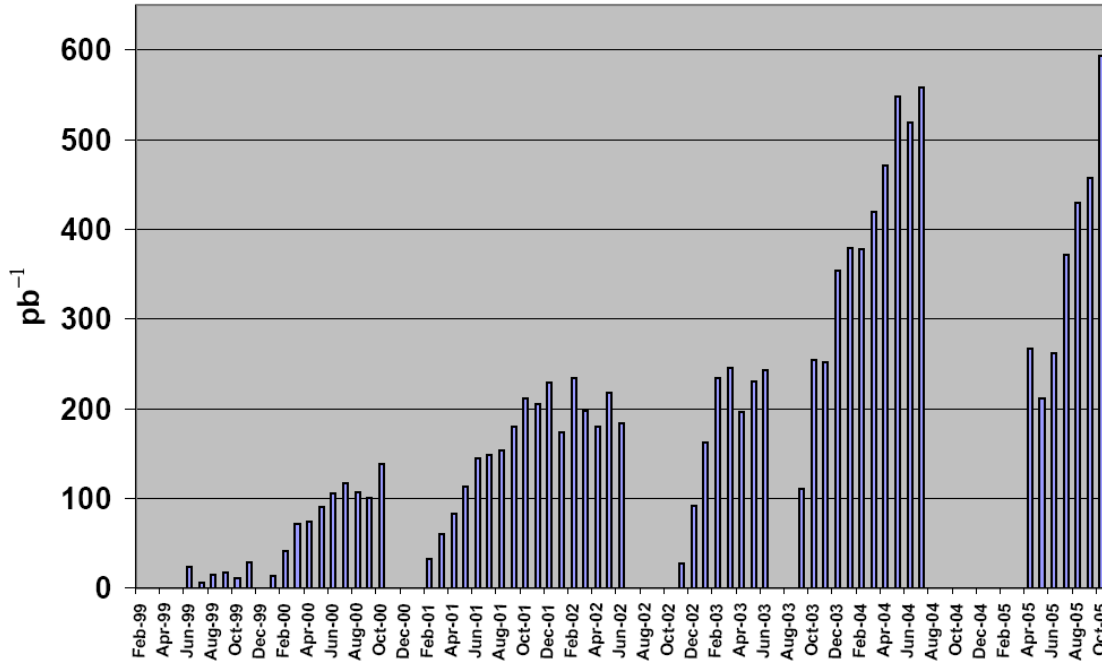


Figure 6: PEP-II integrated luminosity per month since May 1999.

## PEP-II Records

Last update:  
Oct 10, 2005

### Peak Luminosity

$$10.025 \times 10^{33} \text{ cm}^{-2} \text{ sec}^{-1}$$

1732 bunches 2940 mA LER 1740 mA HER

Oct 9, 2005

### Integration records of delivered luminosity

<b>Best shift</b> (8 hrs, 0:00, 08:00, 16:00)	<b>247.2</b> pb <sup>-1</sup>	<b>Oct 7, 2005</b>
<b>Best 3 shifts in a row</b>	<b>727.8</b> pb <sup>-1</sup>	<b>Oct 7, 2005</b>
<b>Best day</b>	<b>710.5</b> pb <sup>-1</sup>	<b>May 24, 2004</b>
<b>Best 7 days</b> (0:00 to 0:00)	<b>4.464</b> fb <sup>-1</sup>	<b>Jul 25-Jul 31, 2004</b>
<b>Best week</b> (Sun 0:00 to Sat 24:00)	<b>4.464</b> fb <sup>-1</sup>	<b>Jul 25-Jul 31, 2004</b>
<b>Peak HER current</b>	<b>1745</b> mA	<b>Oct 10, 2005</b>
<b>Peak LER current</b>	<b>2995</b> mA	<b>Oct 10, 2005</b>
<b>Best 30 days</b>	<b>16.720</b> fb <sup>-1</sup>	<b>Jul 2 – Jul 31, 2004</b>
<b>Best month</b>	<b>17.036</b> fb <sup>-1</sup>	<b>July 2004</b>
<b>Total delivered</b>	<b>315</b> fb <sup>-1</sup>	

Table I: PEP-II overall performance records

FY2005 Totals - PEP run								
	BaBar	PEP Mach. Dev.	Tuning & Injection	Unsched. Down*	Sched. Off	Total hours	Data delivered to BaBar (fb-1)	Data recorded BaBar (fb-1)
Q1 hours	0	0	0	1736	448	2184	0.0	0.0
Q2 hours	0	0	0	1936	248	2184	0.0	0.0
Q3 hours	1000.6	59.9	466.5	594.6	62.4	2184	17.0	15.7
Q4 hours	1475	106.6	286.2	289.9	26.3	2184	36.5	35.4
<b>FY2005 Total hours</b>	<b>2475.6</b>	<b>166.5</b>	<b>752.7</b>	<b>4556.5</b>	<b>784.7</b>	<b>8736</b>	<b>53.5</b>	<b>51.1</b>
(% of total hrs.)	28.3%	1.9%	8.6%	52.2%	9.0%			
Exclude All Sched. Off (% of Sched. On hrs.)	31.1%	2.1%	9.5%	57.3%		7951.3		

\* FY2005 Q1 and Q2 includes directed off for lab-wide investigation, review, and remediation of safety concerns, and re-validation of all systems and procedures.

Table II

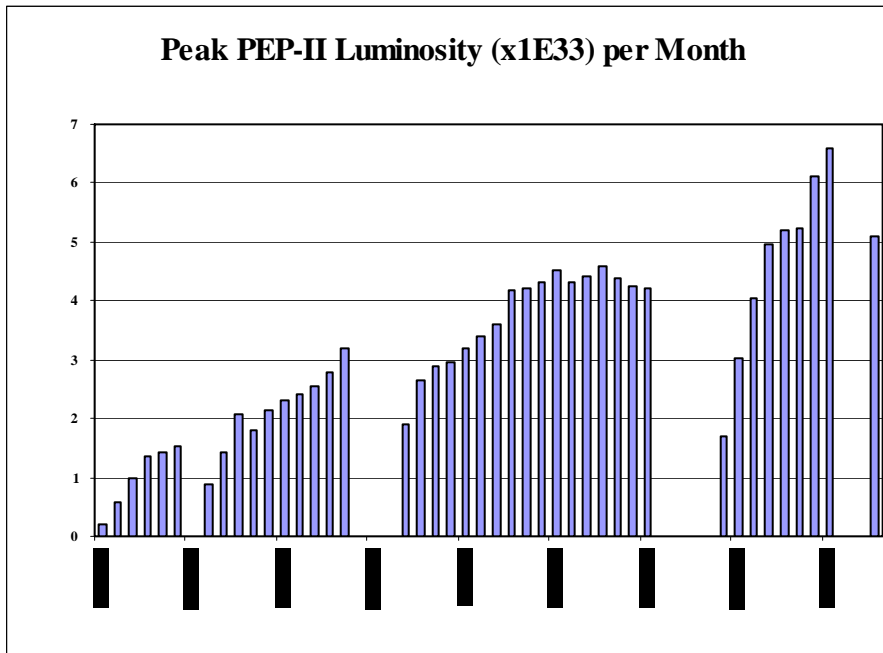


Table II and Figure 7: PEP-II Run statistics for FY2005

## 2. FY05 PROGRESS IN BABAR AT PEP-II by David MacFarlane and Bill Wisniewski

### Overview

Over this past year, the *BABAR* experiment has continued to be spectacularly productive, with many new results on time-dependent and direct  $CP$  asymmetries, rare and semileptonic  $B$  decays, and charm and tau physics. The detector continues to perform extremely well, with an operational efficiency of 97%. Since the start of running in October 1999, *BABAR* has accumulated an integrated luminosity of  $272 \text{ fb}^{-1}$  on the  $\Upsilon(4S)$  resonance, corresponding to 300 M  $B$ -meson pairs, and an additional  $27 \text{ fb}^{-1}$  taken 40 MeV below the resonance. With the delay in the start of Run 5 due to the electrical accident most of the  $52 \text{ fb}^{-1}$  of  $\Upsilon(4S)$  resonance data and  $4 \text{ fb}^{-1}$  of continuum data have been accumulated after May 2005. The analysis of the data has led to a broad range of results and over 175 submitted publications. Of particular note was the large outpouring of new results from the  $B$  Factories for this summer's major conferences, the International Symposium on Lepton-Photon Interactions in Uppsala (LP05) and the International Europhysics Conference of High Energy Physics in Lisbon (HEP2005). In total, *BABAR* contributed 65 conference papers to LP05 and an additional 13 to HEP2005, with *BABAR* speakers giving 19 parallel session talks on the full spectrum of new results at HEP2005, as well as major plenary talks by Francesco Forti (LP05) and Marie-Helene Schune (HEP2005). This is achievement is even more remarkable, given that no significant additional data was available between the summer 2004 and summer 2005 conferences. Clearly, PEP-II and *BABAR* have been highly productive in recording, reconstructing, analyzing and simulating data, more than fulfilling expectations for the promise for exciting physics from the project.

## BABAR Physics Highlights

The *BABAR* physics program, based on this enormous data sample, encompasses three main goals: (1) comprehensive measurement of a complete set *CP*-violating asymmetries in *B* meson decays; (2) systematic exploration of rare decay processes; and (3) detailed studies to elucidate the dynamics of processes involving heavy quarks. The first two goals focus on testing the Standard Model, measuring its parameters, and searching for the effects of new physics, while the third goal is designed to build a solid foundation by elucidating the interplay between electroweak and strong interactions in heavy-quark processes.

During the past year, we have made substantial progress in all three areas. The original discovery of time-dependent *CP* violation in the modes  $B^0 \rightarrow J/\psi K_S^0$ ,  $B^0 \rightarrow J/\psi K_L^0$  and related charmonium channels is by now a precision measurement, with a value for the *CP* violation parameter  $\sin 2\beta = 0.722 \pm 0.040 \pm 0.023$  already shown at ICHEP04. Belle provided a new measurement at LP05, which together with the *BABAR* measurement lowers the world average by about one standard deviation to  $\sin 2\beta = 0.685 \pm 0.032$ . This result provides a precise benchmark for *CP* violating effects within the Standard Model due to interference between amplitudes for *B* decay and *B* mixing. The angle  $\beta$  remains the most precisely measured angle of the Cabibbo-Kobayashi-Masakawa (CKM) unitarity triangle, whose three internal angles  $\beta$ ,  $\alpha$ , and  $\gamma$  characterize *CP* asymmetries in a wide variety of processes. The remarkable predictive power of the Standard Model arises from the fact that both the angles and sides of the unitarity triangle govern the full range of quark transitions in a highly interrelated manner.

Measurements of time-dependent *CP* asymmetries are now being extended to rare decay modes involving so-called  $b \rightarrow s\bar{s}s$  penguin diagrams containing virtual quarks and vector bosons. While such modes, include  $B^0 \rightarrow \phi K^0$ ,  $B^0 \rightarrow \eta' K^0$  and a number of related channels, should show the same *CP* asymmetry as the benchmark charmonium result for  $\sin 2\beta$ , they are also sensitive to new physics at high mass scales beyond those directly produced by present day experiments. *BABAR* reported a comprehensive set of results on *CP* violation studies in these channels at ICHEP04. Updates for many of the channels were provided by Belle at LP05 this summer, while *BABAR* expanded the list of measurements with additional channels and sub-modes. The new penguin channels added to the set of measurements were  $B^0 \rightarrow K_S^0 K_S^0 K_S^0$ ,  $\pi^0 \pi^0 K_S^0$ ,  $\omega K_S^0$ . Figure 1 shows the candidate sample and visible asymmetry for the  $B^0 \rightarrow K_S^0 K_S^0 K_S^0$  channel. In other cases, a  $K_L^0$  was substituted for a  $K_S^0$  to significantly increase the available size of the  $B^0 \rightarrow \eta' K_L^0$  and  $B^0 \rightarrow K^+ K^- K_L^0$  samples. Figure 2 shows an example of the candidate sample for the  $B^0 \rightarrow \eta' K_L^0$  and the observed asymmetry in the time evolution for these events.

A full compilation of measurements of *CP* asymmetries in  $b \rightarrow s\bar{s}s$  penguin modes is shown in Fig. 3. The average value  $0.50 \pm 0.06$  for the product of the amplitude of the sine ( $S_f$ ) term in the time-dependent asymmetry and the *CP* eigenvalue for the final state ( $\eta_{CP}$ ) should be equal to

the well-measured value of  $\sin 2\beta = 0.685 \pm 0.032$ . Intriguingly, this is not the case at present, with a discrepancy at the level of 2.4 standard deviations. This is actually a modest reduction from the 3.7 $\sigma$  significance from a similar suite of measurements at the time of the winter conference, with about one-half the reduction coming from the downward shift in the charmonium average for  $\sin 2\beta$ . Clearly this remains a result to watch in the future as more data is accumulated, since a difference between the charmonium and penguin modes is exactly the kind of signature one would expect from new physics beyond the Standard Model.

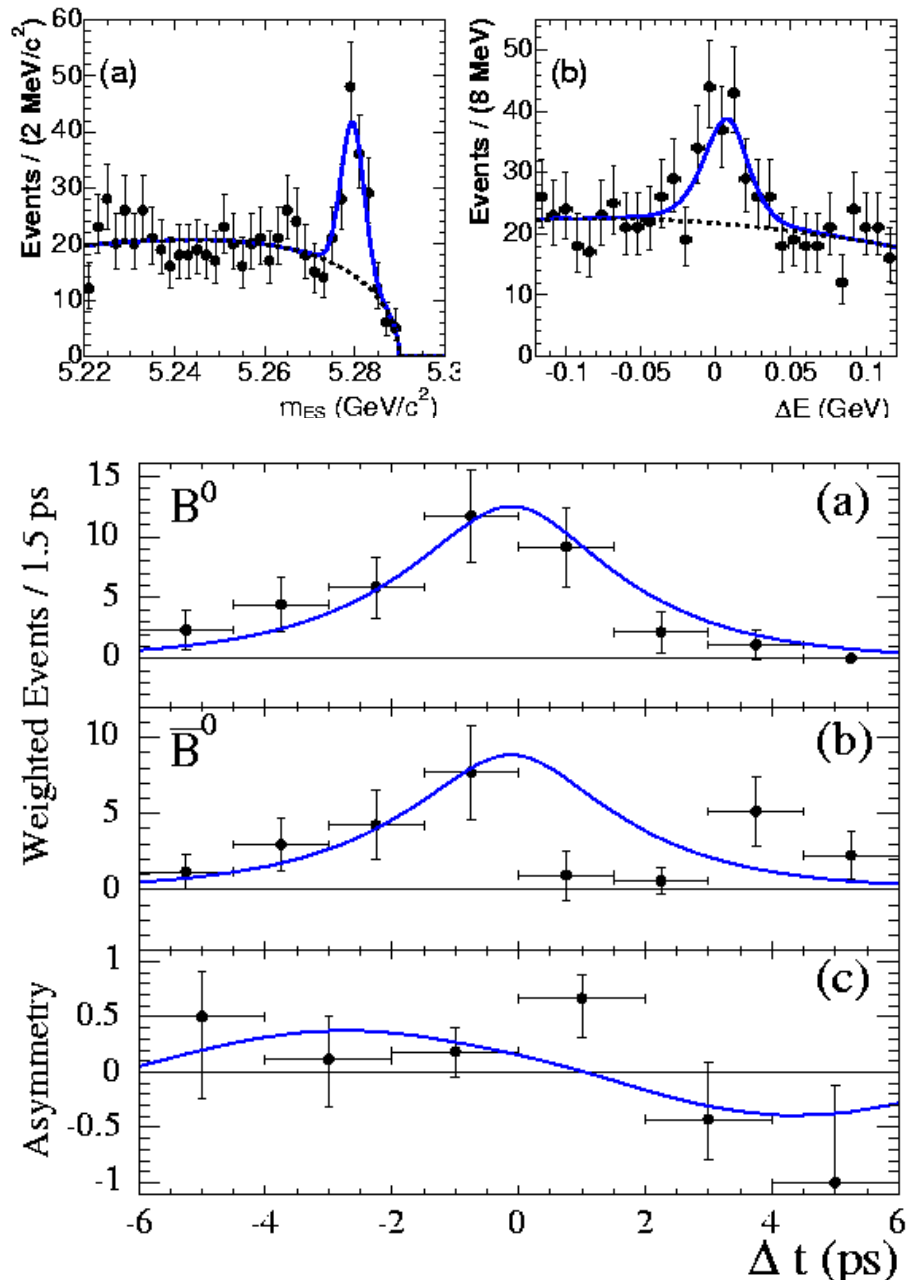


Fig.1. Distribution for the energy-substituted mass  $m_{ES}$  and energy difference  $\Delta E = E - E_{beam}$  for a sample of  $B^0 \rightarrow K_S^0 K_S^0 K_S^0$  (upper) signal events,  $\Delta t$  distributions for  $B^0$ -tagged (lower (a)) and  $\bar{B}^0$ -tagged (lower (b)) events, and visible asymmetry (lower (c)) with overlaid fit results.

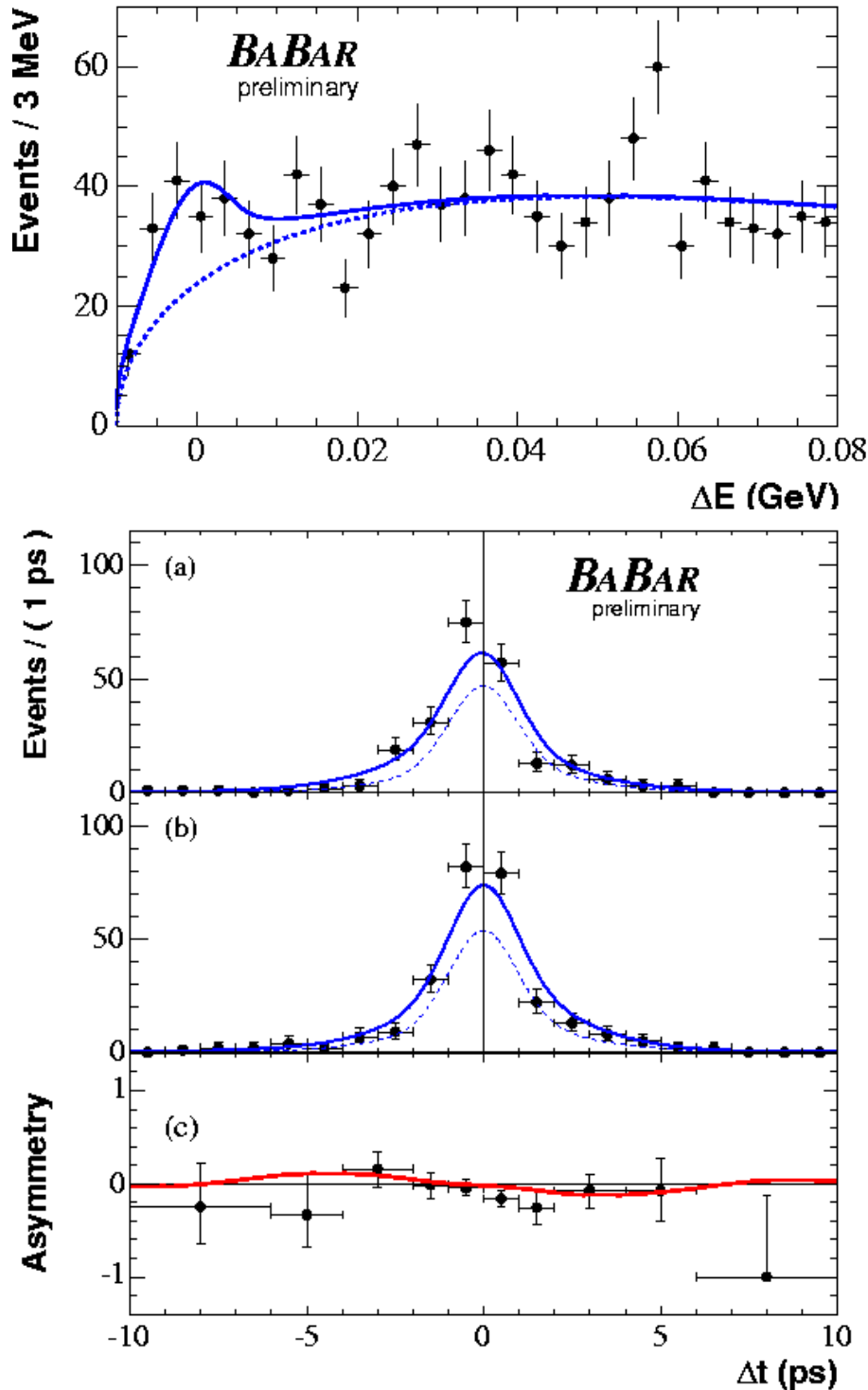


Fig.2. Distribution for the energy difference  $\Delta E = E - E_{beam}$  for a sample of  $B^0 \rightarrow \eta' K_L^0$  (upper) signal events,  $\Delta t$  distributions for  $B^0$ -tagged (lower (a)) and  $\bar{B}^0$ -tagged (lower (b)) events, and visible asymmetry (lower (c)) with overlaid fit results.

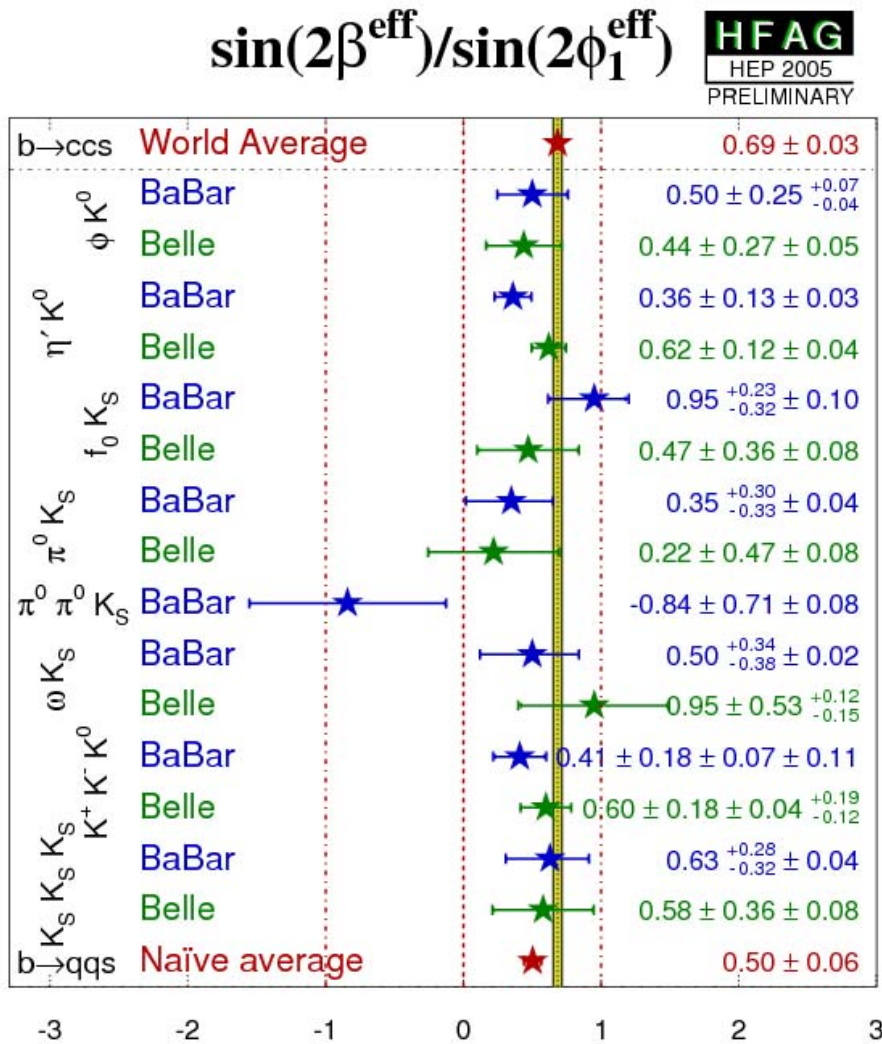


Fig.3. Compilation of fit results for the amplitude of the sine ( $S_f$ ) term in the time-dependent asymmetry multiplied by the  $CP$  eigenvalue for the final state ( $\eta_{CP}$ ) as obtained for various  $b \rightarrow s\bar{s}s$  channels by  $BABAR$  and Belle. The average over the eight channels,  $0.50 \pm 0.06$ , is about 2.4 standard deviations below the precision measurement of  $\sin 2\beta$  obtained in the charmonium modes,  $0.69 \pm 0.03$ .

With increasing size of the available data sample, the focus of the  $CP$  violation program has also turned to measurements related to the remaining angles of the unitarity angles triangle. The

angle  $\phi$  is related to time-dependent asymmetries in two-body modes involving  $b \rightarrow u$  transitions such as  $B^0 \rightarrow \pi^+\pi^-$ ,  $B^0 \rightarrow \rho\pi$ , and  $B^0 \rightarrow \rho^+\rho^-$ . However, the additional complication for many of these channels is the significant contribution of a second important decay mechanism, involving a so-called penguin diagram. Figure 4 summarizes the observed amplitudes for the sine and cosine dependent terms of the asymmetry for the two-body mode  $B^0 \rightarrow \pi^+\pi^-$ . While Belle has claimed to observe significant  $CP$  violation in this channel, along with evidence for direct  $CP$  violation through interference of two competing decay amplitudes, these claims are not supported by the *BABAR* results. Clearly more data will be needed to resolve this important puzzle. A direct measurement of the unitarity angle  $\phi$  requires a complete isospin analysis of the full set of tagged two-body decays. Following the initial observation of the rarest of these modes  $B^0 \rightarrow \pi^0\pi^0$  reported at LP03 by *BABAR*, a first measurement of the flavor-tagged time-integrated asymmetry has now been performed allowing us to constrain the correction due to the additional penguin decay mechanism.

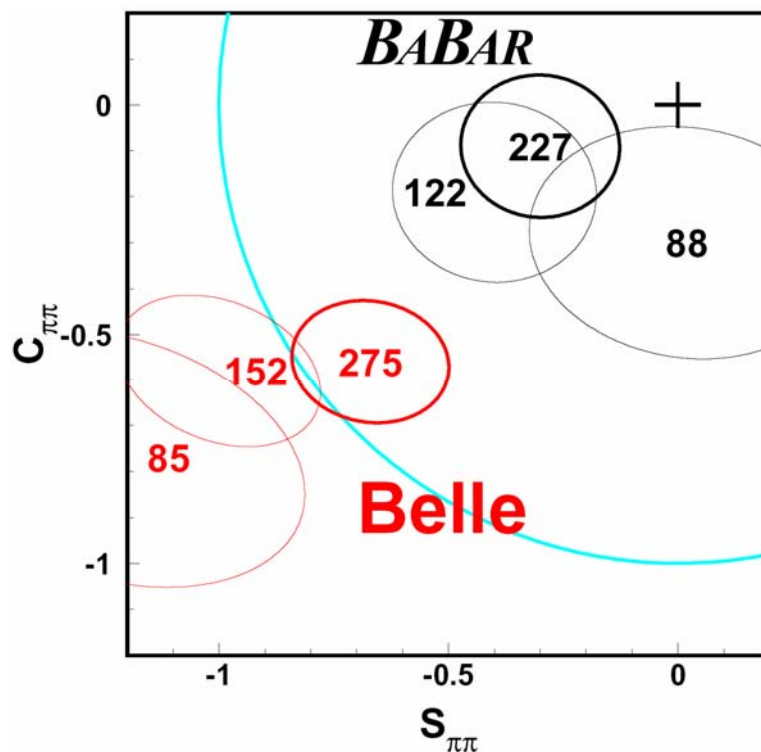


Fig.4. Compilation of fit results for the amplitude of the sine ( $S_{\pi\pi}$ ) and cosine ( $C_{\pi\pi}$ ) terms in the time-dependent asymmetry observed for samples of  $B^0 \rightarrow \pi^+\pi^-$  signal events observed at *BABAR* and Belle. The most recent *BABAR* measurement, reported at ICHEP04 and based on a sample of 227 million  $B\bar{B}$  pairs, while the latest Belle result using 275 million  $B\bar{B}$  pairs was reported at the winter 2005 conferences.

An important development this year in our study of has been the discovery by *BABAR* that  $B^0 \rightarrow \rho^+\rho^-$  has a comparatively small contamination from the penguin amplitude while also being an essentially pure  $CP$  eigenstate. As a result, an analysis of the isospin-related  $\rho\rho$  modes



allows a relatively tight limit on corrections for penguin yields. The observed  $\Delta t$  distributions for tagged samples of  $B^0 \rightarrow \rho^+ \rho^-$  candidates, and the corresponding visible asymmetry, is shown in Fig. 5. On the basis of the observed asymmetry we have obtained a first measurement of the unitarity angle, which we find to be  $\alpha = \left[ 103_{-9}^{+10} \right]^\circ$ . The compilation of available measurements of  $\alpha$  shown in Fig. 6 demonstrates significant progress over the past year, dominated by this exciting result from  $B^0 \rightarrow \rho^+ \rho^-$ .

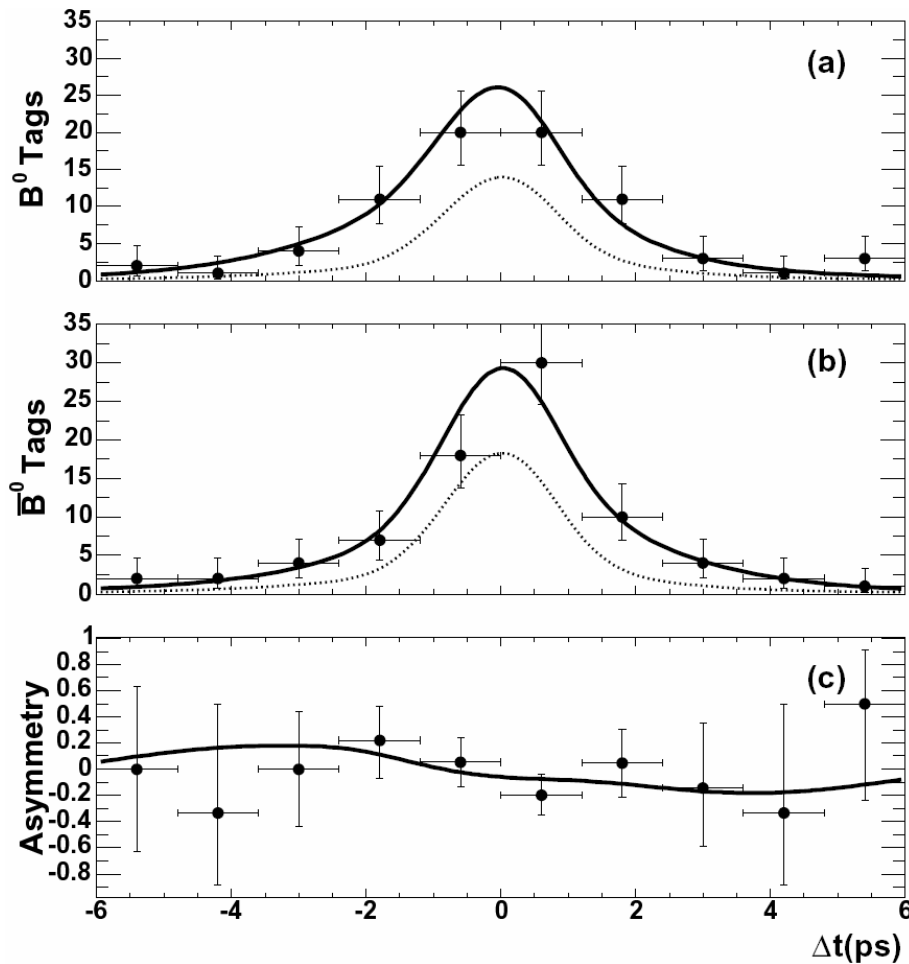


Fig.5.  $\Delta t$  distribution for events enriched in  $B^0 \rightarrow \rho^+ \rho^-$  signal events for  $B^0$ -tagged (upper) and  $\bar{B}^0$ -tagged (middle) events. The dashed line represents the sum of backgrounds and the solid line the sum of signal and backgrounds. The time-dependent  $CP$  asymmetry is shown in the lower panel along with the projected fit result.

Studies have also been continuing on a host of rare charged and neutral  $B$  meson decays that provide a deeper understanding of the role of different "tree" and "penguin" amplitudes in decays to charmless final states. In particular, we are making good progress in understanding how to use the interference between allowed and suppressed amplitudes to gain information about the third

unitarity angle  $\alpha$  where first real measurements are starting to emerge. The basic technique uses the interference between two competing decay mechanisms for  $B^- \rightarrow D^{(*)0} K^{(*)-}$ , one of which involves a  $b \rightarrow u$  transition and therefore the phase  $\alpha$  from the CKM matrix. Interference is possible in cases where the same final state results from the competing decay mechanisms, implying that the decay of the  $D^0$  meson from the sequence  $D^{(*)0} \rightarrow D^0 \pi^0$  or  $D^0 \gamma$  must proceed to a  $CP$  eigenstate (GLW) or through a doubly Cabibbo-suppressed (ADS) decay. Alternatively, the  $D^0$  decay must involve a common multi-body final state such as  $D^0 \rightarrow K_S^0 \pi^+ \pi^-$  (GGSZ). The sensitivity to the phase  $\alpha$  depends on the ratio  $r_B$  of the suppressed to dominant decay mechanism. Measurements using all three methods have been developed over the past year. A summary of the resulting constraints on  $\alpha$  is shown in Fig. 7. The Dalitz plot analysis in particular appears to be very promising for future measurements of  $\alpha$ .

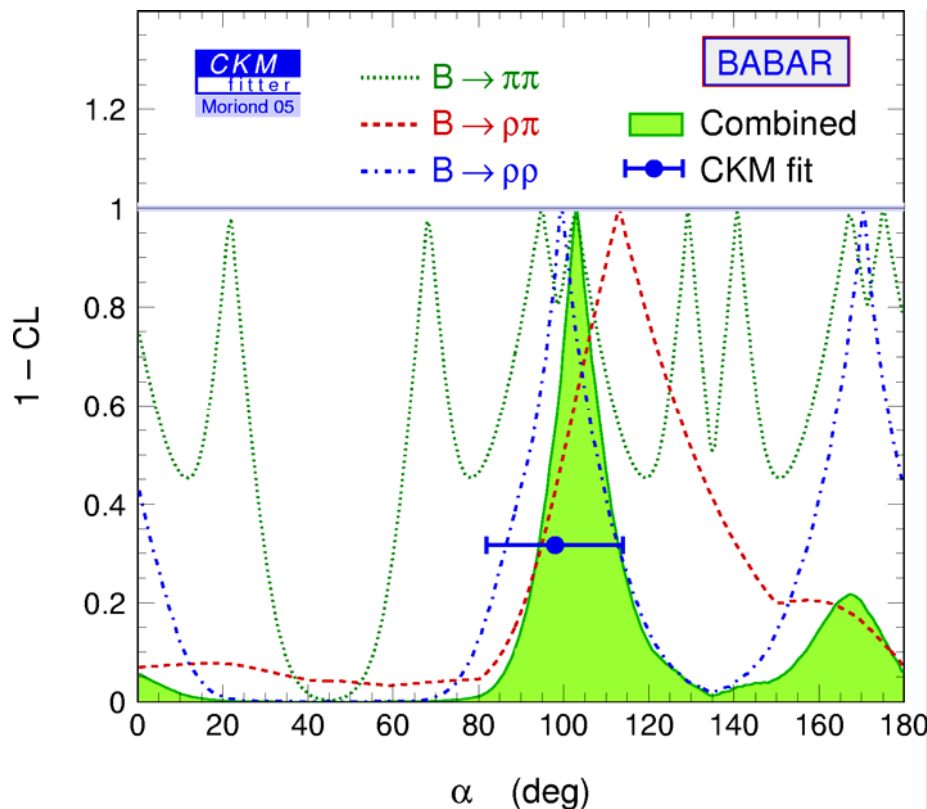


Fig.6. Combined *BABAR* result (shaded region) for direct determination of the unitarity angle  $\alpha$ , based on measurements of  $CP$  asymmetry in  $B \rightarrow \pi\pi$ ,  $B \rightarrow \rho\pi$ , and  $B \rightarrow \rho\rho$ . The point with error bars in the predicted value for  $\alpha$  from indirect measurements of CKM matrix elements.

As already noted the CKM unitarity triangle is a convenient summary of our knowledge of the weak interaction. From a suite of measurements of  $CP$  violation in kaon decays, the  $B$  lifetime and  $V_{cb}$  from semileptonic  $b \rightarrow c \ell \nu$  decays, and  $\Delta m_d$  and  $\Delta m_s$  from  $B_d^0$  and  $B_s^0$  mixing, we are able to indirectly infer the shape of the unitarity triangle and the location of its apex. The upper

plot in Fig. 8 shows with the red-outlined 90% CL allowed region the present knowledge of the unitarity triangle as inferred from this suite of indirect constraints. Measurements of  $CP$  violation in  $B$  decays allow us to determine the interior angles  $\alpha$ ,  $\beta$ , and  $\gamma$ . With the breakthroughs described above in techniques to measure  $\alpha$  and  $\beta$  a significant milestone has been reached this year with the  $B$  Factory data. The lower plot in Fig. 8 shows the constraints on the apex of the unitarity triangle that result from  $CP$  violation measurements in the  $B$  system alone. As can be seen the red-outlined region from the global fit to the direct  $CP$  violation measurements shows an allowed region that is both comparable in size to and consistent with that from the indirect measurements.

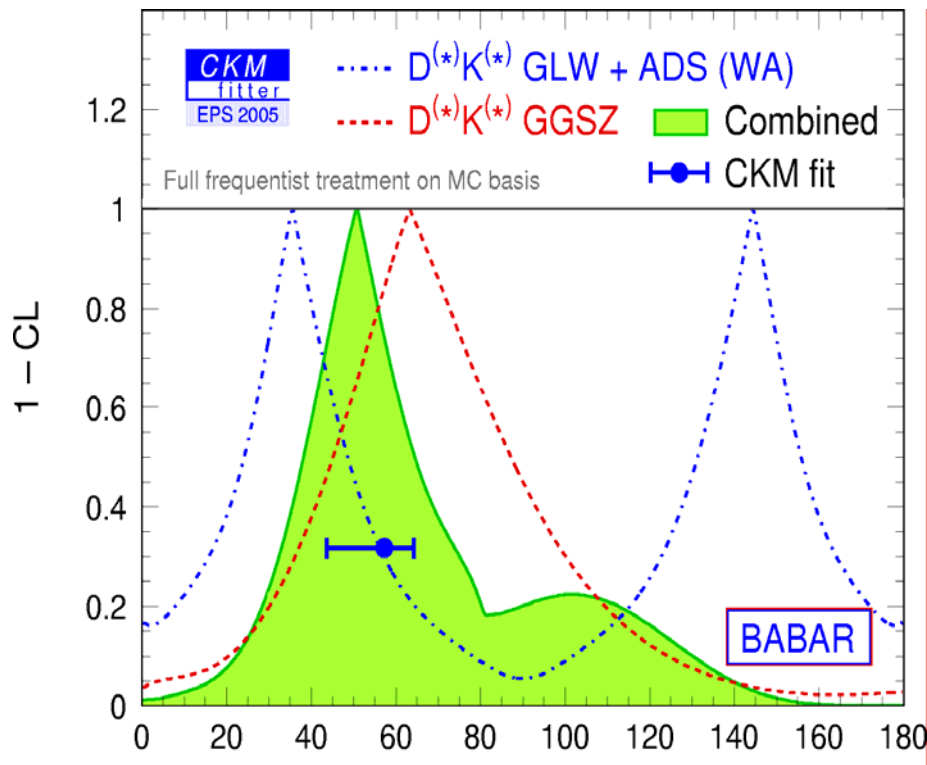


Fig.7. Combined result (shaded region) for direct determination of the unitarity angle  $\alpha$ , based on measurements of  $CP$  asymmetry in  $B \rightarrow D^{(*)}K^{(*)}$  decays using the GLW, ADS, and GGSW methods described in the text. The point with error bars in the predicted value for  $\alpha$  from indirect measurements of CKM matrix elements

The sides of the CKM unitarity triangle are related to the rates for certain quark transitions. Such measurements complement the studies of  $CP$  asymmetries, which are related to the angles of the triangle. We are continuing to refine new, state-of-the-art measurements of the magnitudes of CKM parameters  $V_{cb}$  and  $V_{ub}$  using semileptonic  $B$  decays, and we have studied the detailed dynamical properties of inclusive semileptonic  $B$  decays to extract key theoretical parameters describing  $B$  decay. These studies have reduced the error on  $V_{cb}$  to the 2% level, as a result of a detailed study of the inclusive hadronic and leptonic recoil systems. In particular, measurements of the moments of the inclusive hadronic mass and the electron energy distributions are fit with a

parameterized operator product expansion (OPE) calculation of the inclusive branching fraction, which yields both a precise determination of  $V_{cb}$  as well as the  $b$  quark mass.

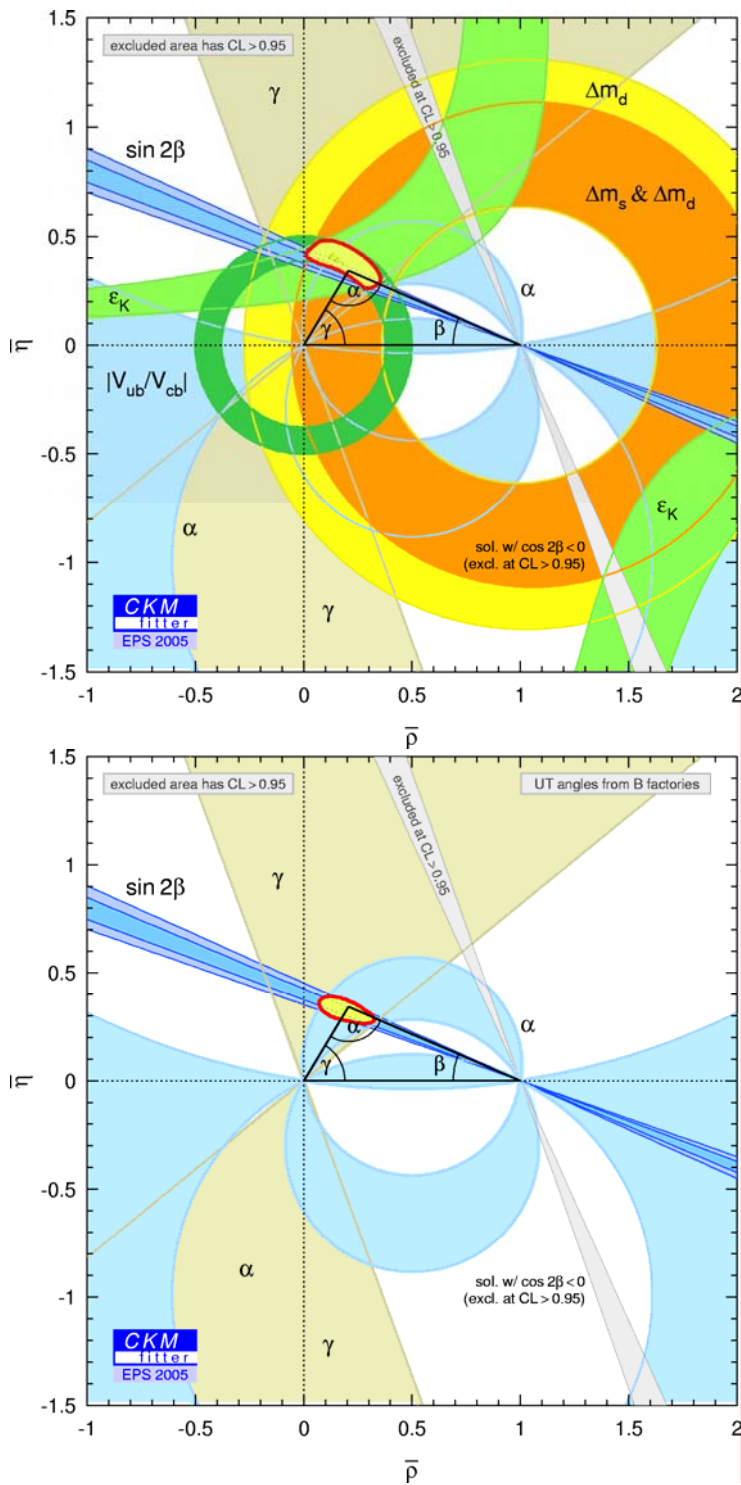


Fig.8. Compilation of indirect and direct measurements of the unitarity triangle. The upper plot shows the allowed region for the apex of the UT, obtained from the indirect constraints of  $\epsilon_K$

from  $CP$  violation in kaon decays,  $|V_{ub}/V_{cb}|$  and  $\Delta m_d, \Delta m_s$  from rare  $B$  decays and mixing. The lower plot shows the 90% CL allowed region (red line) from  $CP$  violation measurements in  $B$  decays alone

Over the past year, we have also made considerable progress in improving the precision of our measurement of  $V_{ub}$ . These measurements involve studies of both inclusive and exclusive semileptonic decays. In this case, the 100-times larger background from  $b \rightarrow c\ell\nu$  transitions makes the measurement particularly challenging from an experimental standpoint. Generally this means that studies of  $b \rightarrow u\ell\nu$  are restricted to certain regions of phase space, which then introduces additional theoretical complications in extracting the full rate and therefore the value of  $V_{ub}$ . However, one very promising method is to exploit the large data sample by using events in which one of the two  $B$  mesons is fully reconstructed in an hadronic decay mode while the other decays inclusively or exclusively via a  $b \rightarrow u\ell\nu$  decay. In such events, the remaining tracks can be analyzed much more easily, allowing a more inclusive measurement that reduces theoretical model dependence on  $V_{ub}$ . An example of such a measurement is given in Fig. 9, which shows the  $q^2$  distribution for signal and background events is a sample obtained by full reconstruction of the tagging  $B$  meson. In the case of hadronic masses  $M_X$  below 1.7 GeV, a region populated by the charmless  $b \rightarrow u\ell\nu$ , we see statistically limited but relatively clean signal. A compilation of current  $V_{ub}$  measurements is given in Fig. 10. The average, dominated by inclusive studies, has already reached a precision of 7.5%. While the exclusive determinations have not quite reached this level of precision yet, we expect substantial progress in the next three years in conjunction with an improved theoretical framework.

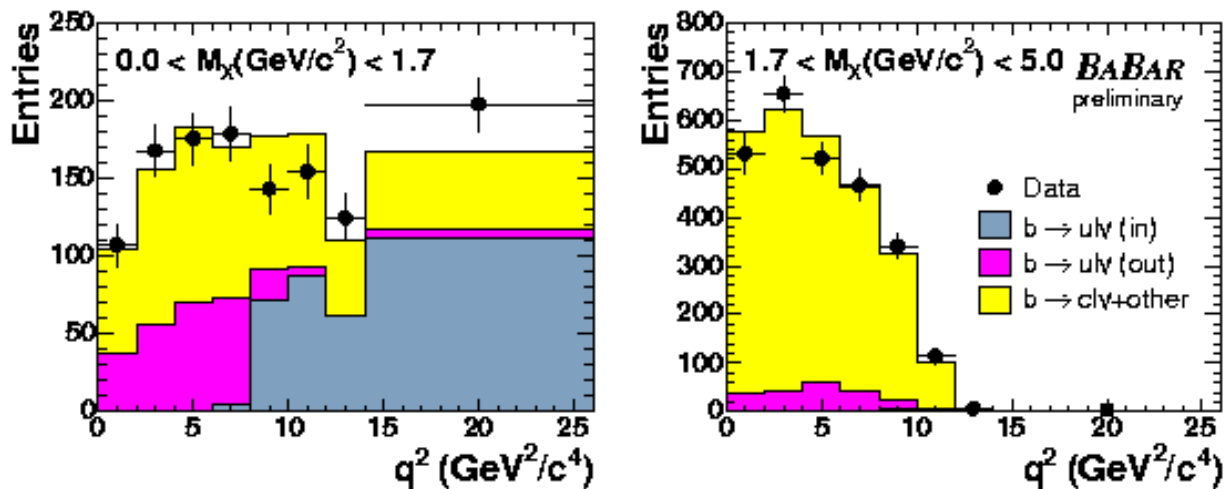


Fig.9.  $q^2$  spectrum from semileptonic  $B$  decays tagged by a fully reconstructed  $B$  meson on the recoil side of the  $\Upsilon(4S)$  event for hadronic masses in the ranges  $0 < M_X < 1.7$  GeV (left) and  $1.7 < M_X < 5.0$  GeV (right). The yellow area is the  $b \rightarrow c\ell\nu$  background, pink is the  $b \rightarrow u\ell\nu$  outside the signal region, while blue is the  $b \rightarrow u\ell\nu$  signal in the region  $M_X < 1.7$  GeV and  $q^2 > 8$  GeV<sup>2</sup>

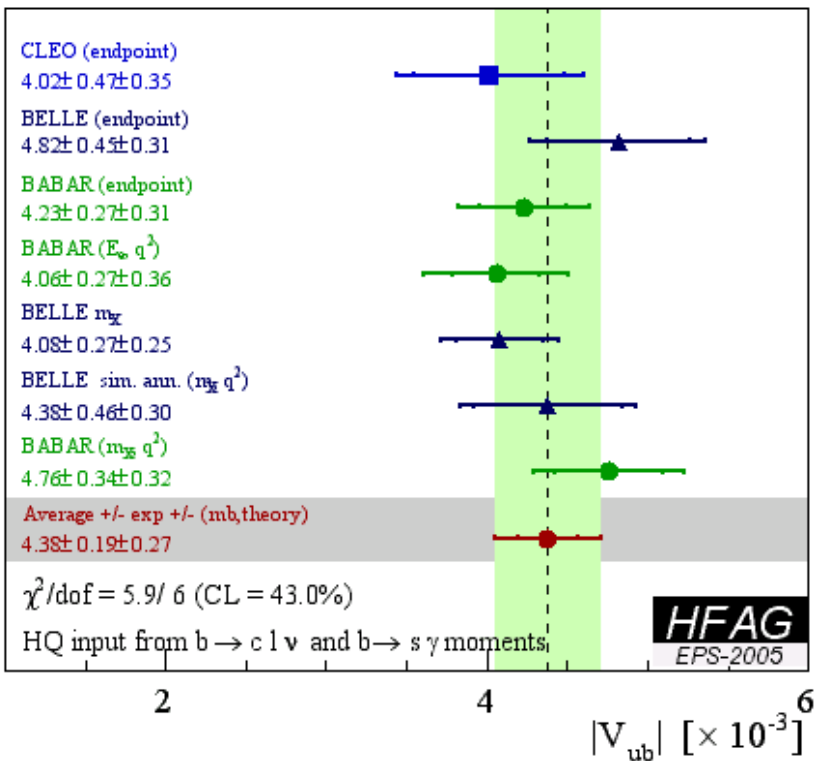


Fig.10. Compilation of available measurements of the quark mixing element  $|V_{ub}|$ . The combined statistical and theoretical error on present world average is 7.5%.

Finally, it should be noted that the range of physics addressed by the *B* Factory program spans a broad range of topics in heavy flavor physics, including beauty, charm, and tau physics, through a variety of production mechanisms, including  $ee$  annihilation, two-photon, and initial-state radiation events. One of the highlights outside the weak interaction physics described above has been the ongoing discovery of unusual high-mass states decaying to charm or charmonium. The latest example was announced by *BABAR* at the LP05 conference this summer in Uppsala. This is a state produced in initial-state radiation events,  $e^+e^- \rightarrow \gamma Y(4260)$ , subsequently decaying to  $J/\psi \pi^+ \pi^-$ . Such a heavy charm-containing object should be very broad, with large branching fractions to pairs of open charm states. However, limits from the total  $ee$  annihilation cross section at 4.26 GeV suggest that the decay width to  $J/\psi \pi^+ \pi^-$  must be unusually large. There are already a large number of theoretical papers contributed to the literature trying to suggest explanations for the unusual properties and mass of the  $Y(4260)$ . The lively debate, with speculations about hybrids, molecules, or other stable states outside the conventional spectroscopy of QCD is yet to be resolved. This work is a reminder of the significant potential for surprises in the very large data samples available in *BABAR* whether in spectroscopy or in weak interaction physics of heavy flavors.

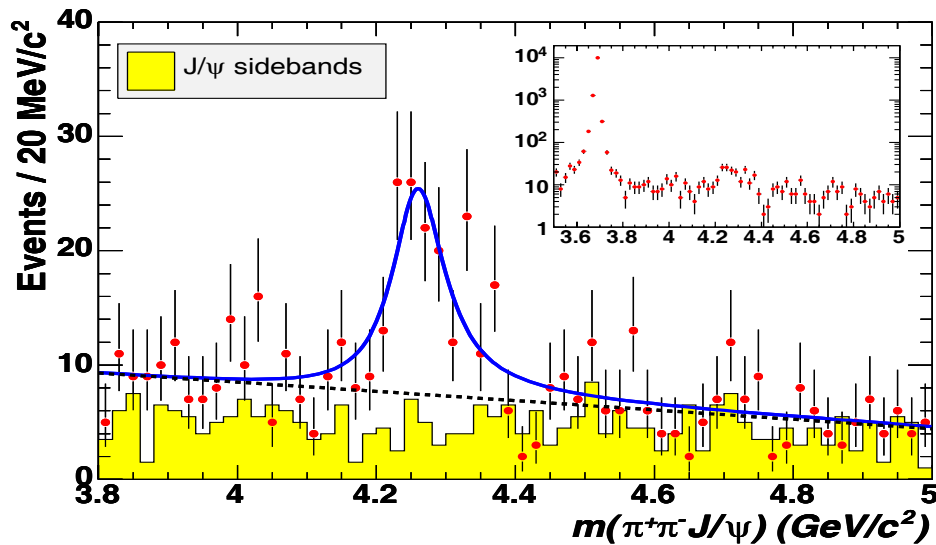


Fig.11. New heavy mass state  $Y(4260)$  observed in initial-state radiation events  $e^+e^- \rightarrow \gamma Y(4260)$  decaying to  $J/\psi\pi^+\pi^-$ .

### **BABAR Detector**

The *BABAR* Detector completed the first portion of its fifth data run in early October 2005 after collecting  $56.3 \text{ fb}^{-1}$  (Fig. 12). The five week October down period briefly interrupts Run 5 to address a couple of accelerator and safety issues: PPS system check-out and replacement of a vacuum chamber whose NEG pump material, in out-gassing due to heat-up associated with the higher luminosities achieved during this run, provided excessive backgrounds to the detector. The detector took advantage of this time to install the next generation of Drift Chamber electronics, as well as to prepare for the Instrumented Flux Return upgrade work that will occur in Summer 2006.

The *BABAR* Machine Detector Interface group continues to understand detector backgrounds using the detailed Monte Carlo simulation (GEANT4) of the interaction region that it developed. The group installed the synchrotron light monitor that was constructed last year, and is developing the software tools to extrapolate the vertical beam size at the interaction point. The MDI group has developed online tools for determining the horizontal and longitudinal beam size at the interaction point, as well for measuring the crossing angle of the beams at the IP, on a real time basis. This has proved to be very useful to the machine physicists and accelerator operators.

MDI activity will receive increased emphasis in the coming years because of the more than double increase in luminosity expected. The activity will aim at ameliorating the effects of backgrounds on the detector.

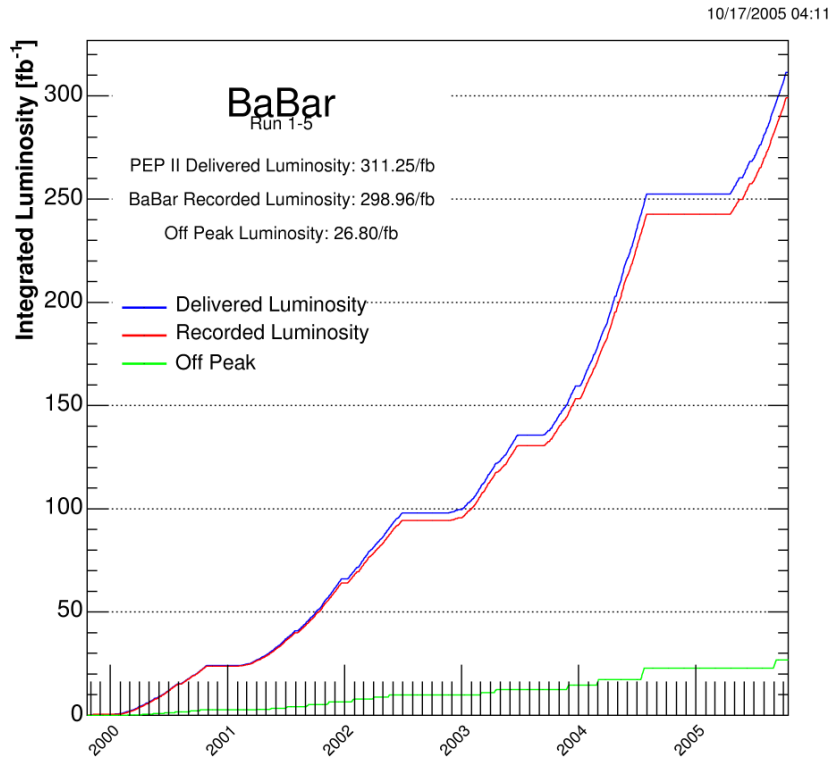


Fig. 12. *BABAR* integrated luminosity (Run 1-5a)

The Silicon Vertex Tracker (SVT), after an initial rocky period, has performed well during the past year. The rocky period was due to fallout of last year's bias current growth problem in the outer layers of the SVT that was identified last year. The redefinition of relative bias voltages in these layers solved the outer layer problems, but produced electric field configurations in a few spots in the middle layer that required a second round of optimization. Effort has been devoted to developing software tools that allow readout of sections of the SVT that have been isolated by local chip damage.

The performance of a narrow band of SVT modules will be severely degraded by high occupancy associated with beam backgrounds. Radiation damage from these backgrounds will render this set of modules useless. The natural time for replacement of these modules would be during the upgrade of the accelerator interaction region at the end of Run 5. However, limitations imposed by the increasing occupancy have led to reconsideration of module replacement at that time. The conclusion, accepted by the collaboration, of the task force which concluded study of this issue in the last year, was that the physics loss is minimal and no module replacement should be attempted.

During the past year the Drift Chamber team has focused on upgrading the front end readout electronics. Beam related backgrounds clog the data pathway from the on-detector electronics to the off-detector readout modules, producing readout deadtime (Fig. 13). Fragments produced in the interaction of radiative Bhabha event electrons and positrons with beam line elements



dominate these backgrounds that grow with luminosity. The fix for this problem has been implemented in two steps. In the first phase, whose implementation was completed during the 11 week downtime following the end of Run 4, the programmable array front end chips were reprogrammed to send half of the waveforms. This reduced the readout dead-time during Run 5a to acceptable levels (i.e., of order a per cent or less), though the limits of this implementation were apparent in dead-time increases that accompanied unusually high backgrounds.

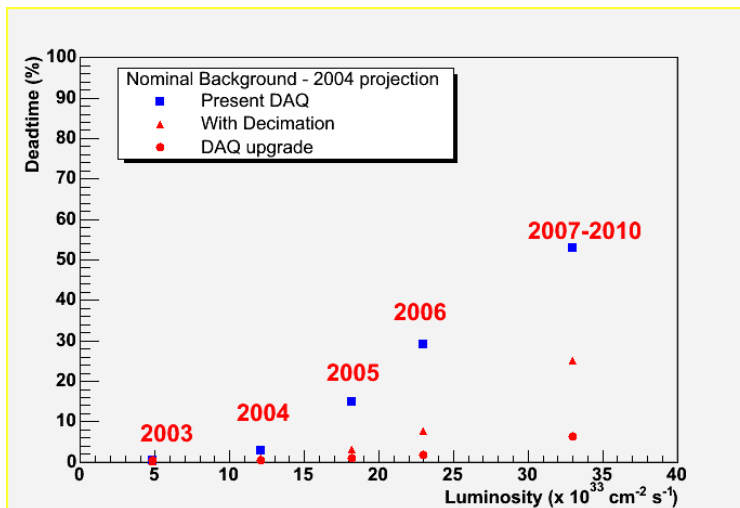


Fig. 13: Dead-time due to DCH readout. Blue squares show extrapolation of original front end electronics; red triangles show extrapolation with phase 1 upgrade; red circles show extrapolation with phase 2 upgrade.

In the second phase the feature extraction algorithms, which are currently executed in the off-detector readout modules, will be moved into modern programmable array chips located in the on-detector electronics. The quantity of data that flows from the DCH will be reduced about another factor of two; dead-time at the highest luminosity projected at the end of the decade will remain acceptably small. The new electronics board (Fig. 14), which uses a modern field programmable gate array and programmable read-only memories, has been designed and tested, and is being installed in the October 2005 shutdown.

The DIRC, which uses Cherenkov light to identify charged particle species, has performed well this year. The Electromagnetic Calorimeter has performed without problems. Effort continued to be focused this year on improvements to the electromagnetic shower reconstruction code and calibration scheme.

The Forward Endcap Resistive Plate Chambers (RPCs) performed efficiently during the fifth data run. The additional steel added during last year's down has decreased beam related background rates in the outer layers of the forward endcap by over a factor of three. This has

permitted all layers to be utilized, allowing the realization of the full benefits of the Summer 2002 upgrade: increased  $\mu$  identification efficiency with improved  $\pi$  rejection. In order to decrease the sensitivity to backgrounds, which increase directly with future luminosity improvements, of portions of the RPCs closest to the beam line, electronics have been developed to operate the RPCs in avalanche mode, rather than streamer mode. Prototype electronics is being installed during the October shutdown during the October shutdown in three RPCs to test this scheme. Studies where water vapor is introduced into the RPC gas have been successfully completed. This boosts the RPC efficiency and is being implemented in all forward endcap chambers.

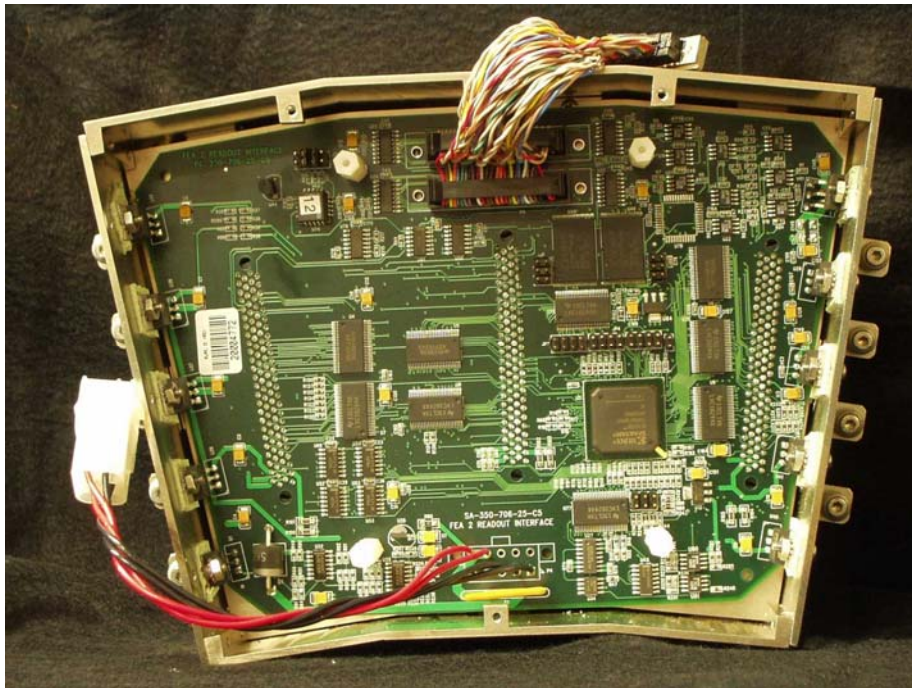


Fig. 14: Phase 2 Drift Chamber readout board, with modern Xilinx FPGA, mounted in a front-end electronics module.

In December 2002 the collaboration selected Limited Streamer Tubes (LSTs) as the replacement technology for the RPCs of the barrel portion of the IFR. Installation of twelve layers of LSTs into the top and bottom sextants of the barrel IFR was completed in mid-October 2004. Brass 7/8" absorber replaces the barrel RPCs in six layers in these sextants to improve the  $\pi/\mu$  rejection ratio. The barrel LSTs, in contrast to the barrel RPCs, are functioning well (Fig. 15). LSTs will be installed in the four remaining barrel IFR sextants at the end of Run 5.

Design and fabrication of tooling for the installation of the remaining four sextants of the barrel IFR is approaching completion. Fig. 17 shows the EMC load transfer fixture that will be used in the LST installation.

The trigger has been upgraded to handle higher luminosity. Additional information from the DCH is used to ensure that events originate close to the interaction point along the beam-line. The new system has performed well during Run 5.

PEP-II is continuing to operate in the “trickle-injection” mode first introduced during Run 4. The modifications introduced to the data acquisition system to support this are working well, and the data acquisition system is being steadily refined to handle the increasing luminosity. As a result *BABAR* continues to maintain its record of recording for physics analysis approximately 98% of the data produced by the accelerator.

At the end of 2003 *BABAR* deployed a new Computing Model with the key new element being the storage of event data in an ensemble of ROOT files with a thin relational database catalog (not required at run time) rather than in an Objectivity/DB Object-Oriented Database. The processing of data acquired since the adoption of the new model continues to demonstrate both the flexibility of the new system and its improved performance. New data are passed through a pre-processing step at SLAC to update and optimize calibrations for the hardware systems. The data are then ported to Padova, where one of several available PC-based Linux farms are used to actually reconstruct the events. Within 24 hours of data acquisition, both steps are complete and data shipped back to SLAC for a final quality assurance evaluation. The resulting fast access to physics quality data both ensures a continuous monitoring of detector performance and permits data to enter analysis very soon after it is acquired. Further work to remove dependencies on Objectivity databases for other auxiliary conditions and environmental information is essentially ready to deploy at this time. These additional changes will improve the portability of the *BABAR* computing environment, enabling laptop analysis for example.

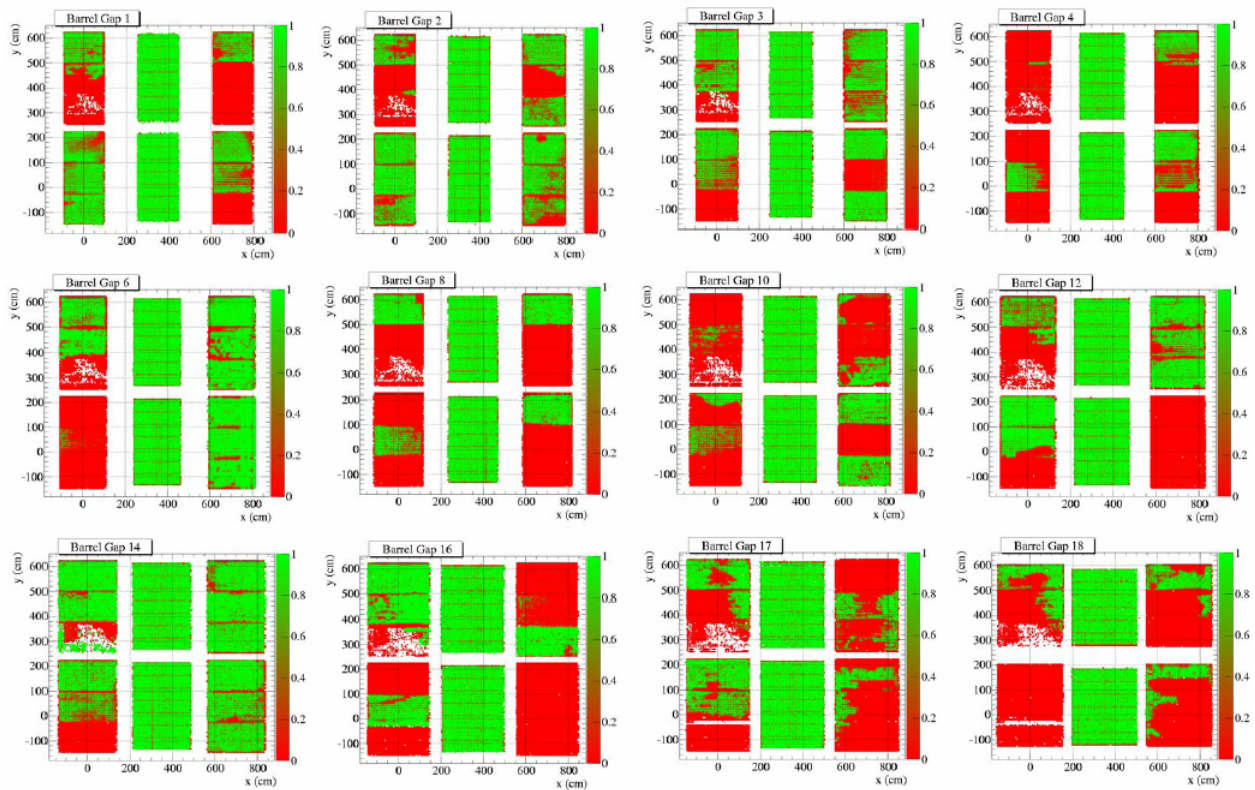


Fig. 15: Hit maps for 12 barrel IFR layers that contain both LSTs and RPCs. Efficient areas are green. In each of the 2x3 postage stamps shows in the upper half the top three sextants of a barrel layer, with the bottom three sextants in the lower half of the postage stamp. The middle sextant in each case has been instrumented with LSTs. Aside from the locations of the wire holders, where the LSTs have no sensitivity, the LSTs are fully efficient. Note that the RPCs have large dead areas.



Fig. 16: LSTs under continuous test. These LSTs will be installed in the remaining four barrel sextants during the Summer 2006 shutdown.

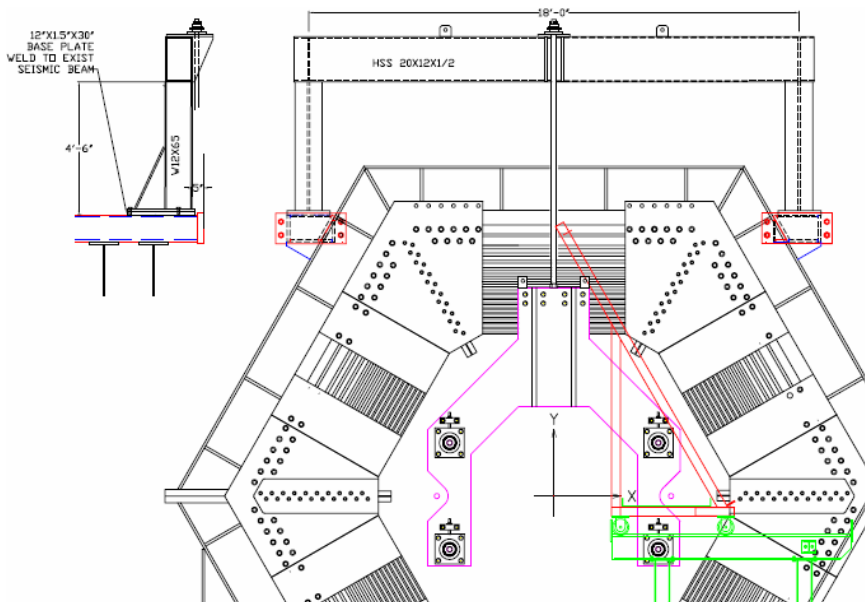


Fig. 17: EMC load transfer fixture. Engineering and safety reviews have been completed for these fixtures.

Following initial reconstruction in Padova, all data are passed through a skim process, which applies about 200 separate physics pre-selections to the data sample and allows much faster and efficient physics analysis of the full data sets. Specific physics selections of the data are made uniquely available at individual *BABAR* Tier-A sites at SLAC and in Europe. Our experience with the new data format, in combination with these reduced physics data samples, has continued to be very positive. It has been a major factor in the continuing high level of physics productivity of the experiment, including our ability to monitor the quality of data in near real time and to add this data to analyses within a matter of days of its being recorded. In addition, the length of time required for a skim of the complete data sample is now short enough to allow central production of new skims several times per year, adding considerably to our ability to quickly attack new areas of physics interest. Finally, the data storage changes have allowed us to utilize Grid techniques for part of our Monte Carlo simulation production, as the first step in exploiting the significant developments and resources available by this means.

### ***BABAR* Future Plans**

The goal of the experiment is to accumulate a full sample of  $500 \text{ fb}^{-1}$  by the end of 2006 and  $1000 \text{ fb}^{-1}$  by September 2008. The collaboration and the laboratory have explored the physics case for this rich *B* physics program, with many important new results that can be anticipated by quadrupling the sample currently used for analysis. The program rests on two main scientific goals. The first is to provide precision measurements of the weak interaction couplings of beauty quarks that will test at a fundamental level the Standard Model of particle physics through a series of over-constraining measurements. The couplings of quarks to the weak interaction, *i.e.*, the elements of the quark mixing matrix, are as basic to the theory as the quark masses. The *B* Factory will substantially improve the precision of our knowledge of both the magnitude of these couplings and the single complex phase that appears to describe all observed matter-antimatter differences, which we refer to as *CP*-violating asymmetries. Over the next three years, additional independent measurements of the quark couplings will achieve a threshold of precision that will, for the first time, allow these new methods to provide further stringent consistency tests. The combination of existing and new constraints will provide a powerful test of the Standard Model.

The second goal is to study *CP* violation and rare decays in beauty, charm, and tau decays for indirect evidence of New Physics beyond the Standard Model. Such searches are possible only because of the ever increasing precision with which we understand the Standard Model, thereby providing a benchmark against which we can distinguish the additional effects of New Physics. Searches for New Physics are of fundamental interest if either convincing new effects are seen or limits can be substantially improved. In general, *CP* violation and rare processes are sensitive to New Physics at high mass scales through their quantum contributions to penguin diagrams, which may involve virtual production of particles from either the Standard Model or New Physics. If there are deviations from the Standard Model, we will have a first exciting look at the properties of New Physics even before it is directly observed at the LHC. However, if no deviations are seen, the *B* Factory program will still provide all important evidence to rule out whole classes of theoretical explanations for new phenomenon discovered at the LHC. The *B* Factory and the LHC are thus complementary tools in the search for New Physics, with the *B* Factory providing a powerful legacy of constraints on the nature of any New Physics directly produced at the LHC.

### 3. FY05 Progress in the Particle Astrophysics Program by Steven Kahn

The Kavli Institute for Particle Astrophysics and Cosmology (KIPAC) has completed its second full academic year. The KIPAC faculty has been joined by Professors Tom Abel and Steve Allen. Tom Abel works primarily in computational cosmology and Steve Allen in the modeling of X-ray clusters of galaxies. Abel is leading a new computational astrophysics research initiative and working well with the SLAC Computing Services. Allen is developing a capability to analyze data from X-ray telescopes which will provide a basis for future research projects. Kirk Gilmore, Glenn Morris and Andy Rasmussen have joined KIPAC in senior staff positions. Only one of the original group of postdocs has moved on. The remaining seven have been joined by Melanie Bowden, Marusa Bradac, Teddy Cheung, Jonathan Granot, David Rapetti and Weiqun Zhang. Over 20 graduate students are now associated with the group. At the administrative level, Jennifer Formichelli has moved to the East Coast after two years of outstanding contribution to the set up and growth of KIPAC, and we are seeking her replacement. Christine Aguilar has also joined the group. The current KIPAC membership can be found at <http://www-group.slac.stanford.edu/kipac/>.

KIPAC has become well-integrated into the SLAC-campus physics community. Joint astrophysics seminars occur alternating between campus and SLAC and there is good coordination with other lecture series in theoretical physics. There are twice weekly morning teas where recent papers are discussed and short research presentations are made by group members. Attendance at these meetings typically varies between 40 and 70. KIPAC has achieved one of its goals of providing an open scientific forum connecting SLAC with campus. These also alternate between campus and SLAC. Looking further afield, further outreach has occurred into the Bay area astrophysics community (extending as far as UC Davis). A major event was the hosting of the 22<sup>nd</sup> Symposium on Relativistic Astrophysics held at Stanford Dec. 13-17, 2004. This had well over 300 participants and was regarded as a very successful meeting.

Administratively, KIPAC has grown within the SLAC reorganization, taking on responsibility for the science phase of GLAST. From the SLAC perspective, it is now organized into seven departments – Computing, GLAST-ISOC, GLAST-Physics, KIPAC-Physics, LSST and SNAP. These departments are being brought under a common administration and involve over 150 people at present.

Progress has continued on the construction of the Fred Kavli Building which should be ready for occupancy in February 2006. In addition, the new Physics-Astrophysics Building on campus should be completed in summer 2006.

The scientific program at KIPAC is now quite diverse. In addition to the work directly related to projects, reported below, over 60 scientific papers, including conference proceedings, have been written by KIPAC members over the past year, and a comparable number of talks has been delivered. Major research concentrations include, in no order:

- cosmological studies of clusters of galaxies, combining observations made using X-ray, optical and radio telescopes

- projects in weak and strong gravitational lensing as well as microlensing, investigations of particle dark matter
- participation in the Sloan Digital Sky Survey, particularly in the discovery and analysis of supernovae
- participation in radio observations of the sources likely to be studied by GLAST
- modeling of pulsars, especially the recently discovered double pulsar
- modeling of gamma ray bursts
- numerical simulations of the growth of structure in the early universe
- analysis of microwave background observations
- calculations of atomic transitions for use in X-ray astronomy
- new ideas in black hole astrophysics

KIPAC look forwards to further growth over the coming year.

### **GLAST**

The Gamma-ray Large Area Space Telescope, GLAST, is a satellite-based experiment under construction to measure the cosmic gamma-ray flux in the energy range 20 MeV to >300 GeV, with supporting measurements for gamma-ray burst transients in the energy range 10 keV-25 MeV. With a sensitivity that is more than a factor 30 greater than that of the EGRET detector on GRO, GLAST will open a new and important window on a wide variety of high-energy phenomena, including super-massive black holes and active galactic nuclei, gamma-ray bursts, supernova remnants and cosmic ray acceleration, and searches for new phenomena such as supersymmetric dark matter annihilations, Lorentz invariance violations, and big-bang particle relics. The launch is scheduled for the fall of 2007.

The Large Area Telescope (LAT) is the primary instrument on GLAST. The LAT collaboration is a novel teaming of particle physicists and high energy astrophysicists. The LAT Principal Investigator (PI) and Spokesperson is Professor Peter Michelson (Stanford and SLAC). The LAT is being developed in a partnership between NASA and the DOE, with substantial contributions from Italy, Japan, France, and Sweden. The LAT project is managed at SLAC.

There was one full collaboration meeting in FY05, at SLAC in August. Continuing the tradition from past years, accompanying the meeting was a full-day science symposium devoted to a specific topic (The Galactic Center Region), providing additional interactions with the broader science community. The Senior Scientist Advisory Committee (SSAC) meets regularly, approximately every six weeks, by teleconference and in person. There is also a monthly "all-hands" meeting for team members resident at, or visiting, SLAC. Science preparation has been proceeding within the context of parallel topical groups, which have been meeting with varying frequency, and an update to that organization was discussed at the recent collaboration meeting.

The first data challenge (DC1) was held in FY04, providing the first end-to-end testing of the instrument simulation, reconstruction, and science analysis tools. Based in part on the lessons



from DC1, the LAT team is now planning for DC2 in early 2006. Care is being taken to minimize conflicts with the main focus of the team, building and testing the flight hardware.

The key detector elements, Calorimeter, Tracker, and Anticoincidence detector were completed during FY05. Twelve of the sixteen towers were installed in the Grid. The thermal/mechanical equipment (grid, X-LAT plate, and radiators) was completed and delivered to SLAC.

**Other highlights included:**

*System Engineering:* In FY05 the instrument documentation was mostly completed. The attention has been on planning for LAT level testing and preparing for the LAT environmental testing.

*Tracker:* The flight Tracker modules were completed in FY05, a tribute to the hard work at USCS, SLAC and INFN in Italy.

*Calorimeter:* All of the flight Calorimeter modules were delivered from the Naval Research Laboratory.

*Anticoincidence Detector:* The ACD was completed at the Goddard Space Flight Center and delivered to SLAC.

*Electronics, Data Acquisition, and Flight Software:* At least one copy of each of the flight modules for the DAQ system is at SLAC. The critical path for the instrument goes through the delivery of the last Event Processing Unit which will be turned over to Integration and Test (I&T) on December 20, 2007.

*Mechanical Systems:* All flight components have been delivered to the Integration and Test group (I&T). The second grid was prepared for strength testing at an outside testing lab. That work will go on in early FY06.

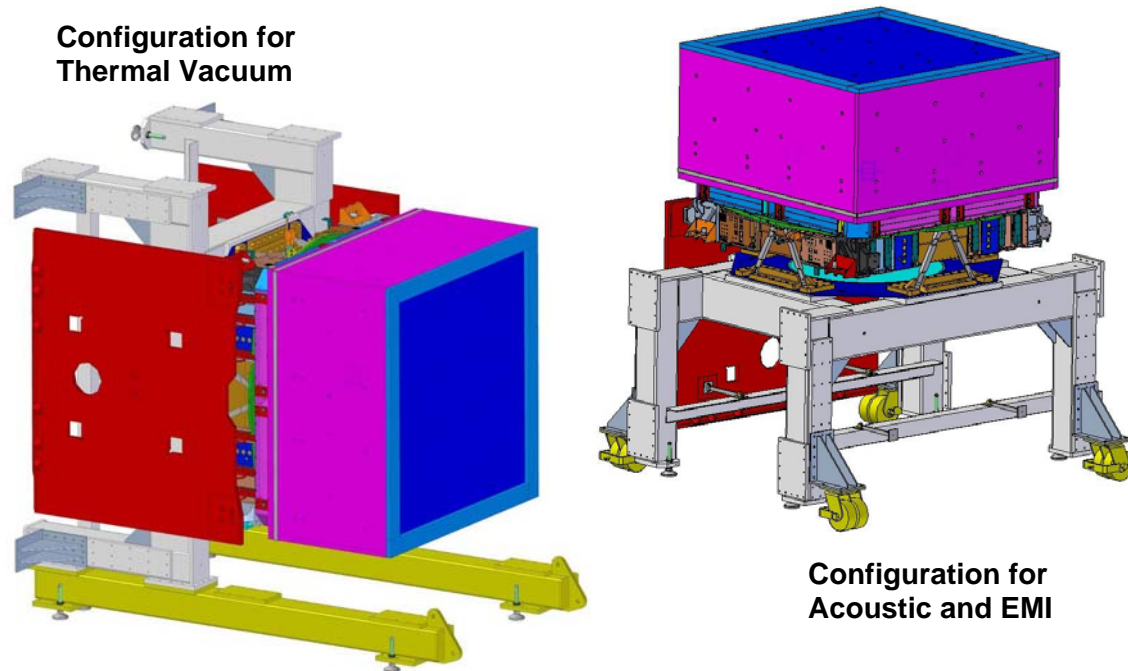
*Integration and Test:* Successfully integrated 12 towers into the grid. Integration and test of the flight hardware is proceeding smoothly. The I&T staff has been preparing the ground test equipment for the environmental test at NRL.



12 towers installed in the grid



Anticoincidence Detector just prior to shipment to SLAC



Ground Support equipment for environmental test at NRL

## LSST

The Large Synoptic Survey Telescope (LSST) is a ground-based dark energy experiment designed to provide strong constraints on the expansion history of the universe via both kinematic measurements (*e.g.* Type 1a supernovae, baryon oscillations), and measurements of the growth of structure with cosmic time using weak gravitational lensing. The design involves a wide-field, large-aperture telescope that produces a faint survey of the optical sky in five color bands every few days.

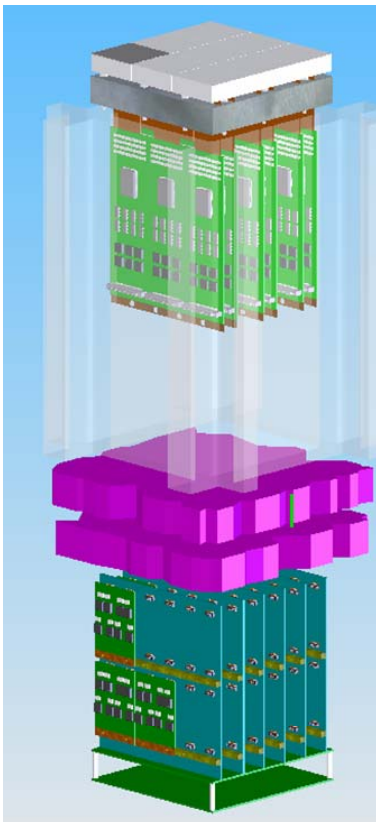
A collaboration led by SLAC has been formed to develop the camera for the LSST. This will be the largest digital camera ever constructed, with a focal plane covering 3.2 billion pixels, and measuring 60 cm in diameter. The camera also includes three large refractive lenses and an array of five optical filters mounted on a carousel. The mechanical tolerances on the system are tight, owing to a very fast optical beam (f1.2). SLAC personnel occupy several leadership positions within the project. Steven Kahn is the Deputy Director of the LSST project overall, and is the Lead Scientist for the Camera. Kirk Gilmore is the Camera Project Manager, and William Althouse is the Project Systems Engineer. Roger Blandford, the Director of KIPAC, is a member of the LSST Corporation Board of Directors.

In the past year, substantial progress has been made on the camera development. We now have a detailed strawman design for a prototype CCD sensor, and have let contracts to a select group of sensor vendors to study sensor fabrication issues. Work has begun on the front-end and back-end electronics as well, which will be tightly integrated within the camera body. At SLAC, attention has focused on the alignment of the overall focal plane and *in situ* monitoring schemes that can maintain this alignment as the telescope is operating. A laboratory in the Collider

Experiment Hall is now undergoing renovation to enable early prototyping of these various concepts. SLAC is also heavily involved in the mechanical design of the camera body, the thermal and vacuum control systems, and the design of the data acquisition system. Significant progress has been made in all of these areas.

In terms of scientific investigations, a group at SLAC has been heavily involved in performing simulations of the experiment, especially with regard to investigating the possible systematics due to the atmosphere for weak lensing investigations. An atmospheric monitoring campaign was performed using the Gemini South and SOAR telescopes on Cerro Pachon in Chile in May 2005. The results of that campaign are currently being advertised.

Two camera face-to-face meetings were held at SLAC in FY05, one in October 2004, and the other in June 2005. The laboratory also hosted a project-wide Science Requirements meeting for LSST.



Schematic of a “raft” of 9 CCD sensors for LSST with their associated front-end and back-end boards. The faint white shading indicates the integrating structure which supports the rafts.

## **SNAP**

The Supernova Acceleration Probe (SNAP) is a proposal for a space-based wide-field telescope designed to study of the physics of dark energy using calibrated Type 1a supernovae as standard candles. The mission will also enable weak lensing studies with high precision over moderate angular scales. The SNAP design includes a large focal plane tiled with both visible-light and infrared-imaging sensors, as well as a visible/IR spectrograph suitable for following up detected supernovae.

SLAC/Stanford proposed to join the SNAP collaboration in August of 2003. That application was formally approved in March 2004. Within the collaboration, SLAC is responsible for the design and development of the SNAP Instrument Control Unit (ICU), which performs electronic supervision of the entire SNAP instrument, executes the science mission, manages the operation of instrument mechanisms and thermal controls, and controls the flow of commands and data between the focal plane electronics, mass memory and spacecraft. SLAC is also responsible for the focal plane guiding system that will allow the SNAP observatory to track its science fields to an accuracy of better than 20 milliarcseconds.

During the past year, a new technical approach was proposed for the guiding system and adopted as the baseline. This system uses four asynchronously operated imaging devices, controlled by a central processor, to collect sufficient photons to generate an appropriate error signal for the spacecraft pointing system. By operating the sensors asynchronously, the integration time for each device can be tailored to the number and brightness of stars available with the field of view. This approach was simulated and compared with worst-case star field density and shown to meet the accuracy requirements. A guiding system prototype is now under development and will be used to deliver flight-like pointing error signals to a tracking test-bed program now under consideration.

SLAC scientists have also played a significant role in formulating the detailed scientific program for SNAP, especially with regard to strong lensing investigations. The SNAP database should reveal a large number of new strong lenses. Measurements of the properties of these lensed images will yield a number of interesting constraints on cosmological models.

## **Other Activities**

### **NuSTAR**

The development of the NuSTAR Small Explorer mission is now ongoing at SLAC. NuSTAR is a hard X-ray focusing mission, led by Caltech, that was selected for an extended Phase A study during the past year. Work is proceeding on further mission definition and risk reduction with an initial confirmation for flight by NASA scheduled for February of 2006. During the past year, SLAC members of the NuSTAR collaboration worked on instrument definition and design. SLAC also hosted a science team meeting for the collaboration.

## PoGO

The PoGO experiment, a balloon-borne hard X-ray polarization observer, has successfully completed the second prototype instrument made of the flight phototubes. The prototype has been tested successfully at KEK Photon Factory, verifying its sensitivity down to 30 keV. The collaboration is now producing flight components with funding awarded in Sweden, in Japan and at Stanford University.



The first PoGO flight phoswich unit installed at the center of the acrylic mechanical structure.

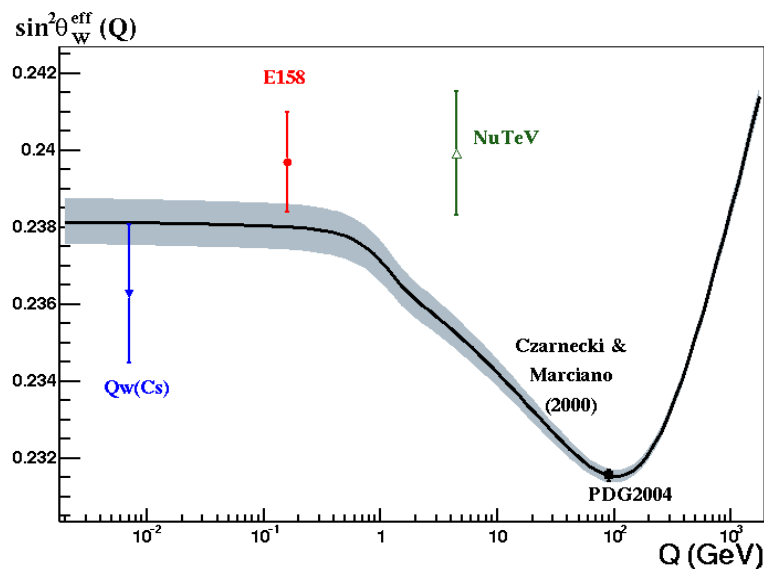
### 4. FY05 Progress: Experiment E158: A Precision Measurement of the Weak Mixing Angle in Møller Scattering by Krishna Kumar and Mike Woods

In September 2003, final data were collected for SLAC experiment E158,<sup>1</sup> which seeks to determine the weak neutral current coupling of electrons to high precision at low  $Q^2$ . This is achieved by measuring the left-right parity violating asymmetry in the Møller scattering of 45 GeV and 48 GeV longitudinally polarized electrons from atomic electrons in a liquid hydrogen target. The final result for the E158 experiment has been published in *Phys. Rev. Lett.* **95**, 081601, 2005. The *PRL* publication was accompanied with a SLAC press release in June 2005, and related press articles appeared on the result in *Nature*, the *CERN Courier* and *Physics Today*. The experiment had 60 collaborators from 10 institutions in the U.S. and France and generated 8 Ph.D. theses. An E158 webpage for the public and the press is <http://www-group.slac.stanford.edu/com/e158/>.

The primary physics goal for E158 is to determine the electron's weak charge and the weak mixing angle parameter,  $\sin^2\theta_W^{\text{eff}}$ , at low momentum transfer,  $Q$ . E158 measures the weak mixing angle parameter to be  $0.2397 \pm 0.0014$ . This is 4% greater than the result at high energy obtained from the SLD and LEP experiments, demonstrating the "running" of the weak mixing

<sup>1</sup> SLAC E158 proposal, K. Kumar spokesman and contact person, (1997)  
([www.slac.stanford.edu/exp/e158/documents/proposal.ps.gz](http://www.slac.stanford.edu/exp/e158/documents/proposal.ps.gz))

angle with a significance of 6.2 standard deviations. The electron's weak charge is approximately given by  $Q_W(e) = -(1-4\sin^2\theta_W^{\text{eff}})$ . E158 finds  $Q_W(e) = -0.041 \pm 0.006$ , approximately  $\frac{1}{2}$  the value expected if there were no running. The demonstration that the electron's weak charge varies with distance, a trait called running, complements previous experiments that established running in electromagnetism and the strong force. E158's measurement probes TeV-scale physics and sets limits on contact interactions, with a 95% CL lower limit for the compositeness scale  $\Lambda_{LL} \sim 10$  TeV. It also sets limits on additional  $Z'$  bosons--for example, the 95% CL lower limit for an SO(10)  $Z'$  is  $\sim 900$  GeV.



s

Figure 1: The  $Q^2$ -dependence of the Weak Mixing Angle: Theory and Experiment. The black curve is the prediction from Czarnecki and Marciano, with the theoretical uncertainty indicated by the shaded region. The E158 result demonstrates the running of the weak mixing angle with a significance of  $6.2\sigma$  from low  $Q^2$  to the  $Z$ -pole.

## 5. FY2005 Self-Appraisal for DOE: ILC Department and NLCTA

### 5. 1. The ILC Department at SLAC

At the end of FY2004, the International Technology Recommendation Panel (ITRP), appointed by the International Committee on Future Accelerators (ICFA) International Linear Collider Steering Committee (ILCSC), recommended that cold technology be pursued as the technology for the main linac of the International Linear Collider (ILC). SLAC has been committed to playing a leadership role in the linear collider independently of the choice of rf technology and, after the technology decision, the SLAC linear collider group began to study ways in which it could contribute to the ILC design.

The SLAC ILC group is internationally recognized for its expertise. SLAC has been a leader in linear collider development for over 25 years. SLAC built and operated the first linear collider,

the SLC, and used that experience to produce an integrated, comprehensive design for a linear collider based on warm rf technology for the accelerating structures. SLAC has accelerator physics expertise in *all* subsystems of the collider from the sources to the Interaction Regions (IR) and this expertise has been refocused on developing a design based on cold rf technology.

With the adoption of the superconducting rf technology for the ILC, SLAC continues to be a major contributor to linear collider development through the broad expertise and unique test facilities. Over the years, significant R&D has been performed on all of the subsystems of the ‘warm’ X-band design and both the ‘warm’ design and ILC design share many common features. Less than 25% of the cost of the superconducting design is in the superconducting cavities or cryomodules – the rest of the collider is based on normal-conducting technology similar to that which SLAC has studied extensively. SLAC is applying the major advances that were made for the X-band design to the ILC.

Thus, during FY2005, the SLAC linear collider R&D program was redirected towards many of the most important issues in the ILC design. The activities in or supported by the SLAC ILC program address 14 of the 15 critical R2 items identified in the ILC Technical Review Committee (TRC) report from 2003 – many of these issues are important to resolve as part of an international Reference Design Report (RDR). In addition, during early FY2005, at the ILC-Americas Meeting at SLAC and the ILC Collaboration Meeting at KEK, elements of the linear collider technology were identified as requiring additional R&D or optimization. SLAC is working on many of these issues including modulator improvements, alternate klystron designs, and rf power distribution options.

In addition, the SLAC accelerator complex provides facilities capable of supporting a wide range of ILC R&D. An L-band rf test facility is being developed in End Station B as part of the NLC Test Accelerator (NLCTA) to benefit from the existing infrastructure. This facility will provide long-term testing of klystrons and modulators, and rf power for coupler and normal-conducting structure testing. The NLCTA beam and beam-line support full power structure testing with beam. Modifications are being made to produce an ILC-type bunch for instrumentation development. End Station A is being reconfigured as a test beam facility for experiments with collimators, IR instrumentation, and detector components. A mockup of key aspects of the IR is being planned for the future. This will be the only experimental area with access to multi-GeV high quality electron beams. Prototype vacuum chambers utilizing various electron cloud suppression techniques will be tested in PEP-II.

The rest of this section will describe the ILC Department organization, participation in the ILC GDE, participation in Reviews and Conferences, and Department safety issues. In the following sections, the close-out of the X-band R&D program, the L-band R&D program, and the Accelerator Design programs will be described. Following this will be short sections describing the operation of the NLC Test Accelerator (NLCTA) which the ILC Department operates to support advanced accelerator R&D as well as ILC R&D and participation in the LHC Accelerator Research Program (LARP) in the form of advanced beam collimators which were spun off from the NLC R&D program.



### *5.1. a. SLAC ILC Department Organization*

Early in FY2005, SLAC renamed its linear collider program the ILC Department at SLAC, and SLAC Director Jonathan Dorfan appointed Tor Raubenheimer to lead the SLAC ILC effort. The group was organized with two deputies, Nan Phinney and Thomas Himel, and four area leaders, John Cornuelle for Mechanical Systems, Ray Larsen for Electrical Systems, Nan Phinney (acting) for Accelerator Design and Tom Markiewicz for Experiments and Prototypes. Following a subsequent laboratory reorganization in mid-2005, the ILC Department now reports directly to the director for Particle and Particle Astrophysics, Persis Drell.

### *5.1. b. ILC GDE Activities*

The ILC Global Design Effort (GDE), which reports to the International Linear Collider Steering Committee of the International Committee for Future Accelerators, was formed following the August decision on cold technology. The director, Barry Barish, formerly of California Institute of Technology and the chair of the International Technology Recommendation Panel, was appointed in March 2005. Shortly thereafter he announced the appointment of the regional directors who are Gerry Dugan of Cornell University as Director for the Americas, Brian Foster of Oxford University as Director for Europe, and Fumihiko Takasaki of KEK as Director for Asia. The GDE Executive Committee was rounded out with the appointment of three accelerator physicists, Tor Raubenheimer (SLAC) for the Americas, Nick Walker (DESY) for Europe, and Kaoru Yokoya (KEK) for Asia.

To date, the GDE comprises some 49 individuals, about 20 FTEs, and is supported by the governments of the three regions; five of the members are from the SLAC ILC Department: Chris Adolphsen, Tom Himel, Tom Markiewicz, Nan Phinney, and Tor Raubenheimer. In addition, Ewan Paterson of SLAC has been asked to organize the Configuration Control and Cost Management. This group or groups will hold the collider configuration and cost estimates and will manage changes to the collider design and R&D program. A detailed charge and budget for this group (or groups) will be resolved in FY2006.

The 1<sup>st</sup> ILC Workshop was held at KEK in Tsukuba, Japan in November 2004. The 2<sup>nd</sup> ILC Workshop was held in Snowmass, CO in August 2005 in conjunction with the ILC Detector groups meeting. The latter was a two-week-long meeting of the working groups, together with a number of newly formed corresponding global groups, with many SLAC ILC members as conveners of both global and working groups. The SLAC ILC group played a major role in formulating the shape and content of both of these ILC Workshops. In both cases, SLAC ILC Department members made significant contributions to the overall meeting structure and to leadership of working and global groups.

During the Snowmass workshop, the first week was devoted to reports from the working groups while the second week was more informal with many ad hoc sessions. The goal of the second week was to select the basic machine parameters and a set of viable alternatives where research efforts would be concentrated so that a baseline parameter set could be decided by the end of CY2005 and a reference design report might be prepared by the end of CY2006. The workshop

was very effective and great progress was made. Summary reports from the working and global groups and responses to a list prepared by Tom Himel of SLAC of about 40 items that required decisions go a long way to describing the baseline design. The structure for preparing the reference design report has not yet been formulated, but should be decided early in CY2006 to allow document completion by the end of the year.

### *5.1. c. Reviews and Meetings*

The ILC group has participated actively in the national and international community through reviews and meeting participation.

In October 2004, SLAC hosted the ILC-Americas meeting. This meeting was organized to prepare for the 1<sup>st</sup> ILC Workshop which was held in November 2005 at KEK in Japan.

In November 2004, the first Linear Collider working group meetings were held at KEK in Tsukuba, Japan. These followed the format of the working groups established in the longstanding SLAC-KEK US-Japan collaboration. This structure proved to be effective for the international ILC organization. The Tsukuba meeting set the framework for future collaboration, but was held before the organization of the GDE directorate.

In January 2005, SLAC hosted the Machine-Detector Interface (MDI) workshop in combination with an ATF-2 workshop. In addition, SLAC ILC Department members were among the conveners of the Daresbury positron workshop in April, and of the Beam Delivery and Interaction Region (BDIR) workshop at Royal Holloway University of London in June.

In March 2005, SLAC hosted the Linear Collider Workshop (LCWS05) at which Barry Barish's appointment to the GDE was announced. SLAC ILC Department members helped organize and convene a number of the technical sessions.

PAC 2005, the biennial international particle accelerator conference, was held in Knoxville, TN in May 2005. Over two dozen papers representing the work of about 40 ILC staff members were presented. In addition, ILC staff members were active in the organization and program committees for the conference.

The SLAC ILC group also played a major role in formulating the shape and content of the two ILC Workshops, the first at KEK in November 2004 and the second at Snowmass in August 2005. In both cases, SLAC ILC Department members made significant contributions to the overall meeting structure and to leadership of working and global groups.

SLAC ILC members also participated in the Nuclear Science Symposium, the International Conference on Magnet Technology, the International Linear Collider Industrial Forums, the 12<sup>th</sup> International Workshop on rf Superconductivity and many other conferences and workshops where they presented papers and shared plans with colleagues without actual linear collider experience and without the depth and breadth of research that backs the SLAC ILC team. Other workshops held at SLAC include an ongoing series on ATCA technology as a possible basis for standardization of ILC electronics.

#### *5.1. d. Collaborations*

The ILC Department has a long history of collaboration with KEK and within the US with LLNL, LBNL, FNAL and BNL. Additional collaborations are ongoing with Queen Mary University of London, Oxford University, the Rutherford Appleton Laboratory, the Daresbury Laboratory and DES, and with the French laboratories CEA Saclay and CEA Orsay.

The Superconducting Module Test Facility (SMTF) is a newly proposed international collaborative facility at Fermilab that would develop a superconducting rf center of excellence in support of ILC. A proposal and more detailed collaboration plans will be available in FY2006. SLAC is an active participant, with Tor Raubenheimer and Chris Adolphsen representing SLAC on the Institutional Board and Chris Adolphsen also on the Technical Board. In FY2005, SLAC fabricated elements of the cryogenic system, started building solid-state switches for Fermilab modulators, and offered use of its electron beam welding facility.

Collaboration at DESY includes work on benchmarking reliability and availability codes and working on the Tesla Test Facility (TTF). The SLAC ILC Department installed rf transverse deflecting structures for monitoring the longitudinal profile measurements. This diagnostic has a resolution of 10 microns and has become indispensable for operation of the FEL. Members of the ILC Department also used concepts and technology developed for the X-band program to measure the higher-order mode (HOM) signals from the TESLA cavities. Such HOM detectors may prove important to align the cavities in the ILC. At DESY's request, the ILC group is now building a set of 40 of these detectors for installation at the TTF. Finally, at the April 2005 TESLA Technology Collaboration (TTC) Board meeting SLAC formally joined the TTC and MOUs are being exchanged.

The ILC Department has a long-standing collaboration with KEK and has worked on X-band rf components and the ATF damping ring. Activities in FY2005 include construction and installation of a replacement extraction kicker that will support a 300-ns-long extraction pulse, development of an ultrafast kicker for testing at ATF, and design of the ATF-2, which would prototype the ILC beam delivery system utilizing the extremely low emittance beam from the ATF damping ring. During FY2005, the SLAC group has worked on three main projects with KEK and has received roughly 500k\$ of US-Japan funding. The ILC Department has had a physical presence at KEK working on the ATF damping ring that averaged roughly 1 FTE. An MOU with KEK on the ATF which covers operation of the ATF and the international construction of the ATF-2 is being finalized. Ewan Paterson of SLAC will chair the ATF International Collaboration Board and Marc Ross, Tor Raubenheimer, and Andrei Seryi of SLAC will be members of the ATF Technical Board.

The End Station A Test Facility, which is being developed to test prototypes of IR beam diagnostics and IR design concepts using the high energy SLAC beam, is a collaboration between SLAC and US and UK universities. Most of the specific experimental proposals have at least one spokesperson from a university in either the UK or the US.

The E166 experiment at SLAC is a collaboration of some 9 laboratories and universities with 50 participating scientists. The experiment will demonstrate production of polarized positrons using an undulator. A second data-taking run has been completed and the data are being evaluated. The success of E166 will provide a strong basis for the undulator-based production of positrons at the ILC.

### *5.1. e. Safety*

At SLAC and in the ILC Department, concern for safety is an integral part of our culture. Following the early FY2005 electrical accident that halted lab operations for several months, all personnel received electrical hazard training, reviewed and updated their JHAMs, and completed all other safety courses recommended by their supervisors. In addition, the NLCTA, a major test facility operated under the ILC Program, had to completely requalify its safe operation procedures to allow start-up. This process was completed professionally and efficiently, requiring no revisions or alterations to the plans. The laboratory chose to use the procedures developed at the NLCTA as a model for other facilities at SLAC.

Additionally, during the site-wide safety stand-down, ILC's Conventional Facilities engineers contributed significantly to the lab-wide effort implementing risk mitigation measures. Arc flash calculations, in accordance with NFPA 70 were performed for every electrical 480 V or higher breaker panel by a team including an ILC power engineer. As a member of the Restart Committee, another ILC engineer was tasked with Seismic Safety inspection of the major test facilities and participated on the Earthquake Safety Citizens Committee. Another was involved with various aspects of environmental safety issues site-wide.

## **5. 2. X-band rf R&D**

With the ITRP decision of the superconducting technology for the ILC, the SLAC X-band program was put on hold. The X-band program consisted of three R&D programs: high gradient structures that were detuned to reduce the long-range wakefields, efficient rf pulse compression, and high power rf sources. Most of the R&D was performed at the NLC Test Accelerator (NLCTA) which is a 350 MeV linac powered with 4 rf stations: three conventional rf stations that were constructed in the late 1990s and one high power rf station that was completed in FY2004 and is referred to as the '8-pack.'

At the time of the ITRP decision, the NLCTA was being modified to be used for a laser acceleration experiment and commitments had been made to CERN to test accelerator structures and KEK to study the wakefield characteristics of the X-band structures. In addition, a collaboration involving Yale University and Institute of Applied Physics in Russia was building hardware to test a novel method of pulse compression.

The ILC Department decided to complete all of these programs since they did not require significant resources. In addition, it was decided to maintain the NLCTA as an operating linac which could be used for future advanced accelerator R&D. To this end, the 8-pack modulator, which was contaminated with beryllium, was decommissioned and will be replaced with a newer 2-pack modulator; the 2-pack modulator would not deliver as much power as the 8-pack but it will still accelerate the beams to roughly 300 MeV.

### 5.2.a. Accelerator Structures

After the ITRP technology recommendation was made, the NLC/ILC group chose to continue some of the X-band (11.4 GHz) structure testing in a program to wrap-up the 15-year-long structure development effort, and to provide useful information for future high gradient applications. Despite the long SLAC-wide down period starting in October (the NLCTA was shut down for about six months), most of this program has been completed. The tests in FY2005 included:

- 1) Characterization of structure performance at pulse lengths shorter than the nominal 400 ns value, at which most testing has been done. Two structures were run at 80-90 MV/m with 30-100 ns pulses after having been processed at 95 MV/m for several days with 100 ns pulses.
- 2) Evaluation of an X-band structure built by CERN that contains tungsten irises, which they found afforded higher gradients in their 30 GHz program. So far, this structure has performed no better than the NLC copper structures. At a pulse length of 200 ns, the breakdown rate is 10 per hour at 65 MV/m (the rates for the NLC structures with 400 ns pulses are about 0.1 per hour at 65 MV/m). The CERN structure will continue to be operated for the next few months to measure the breakdown rate at other pulse lengths.
- 3) Vent tests to characterize structure robustness, in particular, structure sensitivity to air exposure, particle contamination and oxidation. In separate tests, a pair of structures was vented to nitrogen, filtered air and unfiltered air. In all cases, the structures then processed to 65 MV after fewer than about 100 breakdowns and achieved a low breakdown rate (0.1 per hour) after a few days of operation indicating a very robust system. As a final test, one of the structures was heated to 200°C and vented to filtered air for an hour. In this case, 60 MV/m was achieved with 400 ns pulses after about 5000 breakdowns before the processing was terminated.
- 4) Wakefield measurements of a pair of damped and detuned NLC accelerator structures. The measurements were made using the ASSET facility at the upstream end of the SLAC Linac. The results showed good agreement with the expected wakefield, which was the remaining performance goal in a program to demonstrate that the structure design meets NLC requirements.

### 5.2.b. Pulse Compression

In early FY2005, two experiments were approved with the multimoded pulse compression system (SLED) at NLCTA (they are funded through non-ILC sources). Both are aimed at improving the compression system efficiency by changing the match conditions into the delay lines during the pulse. For this purpose, one experiment employs solid-state switches, and the other, plasma switches (the latter experiment is a collaboration with Yale University and the Institute of Applied Physics in Russia). Initial tests with low (mW) rf power showed both performed as expected. However, high power tests have been delayed due to failure of the plasma switch pulsed power supply and then by the decommissioning of the modulator for the rf

source because of safety concerns (see below). Currently, the experimenters are waiting for a new modulator to be installed to conduct both experiments.

### *5.2.c. X-band rf Stations*

The 8-Pack: The 8-Pack modulator, together with four X-band 50 MW XL4 klystrons, was the workhorse of the warm structures test program. The system consisted of a single solid state modulator powering all four klystrons to send rf power into the SLED system. The modulator was the first successful design of a 500 kV unit using solid state. The modulator PLC programmable controller ran all the auxiliary DC power and interlocks for the klystron complex while a low-level rf (LLRF) system provided experimental control of phasing and power to the SLED. All experimental data were collected 24/7 in the control room. A 100 kW DC power supply provided the required 2.2 kV to the modulator cells. After completion of the program, the 8-Pack modulator was decommissioned, but the X-band rf section is to be kept intact for future experiments. In late FY05 the modulator was taken apart and the parts put into storage for possible future use on small modulators or subboosters in the Linac and experimental areas. The materials needed special handling because arcing of the modulator high voltage contacts had left deposits of beryllium dust. In cooperation with ES&H a successful mitigation and monitoring program was put into place during decommissioning.

The Two-Pack: The 2-Pack modulator was designed as a second generation solid-state modulator for driving two 75 MW X-band klystrons. It has many improvements over the 8-Pack design including higher voltage IGBTs for fewer cells, oil cooling instead of water cooling, lower cost cast-cell housings, and specially designed connectors that eliminate the arcing problem. After the technology recommendation, it was earmarked to replace the 8-Pack modulator, where it will power two 50 MW klystrons to accelerate beam to roughly 300 MeV. During early FY2005, the 2-Pack modulator was tested into a water load in the Power Conversion Lab and found to be heat limited at 60 Hz. New heat sinks were designed and installed to meet the 120 Hz requirement. The system is now reassembled and ready for final power testing before moving to NLCTA.

## **5.3. L-band rf**

The SLAC ILC group is in a unique position to aid the development of the rf power sources for the ILC. SLAC has a world-renowned klystron group and the power conversion group developed novel high power switching technologies for modulators for the X-band design. The expertise of both of these groups can be directly applied to the ILC. In addition, there is a clear need for an optimization of the rf distribution system with the many different components that are presently required. To begin this program, in FY2005, SLAC started by creating an L-band rf test station in End Station B next to the NLCTA. This station will be used to gain experience with the L-band rf system and to supply power for structure and coupler testing programs. Additional R&D programs are being carried out on novel modulator and klystron designs. Components from the successful completion of these programs will be used to build a second 10 MW L-band station in ESB in FY2006 or FY2007. Additional stations are expected to be constructed in the future.

### 5.3.a. Modulator

At the time of the technology recommendation, development of a Marx-type modulator for the 500-kV X-band klystrons was redirected toward producing a long pulse, 120-kV unit as an alternative to the ILC baseline pulse-transformer design. The goals were to reduce the size, weight and cost of the modulator, to improve its efficiency, and to eliminate the pulse transformer which is a source of stray fields in the beam enclosure. The all-solid-state modular design that resulted uses IGBTs and a unique droop-compensation scheme of vernier cells to flatten the pulse. Simulations have shown the design to be feasible and a full-scale prototype will be built in FY2006. Presently the main switching circuits have been successfully prototyped and tested into a resistive load and the full cell design is nearing completion. A short stack of six cells will be tested early in FY2006 before the full 16-cell modulator is built.

At the ILC Snowmass meeting in August, the SLAC Marx Modulator was chosen as the Alternate Baseline Design. One reason was that its modular design lends itself to high volume circuit board assembly techniques that can be performed by commodity manufacturing houses. As a result, significant cost savings (~ 40%) are expected over the baseline design. During FY2006, detailed cost modeling and industrialization plans will continue.

In FY2005, the SLAC modulator group also designed and began construction of IGBT switch stacks for two new pulse-transformer modulators being constructed at FNAL for the Superconducting Module Test Facility (SMTF). These switches are more compact and have a higher current carrying capability than the IGBTs previously used for such modulators.

### 5.3.b. Klystrons

At the beginning of FY2005, the focus of research by the Klystron Department was undergoing a major change as a result of the ITRP recommendation. For the previous 12 years, the klystron R&D group was fully engaged in the design and testing of X-band klystrons. After the recommendation, it was decided to complete the 75-MW PPM klystron program by 'mothballing' the project, testing the last tube, and autopsying prior tubes. However the accident at SLAC in October 2004 resulted in the shutdown of the Klystron Department's testing and fabrication facilities. Only by the end of August 2005 was it possible to run the test facilities again, so little of testing program has been completed. However, the L-band klystron requirements and program for ILC were reviewed during the past year.

The existing prototypes for ILC rf power sources consist of three different vendor-produced Multiple Beam Klystrons (MBKs). The Klystron Department has been investigating the merits of a new class of klystrons known as Sheet Beam Klystrons (SBKs). Of particular note was the successful testing of a W-band (95 GHz) SBK during September 2005. The device performed exceedingly well when compared to the 3D simulations. Other SBK devices, which may find applications, are at L-band, as an ILC power source, and Ka-band, as a power source for the CERN CLIC accelerator efforts. Both of these devices were investigated during the past year. Unfortunately, reduced funding for the SLAC ILC program could not support the SBK R&D in FY2006.

Substantial progress was made in the ability to simulate the 3D behavior of klystrons. Structural, magnetic, electrical, beam-interaction, and particle-in-cell codes were improved along with the ability to operate such codes on multiple CPU platforms. Other ILC-related developments during the year included testing of the CPI MBK klystron at CPI for DESY, work on an SBIR with DTI Technologies on a modulator for the ILC klystrons (to be delivered in FY2006), and measurement of the perveance of a Thales 2104U klystron that was acquired for the SLAC L-band source.

### *5.3.c. Rf Distribution*

To distribute the power from a klystron to the cavities in the ILC linacs, the baseline proposal is to have a series of tap-offs along a waveguide that runs parallel to the beam line. There would be a circulator in each cavity feed line followed by a tuner (three-stub or E-H type) to allow control of the cavity phase and  $Q_{\text{ext}}$ . Currently DESY uses off-the-shelf components for the distribution system, which are not necessarily optimized for this application.

The circulator is the largest cost component at about 25% of the rf distribution cost. In FY2005, several alternative distribution schemes were studied that eliminate the circulators but require more precise cavity-to-cavity phasing. The simplest of these schemes feeds the cavities in pairs via 3 dB hybrids. A concern is that in the event of rf breakdown in a coupler or cavity, some fraction of the reflected power will propagate to the other cavities. How this additional power would affect cavity performance has not yet been measured.

### *5.3.d. Coupler*

The power coupler designs for the ILC superconducting cavities are complex devices due to the required cleanliness, high power rf operation, temperature gradients (300 K to 2 K), vacuum isolation (with two rf windows) and tunability requirements. The current ILC baseline design (TTF3) works reasonably well, but the couplers can take up to 200 hours to rf process. To understand what limits the processing, Brian Rusnak from LLNL, in collaboration with SLAC, has been examining the coupler design and its performance. In FY2005, Rusnak showed that multipacting will likely occur in the coupler bellows, which may cause significant outgassing and slow processing. To explore this and other effects, a set of tests has been planned to power various coupler parts including sections with and without bellows, and sections with and without windows. The parts for these tests will be acquired in FY2006 and will be powered using the L-band source being constructed in the End Station B (see Section 5.3.f).

The High Power rf Group at SLAC is considering a fundamental change to the coupler design. Instead of using a coaxial waveguide to transmit the power, an overmoded dielectric coaxial waveguide operating at the  $TE_{01}$  mode would be used. In this case, all the fields would be parallel to the surface, eliminating multipacting and processing issues. This should result in a highly reliable coupler. Furthermore, the use of the  $TE_{01}$  mode, which has no axial currents associated with it, allows the waveguide to be divided into sections that do not touch mechanically. Here, the rf travels in the gap between the sections with virtually no loss. This may prove advantageous for isolating different sections at different temperatures. To date, a  $TE_{01}$  mode launcher for such a transmission system has been designed.



### 5.3.e. L-band Normal-conducting Accelerator Structures

After the technology recommendation was made, the structure group turned its attention from X-band structures to the normal-conducting cavities that are required for the ILC positron source. They have developed an improved design for the positron accelerator that includes both standing wave (SW) and traveling wave (TW) sections. In particular, three types of accelerator structures are proposed:

- 1) 11-cell SW structure. This is a simple  $\pi$  mode SW structure with 11 cells for the high gradient (15 MV/m) positron capture structure. Compared with the baseline design, its advantages are more effective cooling, higher shunt impedance with larger aperture (60 mm), lower rf pulse heating, apparent simplicity and cost saving. The mode and amplitude stability under various cooling conditions for this structure have been theoretically verified.
- 2) 4.3 m  $3\pi/4$  mode TW structure. The parameter 'phase advance per cell' was used to optimize the design of this large aperture, constant gradient, TW structure. The advantages of this design are lower pulse heating, easy installation for long solenoids and no rf reflected power (no circulators).
- 3) 2.2 m  $3\pi/4$  mode TW structure. In order to insert quadrupole magnet triplets in the downstream half of the positron beam line, the 4.3 m TW structures would be divided into two  $\sim$  2.2 m sections and installed with the proper drift space.

The most challenging of these designs is the SW cavity due its relatively high gradient. A prototype is being built, although with only 5 cells to match the near-term power source capability (5 MW) at NLCTA. The mechanical design for this cavity is complete and its fabrication is under way. A high-power test of the cavity is scheduled early in FY2006.

### 5.3.f. L-band Test Station

SLAC has much experience in developing and operating rf power sources, and is quickly becoming the US R&D leader in this area for the ILC. To gain experience with L-band sources and to provide power for warm rf component tests planned in FY2006, construction of an L-band rf station at NLCTA was started in FY2005. For this purpose, a 120 kV converter-style modulator was borrowed from SNS, and an SDI-legacy 5 MW klystron was purchased from Titan (an order for a standard, but more expensive, 5 MW tube was also placed in FY2005). In addition to gaining long-pulse, low-frequency rf operational experience with this system, the SNS modulator will be evaluated for its application in the ILC. It is likely to be more efficient and less expensive than the ILC baseline design, but may be less reliable.

The L-band test stand will provide power to two experimental test areas. One will be used to process coupler components (see Section 5.3d), and the other will be located in the NLCTA beam enclosure to test a prototype positron capture cavity (see S- level rf system is complete and most of the components have been built. The first modulator test into a load is planned in November 2005, and first operation of the klystron is expected in early CY2006.

#### **5.4. ILC Accelerator Design and R&D**

SLAC has more than 20 years of experience with the design of a linear collider and is well positioned to play a leading role in the design of essentially all components of the machine except the cryomodules and cryogenics. The ILC group is actively developing designs for the electron and positron sources, the damping rings, the bunch compressors, the beam delivery and machine-detector interface. In the main linacs, in addition to work on the L-band rf power sources described elsewhere, the effort includes optics and simulations and superconducting quadrupole measurements. The availability simulation developed for the US Technology Options study has been expanded and used as a tool to study various configuration options. SLAC is also involved in developing diagnostics, controls and high-availability hardware. The conventional facilities group is actively collaborating with FNAL to develop site criteria and US candidate sites.

##### *5.4.a. Electron Source*

SLAC now has more than 25 years developing and operating polarized electron sources and more than ten years experience with the polarized electron source developed for the SLC. The baseline design for the ILC adopted at Snowmass 2005 was based on the SLC source. Such an electron source will fulfill the ILC requirements in terms of bunch charge, but a laser system with the required wavelength of 780 nm +/- 20 nm that can generate the required pulse train is challenging and a feasibility demonstration is needed. To support this work, the SLAC Injector Test Facility is currently being upgraded, and experimental R&D towards such a laser system will begin in FY2006.

SLAC continues to have an active program on polarized photocathode research. This program resulted in cathodes capable of routinely delivering polarization well over 90% for the E158 experiment. The present program at the Cathode Test Laboratory is focused on reoptimizing the cathode parameters for the ILC bunch train format and on further improvements in available quantum efficiency and polarization. An additional physicist was hired in FY2005 to augment this effort.

A polarized rf gun would be beneficial for the overall injector design, particularly for simplification of the bunching system, but requires significant R&D. The SLAC group is interested in further development of rf-gun technology and is preparing R&D proposals for future work. The SLAC group is actively forming collaborations nationally and internationally for all aspects of the ILC electron source development.

##### *5.4.b. Positron Source*

SLAC has had a long-standing program of R&D on the design of a conventional positron source and, in FY2005, this was expanded to include design of an undulator-based source. SLAC effort in FY2005 included calculations on positron production in various materials using both electron and photon beams, on positron yield into the ILC damping ring and on heat deposition in the positron capture apparatus due to the drive beam. Additional studies focused on understanding target damage for different beam conditions. SLAC has had a long-term collaboration with

LLNL on target materials and damage studies, which was focused in FY2005 on the actual design of the positron target. This work was able to demonstrate the feasibility of a target for a conventional source, which was not previously believed possible by much of the community.

The SLAC ILC Department was central in the organization and documentation of the Working Group (WG) 3a positron source group at Snowmass 2005. This group agreed for the first time that a conventional solution was viable but chose the undulator-based scheme for the ILC baseline design to provide polarized positrons. SLAC also began several new collaborations on positron sources. The LLNL target effort was expanded to include Liverpool University, UK, which is working on the mechanical design of the positron target under the auspices of the EuroTeV project and a small group from UC Berkeley which is calculating long-term target degradation. A collaboration was formed with Daresbury Laboratory, UK, to look at undulator design and prototyping and a second with ANL on start-to-end simulations of the positron system from upstream of the target to the damping ring. SLAC is working to consolidate these collaborations and other institutions into a single framework for the ILC Baseline Configuration Document (BCD).

SLAC led an international collaboration of approximately 9 institutions and 50 physicists in the E166 experiment whose goal was to demonstrate the feasibility of generating polarized positron beams for the ILC using a helical undulator. The experiment had two one-month runs in FY2005 which were very successful. The data written to disk has low backgrounds and high statistics. Publication of the experimental results is expected soon.

#### *5.4.c. Damping Rings*

The SLAC ILC Department is playing an important role in the design of the Damping Rings (DR) and development of the related technical subsystems, hardware instrumentation, beam dynamics and collective instabilities studies. The ILC requires the damping rings to have extremely small equilibrium emittance, fast damping time and large acceptance, which is a challenging task for the lattice design. In the TESLA design, the damping ring had a large circumference and the international collaboration is investing considerable effort studying alternate configurations with reduced circumference, improved dynamic aperture and reduced space charge effects. In FY2005, SLAC proposed a new damping ring design based on a  $\pi$  cell and noninterleaved sextupoles for increased dynamic aperture at reduced circumference. An energy compressor is under design to reduce the energy spread upstream of the damping ring.

A large number of collaborators worldwide are working on different techniques to develop fast injection-extraction kickers in an effort to shorten the pulse train as much as possible to allow smaller rings. Several pulsers were tried in FY2005 on a kicker at the ATF in KEK. The unit designed by LLNL with SLAC support which drives a bipolar pulse out two deflector plates, looks capable of providing the few ns rise and fall time required for the smaller ring designs. Unfortunately, a reduction in circumference will increase the average current, and cause collective effects to become more severe. SLAC is actively studying several of these effects to evaluate their severity.

For the last few years, SLAC has had a large R&D effort to find possible cures for the electron cloud effect in the positron DR and to mitigate the fast beam ion instability in the electron DR. Studies, in collaboration with CERN, DESY and KEK, include simulations of collective effects, laboratory measurements of the secondary electron yield and installation of test chambers in the PEP-II ring. SLAC is also studying space charge effects, acceptance issues and classical instabilities.

#### *5.4.d. Main linacs*

The SLAC ILC group worked with physicists from LBNL and Cornell University LEPP to develop a design for a two-stage bunch compressor for the ILC. The resulting two-stage design was found to achieve the nominal compression with significantly less emittance growth than the previous single-stage design. In addition, the two-stage compressor can achieve larger compression ratios than are attainable with a single-stage design, providing additional flexibility for the operation of the ILC. The SLAC/LBNL/LEPP design for the two-stage bunch compressor has been accepted as the baseline design for the ILC. Efforts in FY2006 will concentrate on completion and further cost optimization of this design, and on performance comparisons between alternate designs for the ILC bunch compressor.

The SLAC ILC group has taken a leadership role in the study of emittance preservation in the bunch compressor, main linac, and beam delivery system of the ILC (these regions are known collectively as the “Low Emittance Transport,” or “LET”). SLAC hosts a bi-weekly meeting on LET work which is attended by physicists from LBNL, FNAL, and LEPP. Physicists at SLAC are involved in all aspects of LET studies, either directly or in a supervisory/advisory role. In addition, a new postdoc was hired to augment this work, allowing these studies to continue at a higher level of intensity in FY2006.

Beam-based alignment of the quadrupole magnets in the ILC linacs will be required to preserve the small emittances. To achieve the desired accuracy, the quadrupole magnetic center cannot move by more than about 5 microns when the field strength is changed and the beam position needs to be measured with a few microns resolution. In FY2005, a program was begun to show that such requirements can be met. A prototype SC linac quadrupole magnet will be obtained from DESY (built at CIEMAT in Spain) and a warm-bore cryostat is being built for it at SLAC (the initial drawing package is nearing completion). The quadrupole magnetic field will be characterized with a rotating coil system similar to that developed for NLC prototype quads. In parallel to this program, a high-resolution rf cavity BPM has been designed and three prototypes are under construction. They will be tested in End Station A at SLAC in February of 2006 (see Section 5.4.f). Ultimately, both the quadrupole and BPMs will be tested together with beam to demonstrate the required quadrupole shunting performance.

In FY2005, the collimator wakefield experimental apparatus was moved from its original location in SLAC Sector 2 area to End Station A. The End Station A location has the advantages of relaxed vacuum requirements and much easier access. Also during this time, two new sets of collimators (8 apertures total) were designed and constructed by a collaboration between SLAC and Rutherford Laboratory in the UK. The installation of the Collimator Wakefield experimental apparatus in End Station A will be completed in FY2006 and measurements made of the

wakefield kicks from all of the new collimators. These measurements will provide additional insight into the transverse wakefields from resistive and geometric effects in the collimators, as well as a first study of more complicated and realistic collimator geometries.

#### *5.4.e. Beam Delivery System*

SLAC is playing a leading role in the international collaboration on the design of the Beam Delivery System (BDS), including development of required hardware, instrumentation and test facilities. SLAC was key to the early decision by the ILC WG4 to adopt a BDS layout with 2 IRs, one with 20 mrad crossing angle and one with 2 mrad angle. For both IRs, the optics design is based on the local chromaticity compensation final focus developed at SLAC for NLC. SLAC has continued to refine the 20 mrad solution developed for NLC but has also pushed the 2 mrad design. In particular, SLAC designed the collimation system, diagnostics, extraction beam lines and beam dumps.

Many subsystems are being developed in close collaboration with national and international partners. The collimation and machine protection system is being designed together with Fermilab and UK labs. The fast feedback systems are being developed by QMUL UK, with strong participation from SLAC. The superconducting magnets for a larger crossing angle IR are developed by BNL with SLAC providing the optics requirements. The extraction beam lines for a smaller crossing angle IR were developed by Daresbury (UK) and both CEA Saclay and CEA Orsay (France) together with SLAC. For the beam dumps and civil layouts, SLAC is working with Japanese and British groups.

The experimental studies to support a reliable BDS design will be conducted at two test facilities – End Station A at SLAC (described below) and ATF2 at KEK. The ATF2 facility will make use of the uniquely small emittance beam available at the ATF damping ring to achieve a beam size of the requisite 35 nm, develop methods of tuning and maintaining a small beam size for an extended duration, and eventually stabilize the beam with nanometer precision. In FY2005, SLAC contributed to the design of the ATF2 optics and the ATF2 proposal, and in FY2006 and beyond, will contribute in-kind hardware for construction.

#### *5.4.f End Station A Test Facility for Prototypes of Beam Diagnostics and IR Design*

The SLAC Linac can deliver damped bunches with ILC parameters for bunch charge and bunch length to End Station A (ESA). A 10-Hz beam at 28.5-GeV energy can be delivered to ESA, parasitic with PEP-II operation. This facility will be used to prototype and test key components of the BDS and Interaction Region (IR). Initial studies will investigate collimator wakefields, the design and performance capabilities for energy spectrometers, and new rf BPM designs. Future studies might include background and EMI (electromagnetic interference) studies for the feedback IP BPMs and detectors near the beam pipe in the IR. Other possibilities include material damage tests and longitudinal bunch profile measurements.

In FY2005, 3 test beam experiments were approved: T-474 to study a BPM-based energy spectrometer, T-475 to study a synchrotron-stripe energy spectrometer and T-480 to study collimator wakefields and determine the optimal geometry and material for the collimators

needed to eliminate beam halo. The scheduling of these beam tests is planned for early FY2006. They require review and approval by the SLAC safety committees and revalidation of ESA operation for primary beams. The FY2005 effort has focused on implementing additional infrastructure for the beam line in ESA (2 wire scanners for example) and for the experimental data acquisition system (DAQ) and preparing for T-474 and T-480. A collaboration with many user institutions has been developed, in particular with a large number of groups in the UK. The ESA program is described in a contributed paper and poster presented at PAC2005, which had ~60 coauthors from 18 institutions.

#### *5.4.g Diagnostics and Controls*

The most important ILC beam diagnostics are for precision, ultra-high-resolution measurements of position, transverse profile and longitudinal profile. Development of these devices has long been recognized as a high priority for linear collider R&D and SLAC has maintained a leading role in this effort. The most useful test facility for the development of precision position and (transverse) profile monitors is the KEK ATF which routinely produces the lowest emittance beam available worldwide. During the last year the SLAC group, supported by groups from LLNL, LBNL, Cornell University and a group of UK universities, achieved a world-record resolution performance of 15 nm with an rf cavity beam position monitor. This is about a factor of 2 better than the previous performance record. The SLAC group at ATF also supports the effort, lead by the UK, to deploy a laser-based beam profile monitor with resolution better than 1 micron.

For longitudinal profile measurements, the SLAC group has developed a world record precision longitudinal monitor based on a high-power S-band deflecting structure. The device was tested in FY2005 at the DESY Tesla Test Facility and showed resolution of 10 microns. Finally, in support of the superconducting rf cavity development at DESY, the SLAC group has developed a signal-processing system that allows the interpretation of the higher order mode signals generated in the cavity for beam position monitoring. This system has been tested in FY2005 and provides position measurements with resolution better than 10 microns and also provides critical offset information that indicates the placement of the niobium cavities inside the cryostat.

Controls R&D had been largely suspended since the NLC CD0.4 exercise in 2000 to concentrate all available effort on the X-band rf power systems. The only ongoing work on modernizing controls, reported at length in 2004, was a non-ILC project to bring a common multigigabit Ethernet solution to communications and distributed processing in the existing SLAC Linac. However, this work was slowed in FY2005 due to increasing demands from GLAST.

In FY2005, efforts were revived to begin reworking the conceptual models for accelerator controls down to the digital interface electronics associated with beam instruments. In addition, the instrumentation standards used in the controls and instrument systems were reexamined, with the goal of modernization. The need for High Availability design quickly became apparent and a parallel effort to address this more broadly was begun (see Section 5.4.h). In particular, a new commercial standard, the Advanced Telecom Computing Architecture (ATCA), has become available that is designed specifically for high-availability production systems similar to that required by the ILC.

At Snowmass 2005, a controls collaboration was initiated to advance the controls conceptual models towards a baseline, with SLAC, ANL, FNAL and DESY actively contributing. Information on the previous conceptual designs is being exhumed and discussed, along with new concepts on building High Availability architectures. A draft BCD proposal was written after Snowmass and submitted as part of the work of ILC GG2. The next steps will include a cost analysis in support of the main RDR.

#### *5.4.h. Operations and Availability*

An availability simulation was developed by SLAC as part of the 2004 US Technology Options Study. This work was extended in FY2005 in collaboration with DESY and has now progressed to the point that it is having a major impact on the ILC design. The full ILC is now simulated down to the level of components such as power supplies, magnets, vacuum pumps, and BPMs. Studies have shown that if an undulator positron source is used it is necessary to have a keep-alive positron source to regain the availability intrinsic to the conventional source. Comparisons of one vs. two tunnels show that the component availabilities must improve by considerably larger factors for one tunnel than for two. The risk of not achieving the necessary improvements forms most of the justification for having two tunnels. Even then, significant improvements are needed in the component availabilities. These improvements have been calculated and will be used as the basis for high-availability R&D and the costing of the components. DESY is now in the process of benchmarking the code by comparing its calculations for HERA to the past few years of operation.

Because of its size and complexity, the ILC must be designed for very High Availability (HA) from the outset. In particular, the electronics and control systems must meet much higher standards than in the past, but the new ATCA standard mentioned in the previous Section provides a realistic basis and measure for future design. The key principles of HA design are applicable to any electronic system, namely modular design for quick replacement; hot-swap capability for critical points of failure; and 1/n redundancy at the system and/or subunit level. The FY2006 program will include an evaluation of the ATCA standard for applicability to ILC and design of a controls architecture with redundant backbone networks and other HA features listed above.

Finally, a broader standards modernization study and adoption of commercial standards will be encouraged beyond the immediate ILC project. A proposal has been made to other physics research communities to share results from other large projects such as ITER, light sources and experiments like LCLS, astrophysics projects like GLAST, and so on. ILC will concentrate on its own needs but intends to support a broader community standards modernization effort, to gain efficiency through combined efforts and economies of scale in manufacturing costs.

#### *5.4.i. Civil Design*

The SLAC ILC Conventional Facilities (CF) group is working in close collaboration with FNAL on the ILC design and evaluation of several sites in Northern Illinois. A major effort in FY2005 was to develop a process (methodology) for comparing the various sites that could also be used

to compare sites in Asia and Europe. This process is intended to compare the salient features of each location and provide tools to develop a clear understanding of the relative effect that a specific site has on the project as a whole. The analysis of each location considers not only cost of the construction and installation, but also environmental impacts as well as eventual impact on long-term operations. This information was captured in a site assessment matrix. The site assessment matrix was reviewed, discussed and amended into a final working document at Snowmass 2005. A sample site for each region is to be selected for inclusion in the Baseline Configuration Document (BCD) by December 2005.

SLAC is collaborating with the Center for Integrated Facility Engineering (CIFE) at Stanford University to implement a Virtual Design and Construction computer simulation program to facilitate the top-level assessment of major trade-off choices of various sites. A VDC for the Beam Delivery System with choices of one Interaction Region (IR) vs. two IRs was implemented and successfully demonstrated at Snowmass. Work is under way to expand this tool to include other trade-off choices.

### **5.5. NLCTA Operations**

The NLC Test Accelerator (NLCTA) is operated by the ILC Department in support of ILC R&D and advanced accelerator R&D including X-band structure testing and laser acceleration experiments. The operating funds for the NLCTA do not come from the ILC R&D funds but out of the SLAC operating budget.

#### *5.5.a. NLCTA Operations*

During FY2005, the focus at the NLCTA has shifted away from production testing of NLC X-band accelerator structures and towards development of L-band rf power systems. The primary effort has been the installation and preparation of a high power L-band modulator which has been borrowed from the Oak Ridge National Laboratory Spallation Neutron Source. This device has been fully installed and is ready for operation. A 5 MW L-band klystron is installed in a tank socket and is also ready for operation. During FY2006, we expect several thousand hours of modulator operation.

The NLCTA has also been modified in order to provide beam for SLAC E163, a 'Laser Acceleration at NLCTA' experiment. The original thermionic gun was removed and replaced with an S-band rf photocathode gun capable of extremely short pulses. The high-power UV laser has been tested and the rf gun is just beginning full power commissioning. The remainder of the E163 laser acceleration apparatus was installed in late FY2005. Finally, the NLCTA high power X-band sources continue to be used for probing the performance of high gradient copper and tungsten iris structures in collaboration with CERN. This work is expected to finish in early FY2006.

#### *5.5.b. NLCTA Schedule*

During most of the first half of FY2005, the NLCTA was shut down due to the laboratory-wide safety stand down. The facility restarted operation in May of 2005 and is now operating routinely in support of the X-band structure testing program and experiment E163. In FY2006,



the NLCTA will operate approximately 1,000 hours for E163, including commissioning. Full E163 operation will start in March 2006. Around that time, a prototype high-power, normal-conducting ILC L-band accelerator section for positron capture will also be installed. Power from the SNS modulator will be routed to the structure for about 1,000 hours of structure operation before the end of the fiscal year. Late in FY2006, the prototype Marx-bank modulator will be transferred from the power supply engineering area to End Station B. This promising new device would provide high-power pulses to ILC klystrons at a substantially reduced cost, without large transformers or oil tanks.

### 5.5.c. NLCTA Safety

Following the arc-flash incident at SLAC in early FY2005, the laboratory director issued instructions resulting in a full cessation of operations, a comprehensive safety review and a restart plan. The NLCTA restart plan was validated in April 2005 and permission to resume operation followed shortly afterward. The NLCTA implementation of the DOE 'Integrated Safety Management System' (ISMS) has been singled out by the laboratory management and by the SLAC DOE site office as being 'exemplary' and showing 'best practice among DOE labs.' The ISMS practice at NLCTA includes a 5 day per week 7:30 AM 'tailgate' meeting at which all work in the area is discussed and hazard evaluation and mitigation is reviewed. This type of meeting has since been adopted at other SLAC facilities and has proven effective, both in terms of raising safety awareness and in providing valuable feedback from SLAC working staff to the area managers.

### 5.6. LHC Accelerator Research Program (LARP) Collimators

The LHC collimator R&D program developed out of a request from CERN to study the applicability to the LHC of the 'consumable' collimator technology that was developed for the NLC. As the project became better defined, it was added to the US LHC Accelerator Research Proposal. All funding for this program flows through LARP, although the program is administered out of the ILC Department, where the technological concepts originated and the people driving the effort are located.

The LHC collimation system will be installed in two phases. The first phase devices are carbon-jaw collimators that can survive the direct impact of up to 8 nominal-intensity bunches, a rare but regularly foreseen accident condition. The system will have adequate efficiency and low enough impedance for start-up luminosity of 10% nominal design or  $1 \times 10^{33} \text{ cm}^{-2} \text{ s}^{-1}$ . A system based on metal collimators with improved efficiency and lower impedance must be devised and installed before the LHC can reach the full design luminosity of  $1 \times 10^{34} \text{ cm}^{-2} \text{ s}^{-1}$ .

The ILC Department has proposed to design and prototype these so-called LHC Phase II collimators as an extrapolation of the design that was developed and prototyped for the NLC. The basic concept is one that replaces classic rectangular jaws with cylindrical jaws that can rotate to present a fresh surface to the beam if the surface is damaged in an accidental beam abort. Relative to the NLC design, the LHC jaws must be longer, of a smaller diameter and each provided with ~12 kW of water cooling. In FY2005, tracking studies, energy deposition studies, and finite element analyses were used to determine the optimal design of the collimators. This information, together with relevant 3-D CAD design drawings, was assembled into a conceptual

design report for a first collimator prototype. It is planned to build and test the thermomechanical properties of this prototype in FY2006.

### **6.A. Advanced Accelerator Research Department-A by Ronald Ruth**

Accelerator Research Department-A has worked on a wide variety of topics this past year. The work has three main thrusts: performance enhancement of current accelerators at SLAC such as PEP-II, research and design for near-future facilities such as ILC, upgrades to PEP-II or LCLS, and research in fundamental aspects of accelerator and beam physics. The department is divided into several groups: selected topics from each group are discussed below.

#### ***Electronics Research***

The Electronics Research group in ARDA combines interests in particle beam dynamics with technology development of fast signal processing and feedback control systems. Electronics Research combines SLAC staff with Stanford graduate students in Applied Physics and Electrical Engineering to provide both accelerator physics and detailed technology skills for accelerator projects. The group's pioneering hardware and software instability control systems have been implemented at labs in the US, Europe and Asia. During the year the group has presented results through 14 publications and an invited talk at the Particle Accelerator Conference, and John Fox taught a course (rf Engineering and Signal Processing) for the US Particle Accelerator school, as well as Stanford courses in Applied Physics. The group comprises four full-time SLAC staff and two Stanford graduate students in Applied Physics and Electrical Engineering.

The group has been central in machine physics studies to better understand the interactions of the PEP-II rf systems, with their complex impedance-reducing feedback architectures, and the longitudinal dynamics of the machine. In 2005 we have continued our focus on high-current configuration and operation of the rf systems through machine physics experiments, nonlinear numeric simulation and analytical studies. The increases in PEP-II currents and luminosity have been possible because of the group's development and commissioning in 2005 of the Low Group Delay Woofer (LGDW). The capabilities of the original rf system implementation were exceeded this year.

We have been working on several fronts to combat these instability limits as machine currents increase. One effort, the LGDW, offers a path to higher gain in the instability control feedback. The other path requires changes in the low-level rf signal processing in PEP-II to better reduce the cavity fundamental impedance via the direct and comb feedback loops. A parallel effort is still under way to measure and control the HOM coupled bunch instabilities in PEP-II via the broadband-coupled bunch feedback systems.

The LGDW, along with the interconnection to the broadband feedback, is shown schematically in the Figures 1 and 2. The channel is a separate programmable 9.81 MHz sampling rate 14 tap FIR control filter, which offers greater flexibility in low mode control via a lower group delay around the control path. A prototype LGDW was constructed and commissioned in the HER in May 2004. This initial success was followed with an Accelerator Improvement Project (AIP) to

construct two complete production control channels for both HER and LER. This AIP (led by Dmitry Teytelman and Dan Van Winkle) was completed on time with successful commissioning of new HER and LER control channels in spring 2005. The commissioning of the LGDW in the LER and HER allowed a direct increase in operating currents to the 1650 mA (HER) on 2650 mA (LER) levels which give PEP-II its record luminosities. Of equal importance is the improvement of operating margins, so that the number of rf aborts due to longitudinal instability in the HER was greatly reduced.

Another PEP-II research area involves techniques to linearize the high-power klystrons. Our efforts in the past three years have led to the understanding that saturation effects in the 1.2 MW PEP-II klystrons significantly reduce the effectiveness of the impedance control loops. Our modeling efforts have been confirmed by physical measurements of the in-cavity longitudinal modes in PEP-II. The effect of this saturation is so significant that the problem must be attacked at the source, in addition to feedback control via the LGDW and broadband systems.

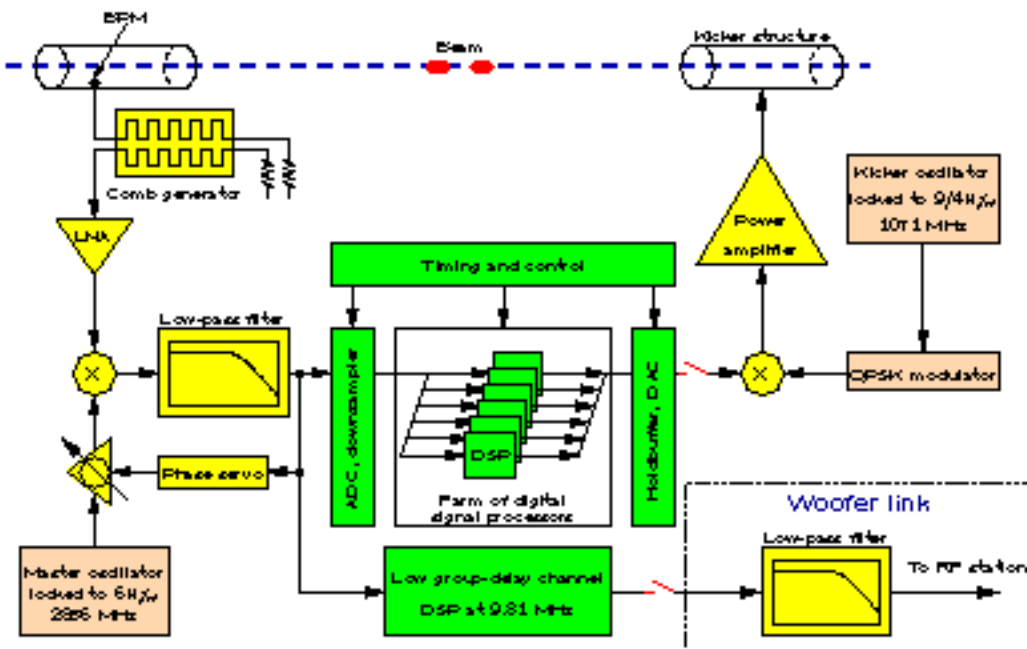


Figure 1: The low group delay woofer channel and the broadband feedback channel.

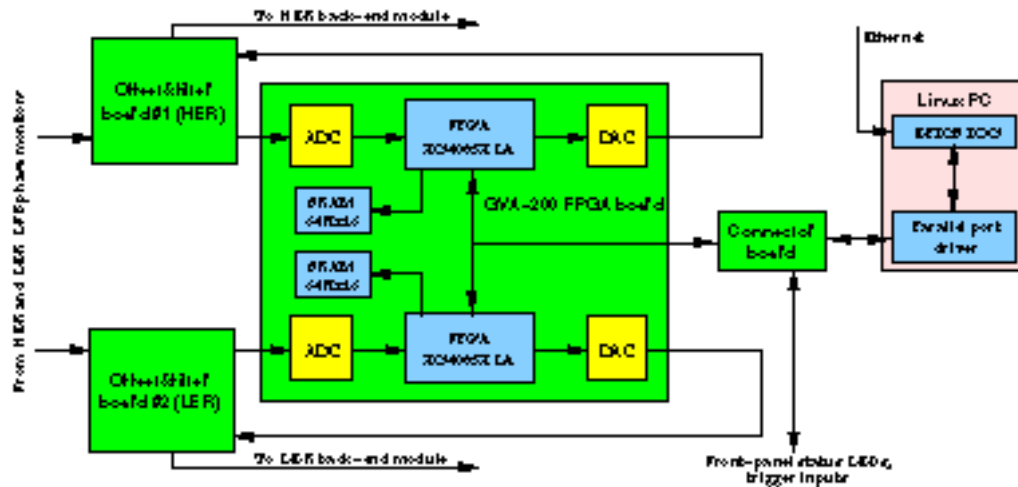


Figure 2: Block diagram of the low group delay woofer processing.

Figure 3 shows the essential idea behind the klystron linearizer. Essentially, a feedback loop and compensation circuit are used around the klystron to enforce a linear input to output amplitude gain characteristic. The action of the feedback path is to create a distorted, nonlinear input to the klystron, such that after the nonlinear klystron gain, the result is a linear gain block.

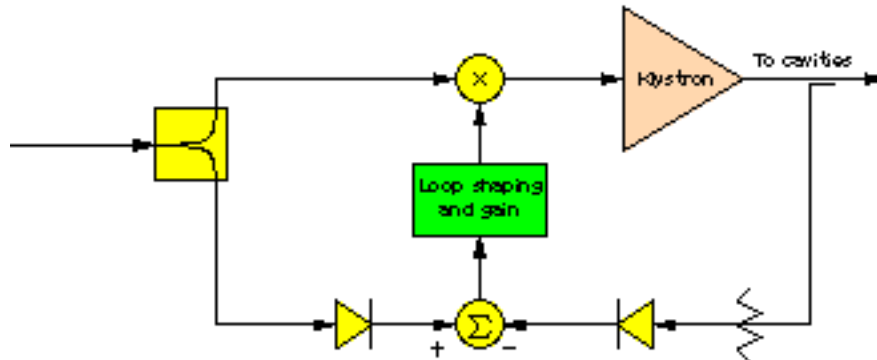


Figure 3: Block diagram of the klystron linearizer.

In the past two years, our group has developed prototypes of this nonlinear processing channel, tested with full-power klystrons, plus a machine development effort to understand the operation of the linearizer interaction with the complex LLRF systems. These linearizers are a mix of rf circuitry plus a digital processor used for gain compensation to keep the closed-loop frequency response stable. We constructed 5 prototype linearizers, and they were used in a machine development effort in the LER to better understand the configuration of the rf systems with such a linearizer, as well as to measure the impact of the linearized klystron on low mode instability growth rates. Based on the success of these prototypes, an AIP project has been initiated to develop fully integrated linearizers for the PEP-II rf systems in the LER and HER. This project is led by Dan Van Winkle.

Our group has continued to develop high-speed signal processing systems, and this last year we have continued the detailed circuit and signal processing system designs for a 1.5 GSample/s  
10/31/2005

feedback processing channel. This new architecture is of direct applicability to PEP-II and other collider needs and can implement either longitudinal (down sampled) or transverse (not down sampled) processing systems. It represents a significant advance in the processing speed and density previously achieved. The initial development has been done in conjunction with Dr. Makoto Tobiya of KEK, and has progressed to include a significant funding component under the US-Japan Cooperative Program in High Energy Physics. We continue to refine and improve our conceptual prototype. In the past year a 1/4 capacity processing prototype (the Gproto) was developed by Dmitry Teytelman as a proof-of-concept demonstrator. This Gproto system has capabilities to run transverse or longitudinal coupled-bunch feedback algorithms at a 500 Megasample/s rate. This prototype channel has been tested successfully at LNF-INFN on the DAFNE E+ ring and at the PEP-II LER ring. The Gproto system development includes reconfigurable control filter algorithms which allow the hardware to run at various facilities. Software includes the control filters as well as monitor diagnostics showing bunch motion spectra (see Fig. 4). These tools are useful for operations to observe injection matching as well as to understand control margins in the machine. Progress on the 1.5 GS/s full capacity channel this last year has been unfortunately slower than we would like, as manpower was concentrated on the LGDW and Klystron Linearizer projects.

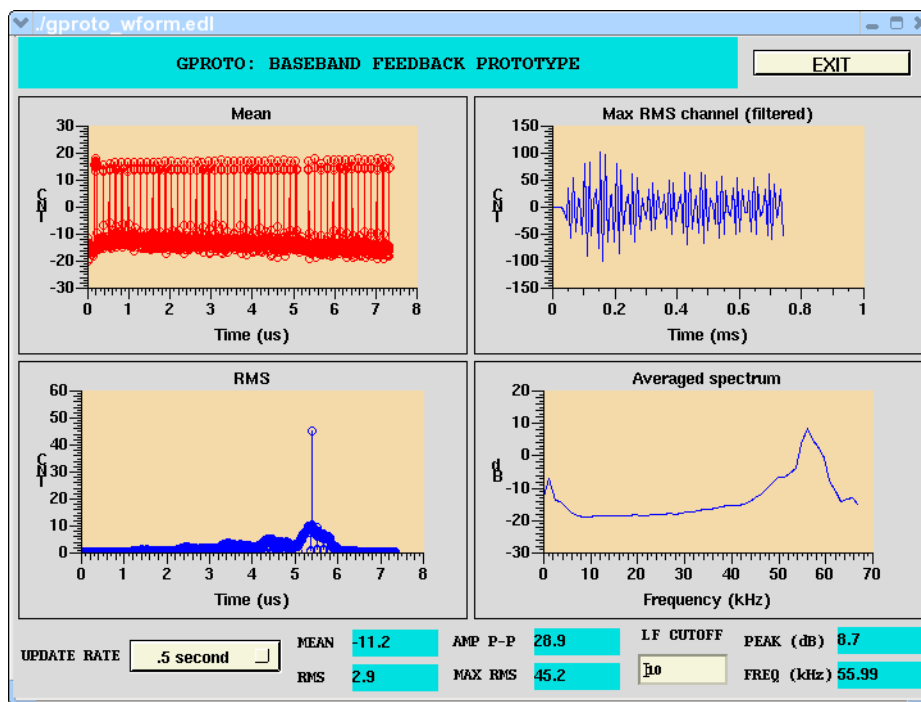


Figure 4: Plot of LER vertical mean and RMS motion around a turn, oscillation of the bunch with the largest RMS, and averaged bunch spectrum. Update rates of 2 Hz are supported.

Figure 5 shows the digital filter used for vertical transverse feedback tests in the PEP-II LER ring. At the operating point for the vertical tune the filter phase is 90 degrees (resistive damping). The digital filter structure is flexible and allows rapid tuning to machine conditions.

The modeling effort to study the dynamics of the rf systems in PEP-II is necessary to predict the behavior of the systems at upgraded currents and to evaluate possible new control techniques or new control hardware for the low level rf systems.

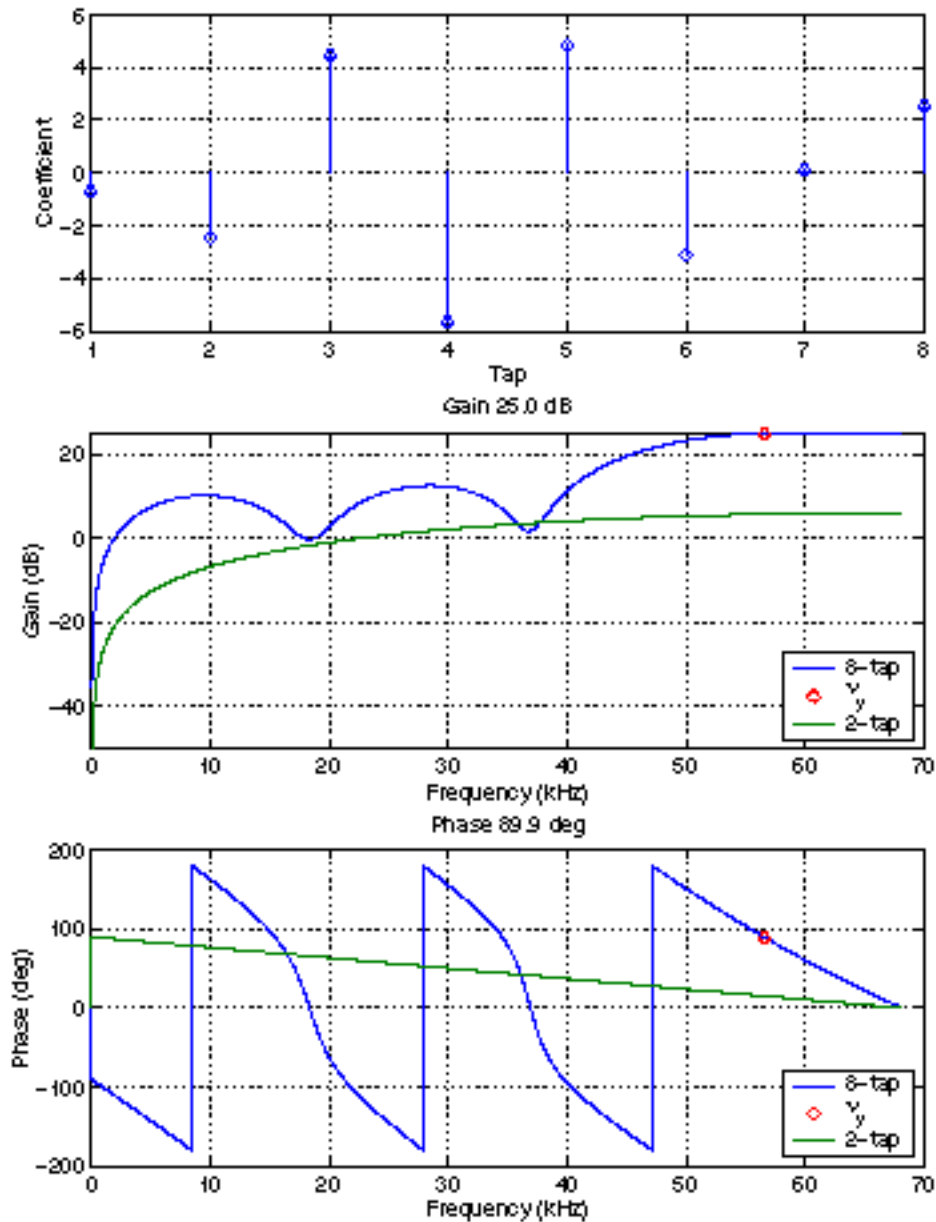


Figure 5: PEP-II LER vertical transverse feedback digital filter.

The rf system and accelerator dynamics simulation is a nonlinear time domain simulation which models the direct and comb loop behavior in the rf systems, as well as the interaction of the high current beam with the rf cavities and high power klystrons. This model has been expanded to allow the simulation of the HER ring with 2 and 4 cavity rf stations. The essential elements of the nonlinear time domain model are shown in Fig. 6.

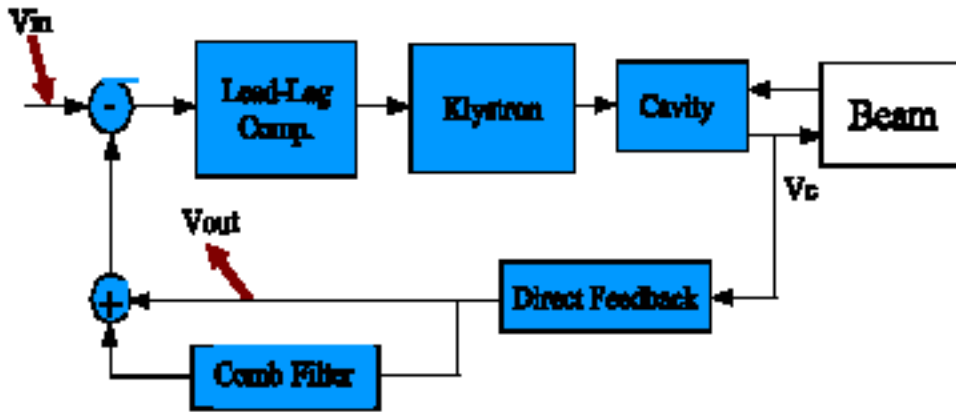


Figure 6: Nonlinear time domain model

The simulation model can be used to predict instability growth rates and modal patterns as shown in Figures 7 and 8. By simulating existing conditions, and comparing the results to actual machine operating data, the validity of the model can be tested. The model can then be used to predict higher-current operation of the machine and to evaluate new operating configurations and stability margins for future operating points.

Our group added a new staff rf engineer - Claudio Rivetta, who is directly involved in rf system analysis and modeling for PEP-II (Claudio just finished his Ph.D. in control theory). Claudio is working with Themis Mastorides (Ph.D. student from the Stanford Electrical Engineering Department).

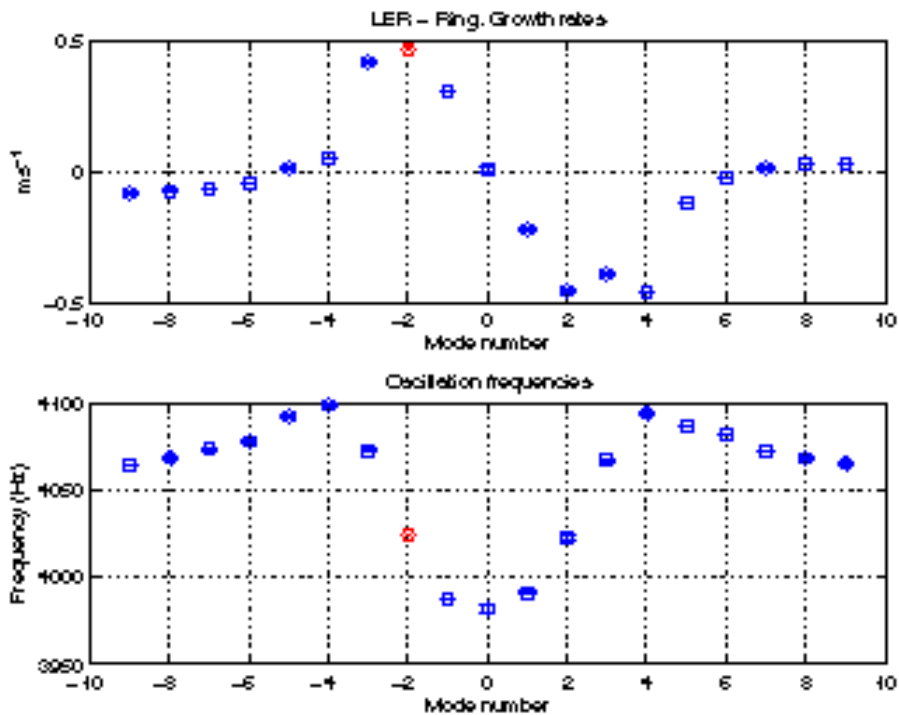


Figure 7: The predicted modal growth rates for PEP-II at 2A

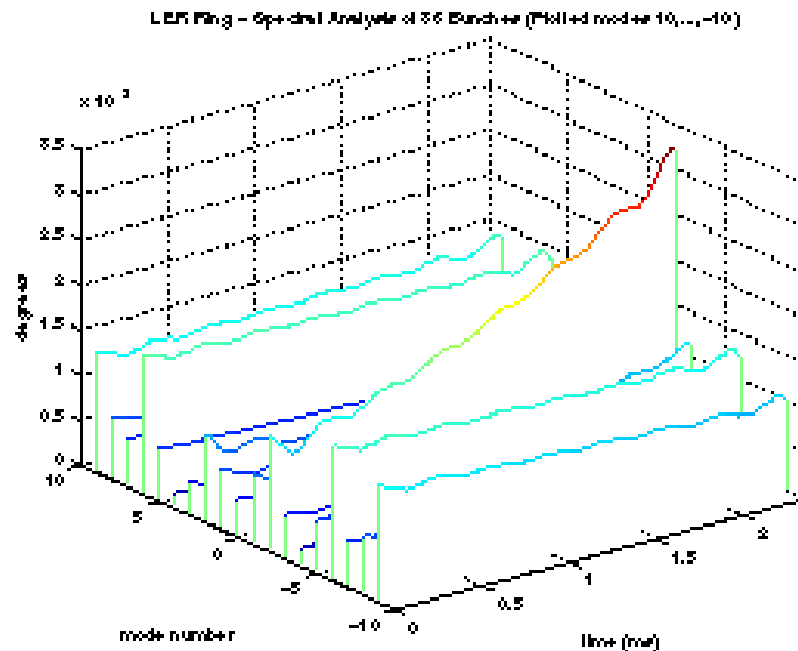


Figure 8: Time evolution of the growth of unstable modes in the PEP-II LER as predicted by the simulation

### *Collective Effects*

The Collective Effects Group continued studies of beam physics in the Linac Coherent Light Source (LCLS). We have carried out calculations of wakes and impedances for various machines. We were also involved in stability studies for the ILC damping rings.

*Resistive wall wakefields in the LCLS undulator:* The previous study of the resistive wall wakefield in the LCLS undulator was continued and compared with the reflectivity measurements carried out at Brookhaven (Bane and Stupakov, LCLS-TN-05-6). These measurements allowed one to infer the conductivity and the relaxation time for copper and aluminum in the range of frequencies corresponding to the LCLS bunch length (about 25 microns rms). They gave experimental confirmation of the advantage of using an aluminum vacuum chamber over using the copper one.

*FELs with slowly varying beam and undulator parameters:* Motivated by the effect of resistive wall wakefield effects in the LCLS undulator, the theory of free electron lasers with slowly varying beam and undulator parameters has been developed and published in *PRSTAB* (Huang and Stupakov, **8**, 040702, 2005). The theory predicts that a linear energy variation along the undulator distance can reduce the gain length in the exponential growth regime and improve the saturated power by about a factor of 2 compared with a constant-parameter FEL (see Fig. 9). Applied to the effect of wakefields, this theory indicates the advantage of using the aluminum vacuum chamber over the copper one. The results of this study were incorporated into the design decisions of the LCLS project.



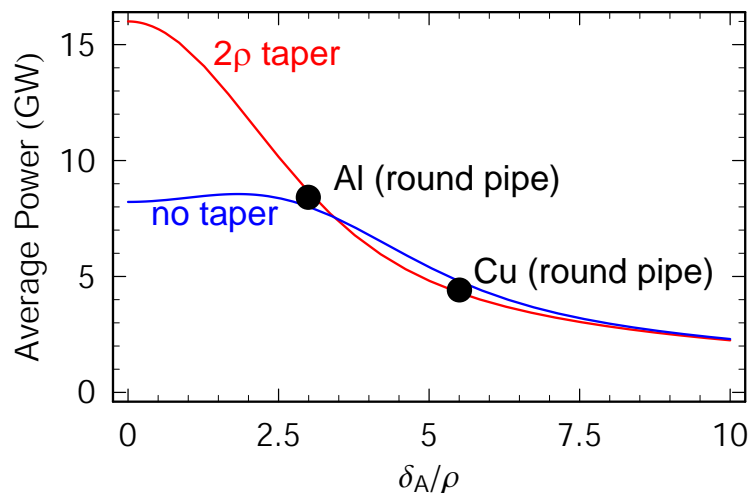


Figure 9: LCLS X-ray power versus the wake amplitude for a prescribed tapered undulator (red) and without any taper (blue). The dots indicate the values for the aluminum and copper vacuum pipe of round cross section

*Calculation of wakefields and impedances for various machines:* We continued to work on the theory of wakefields and impedances in accelerators. The wakefield in a dielectric pipe with a frequency-dependent dielectric constant was computed and applied to a laser-driven dielectric accelerator (Siemann and Chao, *SLAC-PUB-11167*); wakefields for LCLS transitions were calculated by Bane and Zagorodnov (*SLAC-PUB-11388*); transient wakefield in short inserts were calculated by Stupakov (*PRSTAB* **8**, 044401, 2005); various impedances were calculated by K. Bane for the proposal of the next incarnation of the Accelerator Test Facility at KEK for the ILC (*SLAC-PUB-11202*).

*Longitudinal space-charge effects in photoinjectors:* Longitudinal phase space properties of a photoinjector beam are important in many areas of high-brightness beam applications, such as bunch compression, transverse-to-longitudinal emittance exchange, and high-gain free electron lasers. In a recent paper (Huang et al., *SLAC-PUB-11240*), both the rf and the space charge contributions to the uncorrelated energy spread of the beam generated from a laser-driven rf gun were studied. Analytical expressions for the uncorrelated energy spread and the longitudinal emittance were compared with numerical simulations and recent experimental results.

*LiTrack computer code:* LiTrack is a fast 2D code to study longitudinal aspects of beam dynamics. It is based on an earlier code originally written by K. Bane, which is now ported to MATLAB (Bane and Emma, *SLAC-PUB-11035*), with additional features such as graphical user interface, prompt output plotting, and functional call within a script. This single-bunch tracking code includes rf acceleration, bunch compression to 3rd order, geometric and resistive short-range wakefields, aperture limits, synchrotron radiation, and flexible output plotting. The code was used to design both the LCLS and the SPPS projects at SLAC.

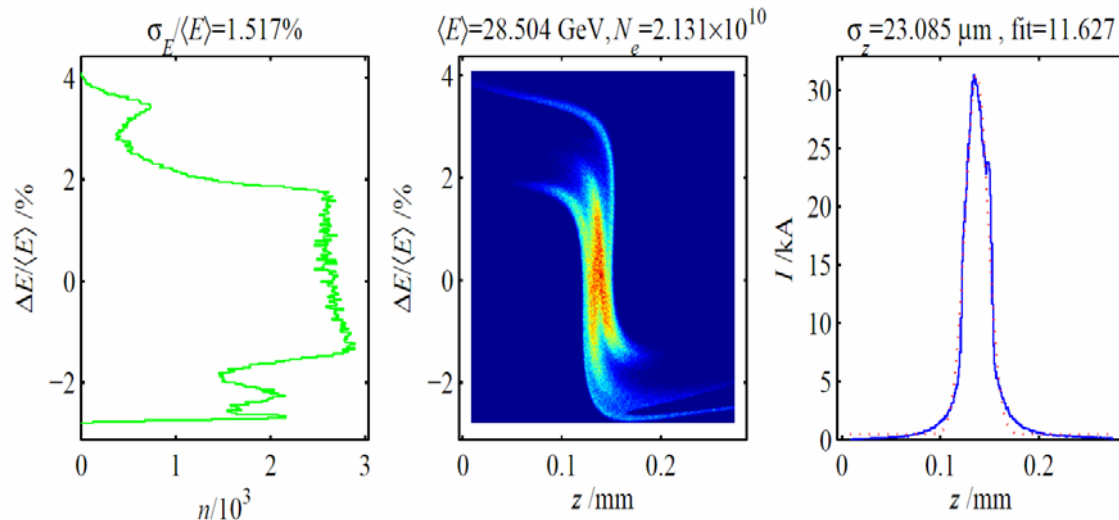


Figure 10: LiTrack output plots for SPPS with energy profile (left), longitudinal phase space (center), and bunch length profile (right).

*Dark current simulations for NLC structure:* The study of dark currents in the NLC structures has been completed and published in *PRSTAB* **8**, 064401, 2005.

*Study of stability and impedance for ILC damping rings:* Several members of the group are now involved in the stability study of the ILC damping rings. A talk on the first results of the stability analysis was given at the Snowmass workshop, August 2005.

*Beam-Ion Instability:* The results of the experimental measurements at Berlin Electron Storage Ring for Synchrotron Radiation (BESSY-II) were analyzed by Heifets and Teytelman (*PRSTAB* **8**, 064402, 2005). Grow/damp measurements of the transverse coupled-bunch instabilities were performed using a multibunch feedback system and a synchronized time-domain bunch motion recorder. The results of these experiments were compared with theoretical predictions, and it was concluded that a plausible explanation of the instability is the beam-ion interaction in the ring.

*Dust particle dynamics:* A new study of dust macroparticles in storage rings explaining the long duration of the dust events observed in the PEP-II B-factory and BEPC-II machines has been carried out (Heifets et al., *PRSTAB* **8**, 061002, 2005). Previous models predicted the lifetime of dust particles to be many orders of magnitude shorter than observed in the experiments. The new explanation proposed by the authors is based on two-dimensional oscillations of the macroparticles in which they remain far from the beam most of the time and only occasionally traverse the beam orbit.

### ***Lattice Dynamics***

Since the August, 2004 decision to use superconducting cavities as the acceleration technology for a next-generation linear collider, we have started design work for the ILC. We have made significant contributions to the improvement of the lattices for the beam delivery system and damping rings. In the same period, we continued to work on the PEP-II machine optics and beam-beam effects and made major contributions to the luminosity recovery after the unexpected long shut-down.

*Study of beam-beam effects in an  $e^+e^-$  collider:* Collaborating with W. Kozannecki, I. Narsky, J. Seeman, and M. Sullivan, we have studied the effects of the head-on and small crossing angle collisions at PEP-II. In a series of dedicated experiments, we measured the dependence of the PEP-II luminosity performance on small horizontal crossing angles and on the horizontal separation at the first parasitic crossing. The experiment was carried out by varying the IP angle of one of the beams in two different bunch patterns, one with and one without parasitic crossing. The measurements showed satisfactory agreement with three-dimensional beam-beam simulation. The work was reported at PAC 05 and was written as SLAC-PUB-11216.

Based on the experimental and simulation work, Yunhai Cai has given an invited talk about the beam-beam effects in  $e^+e^-$  storage rings at the Particle Accelerator Conference, May 2005, Knoxville, TN. The talk gave a comprehensive review of simulation method based on the particle-in-cell and broad comparisons between experiments and simulations. The topics included the beam-beam limits, crossing angle, parasitic collisions, beam-beam spectrum, and beam-beam lifetime. The work was written as *SLAC-PUB-11179* and published in the proceedings of the conference.

*ILC beam delivery system design:* We designed the conceptual optics for the ILC extraction lines for two options of IP crossing angle: 1) 14 to 20 mrad and 2) 2 mrad. The main challenge of the ILC extraction design is to achieve a very large energy acceptance needed for safe transport of the high power disrupted beam with expected energy spread of 60% to 80%. The advantage of the 14-20 mrad option is that there is sufficient beam separation after the IP for an independent extraction line. In the 2 mrad option, the extracted beam must travel off-center through the incoming beamline quadrupoles and sextupoles near the IP. This significantly complicates the extraction design, but the advantage of the smaller angle is that the crab cavity may not be required and the detector background from backscattering may be reduced. Both designs include two diagnostic chicanes and the second beam focus for energy and polarization measurements. The quadrupole focusing and magnet apertures were optimized to achieve an acceptable level of beam loss for the ILC nominal luminosity beam parameters. Protection collimators are included to further minimize beam loss on magnets and to limit the beam size at the dump. These designs have been presented and published at the LCWS 2005, PAC 2005 and Snowmass 2005 conferences. They will be further developed for the ILC CDR.

*ILC damping rings design:* The current designs of damping rings for ILC do not have adequate acceptance for the injected positron beam when the nonlinear wigglers are properly taken into account in the calculation of dynamic aperture. Over the past year, we have designed two damping rings (3-km and 17-km circumferences) based on different types of cell. The dynamic aperture has been significantly improved by the pairing of sextupoles for the cancellation of their nonlinearity. This work was reported at the Wiggle 2005 workshop, February 2005, Frascati, Italy and was written as *SLAC-PUB-11084* and *SLAC-PUB-11208*. As a result, we are coordinating an international effort to evaluate seven possible designs of the ILC damping ring for the selection of a baseline design by the end of this year.

*Single-particle dynamics:* To model realistic wigglers in damping rings, we have developed a new hybrid symplectic integrator for fast and accurate tracking of particle in storage rings. The

method was implemented in LEGO and used to study and improve the dynamic aperture in the designed damping ring. This work was also documented in SLAC-PUB-11084.

The leading Lie generators, including the chromatic effects, due to hard-edge fringe field of single multipole and solenoid were derived from the vector potentials within a Hamiltonian system. These nonlinear generators were applied to the interaction region of PEP-II to analyze the linear errors due to the feed-down from the off-centered quadrupoles and solenoid. The nonlinear effects of tune shifts at large amplitude, the synchrotron sidebands near half integer and their impacts on the dynamic aperture were studied. This work was presented at PAC 2005 and was written as *SLAC-PUB-11181*.

Upgrade object-oriented nonlinear differential-Lie algebraic library: Zlib. Symplectic map tracking with a mixed-variable generating function has been implemented to Zlib. It allows fast, turn-by-turn particle tracking so as to ease beam-beam study with the nonlinear effects from the lattice nonlinearities included.

*Precision measurement for PEP-II optics and its improvement:* As PEP-II luminosity gets better, further improvement demands finer optics. This requires detail and precise optics measurement. Model-Independent Analysis (MIA), which was developed for PEP-II optics measurement, has been upgraded continuously for measurement precision and model-fitting speed. To add to the fine precision, we have recently upgraded MIA with fitting of the one-turn linear maps, in addition to the fitting of the Greens functions and phase advances. We have also figured out precise measurement of betatron motion invariant ratio so as to add a key constraint to MIA, which results in improved coupling measurement.

The accurate measurement leads us to a reliable virtual accelerator, so we can study solutions on a computer for correcting and improving the PEP-II machine optics (presented and published in PAC2005; *SLAC-PUB-11209*). Indeed, for the current PEP-II run, we have made a major contribution by improving the optics to bringing up the luminosity after the long shut-down.

*Beam dynamics studies for PEP-II:* In PEP-II studies, we have investigated the effect of nonlinear fringe field in quadrupoles on dynamic aperture near the half-integer resonance. Tracking simulations using LEGO showed that the fringe field generates octupole synchrotron resonances, which reduce the available tune space near the half-integer resonance and degrade the dynamic aperture. This effect is more severe on the LER because of the lower synchrotron tune and unfavorable sign of the third order chromaticity, which limits how close the working point, can be to the half-integer. In another study, we evaluated the first-order coupling at the IP as a function of energy. It has been shown that the nominal chromatic coupling at the IP is not very strong. It produces less than 5 mrad of tilt angle at the IP and only moderately increases the beam ellipse aspect ratio to 0.04 at large  $\delta E/E$ . We have also investigated an option of using antisymmetric horizontal offsets at “-I” sextupole pairs to increase the LER emittance from 24 to 48 nm, as an alternative to using wigglers. Three sextupole knobs have been designed to produce a local perturbation of the horizontal dispersion in the LER arcs 7 and 9. It has been shown that very large sextupole offsets (at least 10 mm) are needed to achieve the 48 nm emittance. Using smaller but more practical offsets would create only minor emittance adjustment.

*Lattice design for SABER project:* We have designed preliminary optics for the SABER project using the SLC South arc. This includes the 1 km bypass optics, a simple final focus optics with  $x/y \text{ beta}^* = 10/1 \text{ cm}$ , and tracking simulations. A chromatic correction using two sextupoles was included in the bypass to reduce the chromatic beam size growth. Tracking simulations (with K. Bane) showed that achieving the required 30-micron bunch length is possible, and the  $x/y$  beam size and magnet parameters are reasonable. However, a better final focus, with a localized chromatic correction, is needed to achieve the specified 10 micron  $x/y$  beam size at the IP. This study will continue.

### ***Accelerator Structures***

The mission of the rf Structures Group is to design, engineer, and test a variety of accelerator structures with superior properties in high rf efficiency, good higher order mode suppression, and high gradient performance. Our activities span design theory and practice, simulation, structure related beam dynamics studies, fabrication technology, microwave measurements, structure characterization, and high power experiments. We support accelerator R&D programs at SLAC including the ILC, LCLS, and others.

After the International Technology Recommendation Panel (ITRP) announced, in August 2004, the decision to select superconducting technology for a future linear collider, we quickly adjusted our R&D program from normal conducting X-band NLC structures to embrace the ILC opportunity with enthusiasm and to support SLAC photon science projects.

*Completing X-band Structure Studies for the NLC Main Linac:* As the prototype with all necessary HDDS structure features for the NLC main linac accelerator, two H60VG4SL17 type structures have been completed. Figure 11 shows four HOM couplers in both input and output ends. The predicted wakefields and their measurement results obtained in early 2005 are shown in Fig. 12. The HOM modes wakefield suppression has met all the NLC design requirements. This excellent agreement between theory and experimental measurements has proven our success in the accelerator design, analysis, and fabrication technologies.

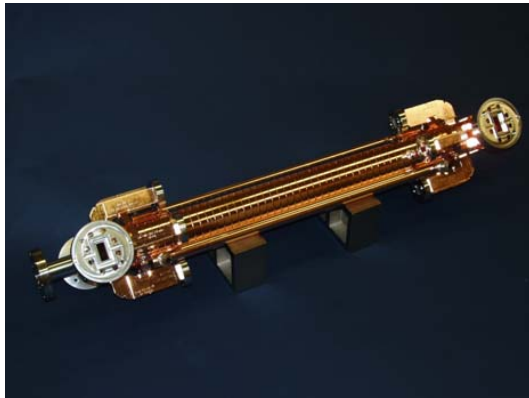


Figure 11: H60VG4SL17 – the prototype accelerator structure for the NLC main linac.

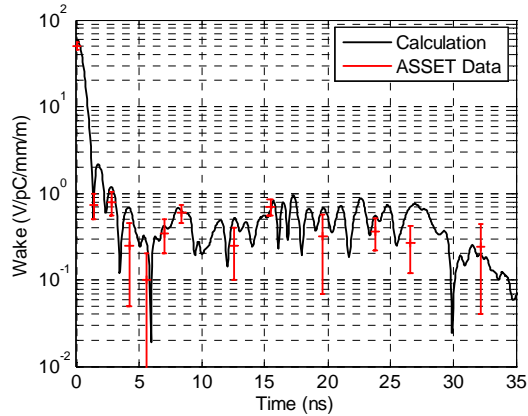


Figure 12: Envelope of calculated wakefield of two-fold interleaved structures as a function of the distance behind a driving bunch (black line) and the measurement data with error bars (red crosses).

Research program for the ILC

1. We conducted feasibility studies of recirculating traveling-wave linacs for the ILC main linacs.
2. We have also proposed an improved alternative design for an L-band normal-conducting accelerating system for the ILC positron source, including both standing wave and traveling wave sections. Figure 13 shows a schematic layout of the ILC positron source.

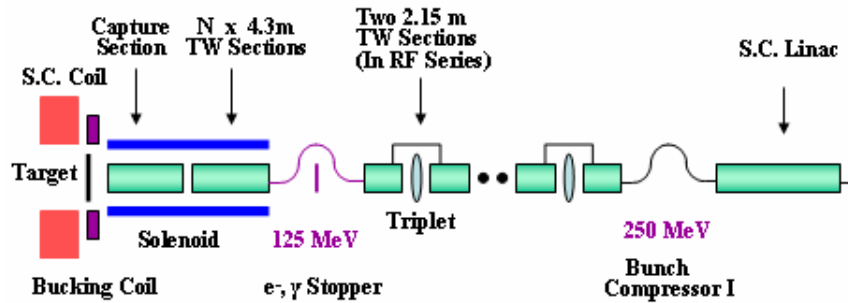


Figure 13: Schematic layout of the ILC positron source.

i. 11-cell Standing Wave structure

We have designed a simple  $\pi$ -mode standing wave (SW) structure with 11 cells for the high gradient (15 MV/m) positron capture structure. The advantages are a more effective cooling system, higher shunt impedance with larger aperture (60 mm), lower rf pulse heating, apparent simplicity, and cost savings. The mode and amplitude stability for this type of structure have been shown theoretically to be feasible.

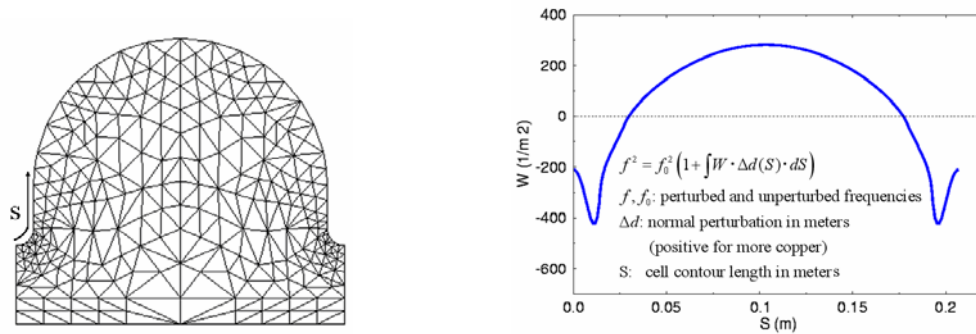


Figure 14: Cell profile of 1.27 m long  $\pi$  mode SW structure and the frequency perturbation weighting function along the cell surface.

#### ii. 4.3-m $3\pi/4$ -mode Traveling Wave structure

The “phase advance per cell” has been used as a knob for designing large aperture, constant gradient traveling wave (TW) structures in order to optimize the rf efficiency. The advantages are lower pulse heating, easy installation for long solenoids, no need for rf reflection protection (circulators), apparent simplicity, and cost savings.

We have also designed a special 4.3-m TW section with larger iris (6 cm) and thicker disc (1.7 cm) at the front end (right three profiles in Fig. 15). It can be used for realizing a deceleration scheme for higher positron capturing.

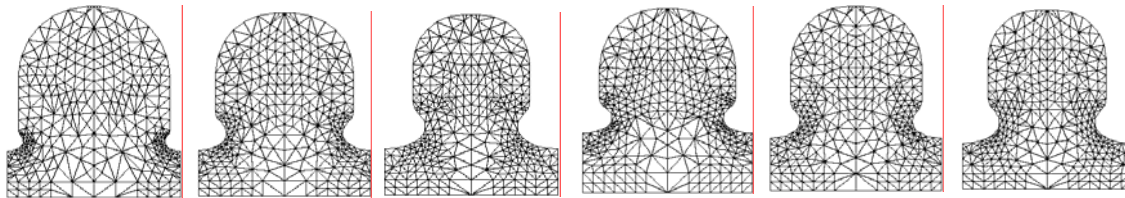


Figure 15: Profiles of the first, middle and last cell for 4.3m  $3\pi/4$  Mode TW structures, regular (left three) and special section (right three).

#### iii. Pair of two 2.2-m $3\pi/4$ -mode TW structures

In order to insert quadrupole triplets for transverse focusing of positrons with energy beyond 125 MeV, we plan to divide the regular 4.3-m TW structure into two  $\sim 2.2$ -m sections and install them with proper drift spacing as shown in Fig. 13. The rf power from the output coupler of the first section feeds into the second section.

We have made a theoretical feasibility analysis of rf and beam acceleration stabilities under different cooling conditions. The design work for a 5-cell test L-band standing-wave accelerator section is completed and its fabrication has begun.

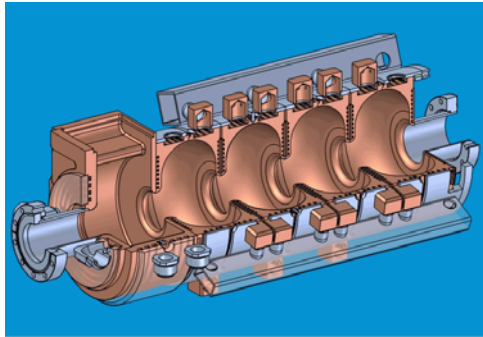


Figure 16. L-band NC SW test accelerator structure for the ILC positron source.

3. We are participating in beam dynamics studies aimed at increasing the positron yield for the ILC positron sources. Phasing the positron capture section so that it initially decelerates and bunches the positrons can shorten the bunch and produce a positron bunch with significantly smaller longitudinal emittance. We have completed the conceptual design of the ILC positron preaccelerator system for both conventional and undulator-based positron source with acceleration and initial deceleration scheme.

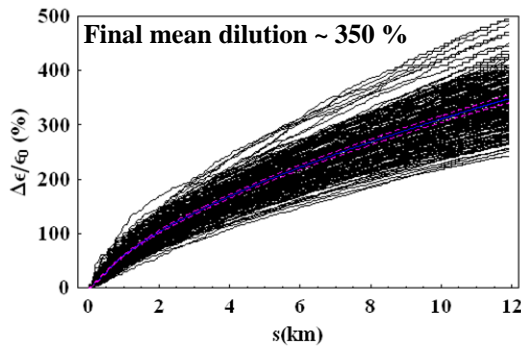


Figure 17. Equal tune of 60-60 in both planes of the lattice.

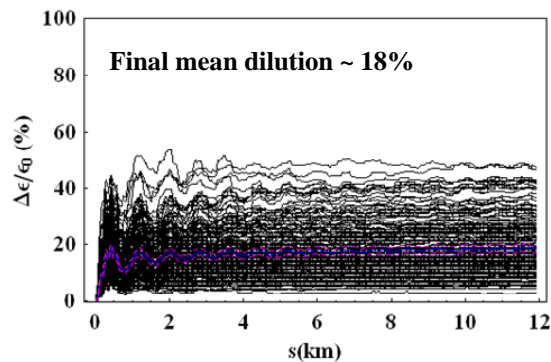


Figure 18. Splitting the tune of the lattice 90-60 in x-y plane.

4. Theoretical modeling of wakefield and emittance dilution for the ILC: The progress of the bunches in high-energy linear colliders is disrupted by the trailing wakefield left behind each driving bunch, and this can lead to a severe dilution in the luminosity of the colliding beams. In an ideal accelerating structure, the horizontal and vertical modes of the dipole wakefield are degenerate. Inevitable manufacturing errors will remove the degeneracy and create two dipole eigenmodes of slightly different frequencies lying in diagonal planes. These dipole wakefields will couple the horizontal and vertical motions of the beam. We have investigated the consequences on the final emittance dilution of the beam for this coupling in L-band superconducting linear colliders. Means to ameliorate the severe emittance dilution that occurs due to this mode coupling have included splitting the horizontal-vertical phase advance per cell of the linac's lattice. The vertical tune remains fixed at a phase advance of 60 degrees per cell, whereas the horizontal has been varied from 70 to 90 degrees. In all cases, the emittance dilution has been reduced to of the order of 20%. The emittance dilution for 200 possible linear colliders



is shown in Figures 17 and 18, in which the dramatic effect of splitting the tune of the lattice is illustrated. Further research is ongoing on the influence of trapped higher order modes on emittance dilution in particular.

5. We have given engineering support to several other SLAC projects such as the ILC superconducting quadrupoles and the remote positioning cam support system for LCLS undulator measurement.

#### Other Accelerator-structure-related Research Programs

1. We are actively participating in the S-band structure-related work for the LCLS project, including design discussions for the microwave gun, modification of the accelerator sections and preparation for structure measurements. We have designed and fabricated a horizontal bead pulling setup. The two 9.5 ft sections and six 10 ft sections have been evaluated. We have provided some important suggestions for the LCLS injector engineering. We will measure and characterize two rf deflectors. We will perform complete microwave measurement and tuning of the 1st microwave gun. The analysis of test results will contribute to the future upgraded gun design.

2. *Progress in wire measurement for accelerator studies:* A wire-based structure experimental method is being developed to analyze quickly and inexpensively the wakefield suppression properties of accelerator structures. In order to automate the measurement, the position of a 300-micron thick brass wire is moved by micro-stepping motors and controlled by measurement software. Data acquisition with an HP8510 network analyzer has been successfully accomplished on a SW20PI-L standing wave accelerator structure. The recorded S-parameters are used to compute the impedances for the monopole band and higher dipole mode bands.



Figure 19: Microwave measurement of an S-band TW structure for LCLS structure.



Figure 20: Wire measurement set-up with a SW structure.

3. The Micro Linac is a small, SW linac for a low-cost radiography source with dosage larger than 100 Ci intended to replace radioactive sources, which can potentially be used for “dirty bombs”. We have contributed both the electrical and mechanical designs for these accelerator structures.

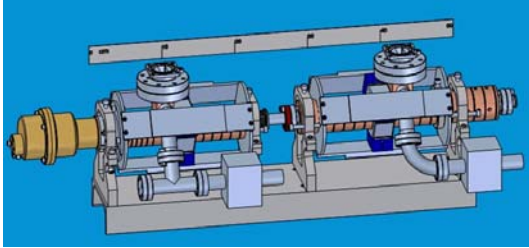


Figure 21: Micro Linac as low-cost radiography Source for security inspection

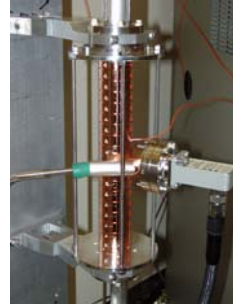


Figure 22: An accelerator section of the Micro Linac under test

### ***High Power rf***

During this fiscal year we continued our developments of X-band rf systems and components. The main thrust of our research is pushing the limits on ultra-high-power active systems. We are developing three different systems: semiconductor-based rf switches, nonreciprocal magnetic-material-based switches and plasma excited rf switches. These developments will immediately enhance the performance of the X-band pulse compression systems, and we plan to test them at high power using the 8-pack rf system at the NLCTA. However, the impact of these developments is by far more important than the pulse compression applications. The technology developed for spatially combined rf switches in a moderately overmoded waveguide should lead to novel high power sources based on semiconductor technology, with great impact on rf sources for accelerators and other applications.

To support these active systems we had to develop three new passive components. The first of these is a new  $TE_{01}$  mode tee. The structure of this tee is shown in Fig. 23. With a movable short circuit at the end of the symmetrical port, the device becomes a two port network with an arbitrary reflection/transmission coefficient. The measured total loss is less than 1%. The device uses the  $TE_{01}$  mode in all its ports, and the transition from circular to rectangular waveguide yields the  $TE_{20}$  mode in the interior, for which the E-plane tee junction is matched. Because it is overmoded and because there are no axial currents at the terminal planes, the device is suitable for ultra-high-power operation.

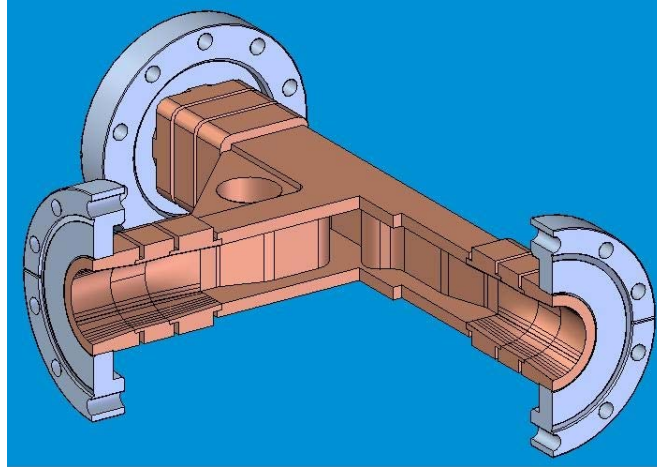


Figure 23: TE<sub>01</sub>-mode matched tee.

Also during this year, we developed a new TE<sub>01</sub> mode phase shifter. This device is also suitable for ultra high power operation and has been tested with total losses of less than 1%. This particular device is needed by other test facilities and will be duplicated and used at the NRL magnicon facility in the testing of dielectric loaded accelerator structures designed at ANL.

Finally, we designed and tested a broad-band compact (~ 4 wavelengths long) TE<sub>01</sub> mode converter. The design of the device builds on our experience in this field and is the ultimate in terms of power handling capability and low-loss design. The total parasitic mode loss is less than -50 dB at the operating frequency of 11.424 GHz, and it has a bandwidth of about 1 GHz where these losses are less than -20 dB. This device will become the standard for mode converters.

Our progress in active semiconductor components which utilize these passive components is described below. The schematic layout of the switch window is shown in Fig. 24. The window is inserted into the gap between two 1.3-inch diameter waveguides. The P/N doping regions and metal lines are radial, so they are perpendicular to the E-field of the TE<sub>01</sub> mode. The PIN diodes form a narrow ring at the peak E-field radius inside the waveguide, and the silicon will reflect microwaves most efficiently when carriers are injected. There is a narrow metal ring inside the diode ring, which provides bias for N doped lines where metal connection from outside of the diode ring is not practical. The metal ring can minimize the reflection from the silicon wafer when the diodes are off, and assist reflection when the diodes are on, so the switch requires fewer injected carriers. The silicon inside the metal ring can be cut to further reduce insertion losses. The 1.3-inch diameter of the waveguide is close to cut off, which reduces the carrier density needed for reflection and increases the switching speed, but compromises power handling capacity and rf losses. 'Floatzone' silicon wafers with 500-micron thickness are used to build the switches, although thinner wafers will have lower loss.

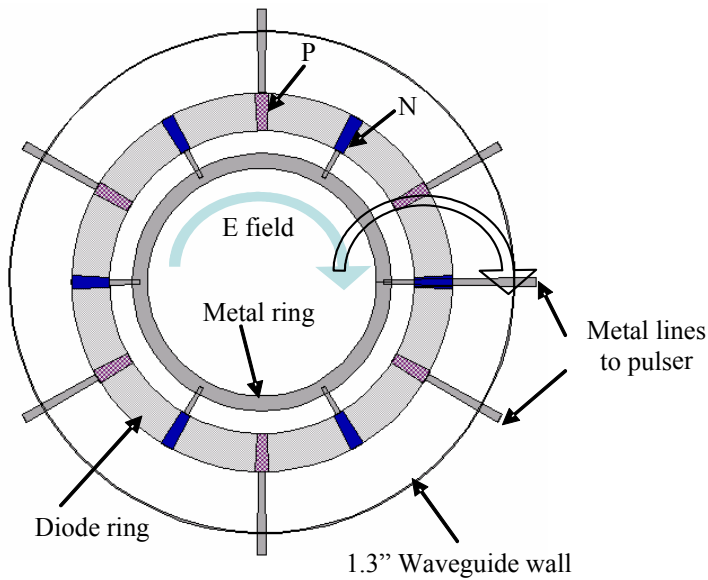


Figure 24: Schematic layout of the active window (top view).

The structure is simulated with the HFSS code. When diodes are off, the window has 3% loss and 97% transmission, compared to almost full reflection without the metal ring. When diodes are on, assuming a 50 micron thick carrier layer is formed under the wafer surface, transmission is less than 1%. The losses will be 10% if the carrier density is  $5 \times 10^{16}/\text{cm}^3$  and 3% if the carrier density is  $5 \times 10^{17}/\text{cm}^3$ .

We built this device directly on a silicon wafer and on a SOI wafer with a device layer of about 50 micron thickness. The diode fabrication processes are simulated with Tsuprem4, and then the electrical properties of the diodes are simulated with MEDICI, using the results from Tsuprem4. Simulation results show that, for devices with 60- $\mu\text{m}$  depth powered by a 1 kV pulser with  $1\Omega$  internal resistance and 30 ns rise time, a 50  $\mu\text{m}$  carrier layer with carrier density averaging  $1 \times 10^{16}/\text{cm}^3$  can be formed in about 100 ns and reach  $5 \times 10^{16}/\text{cm}^3$  in about 300 ns. To enhance the switching speed further, the 3D structure shown in Fig. 25 is desirable. This 3D structure can inject carriers more uniformly into the intrinsic silicon layer, making the switch much faster. Our simulation shows that with same power supply,  $10^{16}/\text{cm}^3$  average carrier density can be achieved in less than 50 ns (20 ns more than the assumed power supply rise time), and  $5 \times 10^{16}/\text{cm}^3$  in about 70 ns.

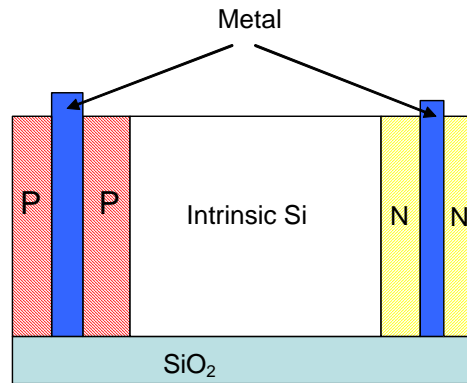


Figure 25: Structure of the 3D SOI PIN diode.

Low power testing has been performed by placing the switch assembly at the symmetrical port of the three-port tee device described above. The switch is powered by a homemade circuit driving two IGBT transistors. The current output of this circuit is monitored by a  $0.2 \Omega$  low inductance resistor. At 1 kV, the current output rises to 300 A in about 40 ns and then reaches 800 A in 300 ns.

Figure 26 shows the time response of the switch module with a bulk silicon switch. Two current pulse power supply boards are used in parallel. Switching time is about 300 ns. The loss is measured at about 15%.

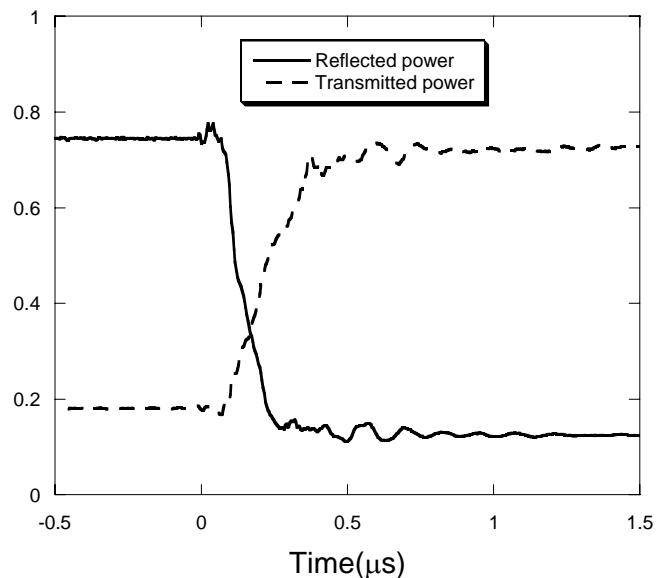


Figure 26: Time response of the switch module with a bulk silicon switch.

After the linear collider technology decision, our group started a new research direction to help improve the quality of the rf system of the ILC. The present design for an ILC main linac fundamental mode coupler is very complicated and expensive. We could contribute to the modification of these devices to increase their reliability and decrease their cost. We would like to change the design of these couplers in a fundamental way. Instead of using a coaxial waveguide to transmit the power we would use an overmoded dielectric coaxial waveguide

operating at the  $TE_{01}$  mode. All the fields in this case would be parallel to the surface, eliminating multipacting and processing issues. This would result in a highly reliable coupler. Furthermore, the use of the  $TE_{01}$  mode, which has no axial currents associated with it, allows us to divide the waveguide into sections that do not touch each other mechanically. The rf in this case travels in the gap between the sections with virtually no loss. This may prove advantageous for isolating different sections at different temperatures and in different vacuum enclosures.

We have developed the first launcher for this mode. The dielectric material of choice is alumina. We plan to test this device at high power and, if successful, proceed to further developments, not only for couplers but also for other devices, such as circulators. A novel circulator idea was suggested for X-band based on the  $TE_{01}$  mode<sup>2</sup>. This idea could be extended to L-band, provided the success of the mode launching scheme. This holds the promise of reliable circulators at power levels near 10 MW at L-band.

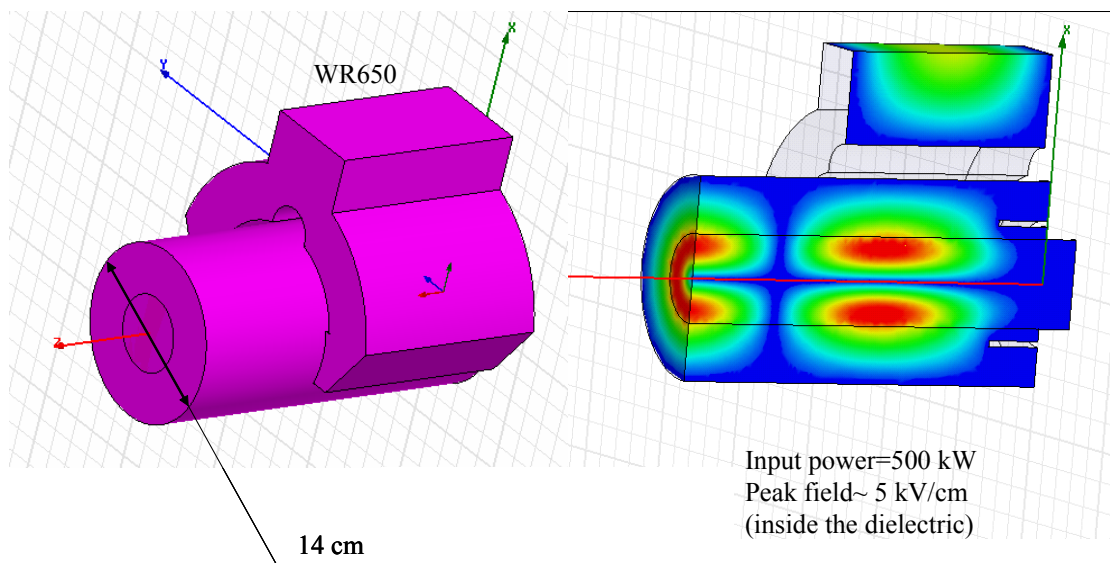


Figure 27:  $TE_{01}$  mode launcher in a dielectric loaded waveguide.

To justify further development, one must demonstrate the feasibility of propagating rf power in such a mode inside the dielectric. To this end, we would like to build two of the above mode launchers and test them back-to-back at high power.

Superconducting rf cavities are used with increasing frequency in accelerators. Niobium is the standard superconducting material used. Its ultimate potential has taken a long time to reach, in part because cavity issues and issues related to the intrinsic properties of the material were confronted simultaneously. Much progress in increasing gradient has been made over the past decade, overcoming problems of multipacting, field emission, and quenching triggered by surface impurities. The fundamental surface magnetic field quenching limit for niobium remains a hard limitation on accelerating gradients sustainable with this technology. Removing power deposited at the operating temperature of 4.2 K through the cryogenics system is expensive.

<sup>2</sup> S. Tantawi, "Overmoded high-power rf magnetic switches and circulators, *Proceedings IEEE Particle Accelerator Conference*, **2**, 1216-1218, 2001.

Further exploration of different materials and preparation techniques may offer a path to acceptable performance at higher temperatures. It is also desirable to understand the response of superconducting materials to high magnetic fields on short time scales.

For this purpose, we have designed a resonant test cavity, shown in Fig. 28. One wall of the cavity is formed by a flat sample of superconducting material; the rest of the cavity is copper or niobium. The H field on the sample wall is 75% higher than on any other surface. Multipacting is avoided by use of a mode with no surface electric field. The cavity will be resonated through a coupling iris with high-power rf pulses at superconducting temperature until the sample wall quenches, as detected by an abrupt change in the quality factor. This experiment will allow us to measure critical magnetic fields and the pulse time dependence of quenching with minimal cost and effort. Experiments done at low power will measure the critical temperature of superconducting samples.



Figure 28: Copper cavity for superconducting materials testing. The bottom flange holds the test sample. Attached to the cavity is the  $TE_{01}$  mode launcher described above, through which it is coupled.

Thus far, as an initial experiment, we have tested our mushroom-shaped cavity with a copper disk installed as the sample wall. With a new, high-purity mode launcher attached to excite it symmetrically with a  $TE_{01}$  mode, we installed it in a Dewar and brought it down to liquid helium temperature. Using a network analyzer, we carefully measured the frequency response around the X-band resonance. From fits to these data, we measured the resonant frequency, loaded  $Q$ , and coupling beta, and from these derived the unloaded and external  $Q$ s. This measurement was repeated periodically as the cavity was allowed to slowly return to room temperature over several days.

The measured increase in  $Q_0$  from room temperature to 4.2 K that we measured was a factor of  $\sim 2.35$ . From the theoretical models, however, one is led to expect a greater increase, by about a factor of two. We need to understand this and suspect it may be related to the “anomalous skin effect” and the fact that part of the cavity is formed from copper-plated stainless steel. We will modify the cavity prior to the next test. In November, we plan to measure the critical temperature of a sample of  $MgB_2$  sent to us from Los Alamos National Laboratory by T. Tajima.

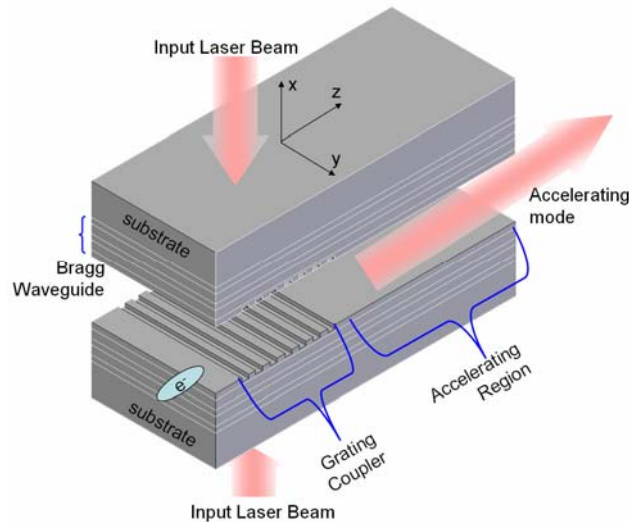


Figure 29: Optical accelerator with integrated optical Gaussian beam coupler.

Our efforts in advanced accelerator concepts continue. We designed a Bragg optical waveguide consisting of multiple dielectric layers with alternating indices of refraction, which is an excellent option to form electron accelerating structures powered by high-power laser sources. The Bragg waveguide provides confinement of a synchronous speed-of-light mode with extremely low loss. However, the laser field cannot be coupled into the structure collinearly with the electron beam. There are three requirements in designing an input coupler for a Bragg electron accelerator: side coupling, selective mode excitation, and high coupling efficiency. We studied a side-coupling scheme using a Bragg-grating-assisted input coupler to inject the laser field into the waveguide. Side coupling is achieved by a second-order Bragg grating with period on the order of the optical wavelength. The phase-matching condition results in resonance coupling, thus providing selective mode excitation capability. The coupling efficiency is limited by profile matching between the outgoing beam and the incoming beam, which normally has a Gaussian profile. We have demonstrated a nonuniform distributed grating structure, generating an outgoing beam with Gaussian profile and therefore increasing the coupling efficiency (see Fig. 29).

Fundamental understanding of high gradient limits in room temperature rf accelerator structures is the most important topic for future accelerators and colliders such as CLIC. We have helped organize a nationwide research collaboration on the topic. This collaboration held its first workshop in August 2005, and we are now in the process of starting the scientific program.

The work being done at SLAC in this regard is described briefly. Understanding the frequency scaling of the rf breakdown limit is fundamental for CLIC and for advancing the art of high



gradient accelerators. To this end, we have started the design of a series of experiments aimed at studying the basic physics of the problem. Because of the multiphysics nature of the problem, we had to design our experiments so that they do not neglect the physics that enters when building complicated accelerator structures and at the same time keep them simple enough to simulate and diagnose. We used waveguide with different cross sections. These had different distributions of magnetic and electric fields on the surface, with the same power flow, energy per pulse, surface area, and peak electric field. We also introduced the concept of the single cell traveling wave structure – a cell that has the boundary conditions of an infinite periodic structure. In collaboration with KEK, we built several single-cell test pieces made either of copper or molybdenum or with a combination of the two elements. These were cold tested to our satisfaction and are being prepared for high-power testing. In order to do breakdown experiments with a single cell accelerator structure, we have had to construct a special enclosure to shield radiation. However, the testing was delayed due to the lab-wide shutdown in 2004. We will continue this activity in FY2006. We also intend to collaborate with the CLIC group from CERN on this research.

### *Astrophysics Group*

During the past year the group's activities have included theoretical, observational and experimental studies of particle astrophysics and cosmology. Specifically, the theoretical research has been focused on the nature of dark matter and dark energy and on ultra-high-energy cosmic ray acceleration mechanisms. The observational research focused on the "intermediate lensing" studies. The experimental activities centered around the program on Laboratory Astrophysics. The group now consists of four senior physicists, two postdoctoral research associates, and one Stanford graduate student. The group also had one visiting professor and three visiting students from the Center for Cosmology and Particle Astrophysics (CosPA) in Taiwan and one visiting professor and one student from Reed College in Oregon. Most of the research projects have been carried out in collaboration with world-leading theorists and experimental groups. The major activities are described below.

#### *Theoretical Activities:*

- Black Hole Remnants as Dark Matter

Together with R. Adler and D. Santiago (both of Stanford), P. Chen proposed a "generalized uncertainty principle" (GUP) where gravity effects are included. The GUP predicts the existence of a fundamental length, which happens to be the Planck length. By applying this GUP to black hole evaporation, it was shown that BH's cannot evaporate entirely, but should leave with a remnant at Planck mass ( $\sim 10^{19}$  GeV). Such remnants from primordial black holes are an interesting candidate for dark matter. When combining this theory with the "Hybrid Inflation" model of A. Linde and others, P. Chen has recently found that the abundance of these BHRs is of the right order of magnitude for the dark matter. During last year, K. Thompson, P. Chen, and R. Adler further studied the cosmology of the post-inflation "black hole" epoch. A formal paper on this project is being prepared. In a separate effort, P. Chen and M. Shmakova, in collaboration with K. Dasgupta, S. Narayan, and M. Zieglermann, have published a paper (120 pages) in JHEP

on “brane inflation”, where the scenario of D3/D7 brane collision to manifest the hybrid inflation model was investigated and the issue of primordial black holes so induced was discussed.

- Dark Energy

In September 2004 P. Chen and Je-An Gu (CosPA) proposed a new model for dark energy (arXiv: astro-ph/0409238), entitled “Casimir Effect in a Supersymmetry-Breaking Brane-World as Dark Energy.” By insisting that SUSY is perfectly preserved in the “bulk,” but broken only on the D3 brane, Chen and Gu were able to show that the Casimir energy on the brane induced by the periodic boundary condition in the extra dimensions can be strongly suppressed. SUSY guarantees the perfect cancellation of the vacuum energy in the bulk. Its breaking on the brane then provides the vacuum energy “difference” between the graviton and the gravitino modes. This new theory looks very promising, and Chen and Gu are continuing collaboration on the project.

*Observational Activities:*

J. Irwin has developed a novel approach, based on his theoretical expertise in particle beam optics, to weak gravitational lensing analysis. It is proposed that higher multipole, such as sextupole, moments beyond the conventional quadrupole moment, can in principle be extracted from observation, which would provide extra information in the gravitational lensing studies. Applying this new method to the Hubble Deep Field data, Irwin and Marina Shmakova have found evidence of the existence of sub-galactic dark matter structures. They have posted a paper on the arXiv to report on this finding. P. Chen, J. Irwin, and M. Shmakova have been accepted as Guest Members of the SNAP collaboration. They expect to contribute to the gravitational lensing and dark energy search efforts in SNAP. Prof. Mary James and a student of hers are currently long-term visitors to the group who collaborate on this project.

*Experimental Activities:*

- E165: Fluorescence in Air from Showers (FLASH) Experiment

Recent observations of ultra-high-energy cosmic rays reported super-GZK events above  $10^{20}$  eV. However, the two major experiments, the ground-array air shower detector AGASA and the High Resolution Fly's Eye (HiRes) fluorescence detector, exhibit an apparent discrepancy in the observed absolute flux and in the spectral shape. Because of the importance of the physics involved, both groups are currently studying systematic effects that might contribute to the discrepancy. One such effect is the air fluorescence yield.

A proof-of-principle experiment, T-461, using the SLAC FFTB beams to trigger air fluorescence was carried out successfully in the FFTB in June 2002. A formal proposal (E165) by a five-institution international collaboration, “FLASH,” was approved later in November 2002. The first of three runs of this experiment, the “Thin Target Phase,” had been carried out successfully in September 2003. In June 2004, there was a successful “Thick Target” run, and in July a hybrid run was carried out. By the end of summer 2004, the data acquisition phase of E165 was essentially over.

The major activity during FY05 was data analysis and publications. The data collected from E165 were very good. Two presentations, one on FLASH's Thin Target results and the other on its Thick Target results, were presented at the important biannual International Cosmic Ray Conference in India, August 2005. The major publication on Thin Target results, lead by Kevin Reil, is near ready for release.

- Research and Development of other LabAstro Experiments

An R&D effort has been under way in preparing LabAstro experiments beyond FLASH. One major direction is an experiment to investigate the astrophysical dynamics involved in cosmic particle accelerations and jet-plasma interaction. K. Reil, P. Chen, and R. Sydora (Alberta, Canada) have been actively pursuing simulations of Alfvén-wave induced plasma wakefield acceleration. The simulation results support the original notion of an Alfvén shock induced plasma wakefield acceleration mechanism. A formal paper that reports on this finding is currently under preparation. J. Ng and R. Noble at SLAC have been pursuing simulations of jet dynamics, which have yielded exciting results reported in their paper submitted to *Phys. Rev. Lett.* for publication.

- R&D on SALSA

The group has engaged in R&D on a new initiative, the Saltdome Shower Array (SALSA), in an attempt to detect ultra-high-energy cosmic neutrinos with sufficient statistics. If successful, this experiment will have significant impact on astrophysics as well as particle physics. It should help to discern the origin of cosmic ray production sites. On the other hand, with the center-of-mass energy at  $\sim 100$  TeV, when such a neutrino interacts with a proton in the salt, it should also provide important insights into particle physics at an energy frontier which is about an order of magnitude higher than that of LHC.

### **6.B. FY05 Progress: Accelerator Research Department B (ARDB) by Robert Siemann**

Accelerator Research Department B (ARDB) conducts research into the physics and technology of accelerators with a strong emphasis on high-gradient acceleration and advanced concepts.

A UCLA, USC, SLAC/ARDB collaboration is continuing with an experimental program to study all aspects of beam-driven plasma wakefield acceleration. The SLAC beams offer a unique opportunity for this, and there have been fourteen experimental runs (as experiments E157, E162, E164, and E164X) for over fourteen months of beam time from June 1999 through August 2005. The E157 and E162 data have been analyzed, and the results have been published in thirteen papers in peer-reviewed journals.

Experiments E164 and E164X emphasized short bunches made possible by the installation of a compressor chicane in the linac. These experiments were motivated by simulations and theoretical results that predicted that the acceleration gradient would vary as the inverse of the square of the bunch length provided the ratio of the bunch length to plasma wavelength was held constant. The main features of the experiments were an extremely short bunch length, 0.02 to 0.1

mm, and a 10 cm long, high density plasma source capable of reaching densities above  $3.5 \times 10^{17}$  cm<sup>-3</sup>. Innovative instrumentation to measure and monitor the bunch length was also required and was an integral part of these experiments. It was discovered in FY03 that there was significant beam generation of plasma, and experiments performed in FY04 showed large acceleration gradients. These data were analyzed in FY05, and the results were published in an article featured on the cover of *Physical Review Letters*.

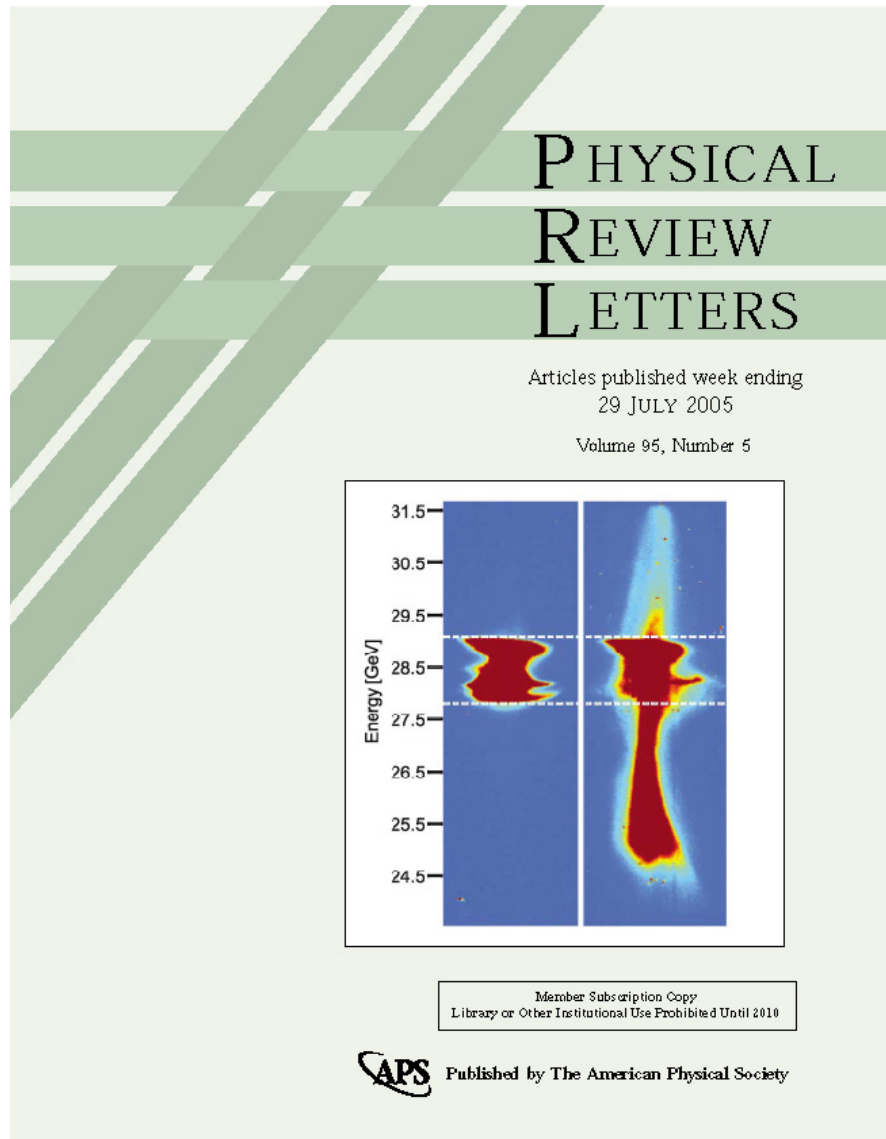
- M. J. Hogan, et al., « Multi-GeV Energy Gain in a Plasma Wakefield Accelerator, “ *Physical Review Letters* **95**, 054802, 2005.

In this paper, which has been widely recognized as a milestone in the development of plasma accelerators, it was shown that accelerating gradient in excess 27 GeV/m were sustained for 10 cm of plasma length resulting in energy gains of 2.7 GeV.

The energy aperture of the beamline downstream of the plasma limited the energy gain and plasma length in E164 and E164X. That aperture restriction was identified and removed, and in an experimental run in August 2005 energy gains of more than 10 GeV were observed using a 30-cm-long plasma. The experiments demonstrating this new world-record energy gain were in progress just when the previous results in Hogan et al were being published and widely cited.

In addition to the acceleration, we observed and measured some of the properties of a new phenomenon, accelerated electrons that originate from the plasma at high gradients. Analysis of the data from the August 2005 experiment and further plasma accelerator developments will be major activities in FY06.

Lasers have extraordinary potential as accelerator power sources. Their large fluence leads to the possibility of high gradients. This was realized soon after the invention of the laser, but, until recently, the laser has not been a practical power source because of low efficiency. Recent developments have raised the efficiency of solid-state, mode-locked lasers to well above 10%. This has changed the situation, and laser driven accelerators have become a major activity of the ARDB program. The ARDB laser acceleration studies, performed in collaboration with Stanford physicists, are wide-ranging and have both experimental and theoretical aspects.



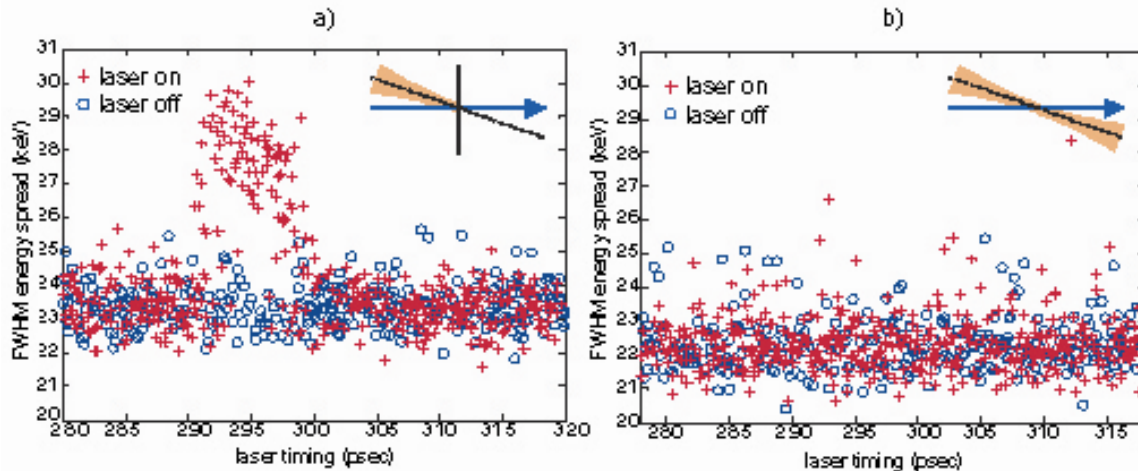
The multi-GeV energy gain reported by M. Hogan et al was featured on the July 29, 2005 cover of *Physical Review Letters*.

Experiments at the Hansen Experimental Physics Laboratory on the Stanford campus that address fundamental and practical aspects of lasers were completed in FY05 and the results submitted and accepted for publication.

- T. Plettner et al, “Visible-Laser Acceleration Of Relativistic Electrons In A Semi-Infinite Vacuum,” *Physical Review Letters* **95**, 134801, 2005.
- C. M. S. Sears et al., “High Harmonic Inverse Free Electron Laser Interaction at 800 nm,” accepted for publication in *Physical Review Letters*.

A new particle acceleration mechanism was demonstrated using 800-nm laser radiation to accelerate relativistic electrons in a semi-infinite vacuum in the Plettner et al. paper. The experimental demonstration was the first of its kind and was a proof-of-principle for the concept of laser-driven particle acceleration in a structure loaded vacuum. We observed up to 30 keV

energy modulation corresponding to a 40 MeV/m peak gradient. The energy modulation was observed to scale linearly with the laser electric field and showed the expected laser-polarization dependence. Furthermore, as expected, laser acceleration occurred only in the presence of a boundary that limited the laser-electron interaction to a finite distance.



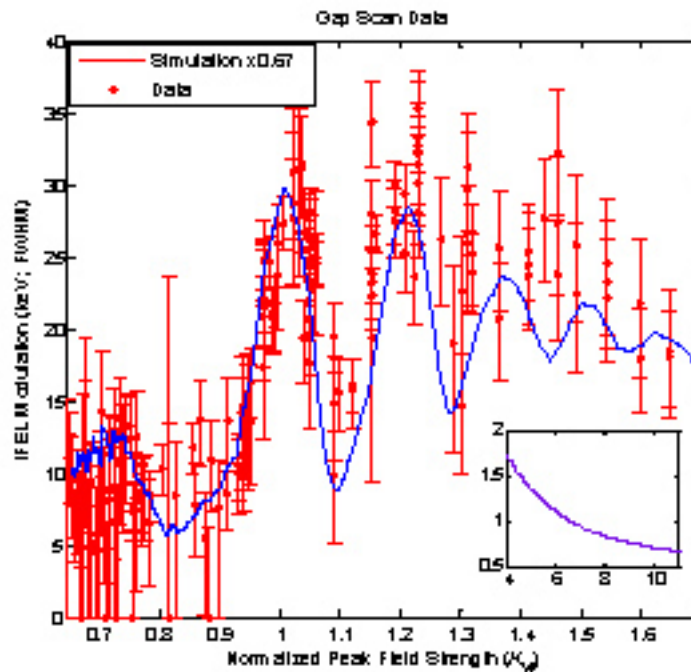
Experimental confirmation of laser acceleration from T. Plettner et al

The first direct observation of a higher order inverse free electron laser (IFEL) interaction was presented by Sears et al. Interaction was observed at the 4th, 5th, and 6th harmonics from an IFEL operating at 800 nm. The harmonic spacing, relative harmonic strength, and transverse beam overlap of the interaction were all in good agreement with tracking simulations. The IFEL interaction is important for forming bunches of electrons spaced at the laser wavelength, and this experiment was a first step in realizing an IFEL optical buncher.

Research in laser acceleration will move from the Stanford campus to SLAC where it has been approved as experiment E163. E163 will be located at the NLCTA (Next Linear Collider Test Accelerator). Designing and building the E163 infrastructure has been a major activity during FY05. The laser-driven rf electron source was installed at the NLCTA. An environmentally controlled clean room was constructed for the E163 laser systems, these lasers were moved to this new clean room and commissioned there, and magnet fabrication is nearly complete. Conditioning of the electron source is imminent, and the beam line should be complete and experiments starting in FY06.

Laser accelerator structures are being designed primarily using computer simulations. The emphasis remains on photonic crystals that could be fabricated by either optical fiber drawing or lithography. Studies of energy efficiency continued, and another manuscript was published. In this paper the optimum energy efficiency of a laser driven linear accelerator was calculated. It was shown that it could be enhanced incorporating the accelerator into a cavity that is pumped by an external laser, and the effects of multiple bunches was considered.

- Y. C. Neil Na et al, "Energy Efficiency of an Intracavity Coupled, Laser-Driven Linear Accelerator Pumped by an External Laser," *Physical Review Special Topics – Accelerators and Beams* **8**, 031301, 2005.



Scan of the IFEL gap comparing measurements and simulations and showing the harmonic IFEL interaction. (C. M. S. Sears et al)

The ARDB research program would not be possible without collaborations with colleagues from UCLA, USC, and Stanford who are an integral part of every activity. This research would also be impossible without students, and their education is an important part of the ARDB program. One of our students completed her PhD degree in FY05

- Caoliann O'Connell (Ph. D., Stanford University, August 2005) "Plasma Production via Field Ionization."

There are eight ARDB graduate students at the present time, and three students from collaborating institutions are working with ARDB on their dissertations.

## 7. FY05 Progress in Advanced Computations Research by Kwok Ko

During FY05, research in ACD covered parallel code development, collaborations in computational science, and accelerator modelling for projects across the Office of Science. Efforts were also devoted to the annual SciDAC Principal Investigators (PI) meeting, to the Joule report for the DOE MICS Office and to the preparation for the US Particle Accelerator School (USPAS). Progress and highlights in each of these areas are summarized below.

### *Parallel Code Development*

Complex Solver in Omega3P – A major advance was achieved for the parallel eigenmode solver Omega3P to enable the modeling of rf cavities coupled to matched waveguides. Because of the power flow out of the cavity, the eigenmode frequency now becomes complex. Of interest is the  $Q_{ext}$  which is given by one-half the ratio of the real to imaginary part of the frequency and provides a measure of the mode damping effect. The complex eigenfrequency is obtained by

solving a nonlinear eigenvalue problem, the details of which are described in a later section on computational science collaborations. This new solver has been ported to the IBM SP3 at NERSC and the Cray X1E at NLCF for use in the ILC and JLab applications and the results are reported in a later section on accelerating modeling.

Wakefield Simulation with T3P – Several new features have been implemented into the parallel time-domain solver T3P to facilitate wakefield simulation including a beam port boundary condition for arbitrary beam-pipe cross section, a wakefield monitor and an improved beam projection. Wakefield benchmarks on standard geometries against MAFIA have been done while work on improving accuracy and performance continues. Applications to the ILC cavities and the MIT Photon-Band-Gap (PBG) structure are in progress. A 6-cell PBG structure has been fabricated at MIT and reached 35 MV/m in cold tests. (E.I. Smirnova, et al., *Phys. Rev. Lett.* **95**, 074801, 2005). The wakefield simulation of this structure with T3P constitutes one main task for the DOE SBIR Phase 1 project with STAR, Inc. whose goal is to develop an advanced simulation toolkit for PBG Accelerators.

Multipacting Calculation in Track3P – Upon successful completion of dark current simulation in the NLC structure, the development of the parallel particle tracking code Track3P has turned to multipacting calculations in superconducting rf structures. The new capability has been benchmarked against MULTIPAC on the TTF and SNS cavities in determining multipacting barriers. Figure 1 shows the Track3P calculations of multipacting in KEK's ICHIRO cavity and tests show a soft barrier at field gradient of 23 MV/m as numerically predicted. The study of multipacting in the new KEK input coupler design for the ICHIRO cavity is ongoing.

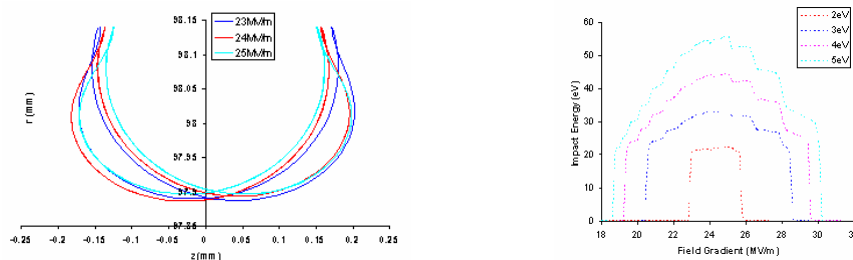


Figure 1: Track3P computed multipacting trajectories (left) and multipacting barriers (right) in the ICHIRO cavity

PIC3P for RF Gun Design – Under development is a new parallel particle-in-cell code, PIC3P, which is based on the finite element method specifically for high fidelity simulation of rf guns. All existing gun codes use structured grids which have difficulty in modeling complex geometries precisely. Particle methods on unstructured grids remain an open research topic and a pioneering effort is under way to make a breakthrough on this challenging computational problem. When completed, the new tool will be extremely useful for designing the rf guns that are required to drive the next generation of ERLs and FELs such as the LCLS II.



**Accelerating Modeling**

SRF Cavities for the ILC and JLab – An international team comprising DESY, KEK, JLab, FNAL and SLAC is collaborating to realize the Low-Loss (LL) cavity design for the ILC (see Figure 2). The LL cell shape presents a higher accelerating gradient than the standard TESLA shape (46.5 MV/m versus 35 MV/m from experiment) and the LL cavity has 20% less cryogenic loss. An important issue in the LL cavity design is HOM damping. Omega3P with quadratic elements was used to calculate the  $Q_{ext}$  of the dipole modes in the first LL design with a given configuration of the HOM couplers. Figure 3 shows how the mesh model of the cavity is partitioned with ParMETIS onto different processors. The  $Q_{ext}$  for the first 5 dipole bands are displayed in Figure 4 (left). It was found that a third band mode with significant R/Q is well trapped so efforts are under way to reduce its  $Q_{ext}$  (see section on shape optimization). On the IBM SP at NERSC, these computations required 300 GB of memory on 738 CPUs and generated results at the rate of 18 modes per hour.

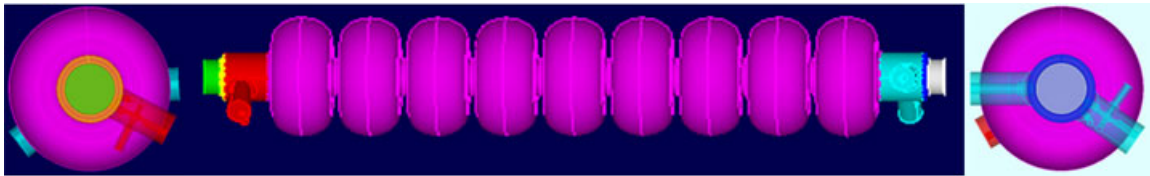


Figure 2: Model of the ILC LL cavity design

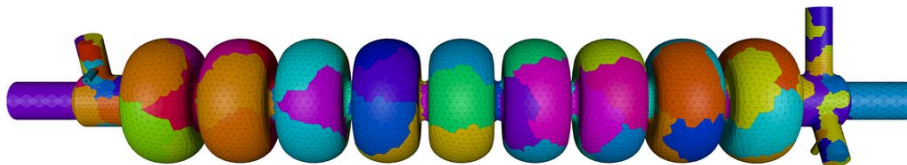


Figure 3: Partitioned mesh model of the LL cavity

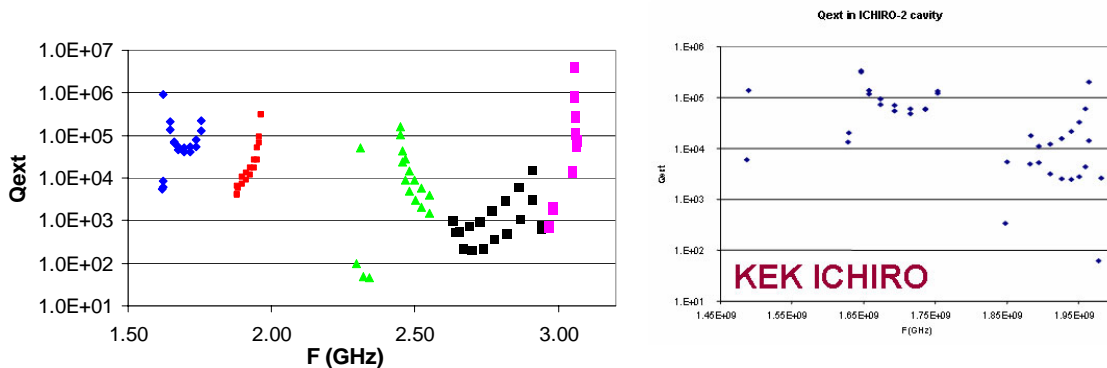


Figure 4: Omega3P results for the  $Q_{ext}$  of dipole modes in the LL cavity (left) and ICHIRO cavity (right).

Similar calculations have been performed for the KEK version of the LL cavity design, named the ICHIRO cavity, on the Cray X1E at NLCF. HOM damping results for a preliminary design are shown in Figure 4 (right) and since this cavity has a larger beam pipe, only two dipole bands are below cutoff. Different HOM coupler designs/configurations are being explored to further improve the damping.



Figure 5: (Left) Low  $Q_{\text{ext}}$  polarization of a dipole mode in JLab's 7-cell cavity, (right) high  $Q_{\text{ext}}$  polarization of same mode causing the BBU instability.

ACD and JLab have been collaborating on the comparison between Omega3P calculations and HOM measurements on JLab's 7-cell SRF cavity in operation in their FEL. Good agreement was found and simulation further identified the high  $Q_{\text{ext}}$  dipole mode that contributed to the beam breakup (BBU) instability in the machine.

ILC L-band Structures and S-band BPM – The prototype for a L-band 5-cell  $\pi$ -mode SW structure, half of the 11-cell SW structure proposed for the ILC positron source, was modeled using Omega3P. The design was optimized for low pulse heating and large cell aperture to improve stability and beam acceptance, while maintaining the same efficiency as the TESLA biperiodic SW design. The simplicity of the  $\pi$ -mode cell geometry (Figure 6) allows for more straightforward engineering of the thermal and mechanical designs. The final dimensions of this prototype have been generated for fabrication. Work has begun on a  $3\pi/4$  TW structure design chosen for higher rf efficiency for the positron preacceleration.

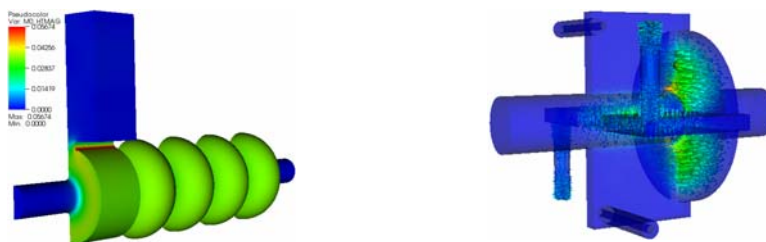


Figure 6: (Left) 5-cell  $\pi$ -mode SW L-band structure for the ILC positron source, (right) S-band BPM for the ILC cryomodule quadrupole.

Omega3P was also used to design the S-band BPM for the ILC cryomodule quadrupole. This design employs an innovative selective coupling scheme (Figure 6) in which the output couples only to the position sensitive mode and rejects the  $TM_{01}$  mode. Another important design feature is the easy access to the device for cleaning purposes. A prototype is being manufactured.

LCLS Input Coupler and Component Design – Although the coupler designs for the rf gun cavity and the L0A/B structures were completed a year ago, modeling efforts have continued to support design changes due to mechanical considerations and the effect of tolerances was also analyzed. In addition, power splitter and mitered bend waveguide components are being designed for both couplers. One power-splitter design using the parallel S-parameter code S3P is shown in Figure 7. Fabrication of these rf components is under way.

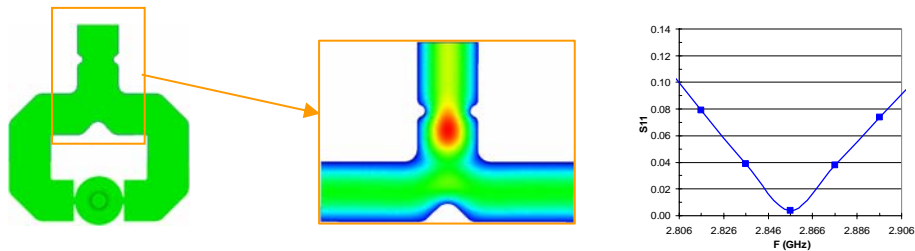


Figure 7: (Left) Power splitter design for the LCLS dual-feed input coupler, (Middle) field distribution of transmitted wave from S3P, (Right) Match of the power splitter calculated with S3P.

PEP-II Vertex Bellows - The PEP-II accelerator is operating at increasingly higher currents and shorter bunches to increase luminosity. As a result, higher higher-order-mode (HOM) power is generated that can cause overheating at beam-line components such as the vertex bellows near the IR. The vertex bellows has a complicated 3-D geometry with disparate length scales (see Figure 8), ranging from 60 microns in the gap between the contact fingers to 2.5 cm for the radius of the vacuum chamber. Plans are to mount ceramic tiles on the bellows convolution to damp the localized modes excited by the beam (Figure 8). With the complex solver in Omega3P the damping calculations show that the  $Q_0$  of the bellows modes can be reduced to below 30.

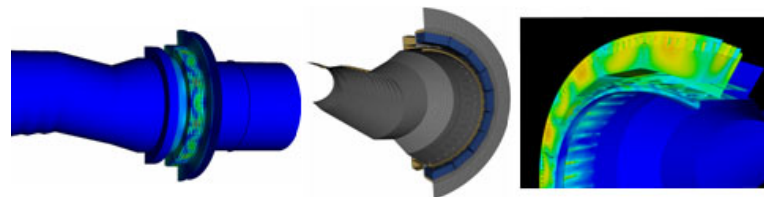


Figure 8: (Left) Localized mode in the PEP-II vertex bellows; (Middle) Ceramic tiles mounted on bellows convolution; (Right) Dielectric loss of trapped mode calculated with Omega3P.

### ***Collaborations in Computational Science***

Nonlinear Eigenvalue Problem in Waveguide Loaded Cavities – In modeling waveguide-loaded cavities, the boundary conditions at the waveguide ports are a function of the eigenvalue if the matched outgoing wave conditions are applied. In this case, the eigenvalue problem for finding the normal modes becomes nonlinear. If only one waveguide cutoff is assumed, the nonlinear

problem can be transformed to a quadratic eigenvalue problem (QEP). Working with LBNL and UC Davis under SciDAC, two algorithms have been developed to solve the QEP. The first algorithm follows the Second Order Arnoldi (SOAR) method which generates an orthogonal basis set for the second order Krylov subspace. When used with the standard Rayleigh-Ritz orthogonal projection technique, SOAR can be directly applied to the QEP while preserving its structure and properties. The second algorithm is a straightforward scheme called self-consistent iteration (SCI) which is also applicable to nonlinear eigenvalue problems with multiple waveguide modes. The method proceeds by simple successive approximation starting with the linear solutions without the waveguide terms and then iterating until the residual of the nonlinear eigensystem is below a specified tolerance. Although a theory is lacking to guarantee convergence, in practice, this algorithm often converges within a few iterations.

SOAR is used for Omega3P calculations of modes that are below beam-pipe cutoff as all the couplers (fundamental and HOM) are terminated in coaxial lines. For modes above cutoff, the SCI is applied. These solvers have been benchmarked on simple geometries against other codes, and have proven to be accurate in modeling complex cavities when compared with measurements on the TTF cavity (see Figure 9) as well as the FEL cavity at JLab. Together with higher order elements and parallel computing in Omega3P, these new solvers have enabled entire 3D complicated open structures such as the TTF cavity to be modeled for the first time, and since then on a routine basis.

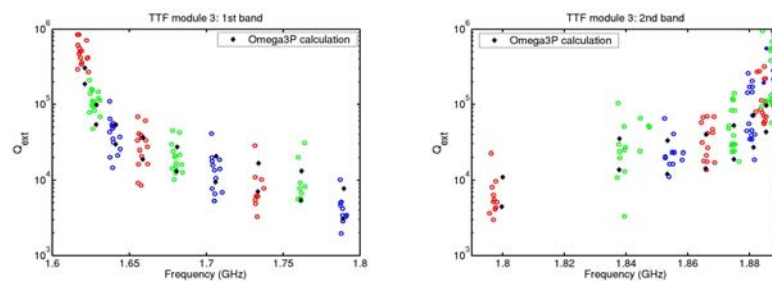


Figure 9 Comparison between Omega3P results (ideal TTF cavity) and measurements (8 TTF cavities in a cryomodule) for the 1<sup>st</sup> dipole band (left) and the 2<sup>nd</sup> dipole band. (right).

Mode Rotation and Visualization Cluster – New visualization tools developed in collaboration with UC Davis under SciDAC are being used to analyze the HOMs in the ILC cavity so that their effect on the beam can be better understood. Of particular interest is a new effect uncovered by visualization showing the time evolution of the HOM fields. In a fully 3-D geometry with no symmetry as is the case in the LL cavity, the degeneracy of the dipole mode is split and the two resulting modes can couple to each other if their resonance widths (due to damping) exceed the mode separation. This overlap leads to mode mixing resulting in fields that are elliptically polarized and causing them to rotate in time (see Figure 10). The formulation for calculating the mode rotation effect on the ILC beam dynamics has been developed and the implementation within LIAR is in progress.

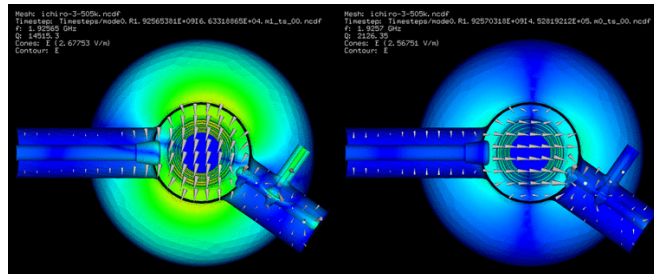


Figure 10: Snapshot of two coupled degenerate modes that rotate in the ILC LL cavity (cones and contours are electric fields)

Working with the High Performance Computing Group at SLAC's SCCS on the hardware side and the Visualization and Graphics Research Group at UC Davis on the software side, ACD has acquired a high performance Linux cluster with the plan to develop advanced visualization tools to aid in accelerator design. This new visualization cluster has 8 nodes, each with 4 GB memory (for a total of 32 GB), an nVidia GeForce 7800 GTX graphics board, dual AMD Opteron CPUs, and 250 GB hard drive storage with another 73 GB of high speed system storage. The nodes communicate over a high-speed, very-low-latency (less than 2 microseconds) Quadrics QsNet II network. Images will be rendered and composited entirely within the cluster/server with the final frames sent out to visualization client software running on user desktops.

Two types of visualization capabilities are envisioned for this cluster. First, a browser with focus-in-context feature will be developed in collaboration with UC Davis for fast and efficient visualization and comparison of many mode patterns. For example, one can select specific modes from a  $Q_{\text{ext}}$  vs. frequency plot and request the simultaneous display/animation of fields for direct comparison. The images and animations are computed and stored on the cluster/server which will be configured to support multiple clients. In further collaboration with UC Davis, a parallel rendering capability will be implemented to generate images from very large datasets by rendering the partitioned data and assembling subimages to display a final image on a visualization node. A prototype code has already demonstrated the efficacy of the approach.

Shape Optimization to Detrap High-Q Modes – Although simulation is already playing an important role in accelerating cavity design, shape optimization is still essentially a manual iterative process. A SciDAC collaboration involving SLAC, CMU, Columbia, LBNL, SNL and LLNL is focusing on developing a parallel, automated shape optimization capability by bringing together DOE's expertise in optimization, in adaptive mesh control and mesh smoothing, and in cavity design to implement a new design procedure through the application of state-of-the-art algorithms in large-scale PDE-constrained optimization. The approach has been used to detrap a localized dipole mode in the ILC LL cavity as shown in Figure 11. The goal is to optimize the end cells of the cavity so as to increase the mode energy there for stronger damping by the HOM couplers while keeping the accelerating and other dipole modes unchanged. A preliminary result from a primitive prototype is shown in Figure 11 while efforts of the collaboration are continuing.



Figure 11 (Left) Field pattern of a trapped mode in the ILC LL cavity with little fields in the end cells, (Right) design variables of the end cell and the optimized (red) vs. original (purple) geometry.

Parallel Meshing – Modeling the ILC cryomodule consisting of 8 to 12 SRF cavities will be far beyond the single CPU memory limitation of existing meshing software. A SciDAC collaboration with University of Wisconsin and Sandia Lab is working on a parallel meshing capability based on a solid model that uses the CHACO graph library to partition the geometry into subdomains and distribute them onto different processors. First, 2-D Meshes are generated for all the interfaces among subdomains which are then passed onto individual processors to ensure the connectivity at the subdomain boundaries. After that, meshes for the subdomains are generated separately without the need for communication. Figure 12 shows the test case for an ILC cavity mesh without couplers generated from four subdomains. Work has started on meshing a chain of 4 cavities in preparation for simulating the first KEK test cryomodule which will be constructed in the next year or two.

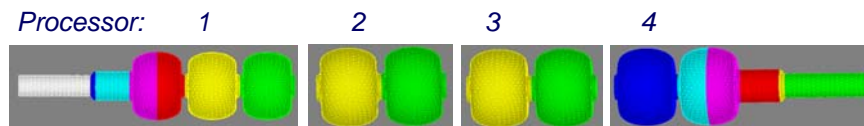


Figure 12: CAD based partitioning of the simplified ILC cavity for parallel meshing

SciDAC PI Conference – ACD contributed an invited talk and a poster paper at the 2005 SciDAC PI Conference which was by invitation only. Five invited talks from other SciDAC projects included materials on the collaborations with ACD on computational science research. All the papers have been published in the *Journal of Physics: Conference Series*, **16**, 2005:

K. Ko et al., “Impact of SciDAC on accelerator projects across the Office of Science through electromagnetic modeling,” (SLAC).

L. Lee et al., “Achievements in ISICs/SAPP collaborations for electromagnetic modeling of accelerators,” (SLAC).

V. Akcelik et al., “Adjoint methods for electromagnetic shape optimization of the low-loss cavity for the International Linear Collider,” (CMU, SLAC, Columbia, LBNL).

C. Yang et al., “Solving large-scale eigenvalue problems in SciDAC applications,” (LBNL).

X. S. Li et al, The roles of sparse direct methods in large-scale simulations (LBNL)

T. Tautges et al., “Interoperable geometry and mesh components for SciDAC applications,” (SNL).

K. Ma et al., “Scientific discovery through advanced visualization,” (UC Davis).

**DOE MICS Joule Report and X1E Allocation Award** – The Omega3P code was among the six parallel simulation codes in the Office of Science (SC) domain selected by the DOE MICS Office for the Application Software Case Studies in FY05 (Joule Report) for submission to OMB. For this report, the progress in software implementation and code performance on SC’s computing platforms was documented at the end of each quarter with an overall evaluation at year end. In the final report on Omega3P, the enhancement in science-driven performance measured on the IBM SP3 at NERSC is 81.3% while the increase in science capability is by a factor of ~3.89. These numbers were obtained by comparing the simulation in the first quarter of the TTF cavity using 743K tetrahedral elements and linear basis functions with that of the LL cavity in the 4<sup>th</sup> quarter when 523K tetrahedral elements with quadratic basis functions and second-order geometry were used. The SCI algorithm was used for the TTF cavity while the SOAR method was applied to the LL cavity. The performance metric was 1.23 seconds/eigenmode/processor for the TTF cavity versus 0.229 seconds/eigenmode/processor for the LL cavity. The science capability was measured by 816K degrees of freedom (DOF) used for the TTF cavity versus 3181K DOFs for the LL cavity.

In addition, ACD won a large time allocation award (200K MSP hours) from MICS on the new Cray X1E supercomputer (peak performance 18.5 teraflops) sited at the National Leadership Computing Facility (NLCF) in ORNL under the project “Computational Design of the Low-Loss Accelerating Cavity for the International Linear Collider.”

**US Particle Accelerator School** – In June at Cornell, ACD taught, for the first time, the USPAS course “Computational Methods in Electromagnetism” without the use of any commercial software. ACD’s electromagnetic codes were ported to the Windows PC platform and interfaced to the mesh generator CUBIT and the postprocessor VISIT, allowing students to perform numerical exercises in rf cavity design and analysis. CUBIT from Sandia and VISIT from LLNL are both public domain codes. With further support, this simulation package could potentially be developed into a replacement for existing rf modeling software from commercial vendors.

## **8. FY05 High Polarization Electron Source/Accelerator Materials Development by Bob Kirby and Takashi Maruyama**

The Physical Electronics Group, now the **Surface and Materials Science Department (SMS)** contributes to SLAC's accomplishments in a number of areas, by using vacuum and materials expertise to support the development of novel electron sources, detectors and accelerating structures. Current areas of focus include a high-polarization, high-current electron source for the ILC, metal photocathodes for the LCLS photoinjector, and surface-analytical research and development on methods for suppressing collective electron instabilities in high current positron/proton storage rings.

SMS engages in a continuing research collaboration with ARD-A's Experimental Group A, Sources and Polarization Group, and the University of Wisconsin on the development of **high-polarization, high-current semiconductor electron sources**, originally for E122, then for the SLC and End Station A experiments, and currently for the ILC. Polarizations as high as 78% were produced for the Stanford Linear Collider (SLC) from photocathodes based on a thin GaAs epilayer grown on GaAsP. However, after 10 years of experience with many cathode samples at

several laboratories, the maximum polarization using the GaAs/GaAsP single strained-layer design cathode remains limited to 80%, while the quantum efficiency (QE) for a 100-nm epilayer is only 0.3% or less. Two known factors limit the polarization of these cathodes: 1) a limited band splitting; and 2) a relaxation of the strain in the surface epilayer. Strained superlattice structures, consisting of very thin quantum well layers alternating with lattice-mismatched barrier layers are excellent candidates for achieving higher polarization because they address these two issues. Due to the difference in the effective mass of the heavy- and light holes, a superlattice exhibits a natural splitting of the valence band, which adds to the strain-induced splitting. In addition, each of the superlattice layers is thinner than the critical thickness for strain relaxation. Supported by a DOE SBIR Phase II program, strained-superlattice photocathodes based on GaAs and GaAsP have been investigated in collaboration with SVT Associates, who grow such wafers using molecular-beam-epitaxy (MBE). The principal structural parameters (well and barrier thickness, phosphorus fraction, and the number of superlattice periods) were varied systematically to discover the optimal structural details. A heavy-hole/light-hole energy splitting of 90 meV was achieved, and the heavy- and light-hole excitations are clearly observed in the QE spectra for the first time. Spin polarization as high as 86% is reproducibly observed with the QE exceeding 1%. The essential results of the SBIR have been published in *Applied Physics Letters* **85**, 2640, 2004.

Although the SBIR was successful in achieving higher polarization and higher QE than strained GaAs, the goal of > 90% polarization, for the ILC, was not achieved. The polarization appeared saturated at about 85% and a spin-depolarization mechanism seemed to be present. To investigate the spin-depolarization mechanism, we are investigating three structures:

- 1) GaAs/InGaP strained-superlattice structure – This is a structure similar to the GaAs/GaAsP strained-superlattice structure, but with the GaAsP barrier layers replaced by InGaP. The GaAs layers are quantum wells and continue to be strained. The spin-orbit interaction in InGaP is three times smaller than in GaAsP, and the spin depolarization is expected to be smaller. Since the band gap energy in InGaP is larger than in GaAsP, higher QE is also expected. A new DOE SBIR has been awarded to SVT Associates to investigate this structure.
- 2) GaAs/AlInGaAs strained-superlattice structure – Our long-time collaborator at St. Petersburg in Russia has reported 91% polarization from this structure. The aluminum content determines the formation of a barrier in the conduction band, while adding indium leads to conduction band lowering, so that the conduction band offset can be completely compensated by an appropriate choice of the aluminum and indium contents. As a result, higher vertical electron mobility and a lower spin relaxation rate are achieved. A test wafer grown by SVT Associates yielded 85% polarization.
- 3) Biased photocathodes – The spin depolarization apparently takes place during transport in the conduction band and in the band bending region. By applying a bias voltage, the electron drift velocity can be controlled and the band bending can be altered. The bias across the device is achieved through a metallic grid photolithographically grown atop the emitting GaAs surface and a back contact to the substrate GaAs. Supported by a DOE STTR Phase II program, spin-polarized photoemission from metal-gridded cathodes is currently being investigated in collaboration with Saxet Surface Science.



**Electron cloud disruption** of positively-charged beams is a significant problem in high-current positron and proton rings, and is expected to be a problem in the LHC main ring and the **ILC positron Damping Ring**. Heating by very low energy secondary electrons endangers the LHC beam chamber cryogenic budget. SMS's X-ray photoelectron spectrometer (XPS) makes secondary electron yield (SEY), as well as surface chemical valence, measurements down to 10 eV primary electron energy. In FY05, secondary yield and XPS measurements continued on yield-suppressing titanium nitride (TiN) and nonevaporable getter (NEG) coatings. Yields from **grooved surfaces** of aluminum (Al) were particularly interesting in that grooving plus TiN coating have a cumulative yield-lowering effect. Various grooving profiles were measured, bare or with TiN coating, with coated values as low as 1.2, before electron conditioning (which lowers the yield further during commissioning).

NEG coating of beam chamber walls is promising because of its residual gas pumping capability. It also acts as a diffusion barrier for gas permeating out from the chamber wall. NEG-coated Al surfaces showed acceptably low yields, even after gas saturation of the NEG. On the other hand, measurements following electron conditioning and re-contamination of uncoated flat Al material showed conclusively that electron conditioning alone cannot reduce the yield below 2. A yield of  $< 1.9$  is essential for electron cloud suppression. NEG and TiN-coated Al and stainless steel gave SEYs of  $< 1.7$  after recontamination and  $< 1.2$  after electron conditioning.

In FY06, coated pieces of flat and grooved chamber wall will be inserted into the PEP-II ring to determine the effect of photon scrubbing on SEY. The samples will be transported, after exposure and under vacuum, to the XPS chamber for yield measurement. Next for laboratory experiments will be yield measurements following simulated residual gas ion bombardment of the coatings, using an ion gun.

The superconducting **accelerating cavities** for the **ILC** will be constructed of high resistivity ratio (RRR) niobium (Nb) sheet. Excessive oxygen within the microwave skin depth (several microns) will reduce the RRR and increase resistive losses. Using XPS and a heating sample holder, we measured the thickness of the native oxide layer on several Nb samples following bake-out simulations in order to discover whether baking is sufficient to remove the native oxide layer and restore the high RRR. Results showed that the oxide layer slowly dissolves into the Nb bulk at 500°C, leaving an 0.5 nanometer residual layer of Nb<sub>2</sub>O that will require a much higher temperature (~1200°C) to decompose.

The Linear Coherent Light Source (**LCLS**) injector is scheduled to commission with a **metal photocathode** having a **quantum photo-efficiency (QE)** of  $> 2 \times 10^{-5}$  at the exciting laser wavelength of 255 nm. Ideally, cathodes will be prequalified for installation by measuring the QE offsite and processing the cathode to maximize the QE. Then, after installation at the injector, only a modest bake out would be required to remove adsorbed water and hydrocarbons. Downstream contamination of the surface during beam operation will require either periodic rebaking (with its inherent risk of opening a vacuum leak) or using *in situ* ion or atom bombardment to remove the contamination. Previously, laser desorption cleaning by others has been shown to be of marginal success and irrevocably damages the emitting surface. A program is underway in SMS to qualify cathodes by XPS (characterize the contamination), atomic force

microscopy (AFM, measures surface roughness), and to measure the QE from 190-300 nm. In a model approach, diamond-machined copper coupons have been baked out in the XPS system, which improved their QE by 3-4 orders of magnitude, depending on initial QE, to  $> 2 \times 10^{-4}$  at 255 nm. Surfaces were allowed to sorb residual gas for several weeks, by which time the QE degraded a factor of two. A brief bombardment with 1 keV argon ions restored the QE to its previous high level. Copper coupons were also cleaned to similarly good QE by ions only (no bake-out), even **hydrogen ions**. The AFM showed no surface roughness change caused by the bombardment. That suggests that the emittance would also not have been affected.

In FY06, we plan to systematically clean coupons with hydrogen ions only, expose to room air, re-bombard and determine the conditions that are most efficient for **making high-QE cathodes** that are easily restorable in the injector with an in-situ ion gun or microwave discharge. A cathode will be similarly treated and installed in the LCLC Gun Test Facility at SSRL.

### **9. FY05 Progress in Fractional Charge Particle Research (Martin Perl)**

A highly automated Millikan oil drop apparatus, with extensive feedback and self regulating controls, has been used throughout all of FY2005 to search for fractional charge elementary particles in meteoritic material suspended in a special mineral oil. The apparatus was developed and first tested in FY2003. This search will conclude in FY2007. When concluded, this will provide a very substantial search for fractional charge particles in meteoritic material and the most extensive search ever carried out in mineral oil.

The reason for searching for fractional charge elementary particles in meteoritic material is that this material that comes from asteroids formed about 5 billion years ago is one of the least processed material in the solar system, and is one of the best candidates for containing fractional charge particles. The experimenters believe that asteroidal material is about one million times more likely to contain fractional charge particles, if they exist, compared to terrestrial material.

### **10. FY05 Progress in the Test Experiment Program (Coordinated by Roger Ericsson)**

The test experiment program was resumed after the accelerator had been restarted and the first runs of the main Final Focus Test Beam (FFTB) program had been completed. Beam for the tests was delivered in intervals between SPPS, E166, and E-164X runs. Since beam cannot be delivered to the FFTB and End Station A (ESA) simultaneously, the opportunity was taken, while installation was going on in FFTB, to send beam to ESA. This allowed an ESA secondary beam of less than one particle per pulse to be delivered for T-469, a characterization of an advanced *Cerenkov* technique. The other test experiments required the beam characteristics of the FFTB. T-478 and T-481 needed the small spot size and the subpicosecond pulses to study magnetic film switching properties and wakefield acceleration, respectively. T-482 made use of the pellicles available in the beam, and the SPPS X-ray beam line and its detectors, to characterize transition radiation.

**T-469, DIRC R&D Program: D.W.G.S. Leith, J. VaVra**

The experiment used a beam of  $\sim 1$  particle per pulse to test the performance of a quartz bar *Cerenkov* detector. The detector is a development of the DIRC particle identifier in BaBar. It uses a spare quartz bar from BaBar, but incorporates multipixel photomultiplier tubes, and electronics affording high resolution in both space and time coordinates.

The DIRC system at BaBar affords excellent particle identification in the relevant particle energy range. In possible future applications at much higher luminosity, limitations to the technique are expected to arise from beam induced backgrounds in the large water tank that serves as an optical coupler between the quartz and the photomultiplier tubes. In addition, the *Cerenkov* cone reconstruction resolution is limited by the optical dispersion in the quartz (the variation in the light propagation speed with wavelength). Both of these concerns are being addressed in this test. By using parallel-to-point focusing optics and light detectors with millimeter size pixels, rather than 3 cm pixels, the size of the coupling fluid tank can be reduced by two orders of magnitude. The pixellated photomultipliers also have excellent timing characteristics, and coupling that with multi-channel electronics with high resolution timing, the optical dispersion in the long quartz bar can be corrected by measuring its time of propagation to  $\sim 100$  ps.

The 3.6-meter-long quartz bar has been mounted on a movable stage at the downstream end of End Station A, where the low-intensity secondary beam was delivered. Light from the end of the quartz was focused, by a 50-cm focal length mirror, on to an array of six 64-pixel photomultipliers of various designs. The optical coupling from the quartz to the photon detectors was achieved by using mineral oil. Detectors were from Burle (multichannel plates) and Hamamatsu (foil dynodes). About 200 channels of preamplifiers using Elantek chips, and custom developed constant fraction discriminators, provided tight timing signals to a TDC system. The timing fiducial was derived from the linac timing system, and was monitored for drift by using a counter in the beam with  $\sim 55$  ps resolution. Preliminary results for the quartz bar system give a time resolution of 100 – 150 ps for single photons. The width of the distribution of photon arrival times was seen to increase with the photon path length, as expected for the optical dispersion in the bar. Analysis continues toward applying the measured arrival times as a correction for dispersion's effect on the reconstructed *Cerenkov* cone, improve the resolution on the measured cone angle, and so enhance the particle identification capability. Further tests with the present system are anticipated early in FY06. Longer term plans include tests with improved photon detectors.

**T-478, Magnetism with Ultrashort Magnetic Field Pulses: H. Siegmann**

The experiment focused the FFTB beam on to a series of very thin magnetic films. It made use of the extremely high magnetic fields around the beam to explore the fast switching characteristics of the materials. Data were taken with pulse lengths of about 80 femtoseconds and also as long as 2 picoseconds for comparison.

The physics being explored is that of the dynamics of precession of ferromagnetic spins. The fastest and most efficient magnetic switching is achieved by letting the magnetization process

about the externally applied field. It has been established that a coherent precession of all the dipoles in the sample requires frequencies no higher than a gigahertz. Faster than this, exchange fields appear to be generated that produce torques on the magnetization, causing random ballistic changes in it that continue after the field pulse has passed. A quantitative understanding of this was the goal of the experiment. It studied the limits of high switching rates by using the strongest and shortest magnetic field pulses available with present technology. The FFTB beam, focused to spots less than 20  $\mu\text{m}$  diameter, was tuned to pulse durations of about 80 fs, and sent through various thin magnetic films on various substrates. The magnetic field of the beam falls off with radius, allowing a wide range of field strengths approaching a megagauss to be studied at distances of 50 to several hundred microns from the place where the beam penetrated.

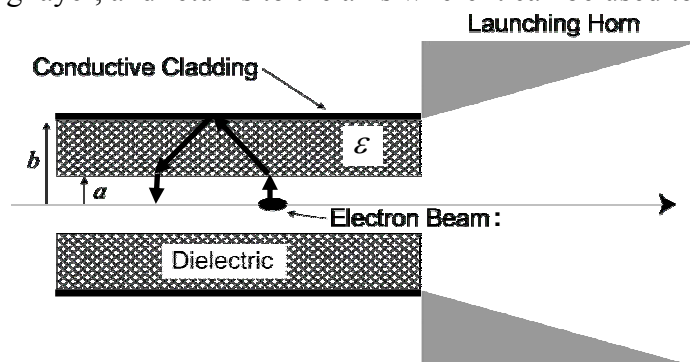
The apparatus was installed at the main focus of FFTB, and considerable care was taken to establish a suitable beam focused at the plane of the samples. The premagnetized samples were then exposed to one or more beam pulses. After recovery, it is necessary to measure the field contours in the absence of oxygen, using a microprobe.

This work is proceeding, and detailed results will be available in several months, although interpretation may require some further time.

#### **T-481: Cherenkov Wakefield Acceleration Experiment: M.C. Thompson, LLNL.**

With the recent theoretical and experimental interest in laser acceleration, the issue of using dielectrics to support large accelerating fields has gained prominence. Various analyses have indicated that GV/m accelerating fields should be possible in dielectric-based laser accelerators, as long as illumination times are very short. Dielectric accelerators may also be powered directly by charged particle beams, via wake-field excitation. This mechanism has been studied in depth over the last several years, but with the maximum fields limited to 10's of MeV/m by the lack of ultra-short drive beams. According to the wakefield scaling laws, however, the recently achieved 20  $\mu\text{m}$  pulse-length beams obtained at the SLAC FFTB facility may give over GeV/m longitudinal fields in dielectric wakefield accelerator systems. T-481 uses the unique FFTB beam to examine ultra-high field wakefields (i.e., coherent Cerenkov excitation) in dielectrics.

An electron-beam-driven dielectric wakefield accelerator is essentially a uniform dielectric tube coated on the outside with a conductor. When an intense electron beam passes through center of the tube its electric field bends at the Cerenkov angle within the dielectric, reflects off the outside conducting layer, and returns to the axis where it can be used to accelerate other particles.



### Schematic of the dielectric wake experiment.

The experiment is the first in the GV/m regime of electron beam driven dielectric wakefield accelerators and the primary goals are to assess dielectric material survivability and verify the achieved wakefield magnitude. The experiment uses dielectric tubes of commercially available synthetic fused silica with 100 and 200  $\mu\text{m}$  IDs, and 325  $\mu\text{m}$  ODs. Tube lengths are limited to a few centimeters in order to mitigate alignment issues. While theory and simulation predict that the peak decelerating field experienced by the beam in these tubes will be as high as 8 GV/m, the energy gained or lost by beam particles can only be on the order of 10 MeV due to the short tube length. By comparison, the full energy spread of the highly compressed FFTB beam is several GeV. Consequently, energy changes are not resolvable in this experiment. The primary signatures of high-field dielectric wakes in the experiment are therefore the detection of material breakdown and measurement of coherent Cerenkov radiation produced in the dielectric.

The first phase of T-481 was conducted in a 48-hour run in mid-August 2005. The primary objective of the first test beam run was to determine the average breakdown field of the fused silica capillary tubing and thus the maximum sustainable accelerating field within the dielectric structure. The FFTB beam was successfully propagated through several capillary tubes and large amounts of data were collected, primarily images of the visible light emissions from the dielectric tube at various levels of beam compression. This is directly related to the strength of the fields on the inner surface of the dielectric. Analysis of the data is ongoing but initial examination clearly shows the onset of breakdown when fields reach  $\sim 4$  GeV/m at the dielectric surface (equivalent to a  $\sim 2$  GeV/m on-axis accelerating field).

Analysis of the physical condition of the dielectric tubes after their exposure to breakdown fields also gives information on failure mode. While we had expected most of the damage to the tubes to occur in the bulk of the fused silica, the most dramatic damage sustained was the vaporization of the aluminum cladding, with varying degrees of cladding loss. In general, the amount of cladding that remained after exposure decreased as either the number of shots and/or the beam current increased. The current theory is that the cladding loss results from resistive heating in the cladding as the beam's image charge travels through it. An initial rudimentary calculation seems to confirm this conclusion. Analysis of bulk damage to the fused silica is still in progress. However, it appears that the ability of dielectric structures to sustain accelerating fields above 1 GeV/m has been demonstrated.

A second run for T-481 is planned in early 2006, so that measurements of the coherent Cerenkov radiation (CCR) can be made. The quantity and spectral distribution of the CCR produced in the dielectric as part of the wake excitation process is directly related to the wakefield strength. Measuring the CCR will allow verification of the strength of the fields within the dielectric at breakdown. Currently, the field levels are deduced from the known structure and beam parameters.

**T-482, Investigation of XTR as an Electron-Beam Diagnostic: A.Lumpkin APS/ANL**

Transition radiation in the X-ray range, emitted sharply in the forward direction relative to the electron beam, has excellent optical diffraction characteristics and traces the divergence envelope of the initiating electron beam over extremely long distances. As a consequence, it could in principle be used as a tool for remote characterization of the divergence and mean trajectory angle of the electron beam. This test was intended to characterize the signal, comparing it with the SPPS undulator X-rays.

The experiment takes advantage of the existing FFTB and SPPS infrastructure. It was predicted that appreciable numbers of X-ray photons would be emitted in the forward direction as the 28.5-GeV electron beam transits the vacuum-metal foil interfaces. Since XTR is broadband radiation, it was planned to use the same monochromator setup as for the 9-keV SPPS wiggler fundamental, so the monochromator alignment was a prerequisite. This first step was not accomplished on the 8/21 startup shift due to the loss of monochromator stepper motor references in the computer. The shift was rescheduled the last day of the SPPS run, so the three-element monochromator was indeed tuned for 9-keV X-rays. The next step was obtaining reference images of these X-rays in the X-ray CCD camera. This had to be done without cooling the sensor because the camera was not leak tight at this time. It had been pumped out two days earlier. Attenuation was added with Al foils in front of the camera to obtain reference intensity and position data. The wiggler gap was then opened and the attenuators (~4000 factor in Al foils) removed to characterize the X-ray synchrotron radiation background from the upstream dipole. A horizontal angle shift was noted between the two sources. This implies the e-beam must have steering after the wiggler and before the dipole.

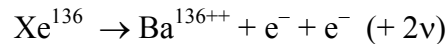
The thin Ti foils from the E-164X experiment were then inserted in various combinations. They are regularly used for backward optical transition radiation (OTR) imaging of the beam size in support of the plasma wakefield experiments. Two foil stations are before the wiggler and about 100 m from the SPPS diagnostics station. Another foil station is located downstream of the wiggler and about 80 m from this diagnostics station. In principle, these two source distances would give different annular radii for angular distribution patterns at the X-ray CCD.

Due to drifts in the camera backgrounds and the electron beam, the results of “foils out” versus “foils in” were inconclusive on this first run. Some intriguing images were recorded, with some distorted annular structures, during the “foils in” running which will be processed further at ANL. For a future test it is planned to run with the CCD camera cooled to reduce background noise, and at some later time a stack of foils may be installed to boost the XTR signal.

**11. FY05 PROGRESS FOR THE EXO DOUBLE-BETA-DECAY R&D PROGRAM by Peter Rowson**

SLAC groups SLD (M. Breidenbach, C. Hall, D. MacKay, A. Odian, P.C. Rowson and K. Wamba) and A (C. Prescott) have been collaborating with the Stanford Physics Department group of G. Gratta, and with others, in an R&D program to test the feasibility of a novel large-scale double-beta-decay experiment. This experiment, known as EXO (for Enriched Xenon

Observatory) proposes to use a large quantity (>1 ton) of Xenon enriched in the Xe136 isotope as both a decay and detection medium. The double beta decay process,



can proceed in the two neutrino ( $2\nu\beta\beta$ ) mode expected from the Standard Model (and which has already been observed in several nuclei other than  $\text{Xe}^{136}$ ), or possibly in the neutrinoless ( $0\nu\beta\beta$ ) mode. The  $0\nu\beta\beta$  process is expected to occur only if neutrinos are Majorana particles, and at a rate proportional to the square of an “effective” neutrino mass, and hence its observation would serve a mass measurement and as the first demonstration that Majorana neutrinos occur in nature. Xenon’s excellent calorimetric properties (necessary to distinguish the broad beta spectrum of the electron energy sum in the  $2\nu\beta\beta$  process from the line spectrum in the two-body  $0\nu\beta\beta$  decay), readily achievable high purity, and lack of worrisome radioactive isotopes make this element an attractive candidate for a low background experiment. In addition, we propose to operate the rare decay search in a coincidence mode, by identifying the barium daughter nucleus of double beta decay on an event-by-event basis. Barium identification is accomplished by a laser fluorescence technique that is sensitive enough to observe a single ion and, in principle, to distinguish the various barium isotopes.

To date, the R&D efforts at SLAC and Stanford have focused on a liquid xenon (LXe) TPC design, where the barium identification would be accomplished by removing the ion from the LXe using an electrostatic probe, and then delivering the ion to an as-yet-unspecified laser system. The campus group has successfully constructed and operated a laser-illuminated ion trap for barium and has observed single barium ions. In addition, they have demonstrated state-of-the-art energy resolution in LXe (which occurs at electric fields >4 kV/cm) and have preliminary results showing resolution enhancement when the scintillation light produced in xenon, in addition to ionization, is collected.

The logistical problems connected with the procurement of a large amount (~10 tons) of isotopically enriched  $\text{Xe}^{136}$  are being dealt with under the Nuclear-Nonproliferation programs of DOE. To date, we have obtained 200 kg of xenon isotopically enriched to 80% in  $\text{Xe}^{136}$ . The site for such an experiment must be deep underground to minimize cosmic ray backgrounds

A prototype that does not employ barium identification is presently being designed and built. It is our intention to construct a 200 kg prototype for use in the DOE-operated underground facility WIPP (Waste Isolation Pilot Plant) in Carlsbad, NM. This prototype would collect useful data for TPC performance, would definitively observe  $2\nu\beta\beta$  in  $\text{Xe}^{136}$  for the first time, and would accumulate the large number of  $2\nu\beta\beta$  decays needed to characterize this important background. In addition, a design goal is that the prototype has sufficient sensitivity to test with one or two years of data the recent and very controversial claims from the Moscow-Heidelberg  $\text{Ge}^{76}$  experiment that they have observed  $0\nu\beta\beta$  events.

### **SLAC Activities: R&D**

At SLAC, we have constructed a xenon purification system that is operated at ultra-high vacuum along with a xenon purity monitor (XPM). The purifier employs a heated zirconium metal getter

to remove nonnoble gas contaminants (nominally to the 0.1 ppb level), as well as distillation capability (to remove Argon). The XPM drift electrons produced from a UV-laser-illuminated cathode in LXe across a gap and measures the transport efficiency. The XPM was upgraded this year to include a longer drift region (60 mm was increased to 109 mm) for improved sensitivity to impurities. We have confirmed electron lifetimes as high as 4 ms in purified LXe in this way (more typically, results are  $\sim 1$  ms), and have reproduced electron drift velocities available in the literature. In addition, we have recently replaced our cold-finger/liquid-nitrogen (LN) cooling system for the XPM with a refrigerator that cools HFE-7000, a hydrofluoroether, into which the XPM is submerged. The HFE may serve as both a coolant and a radiation shield for the prototype detector, and also alleviates safety concerns regarding large volumes of LN at the WIPP underground facility. The new HFE-based system is working well.

We have continued a series of experiments to test the feasibility of electrostatic ion extraction from xenon. The “probe-test cell” incorporates a movable electrostatic probe, and an instrumented volume (PMTs, Si barrier detectors) for LXe or gaseous Xe containing a pair of HV electrodes. One of the electrodes holds a weak  $U^{230}$  source which undergoes two  $\alpha$  decays and emits  $Th^{228}$  and  $Ra^{222}$  ions into the Xe. We have seen that the probe tip, if set to negative potential, collects radioactive ions (thorium and radium  $\alpha$  decays confirm presence of the species). The apparatus has been used to measure ion mobility in LXe, an important issue as the barium ions will be produced in an electric field. The result obtained for thorium ions ( $0.24 \pm 0.02$  cm<sup>2</sup>/kVs) confirms the low mobility of metal ions in LXe observed by other groups. Recently, the probe was replaced with a “cryoprobe.” The cryoprobe is equipped with internal plumbing that functions as a Joule-Thompson expansion cooler, using high pressure argon gas. The probe tip is thereby cooled to below the freezing point of xenon, and ions are trapped in xenon ice. By this means, we have demonstrated that captured ions may be released by thawing the xenon ice, preventing irreversible attachment to a bare metal or dielectric probe tip.

A second approach using a “hot probe” is under study. We have seen in the literature how an appropriately chosen metal surface (e.g., platinum) can have a work function that favors the release of adsorbed metal atoms (e.g., barium) in a ionized state when heated to modest,  $\sim 500^\circ\text{C}$ , temperatures. An R&D program is under way to test this approach to barium ion release.

### **SLAC Activities : EXO200**

A substantial effort is now focused on development of the 200 kg prototype for installation at WIPP, which has been named “EXO200.” The EXO200 TPC detector will incorporate a  $\sim 20$  cm drift region, a maximum electric field of  $\sim 3$  kV/cm, and a detection plane consisting of wire grids and/or pads and large- area amplification photodiodes (LAAPDs).

The design of the EXO200 apparatus is nearly complete, and many major components are already being fabricated. The large low-radioactivity-copper cryostat will be delivered to Stanford campus soon. The custom-made modular clean rooms that will house the experiment at WIPP are already complete and installed in the Stanford HEPL facility, and are ready to receive the cryostat. Low-radioactivity shielding lead is being prepared and soon will appear at HEPL. The refrigeration systems, and xenon handling systems, which were designed by the SLAC team, are nearly complete and will be tested at HEPL in the coming months. Extensive



testing of the entire system at HEPL is planned prior to disassembly of the six clean-room modules, which will be loaded with the apparatus by that time, for shipment to WIPP.

A major effort is under way now to finalize the design of the xenon pressure vessel and the TPC electrode structure that it will contain. This effort is co-lead by a SLAC team of physicists and mechanical engineers, along with our colleagues at Stanford. It is planned that construction of the vessel and TPC would begin early next calendar year, and be complete by the summer of 2006.

Work is under way at SLAC to study light collection technologies for EXO200. As mentioned earlier, if ionization collection is supplemented by the collection of the 175 nm scintillation light produced in xenon, improvements in energy resolution are possible. The SLAC group has coauthored a paper, submitted to *Phys. Rev. B.*, on observations of ionization and scintillation correlation effects in LXe performed by the Stanford campus group (available in the LANL E-print server at [http://xxx.lanl.gov/PS\\_cache/hep-ex/pdf/0303/0303008.pdf](http://xxx.lanl.gov/PS_cache/hep-ex/pdf/0303/0303008.pdf)). We are measuring the performance of LAAPDs, and are preparing to release an order for a large number (~600) of these devices for use in EXO200.

The SLAC group has, thanks to assistance from local electrical-engineering manpower, designed and started production of the ~200 channels of low-noise, charge-sensitive preamps, and associated digitization and control modules for EXO200.

A SLAC group is leading the effort to produce a complete detector Monte Carlo, and in addition, event reconstruction software to be used for the prototype. A first pass version is ready now and has been extensively used.

The design of a full-scale device incorporating barium identification will follow pending the results of our R&D and prototyping efforts.

## **12. FY05 Progress in Theoretical Physics by Michael Peskin**

The research of the Theoretical Physics Group ranges from the development of fundamental theories such as M-theory, string theory, and higher dimensional theories at very short distances to detailed calculations and tests of theories directly relevant to high-energy physics experiments at SLAC and elsewhere. This section summarizes the current activities of the Theory Group and a few of its important achievements in FY2005.

**Physics at the International Linear Collider** – The Theory Group is intensively involved in all aspects of physics related to the development of the next-generation linear electron-positron collider (ILC). Much of the work involves understanding how to use the unique capabilities of the linear collider environment, such as beam polarization, highly efficient heavy-quark tagging, and the possibility of backward-scattered photon beams, to test aspects of new physics at very high energies that would otherwise be inaccessible. It includes analyses of linear collider experiments on the most familiar models of the next energy scale in physics, including studies of the measurement of the parameters of the spectrum of supersymmetric particles of possible strong interactions coupling to the Higgs sector and the top quark. It also includes exploration of

a wide variety of newly proposed models, some of which are discussed in later sections. Each phenomenon has a specific experimental realization at the linear collider, and we are making an effort to understand the systematic picture of how these effects can be found and distinguished. Complementing these theoretical studies, a general-purpose simulation program for ILC events has been created that allows a theoretical calculation of any new process to be easily turned into an event generator incorporating realistic beam and polarization effects.

Over the past year, we have been studying the specific linear collider experiments that might give insight into recent discoveries in cosmology. Cosmic dark matter, in particular, is likely to be produced at the ILC. In fact, the ILC provides an environment for the precision measurement of couplings needed to understand its cosmic relic density microscopically. In the past year, we have investigated this issue quantitatively for the example of supersymmetric dark matter, through Monte Carlo exploration of the large parameter space of models. The study has revealed that data from the ILC can be used in combination with astrophysical observations to test the hypothesis that supersymmetric particles make up the dark matter, and to measure the density of dark matter at many specific locations in the galaxy.

**Physics at Bottom Factories** – The Theory Group is intensively involved in all aspects of physics related to the physics of  $B$  factories, and the  $BABAR$  experimental programs in  $B$  physics and two-photon collisions. On one hand, members of the group have devised new methods for measuring the parameters of CP violation in the Standard Model from analyzing detailed aspects of specific rare  $B$  decay modes. At the same time, models of CP violation beyond the Standard Model have been intensively studied, as well as the reactions involving ‘penguin’ diagrams that are expected to probe for these effects most sensitively. In the past year, our work has clarified the theory of exclusive  $b \rightarrow u$  weak transitions and how experimental measurements of exclusive reactions can be used to produce an accurate determination of the weak interaction mixing parameter  $V_{ub}$ .

**Development of Quantum Chromodynamics** – Although there is strong evidence that Quantum Chromodynamics (QCD) is the fundamental theory of the strong interactions, there is much room for improvement in the methods by which QCD is applied to compute predictions for specific processes. Members of the Theory Group have devised improved computational methods for QCD both for high-precision studies and for the extension of QCD calculations to new regimes. These include the development of ‘commensurate scale relations’ which aid in removing scale and scheme ambiguities from QCD calculations, and the development of renormalization schemes that are analytic in the quark masses. These also include applications of QCD to exclusive  $B$  decays, charmonium production at high-energy colliders, and hadron and lepton production from nuclear targets. In the past year, members of our group have been studying new methods for computing the low-energy properties of the hadron motivated by string theory and duality of 4-dimensional QCD to models based in 5-dimensional de Sitter space. These methods give a very pleasing picture of the meson spectrum in QCD, both at low mass and in the asymptotics of Regge trajectories.

**Computational Perturbative Quantum Chromodynamics** – The most challenging aspect of improving methods for QCD is that of devising methods for high-order Feynman diagram calculations. Members of the Theory Group have been devising methods to simplify the

computation of diagrams involving essentially massless quarks and leptons participating in high-energy collisions. In terms of technical difficulties of QCD computations, the frontier now lies in the calculation of two-loop or NNLO corrections, and in one-loop calculations with a large number of quarks and gluons in the final state. These corrections are essential to interpret the Tevatron and the eventual LHC data to the few-percent level, and to understand the backgrounds to new physics signals at the LHC. Over the past few years, members of the group have taken a leading role in the community in developing methods for the computation of QCD processes at NNLO. In the past year, the work of our group has mainly been devoted to computing one-loop diagrams with many final-state particles, making use of new computational methods based on string theory in twistor space. These methods have made it possible to construct infinite families of tree-level amplitudes for quark, gluon, and Higgs boson reactions. In the past year, members of our group have extended these methods to loop amplitudes, where they seem a promising way to make many computations needed for the LHC analytically tractable.

**Superstring Theory and M-Theory** – Members of the Theory Group have been involved in studies of superstring theory and its possible relevance to elementary particle physics. Superstring theory may give a context for the solution of the cosmological constant problem, the question of why the observed cosmological constant is tens of orders of magnitude smaller than straightforward estimates in quantum field theory. Supersymmetry forces the cosmological constant to be zero, but only if it is an exact symmetry of Nature, not one that is spontaneously broken. It is a very important question whether there is an intermediate solution in which supersymmetry is broken but in such a way that the theory still controls the magnitude of the cosmological constant. A new direction of approach to this problem is related to the fact that the observed universe seems to contain a small positive cosmological constant. The first solution of string theory with a positive cosmological constant was constructed by members of our group in 2003. Since then, we have been developing more powerful methods for string model construction, and these have revealed a wealth of new solutions to string theory with positive cosmological constant.

Models with positive cosmological constant can also be models of inflationary cosmology. We have been using the newest insights into string theory model building to develop new mechanisms for inflation and its endpoint, and to explore signatures of the specific physics of inflation in the cosmic microwave background and other cosmological measurements.

**Realistic Models with Extra Space Dimensions** – Members of the Theory Group have played a central role in the recent development of models of elementary particle physics with large extra space dimensions. The inspiration for these models came from string theory constructions in which elementary particles are bound to a ‘brane,’ a subspace of a higher-dimensional universe. It was realized that, in theories of this type, the additional dimensions may be large, even macroscopic, and that gravity, cosmology, and elementary particle forces can be affected by the new dimensions at energies as low as those currently being probed in accelerators. A wide variety of tests have been devised for effects of higher dimensions that can be carried out at present and future accelerators. In the past year, members of the Theory Group have studied the accelerator tests and constraints on models of the ‘Randall-Sundrum’ type, in which matter, gauge bosons, and Higgs bosons can live on branes or in an extended 5-dimensional anti-de Sitter space. The various possible geometries of these models, for examples, the variety of

places that the Higgs fields might reside, lead to characteristic predictions about Higgs physics that can be tested at colliders.

**New Theoretical Methods** – Other new theoretical methods being developed by the Theory Group include: applications of object-oriented programming techniques to simulation problems in physics; new methods for solving lattice Hamiltonian systems; light-cone Fock state methods in nonperturbative QCD and nonperturbative studies of QCD in light cone quantization. Iterative renormalization-group-like methods for diagonalizing the Hamiltonians of many-body systems have been applied to 2-dimensional antiferromagnets, with promising results.

### **13. FY05 PROGRESS IN THE KLYSTRON DEPARTMENT BY GEORGE CARYOTKIS**

#### **Klystron Manufacturing**

The safety shut down at the beginning of the fiscal year and the subsequent restart process posed severe limitations on our production activities this year. Only seven 5045 klystrons (2 new, 5 rebuilds) were produced during the year. The annual 5045 production yield remains at 100% since there have been no test failures (except for two experimental tubes) of new or rebuilt 5045 klystrons since 2000. 5045 gallery MTBF is approximately 60,000 hours (an accurate MTBF cannot be calculated at present because of the large backlog of untested gallery returns). There are 20 on-line 5045's exceeding 100,000 hours.

The SLAC PEP II klystron S/N BFK-002B was completed and is currently finishing up test with excellent performance. Five klystrons (BFK-001A, -003A, -004A, -005A, and -006A) are installed and running in the PEP II HER. No SLAC-built PEP II klystrons have failed in service. There are currently four more klystrons in production. These are scheduled to be completed in 2-3 month intervals during this fiscal year. An order for two additional klystrons has been placed for delivery in FY07.

In addition, an XL4 klystron (XL4-14A) was completed and is now awaiting test. This is the first of two XL4's being produced for use by LCLS.

#### **Engineering**

At the beginning of FY2005, klystron research made a major change in emphasis due to the International Technology Recommendation Panel's recommendation that the entire LC community pursue the cold technology. At that time, the R&D group was fully engaged in design and test of X-band PPM klystrons. We were enacting a plan to finish up this work by "mothballing" the project, complete a final test on our last tube, and autopsy earlier tubes, when the worker accident occurred. The resulting shutdown of the klystron department resulted in the loss of use of our cranes, testing and fabrication facilities. Only by the end of August 2005, were we able to get our test facilities up and running. By the end of September 2005, we still had no operational cranes in our high bay area in order to move any klystrons. Much effort, perhaps as much as 25% of the available work hours, was also expended writing new procedures for various work in the department in order to conform to new safety regulations. Despite more than an 11-month loss of tube production, many accomplishments of the fiscal year are described below.

The existing prototypes for ILC rf power sources consist of three different vendor-produced Multiple Beam Klystrons (MBKs). At the klystron department we have been investigating the merits of a new class of klystrons known as Sheet Beam Klystrons (SBKs). Of particular note was the successful testing this fiscal year of a W-Band (95 GHz) SBK during September. Note that since this klystron is at 95 GHz and is so small and lightweight, the fabrication and testing of the device was able to proceed without the use of our cranes. The device performed exceedingly well when compared to our 3-dimensional simulations. Other SBK devices, which may find applications, are at L-band, as an ILC power source, and Ka-band, as a power source for the CERN CLIC accelerator efforts. Both these devices were investigated during the year. It is desired that funding for an ILC SBK design will become available soon. There is a recently funded Phase-II SBIR with ELCON where Ka-band SBK devices will be produced and tested with the aid of the klystron department.

We have made substantial progress over the year in our ability to simulate the 3-D behavior of klystrons. Structural, magnetic, electrical, beam-interaction, and particle-in-cell codes have received continued development over the year, along with our ability to operate such codes on multiple-CPU platforms. Three-dimensional simulations are necessary to continue the state-of-the-art development of new devices such as SBKs.

Other areas of development during the year include: work on a 952-MHz rf source design for a "Super B-Factory" design; X-band klystron design for the Linac Coherent Light Source (LCLS); testing, at CPI, of the CPI MBK klystron for DESY; work on an SBIR with DTI Technologies on a modulator for ILC klystrons to be delivered in 2006. In addition, presentations were made throughout the year cataloging the previously described work at various workshops and conferences such as Snowmass, RF2005, and ILC Workshops.

### **Compton X-ray Source**

This fiscal year, very little experimentation has been done on the Compton X-ray Source due to the safety shutdown, which prevented all operations until late in July. During this 10-month period, however, a new interaction chamber has been designed and built. This new chamber will replace the existing chamber and also a downstream Observation Chamber. The new chamber will permit the electron and laser beams to collide at exactly 180 degrees, reducing the tight temporal tolerances of the collision point. The new chamber will also be fitted with additional ports and an optical breadboard, located beneath the beams, designed to allow electrooptic experiments to be run. These experiments are useful for electron bunch length measurements.

In the area of timing jitter, we have been experimenting (during the last two months) with using a precision Local Oscillator and Phase-Locked Loop to reduce the timing jitter between the rf and laser. The laser oscillator will be phase locked to the local oscillator via a piezoelectric device which controls the laser path length. Currently the laser oscillator is the timing fiducial and the inevitable amplitude jitter of the laser introduces rf jitter.

During the next period we will install the new Interaction chamber, and begin X-ray measurements.

#### **14. FY05 Science & Technology Progress in the Radiation Protection Department by Sayed Rokni**

One of the responsibilities of the Radiation Protection Department (RPD) is to perform applied research in the areas related to radiation safety and shielding analyses. Many of these research efforts and results are summarized in SLAC Technical Notes and have been published in various scientific journals. During FY05, the following research topics were investigated:

- Production, attenuation and interactions of radiation with matter.
- Development and characterization of instrumentation.
- Design of shielding and dosimetry for high radiation environments.
- Development, maintenance and benchmarking of radiation production, interaction and transport computer codes.

##### **Neutron Energy Spectra and Yield Measurements**

Development of experimental techniques used in measurements of high-energy (>20 MeV) neutrons, which dictate use of shielding at high-energy accelerator facilities, is an important research goal for the RPD.

Data from the thick target neutron yield experiment carried out in 2004 at the Research Center for Nuclear Physics (RCNP) of Osaka University, Japan, was analyzed using the response functions of the NE213 neutron spectrometer. The response functions of the NE213 were also measured previously at RCNP. The data from the shielding experiment at Osaka University were also analyzed and investigated.

An analysis of experimental data obtained in August 2004 at the CERF facility at CERN has been performed. Using a newly upgraded response matrix and a new calibration curve, unfolding was carried out and good results were obtained for all measured locations. Energy spectra were established behind the various thick shields of concrete and iron for neutrons emitted from a thick copper target bombarded by a 120 GeV/c hadron beam. Experimental neutron energy spectra from 10 MeV to 400 MeV were obtained. MARS15+MCNP calculations were performed to compare with experimental data. Calculation results were within ~20% agreement with the experimental spectra.

Simulations were also made using a simplified geometry for the CERF facility with MARS15+MCNP, FLUKA and MCNPX. Calculations were made with and without the concrete shield using 1- or 120-GeV protons to investigate the differences of the source term and transmission through the shield as calculated by the 3 different codes.

##### **Development of the FLUKA Computer Code**

Universal and powerful Monte Carlo codes are essential tools for the accelerator community. A beta version of a major new (2005.6) release of the FLUKA code has been made available, and the corresponding documentation (Report CERN-2005-10/SLAC –PUB-11506) has been completed. The version has been thoroughly tested and has been used for SLAC shielding calculations since July 2005.

**Radiation Attenuation in Mazes**

The study of attenuation of photons and neutrons of different energies in concrete mazes continued using the FLUKA computer code. An analytical formula was developed that fits the results from these computational simulations so one can quickly and accurately calculate the photon and neutron attenuation in concrete mazes.

**15. FY05 Progress in SSRL OPERATIONS by piro pianetta****FY2005 User Experimental Run**

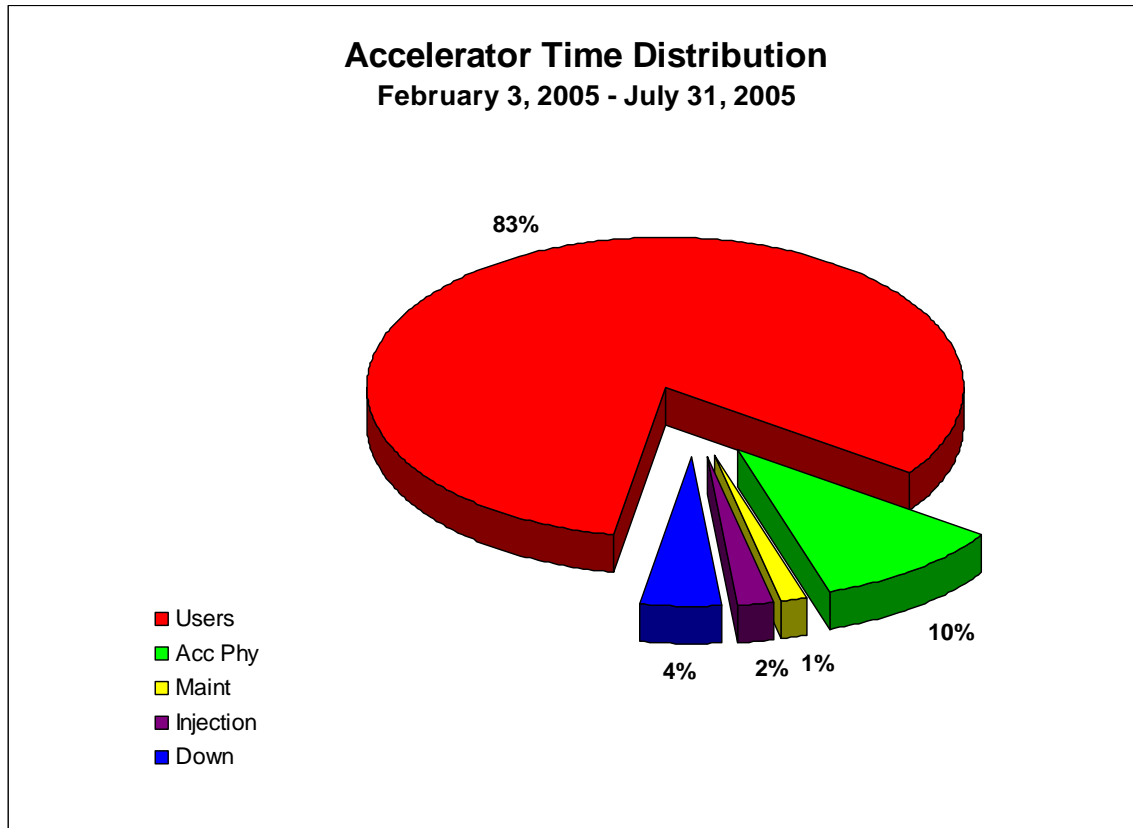
The FY2005 user run (February 4, 2005 – August 1, 2005) delivered 95% of scheduled user shifts. During this time, SSRL supported approximately 760 experimental starts on 19 beam-line stations that were open for users. The User Research Administration office processed and badged over 900 users who came on-site to perform experiments.

Competition for beam-time assignments remains high. When averaged across all available beam lines, the oversubscription rate was approximately 50% (user demand was 150% of available resources).

Users from over 17 countries received beam time at SSRL. Of these users, approximately 89% were from the U.S., spanning 26 states and the District of Columbia. Users were predominantly from American universities (53%) followed by American laboratories (29%), American businesses (7%), foreign universities (8%), and foreign laboratories (3%).







**Distribution of the proposals receiving beam:**

Materials Science	14%
Physics	5%
Chemistry	16%
Polymers	2%
Medical Applications	5%
Biology/Life Sciences	45%
Earth Sciences	3%
Environmental Sciences	5%
Optics	1%
Engineering	3%
Other	1%

***SPEAR3 Project***

The new SPEAR3 light source continued to demonstrate excellent reliability and beam quality during its second user run, which began in early February 2005 and ended on August 1, 2005. The run was delayed from its scheduled October 2004 beginning by a laboratory-wide safety stand down resulting from an electrical accident at the Stanford Linear Accelerator Center (SLAC). Being a new facility, and thanks to the concerted efforts of operations and safety staff

10/31/2005

throughout SLAC, SPEAR3 was the first accelerator at the lab to be validated for restart after the safety stand down, much to the benefit of the user community of the Stanford Synchrotron Radiation Laboratory (SSRL).

The average uptime or beam delivery time to users during this run was 95%. The nominal lifetime at the 100-mA fill current was 60 hours at the end of the run, having increased from an initial 40 hours in January. Orbit stability as measured by the beam position monitoring system was on the order of a few microns, but now that more sensitive experiments have come on line in the new facility, it has been determined that there are significantly larger photon beam excursions in the beam lines. Work has begun in earnest to address these issues at SSRL and to improve orbit and beam-line optics stability, a mission that will undoubtedly occupy the accelerator and beam-line staff for years to come as the demand for higher beam stability steadily increases.

A major milestone was reached during special test periods on June 20 and 21, 2005 when the design current of 500 mA was stored in SPEAR3 for the first time. High-current multibunch stability was achieved without a feedback system by adjusting the SLAC-built digital rf control parameters and by increasing sextupole magnet field strength to provide extra damping. Vacuum pressure and chamber component temperatures were monitored carefully during the tests and no problems were detected. After some vacuum conditioning, beam lifetime at 500 mA was ~14 h, close to the design expectation. More 500-mA tests were conducted near the end of the user run, this time with insertion devices at their operating fields. The first beam line, BL-6, was opened under high current conditions to test newly designed beam line optics, including a liquid nitrogen-cooled monochromator. High-current operation is planned for special periods during the FY2006 user run, with full-time 500-mA operation planned for the FY2007 run, when all SSRL beam lines will have been upgraded for high-current operation.

### **SPEAR3 Accelerator Improvements**

The accelerator improvements reflect the advent of operation of the new SPEAR3 storage ring and the migration to higher-current operation over the next year. The injector underwent a program of improvements that made it more robust and reliable in view of the more demanding SPEAR3 requirements. Such improvements led to considerably more reliable operation during the user run.

*Injector* – A system that digitizes and records the beam injected and ramped in the booster was completed. The White Circuit cell tune monitoring system will be based on the technology used for this system. The low-level rf control system has been tuned to maximize booster ramping efficiency for all bucket timings. Work to characterize gun and linac beam instabilities and to implement a feedback circuit to stabilize the booster White Circuit has begun as part of the work required to implement top-up injection. The Accelerator Physics and Engineering groups continued to study injector performance and limitations and formulate improvement plans.

*Turn-Turn Beam Position Monitors (BPMs)* – Commissioning of the turn-turn BPM system continued. The primary remaining effort for the turn-turn BPM processor project includes verification of signal quality, power levels, timing, noise rejection, signal integrity, and completion of the data communication and software systems. Test tone couplers have been

installed around the SPEAR3 ring and development of test tone processing, which will maintain parallel processing channel gain equalization is in progress. Software tasks include completion of the data acquisition and position-computing programs and integrating the turn-turn BPMs into the orbit feedback system. Digital receiver modules were tested and sent back to the manufacturer for firmware upgrades.

*Synchrotron Light Monitor (SLM)* – The design and fabrication of the cold finger and M0 mirror vacuum chamber assemblies and the first phase radiation shielding was completed and these components were installed in the ring tunnel. The rough vacuum components and optical elements for the optics room were also completed and installed. The work being completed prior to the FY2006 run includes: 1) finalizing the radiation shielding design, obtaining radiation protection system approval from the SLAC Radiation Safety Committee and installing the remaining protection components, and 2) connecting the SLM beam line to the SPEAR3 vacuum chamber. These activities are scheduled for completion by October 2005, with SLM commissioning at the beginning of the FY2006 user run. Work continues to characterize and improve the BL2 pinhole camera system.

*Beam Scrapers* – Low-impedance horizontal and vertical beam scraper modules for the SPEAR3 vacuum chamber were commissioned and used to characterize beam lifetime, injection apertures, and minimum apertures for future insertion devices. Studies are continuing to improve radiation shielding for these devices. The scrapers will enable studies of beam size, lifetime, injection apertures, and minimum apertures for future insertion devices.

*LION Development* – Significant progress was made in developing processing electronics for the Long Ion Chamber (LION) system required for the Beam Containment System before the injection beam current limit can be raised to that commensurate with 500-mA operation. The processing system is relatively complex, requiring extremely sensitive detection electronics having a large dynamic range that is capable of extracting a small injected beam signal out of a large background signal associated with the stored beam.

*Transverse Kickers* – Work began on the design of horizontal and vertical strip line kickers for the storage ring. The kickers will be used to excite transverse beam oscillations for beam studies, and can be used in a transverse multibunch feedback system at higher currents if necessary.

*Orbit Control* – Work has continued on the fast orbit feedback system, first by commissioning a system using only the 54 Bergoz averaged-orbit BPMs, then by adding the turn-turn BPMs operating in averaged-orbit mode. The frequency response of each corrector magnet together with its associated vacuum chamber must be matched with those of all other feedback correctors over a bandwidth of ~100 Hz. The SVD-derived inverse matrix was optimized for best performance, as were the digital filters used to tailor the system time and frequency responses. Work continued to provide an operator interface and data acquisition applications for the new fast orbit feedback system.

*Control System and Application Programs* – Programs have been developed for automatic bucket-filling, TSP flashing, accumulated beam monitoring, temperature monitoring from over 600 thermocouples, Orbit Interlock steering verification, kicker bump compensation, orbit

feedback with photon beam position monitors, and many more. A new program was added for booster current monitoring.

*Double Waist Chicane Lattice* – Tracking studies, frequency map analyses and the consequent optics optimization of the double waist chicane lattice were completed. Magnet families and properties, power supply requirements and beam performance-related design requirements for the chicane vacuum chambers were specified by the Accelerator Physics group. The principal optics components (quadrupoles and power supplies) without the chicane have been installed during the FY2005 shutdown so that the optics can be tested and optimized during the FY2006 run, in advance of the actual BL12 in-vacuum undulator beam line commissioning in FY2007.

*Top-Off Injection* – The design of the system needed for top-off injection with beam line stoppers open began in FY2005. This injection mode, with minimal interruption to users, will enable more frequent beam injection to limit beam current variation, minimizing the variation of thermal power on beam line optical components and improving beam stability for users. Work will begin to implement a booster power supply control system that will permit quick turn-on and -off of the booster beam to avoid continual operation of the power-consuming booster. Design will begin on an improved booster-to-SPEAR3 (BTS) transport line that eliminates several vacuum windows that spoil injected beam emittance. An extensive study of beam-loss modes was initiated to determine what radiation safety components will be required to inject beam into SPEAR3 with open beam-line radiation stoppers. Significant changes to the Personnel Protection System, including the Septum Interlock, will be needed to implement the top-off system. This work will enable the first phase of top-off injection - a mode that will maintain beam current constancy in SPEAR3 to a few percent. A second phase of top-off development that would enable maintaining SPEAR3 beam current constancy to less than 1% will most likely require large-scale improvements to the electron gun and possibly to the booster.

*SPEAR3 Performance and Lattice Upgrades* – The accelerator physics and engineering groups continued to study and tune the SPEAR3 accelerator to maximize its performance and stability. Vertical coupling was reduced to the order of 0.1%, producing brighter beams for users. The compensation of skew quadrupole gradients introduced by the BL5 Elliptically Polarizing Undulator (EPU) was studied and the design of a correction scheme was proposed.

A major study was conducted to identify potential lattice modifications that will enable smaller gap insertion devices (IDs), including the in-vacuum undulator proposed for the new BL12. The “double waist chicane” optics, which accommodates two small-gap IDs in the east long straight section and reduces the vertical beam size in the four matching cell straight sections (one of which will accommodate the BL13 EPU), was selected and studied in detail. A successful configuration having good dynamic aperture was found and approved for implementation by an external review committee.

The accelerator physics and engineering groups continued to study and tune the SPEAR3 accelerator to maximize its performance and stability. With high current operation enabled by the new 500 mA shielding, further measurements of bunch instability modes were conducted. Studies of the sources and cures of orbit instability continued.

*Gun Test Facility* – Important progress was made in understanding the sources of excessive electron beam emittance from a high-charge photocathode gun to be used for the LCLS. Slice emittance measurements determined that most of the increase in projected emittance over slice emittance is due to beam slice offsets and not phase space misalignments, as previously thought. This indicated the presence of a time dependent kick that significantly increases the projected emittance in photocathode rf guns. This discovery sets the path for reducing the projected emittance by determining the source of the time-dependent kick and eliminating it, the next major goal for the GTF.

A scheme to shape the rf pulse driving the gun to reduce the thermal load was tested on the GTF gun. The work will aid in reducing the thermal load for the LCLS rf gun which operates at 120 Hz and with 12 times the load of the GTF gun.

The GTF continued to operate in FY2005 in support of developments for the LCLS injector group. Alternative cathodes can also be installed and tested as needed to determine the maximum obtainable field, evaluate laser cleaning techniques, as well as measuring the cathode quantum efficiency and thermal emittance. The GTF also can be used to test alternate gun designs such as a multi-cell gun optimized for generating polarized electrons. An experiment in ultrafast electron diffraction (UED) is being planned in collaboration with Brown University.

### **Beam Line and Facilities Improvements**

The beam-line and facilities activities are focused on operations and maintenance of the beam lines for users including the Subpicosecond Pulse Source (SPPS), continuing the upgrade of the beam lines for SPEAR3 operations and the construction of two new beam lines.

*Beam Line Upgrade Project* – The SPEAR3 accelerator upgrade was carefully designed to retain the existing insertion device source points and required only minor realignment of the bending magnet beam lines. While this approach preserved the existing capital investment in SSRL beam lines, upgrade and enhancement of these beam lines is required to deliver the full potential of the source improvements to the experimental stations. Consequently, SSRL has engaged in a vigorous program of beam-line upgrades. By the end of 2006 14 insertion device branch lines will have been upgraded for 500-mA SPEAR3 power, while the remaining three insertion device branch lines are scheduled for upgrade completion by the end of 2007. In addition, by the close of 2006 a further six bend magnet branch lines will have completed a first round of upgrades to permit 500-mA operation.

A central aspect of the X-ray insertion device branch line upgrade program is the installation of liquid-nitrogen-cooled (LN) monochromators on 10 of the hard X-ray branch lines. During the 500-mA test run of SPEAR3, initial high-power studies of the liquid-nitrogen-cooled monochromator performance were conducted on the 57-pole wiggler BL6. Analysis of Si(333) rocking curve data indicates that the monochromator crystals experience less than 4  $\mu\text{rad}$  thermal distortion for calculated incident beam powers up to 880 W and 13  $\text{W}/\text{mm}^2$ . Increasing the incident power to the maximum developed by the branch line, resulted in significant thermal distortion (i.e., 26  $\mu\text{rad}$  at 1250 W and 13.8  $\text{W}/\text{mm}^2$ ). While these tests explored the limits of the monochromator crystal thermal distortion using a sensitive higher order reflection, the reflected

flux and rocking curve width of the Si(111) fundamental reflection proved largely insensitive to the incident beam power. Thus these initial tests suggest that the monochromator thermal performance will not provide a serious limitation to wiggler beam line performance under 500-mA run conditions.

As part of the restart validation of SSRL beam lines following the installation of the SPEAR3 accelerator, the SLAC Radiation Protection Department and SSRL conducted a thorough radiation safety review of each beam line for 10- mA operations. A second review is beginning in anticipation of 500-mA operations which will include development of a beam containment system for the beam lines.

*BL1, 2, 3, and 8* – Owing to resource limitations, upgrade activities on the bend magnet beam lines was limited largely to recommissioning the beam lines with the new SPEAR3 source location and upgrade of a few key components and radiation protection systems required for operation with SPEAR3. Notably, new beam transport hutches were completed on BL1 and BL2 and a new experimental hutch was erected for BL1-4. Additional shielding and other radiation safety controls were installed on VUV BL8-1 and BL8-2. Miscellaneous other beam-line shielding elements were modified according to current shielding protocols. The BL1-4  $M_0$  mirror cooling was upgraded. The JUMBO monochromator on BL3-3 was decommissioned. Upgrades to the other bend magnet stations were limited to those essential to operate the beam lines safely at currents greater than 100 mA. In these cases the performance of the beam line will be optimized when the full 500 mA upgrade of the beam line is completed. The present BL7-2  $M_0$  mirror is being relocated to BL2-1 in order to expand the useful energy range of the beam line.

*BL4* – BL4 upgrade activities in FY2004 were largely limited to fabricating hardware in preparation for the FY2006 shutdown installation. These include the BL4-1 and 4-2 LN-cooled monochromators, the monochromator entrance slits, graphite filters, and Be windows for all three branch lines. BL4 shielding was modified according to current shielding protocols to permit 100 mA operations of BL4-2. The BL4-2 upgrade is funded by DOE BER.

*BL5* – The gratings for the BL5-1/2 monochromator were delivered and installed in the spherical grating monochromator (SGM). The BL5-1/2  $M_0$  mirror system and SGM with associated entrance and exit slits were installed on the experimental floor. Assembly and installation of many of the remaining BL5-1/2 500 mA upgrade components continued throughout the fiscal year. The beam transport hutch fabrication was completed and other BL5 shielding was modified according to current shielding protocols to permit 500-mA operations of BL5. The BL5-4  $M_0$  mirror is being upgraded for 500 mA. The BL5 insertion device vacuum chamber will be upgraded for improved ID performance. This will complete the BL5 500-mA upgrade for the start of the FY2006 run.

*BL6* – The  $M_0$  and  $M_1$  mirrors and remaining mask and optics support upgrades for 500 mA were completed. The beam transport hutch fabrication was completed. The remaining BL6 shielding was modified according to current shielding protocols to permit 500 mA operations of BL6. As mentioned above, BL6-2 was successfully operated at 500 mA during the FY2005 run.

*BL7* – Fabrication of the BL7-1 monochromator started. Mechanical testing of key components for the BL7-2 sagittally focusing monochromator commenced as did fabrication of the  $M_0$  mirror systems for all three branch lines. Fabrication of most of the remaining 500-mA BL7 upgrade components will be completed and the upgraded components installed during the first quarter of FY2006. The BL7-2 sagittal focusing LN monochromator development will extend into FY2006. The BL7-1 and BL7-3 upgrades are funded by NIH NCRR.

*BL9* – Installation of the remaining 500-mA BL9 upgrade components will be completed prior to the beginning of the FY2006 run. The BL9 upgrade is funded by DOE BER.

*BL10* – The BL10-1 monochromator entrance slit was replaced with a 500-mA-capable model early in FY2005. Installation of slits, masks, filters, and windows to complete the BL10 500-mA upgrade will be complete prior to the beginning of the FY2006 run.

*BL11* – The additional graphite filter thickness required for 500-mA operations were installed during the summer 2005 shutdown as was a burn-through monitor for the BL11-2 hutch stoppers.

In addition to the beam line upgrade program, SSRL is constructing two new undulator beam lines.

*BL12* – This beam line is funded by the Gordon and Betty Moore Foundation through a grant to the California Institute of Technology and is being optimized for macromolecular crystallography studies. This beam line, which is scheduled to commence commissioning in late 2006, will utilize a small gap, in a vacuum undulator installed in a small beta chicane in the six-meter east straight of SPEAR3. The associated changes in the SPEAR3 magnetic lattice required to produce a double-waist chicane in the 9s long straight section (i.e., East Pit) were extensively studied and reviewed. The double-waist chicane lattice produces two electron beam vertical focus minima in the SPEAR3 9s straight which are suitable for small gap insertion devices. The electron trajectories at these two foci or waists are canted 10 mrad with respect to each other in order to maximize the independence of beam lines developed for each of these two ID sources. The BL12 in-vacuum ID will be located at the downstream waist. The beam-line optics design utilizes moderately demagnifying optics to facilitate optimal coupling of the high brightness X-ray beam to small macromolecular crystals. The experimental infrastructure also will be optimized for small macromolecular crystallography studies. As such, it will include robotic crystal mounting, automatic crystal alignment, and a large area CCD detector. The in-vacuum ID design and fabrication contract has been awarded with delivery scheduled for June 2006. The quadrupole magnet triplet required to create the double waist discussed above was fabricated in the spring and installed during the summer 2005 SPEAR3 shutdown. This will enable machine physics studies of the double-waist lattice during the 2006 run. The three mirrors required for the beam-line optical concept have been ordered with delivery scheduled for February 2006. Modifications to the SPEAR3 concrete shielding enclosure required to extract the beam were completed during the summer 2005 SPEAR3 down time. Procurement of the CCD detector will commence in late FY2005.

*BL13* – The second new undulator beam line, designated BL13, will concentrate on soft X-ray materials science studies. The source consists of a 3.8 m elliptically polarizing undulator currently in fabrication. In the initial configuration the optics are being optimized for a 250-1600 eV band pass using a spherical grating monochromator. The optics design, however, preserves the option to upgrade the beam line through the addition of a second monochromator and associated branch line optics for studies up to 2700eV. In the initial configuration the end stations will accommodate STXM, photoemission, and speckle studies. The beam line is scheduled to commence commissioning in late 2007.

***SSRL Instrumentation and Control Software*** – The XAS-Collect data acquisition software has been ported to the Microsoft Windows operating system. Work is continuing on the VXI Grand Interconnect device driver interface using Microsoft Windows based computers. Enhanced support and integration of EPICS into the SSRL ICS software is underway for the control of the BL5 insertion device.

In order to help protect the SSRL network from off-site intrusions and also to provide for secure isolated networks for instrumentation and control, a network firewall is currently being implemented. The firewall machine chosen for evaluation, a FortiGate 1000, has been installed and is effectively isolating several areas of SSRL using Virtual Local Area Networks, or VLANs. At present this includes all of the SPEAR3 and Injector instrumentation, and one experimental station, BL2-3. The firewall has an easy-to-use Web-based interface, and can be configured to have individual rule sets between different VLANs and groups of computers. As the required rule sets are developed, additional beam lines will be moved behind the firewall. At present no significant problems have been encountered.

***Computers and Networking*** – In order to reduce exposure of network-based instrument control and data acquisition software, a firewall has been installed that isolates the SPEAR control and beam line networks from the regular SSRL network. The complete SPPS experiment and BL controls network was installed and is integrated into the SSRL network. The backbone network was upgraded to Gigabit Ethernet.

***Facilities and Infrastructure*** – The safety review for the LN distribution system has been completed and it is anticipated that the system will be operational in FY2006. As mentioned above, construction of the new alcove from the SPEAR3 9S straight section (i.e., East Pit) and replacement of the SPEAR3 trestle support structure were completed. It should be noted that these projects also accomplish the seismic upgrades for this part of the SPEAR3 tunnel and the trestle. Construction of the second floor of Building 130 to house XLAM which will include laboratories, experimental support areas and offices, utilities, elevator and required systems will continue. Arc flash analysis of all SSRL circuit breakers, correction of OSHA findings and correction of post-start requirements related to electrical findings are all high priority items in the facilities and infrastructure area. Finally, a plan was developed as part of the SLAC infrastructure project to address structures within the SPEAR3 facility requiring reinforcement to meet seismic bracing standards. This project will continue through FY2009.



## Facility Research and Development

***Inelastic Scattering and Advanced Spectroscopy Facility for SPEAR3*** – An Inelastic X-ray Scattering and Advanced Spectroscopy Facility is being developed that will eventually be located at a new SPEAR3 insertion device beam line. Various techniques complementary to the current spectroscopy programs at SSRL will be carried out at this facility. They include X-ray Raman scattering (XRS), resonant inelastic X-ray scattering (RIXS), selective X-ray absorption (S-XAS) and X-ray emission spectroscopy (XES). XRS will widen the range of absorption spectroscopy on low-Z samples, traditionally performed in the soft X-ray range, to systems and sample conditions where the penetration of a hard X-ray probe is essential. XRS can thus provide unique new insight for, e.g., studies of carbonaceous systems related to fossil fuels and hydrogen storage under *in situ* conditions, water and aqueous systems in ambient and extreme conditions, high pressure phases of gases and the formation of methane hydrates. RIXS spectroscopy is a novel technique to study in detail the local electronic structure and spin states of, e.g., 3d transition metal compounds with hard X-rays. As compared to conventional K-edge spectroscopy it can better isolate lowest unoccupied molecular orbital (LUMO) resonances and has less lifetime broadening along the energy transfer axis. Furthermore it provides L-edge/M-edge like information. S-XAS, such as site-selective EXAFS combines the chemical sensitivity of XES with EXAFS to provide more detailed structural information in mixed valence systems. S-XAS can also be used to extend the k-range of EXAFS beyond an absorption edge that otherwise would limit the data collection, hence yielding more accurate determination of neighbor distances. XES contains chemical and structural information complementary to XANES. All of these techniques are valuable in the study of a wide range of systems including man-made and bio catalysts as well as correlated systems.

The first multicrystal component of a new spectrometer to be used for X-ray Raman scattering as well as advanced spectroscopy based on high resolution emission detection was fabricated in FY2004. In summer 2004 several analyzer crystals from different vendors were tested at SSRL BL10-2 and, based on those results, the first set of 7 crystals was ordered. The analyzers arrived in early 2005. Independently the goniometer was completed, and the first experiments (using borrowed analyzers) were performed in December 2004 at the Advanced Photon Source (APS). In particular X-ray Raman scattering measurements on water and D<sub>2</sub>O were performed at low momentum transfer. As part of the SSRL Structural Molecular Biology program proposal to NIH-NCR and DOE-BER (described in the KP11 FTP) funding was requested to: a) make the unit compatible to perform emission scans as required for XES



First multi-crystal component of new analyzer crystals for the various proposed applications related to biological and transition metal systems.

***Molecular Environmental and Interface Science*** – Molecular Environmental and Interface Science (MEIS) research at SSRL focuses on the fundamental interfacial, molecular- and nanoscale processes that control contaminant and nutrient cycling in the biosphere with the goals of elucidating local and global elemental cycles and anthropogenic influences on the environment. Knowledge of these processes is fundamental to developing novel technologies for

remediating environmental contamination and designing environment-friendly industrial processes. Key areas of investigation include: (a) Structural chemistry of water and dissolved solutes, (b) Structural chemistry and reactivity of complex natural environmental materials (biominerals, oxide and sulfide minerals, biofilms, and organic materials) with respect to heavy metals, metalloids, and organics, (c) Reactions at environmental interfaces, including sorption, precipitation and dissolution processes that affect the bioavailability of heavy metals and other contaminants, and (d) Microbial transformations of metals and anions. SSRL-based MEIS research utilizes synchrotron-based X-ray absorption spectroscopy (XAS), wide-angle X-ray scattering (WAXS), small-angle X-ray scattering (SAXS), X-ray standing wave (XSW) spectroscopy, and photoemission spectroscopy (PES). These techniques provide unique capabilities to probe structure/composition/function relationships in complex environmental systems.

A proposal submitted to BER-ERSD to support microspectroscopy and microdiffraction MEIS programs at SSRL has been funded. This resulted in the initiation at SSRL of a programmatic effort to build microspectroscopy and microdiffraction MEIS programs. Instrumentation for a microfocusing capability has been assembled and tested. A focused beam spot size of 2  $\mu\text{m}$  (very close to the theoretical limit) was obtained at 17 keV, far surpassing the first round commissioning goal of 10  $\mu\text{m}$ . Hutch table and optics rail designs were modified to optimize their performance based upon the results from the first commissioning run. A second commissioning run achieved its goals for improved beam/table stability and demonstrated the capability to collect EXAFS spectra at 17 keV.

The Brown Group continued its synchrotron radiation-based research in the following areas: (1) abiotic and biotic oxidation pathways of pyrite surfaces; (2) formation of ternary surface complexes of dicarboxylic acids and metal ions on metal oxide surfaces; (3) interactions of metal ions with biofilm- and organic polymer-coated metal oxide surfaces under *in situ* conditions; (4) XAFS spectroscopy studies of heavy metal contaminated soils; and (5) XAFS, micro-XAFS, and micro-XRD studies of uranium in the Hanford Vadose Zone.

In the area of biogeochemical cycling of manganese in the environment and sorption of ions at oxide-water interfaces (Bargar) *in situ* WAXS and EXAFS measurements of metal-reacted bacteriogenic manganese (Mn) oxides demonstrated the oxides to be nanoparticulate and subnanoparticulate in size. Subsequent measurements showed that sorption of transition and heavy metals to surfaces of the oxides stabilizes very small particle size ( $\sim 1$  nm diam.). It is postulated that sorption of metals passivates dangling surface bonds and thus abates large surface free energy terms. In contrast, incorporation of divalent alkaline earth cations such as  $\text{Ca}^{2+}$  leads to larger particle sizes.  $\mu$ -XAS and  $\mu$ -XRD measurements of bacteriogenic Mn oxides in the field (Pinal Creek, AZ) show a strong similarity to laboratory-produced biooxides, providing a basis for developing a predictive model from lab experiments. Four manuscripts were published, and 11 scientific presentations were given at national/international meetings (one invited talk). A highly successful workshop, "Applications of Synchrotron Techniques for Environmental Microbiology and Biogeochemistry" was held in conjunction with the SSRL Users' Meeting and attracted over 70 attendees.

**Strongly Correlated Materials** – The program of angle-resolved photoemission spectroscopy (ARPES) study of strongly correlated electronic materials continued to be very active and productive in its two main tasks: scientific research and advanced instrumentation development in support of the research.

For research, the focus is to try to get critical information about complex solids that cannot be obtained by any other means. During this period, the primary focus is the many-body interactions that are important to the mechanism for high-temperature superconductivity; however, the research infrastructure developed has also been important to other activities not explicitly listed here.

We have uncovered experimental evidence and developed a theoretical model for an unconventional form of electron-phonon coupling in  $\text{Bi}_2\text{Sr}_2\text{CaCu}_2\text{O}_8$  [Cuk *et al.*, *Phys. Rev. Lett.* **93**, 117003, 2004; Devereaux *et al.*, *Phys. Rev. Lett.* **93**, 117004, 2004]. The conventional wisdom is that electron-phonon coupling is isotropic in nature, even its complex form involves some variation with phonon momentum  $\mathbf{q}$  only. We found instead that electron-phonon coupling in  $\text{Bi}_2\text{Sr}_2\text{CaCu}_2\text{O}_8$ , specifically for the oxygen breathing mode and buckling mode in the important  $\text{CuO}_2$  planes, is highly anisotropic and depends strongly on initial electronic state momentum  $\mathbf{k}$ , as well as the phonon momentum  $\mathbf{q}$ . This finding provides a vivid example demonstrating that one should not extrapolate knowledge obtained from simple metals to complex materials. We show further evidence that this mode of coupling phenomenon persists in all superconducting materials [Cuk *et al.*, *Nature* **432**, 7015, 2004].

An important focus of the research during this period was a systematic investigation of another important cuprate family:  $\text{Ca}_{2-x}\text{Na}_x\text{CuO}_2\text{Cl}_2$ . This material system, which has a stable surface like Bi2212 but does not have the complications due to superstructure, opens up exciting new opportunities to understand the long-standing issue of the chemical potential shift as a function of doping. We have successfully resolved this issue, and found this to be intimately related to the unusually broad spectra seen in undoped material ( $x=0$ ). [Shen *et al.*, *Phys. Rev. Lett.* **93**, 267002, 2004]. The key insight is a coupling of boson fields that gets to be extremely strong and reaches the polaronic regime when the doping of the materials is reduced and the screening gets to be very poor. In a related investigation, we have also uncovered evidence for the d-wave gap to be unstable against disorder in real materials. [Shen *et al.*, *Phys. Rev. B* **69**, 054503, 2004].

In addition to the highlights listed above, we have performed detailed investigations of several other cuprate families, from the comparison of p- and n-doping, to the effect of next nearest neighbor hopping, to the connection between ARPES and transport results. These papers add to the accumulated knowledge of the cuprate superconductors – a necessary process for a comprehensive understanding [Armitage *et al.*, *Phys. Rev. B* **68**, 064517, 2003; Tanaka *et al.*, *Phys. Rev. B* **70**, 092503, 2004].

Important progress was made in understanding the anisotropic quasiparticle dynamics and nature of charge ordering. An intriguing connection between Fermi surface nesting with  $\mathbf{q} = \pi/2$  in  $\text{Ca}_{2-x}\text{Na}_x\text{CuO}_2\text{Cl}_2$  and the striking charge ordering phenomenon with a periodicity of  $4a$  seen by STM has been observed [Shen *et al.*, *Science* **307**, 901, 2005]. The data provide an exciting opportunity to understanding the nature of charge ordering in cuprates – an important current

issue in the field—especially as it will allow understanding of the dual personality of the charge-ordered state, in terms of momentum space and real space descriptions.

Important progress was also made in testing the Fermi liquid concept in two-dimensional  $\text{Sr}_2\text{RuO}_4$ . The Fermi liquid concept has been a cornerstone of our understanding of metals, and the foundation of the band structure description of electrons in solids such as silicon whose success manifests itself in our daily life. Although this concept has been proposed since the 1950s, it has not been rigorously tested in the momentum and frequency domain. We have performed this test and found the picture describes the electronic excitations of solids very well, even down to the details of dimensionality correction [Ingel *et al.*, *Phys. Rev. B*, submitted]. Experiments have been started on the Fermi liquid to non-Fermi liquid evolution via doping through van-Hove singularity (VHS) in  $\text{Sr}_{2-x}\text{La}_x\text{RuO}_4$ . The data are being analyzed. The importance of VHS in 2D solids has been recognized for a long time, but has never been directly observed by tuning via doping, and has never been connected to the Fermi liquid to non-Fermi evolution. The significantly improved momentum resolution enables this investigation.

Our work has continued to uncover evidence for small lattice polaron formation by looking at the Frank-Condon type of broadening in  $\text{Ca}_2\text{CuO}_2\text{Cl}_2$  and  $\text{Sr}_2\text{CuO}_2\text{Cl}_2$ . Small lattice polaron formation and its interplay with magnetic interactions in undoped and underdoped materials have been theoretically suggested for a long time; direct spectroscopic evidence for this behavior does not exist yet. By performing a temperature-dependent investigation, we expect to make progress on this subject.

Progress has been made on the high-energy scale band renormalization from  $t$  scale to  $J$  scale physics in  $\text{Ca}_2\text{CuO}_2\text{Cl}_2$ . This hierarchy of energy scale is important for cuprate physics and has been known for a long time but the specifics of the renormalization have not been experimentally explored due to technical difficulties. We have made good progress in this area.

An understanding of the electronic structure of a novel multilayer cuprate material where the  $\text{CuO}_2$  layers are self-doped has been developed. These materials exhibit a number of surprises as they are very high temperature superconductors although simple valence counting would have put them in the insulating regime. We have uncovered a novel form of self-doping and a number of surprises associated with it.

Important progress has also been made in understanding the role of  $B_{1g}$  phonon coupling and superconducting transition temperatures in multilayer materials such as  $\text{Bi}_2\text{Sr}_2\text{CaCu}_2\text{O}_8$  and  $\text{Bi}_2\text{Sr}_2\text{Ca}_2\text{Cu}_3\text{O}_{10}$ . We found that this mode coupling is much stronger in materials with multilayers of  $\text{CuO}_2$  planes in their unit cells and with higher  $T_c$ , while this coupling is much weaker in cuprates with single  $\text{CuO}_2$  layer and lower  $T_c$ .

Our program of ARPES investigation continues to generate considerable interest in the community. Two of our papers [Lanzara *et al.*, *Nature* **412**, 510, 2001; Damascelli *et al.*, *Rev. Mod. Phys.* **75**, 473, 2003] have recently been identified by the Institute of Scientific Information as among the top 1% of the citation list and are making a significant impact in our field of study.

In addition to research, our program has devoted significant effort to the development of the next generation of instrumentation. These efforts have benefited not only the research program described here, but also other programs at SSRL and ALS.

***Chemical Physics of Surfaces and Liquids*** – The main focus of this research program is to use X-ray spectroscopies to address important questions regarding chemical bonding on surfaces during catalytic reactions and in aqueous solutions. X-ray emission spectroscopy (XES), X-ray absorption spectroscopy (XAS) and X-ray Raman spectroscopy (XRS) provide an atom-specific projection of the electronic structure. Problems related to systems in catalysis, energy technologies, electrochemistry and molecular environmental science are studied using XES, XAS, XRS and density functional theory (DFT) calculations. Probing hydrogen bonding and the structure of liquid water in aqueous systems are new and novel applications of X-ray spectroscopic techniques. Instrument development is an important part of the activity to provide new spectrometers, and enable measurements at high gas pressures and at liquid interfaces.

*Molecular Adsorbates on Surfaces:* XAS and XPS studies were performed on water adsorbed on Ru and Cu surfaces. The recently suggested half dissociated layer of water on Ru(0001) was shown to be incorrect using photoelectron spectroscopy measurements. It was demonstrated that the dissociated state corresponds to the lowest energy but the activation energy barrier is higher than the desorption channel and therefore cannot be reached during vacuum conditions. Different behavior in terms of wetting was found on the (111) and (110) surfaces of Cu that could be related to the difference in substrate electronic structure. The co-adsorption system of oxygen and water on Pt(111) to generate OH species, which is considered as an important intermediate in fuel cell catalysis, was studied. It was demonstrated that the OH species is bonded perpendicular to the surfaces without in-plane hydrogen bonding. Detailed studies have begun of water adsorbed on Cu(110) and Fe<sub>2</sub>O<sub>3</sub> at high pressures using the differential pumped XPS systems, as well as hydrogenation studies of carbon nanotubes for investigations of the potential of carbon as hydrogen storage materials. Studies of water at high pressures and temperatures, different pH and in various aqueous solutions will provide new information to address structure, hydrogen bonding and electronic structure of water in the bulk and in the influence of ions. Another aspect of research will be adsorption and thin film growth of water on different metal and metal oxide surfaces. What is the structure and nature of bonding in the first interface layer and does water grow in an ice- or liquid-like configuration?

*Water in Aqueous Systems:* Proposed new models of the structure of liquid water based on XAS and XRS experiments goes against the existing understanding based on theoretical simulations. This work was considered by *Science Magazine* to be one of the ten most important breakthroughs in 2004. Analysis of EXAFS data on liquid water, based on XRS measurements at the APS, continued, as did the determination of the change in hydrogen bonding network in aqueous solutions containing various ions based on XAS measurements.

*Instrument Development:* A new UHV surface science end-station was completed and installed at BL5. A highly efficient soft X-ray spectrometer optimized for C, N and O K edges has been designed and a differentially-pumped high-pressure cell using cryogenic technology that can be inserted into this UHV system is being assembled.

*Development of Resonant Coherent X-ray Scattering* – The scientific motivation for the development program outlined below is the investigation of the critical fluctuations of a magnetic domain structure at the magnetic-paramagnetic phase transition. This research falls into the general area of critical fluctuations at phase transitions for which theory predicts that the order parameter diverges at the transition temperature. For magnetic phase transitions this implies that the domain size should diverge, i.e., right at the transition temperature a single magnetic domain should extend –momentarily– over the entire sample. However, this has never been observed experimentally. One of the major reasons for this lack of experimental proof is that impurities and defects limit/influence these fluctuations. This limitation can be overcome by studying critical fluctuations in ultra-thin films with quasi 2-dimensional magnetization. Such ferromagnetic films can be prepared essentially defect free by epitaxial growth with thicknesses of only a few monolayers. A further advantage of studying a thin film is that the fluctuations are expected to be much slower in thin films than in bulk materials. To investigate the nature of these critical fluctuations, the following four experiments will be undertaken:

1. *Resonant Small Angle Scattering of Incoherent Soft X-rays*

Resonant scattering at the dichroic L3 absorption edge of magnetic transition metals will yield statistical information about the magnetic domain structure such as average domain size and domain shape. Hence, when investigating the temperature dependence of this statistical information close to the transition temperature, the average domain size of the critical magnetic fluctuations can be derived.

2. *X-ray Photon Correlation Spectroscopy (alias Dynamic ‘Light’ Scattering)*

By scattering of coherent photons, information about the dynamics of the fluctuations can be derived from the time dependence of the scattering intensities. A third generation synchrotron light source like SPEAR3 will enable time-resolving dynamics occurring on the microsecond time regime.

3. *Ultra-Fast, High-Resolution, Lensless Imaging of Magnetic Domain Structures*

One potential application of SLAC’s upcoming X-ray free electron laser LCLS will be ultra-fast, high-resolution lensless imaging. This will allow recording of femtosecond snap shots of the magnetic domain structure at and in the vicinity of the magnetic phase transition. A series of such images will enable distinguishing “real” magnetic fluctuations from defect-pinned fluctuations.

4. *Ultra-fast X-ray Photon Correlation Spectroscopy*

At LCLS, a beam splitter and a delay line will be used to obtain two femtosecond short X-ray pulses separated by a variable delay ranging from a femto- to a few picoseconds. Using both these pulses for lensless imaging of the magnetic domain structure will reveal the dynamics of the magnetization fluctuations on a femto- to picosecond time scale.

A new UHV chamber dedicated to scattering of incoherent and coherent soft X-rays was designed and built in FY2003. Until the completion of the SPEAR3 upgrade at SSRL, this chamber was located at a dedicated branch line of an elliptical polarizing undulator at the third generation synchrotron light source BESSY II in Germany. In close collaboration with the group of Dr. Stefan Eisebitt at BESSY, the potential of lensless imaging techniques has been

investigated over the last few years. Using “oversampled” speckle patterns (the small angle scattering pattern obtained when scattering coherent X-rays) of “geometrically simple” test samples, the phases of the scattering amplitudes have been successfully reconstructed using variants of the well-established Gerchberg-Saxton algorithm. For complex magnetic domain patterns extending over the full field of view, however, it is difficult to demonstrate that the algorithm has converged against the “real” scattering phases – an obvious requirement to establish this phase retrieval as a true imaging technique.

To preserve more information about the scattering phases in the recorded speckle pattern, Fourier transform holography was extended to the X-ray regime. The key element for this is an X-ray opaque mask with a micron-sized sample and a nanometer-sized reference beam aperture. A process based on selective Focused Ion Beam etching has been developed to manufacture the high-aspect ratio reference aperture. With this structure defining the Fourier transform holography geometry, the first X-ray spectro-hologram, i.e., a hologram for which the scattering contrast originates from a dichroism in the scattering cross section, was recorded successfully in early 2004. The spatial resolution of about 50 nm is state-of-the-art and this result was published in the December 16, 2004 issue of *Nature* and highlighted on the cover page of that issue. The experimental simplicity makes this full-field imaging technique ideally suited for single shot imaging at a free electron X-ray laser.

In late spring of FY2004, the experimental setup was shipped back from BESSY. It was located at a dedicated branch line of SSRL’s new spherical grating beam line (BL5) whose source is an elliptically polarizing undulator. In preparation for use on this beam line, the chamber has been modified to best match to the new beam line. In addition to a series of minor upgrades, the multichannel plate detector has been replaced with an in-vacuum CCD camera. Furthermore, the design of a thin film growth chamber has begun. This chamber will be used to grow and characterize the defect-free, monolayer-thickness, thin ferromagnetic films needed for the study of critical magnetic fluctuations.

While BL5 was still in commissioning in early FY2005, parts necessary for the investigation of magnetic fluctuations were incorporated into the experimental setup: *in situ* sample manipulation, temperature control, earth field compensation, and an optical MOKE system to characterize the magnetic properties of the thin films.

***Small and Wide Angle Scattering Studies of Soft Matter and Colloids*** –The end station was upgraded to allow for new SAXS and WAXS capabilities.

The principal upgrade was the provision of a walk-in hutch for the experimental science and a much needed longer optical path, providing X-ray scattering information at lower  $q$  values (and therefore information about larger spatial correlations). This is vital because, as the synthetic control of polymer chemistry increases, particularly through living polymerization techniques, the capabilities of macromolecular design have likewise dramatically increased and so have the physical sizes over which molecules can now be tailored. Many research groups now have the capacity to design macromolecular superstructures where designed order exists on several length scales: gold-coated polymer backbones can be laid inside encompassing hollow cylindrical

structures with micron-scale diameters, for example. These have particular interest in the field of nanoelectronics and IBM is pursuing their development aggressively.

Having already mapped the internal architectures of the components, the new construction succeeds in expanding the SAXS capabilities accordingly to complete the architectural characterization and thus fully evaluate their importance to the nano-electronics field. It is research projects such as these that will be served by this longer optical path.

***Structural Properties of Novel Materials*** – Under the general heading of Novel Materials, there are several major subgroups being explored, including the local structure of noncrystalline materials, the structure of organic and inorganic thin films, the distribution of pore sizes in nanoporous films, the distribution of particle sizes in nanoparticulate materials, the interfacial structure of aqueous solution-solid interfaces, and charge density waves in rare earth tellurides.

***Noncrystalline Materials*** – The X-ray analyzer developed at SSRL and used for the measurement of the structure of amorphous materials was used to measure the structure of liquid water. As expected, the contribution of the Compton scattering peak is significant at a lower scattering vector ( $q$ ) than one sees with the higher-Z materials we have worked with in the past (e.g.,  $\text{MoGe}_3$ ). To determine the feasibility of the experiment, it was performed at 12 keV so that the graphite (0002) reflection could be used. It was found that there is sufficient signal to obtain a scattering pattern. We also learned the best way to produce the liquid water jet which enables us to measure the scattering from water without having a background signal from the sample container.

***Thin Film Structure*** – Pentacene has emerged as a viable candidate for the semiconducting transport layer in organic thin film transistors (OTFTs). While it is recognized that the transport properties of crystalline organic films depend strongly on the molecular packing in the crystal, little is known about the detailed crystal structure of the active transport layers in OTFTs, including pentacene. We have collected grazing-angle incidence X-ray diffraction data for pentacene films grown on amorphous  $\text{SiO}_2$ . The data show that the thin films are crystalline with a large ( $>70$  nm) crystal size, and the pentacene molecules adopt a herringbone arrangement with their long axes tilted only a few degrees from the substrate normal. This molecular packing results in a high intermolecular overlap of the pentacene wave functions that is consistent with the exceptional transport properties of these films. The crystal structure of the pentacene films is not significantly dependent on film thickness up to about 30 nm.

Another class of promising materials for low-performance, thin-film transistors used in displays, is semiconducting polymers of regioregular polythiophene. To investigate the relationship between polymer structure and charge carrier mobility in thin film transistors, grazing incidence diffraction studies have been conducted of regioregular poly(3-hexylthiophene) (P3HT) thin films. These were done as a function of molecular weight (which was previously shown to dramatically affect mobility) and processing conditions. The diffraction shows that for a constant molecular weight the in-plane pi-stacking in the polymer increases with increasing mobility (as expected), but for varying molecular weight, this correlation breaks down. Hence, the mobility-molecular weight relationship is not due to in-plane pi-stacking in the polymer, but rather both disordered domain boundaries and chain length effects result in the observed relationship between molecular weight and mobility.



***Ultra-trace and Microanalysis*** – A microfocus X-ray mirror system using Kirkpatrick-Baez (KB) optics was installed in the back hutch of BL6-2. Prior to installation it was characterized with the Long-trace Profilometer (LTP) at the Center for X-ray Optics (CXRO) at Lawrence Berkeley National Laboratory (LBNL). The mirrors were characterized using X-rays and a focal spot of 2 microns x 2 microns was obtained. The beam-line optics includes a virtual source defined by a high-precision slit in the front of the back hutch. The mirror prior to the monochromator focuses onto this slit, overfilling the aperture. By changing the size of the slit one can change the size of the focal spot downstream of the KB optics, so that a large spot can be used for coarse scanning of a sample (e.g., finding a micrometeorite in a block of aerogel) or a small spot for element mapping of an individual particle.

Applications of TXRF at ultra-high sensitivities continued with an emphasis on developing broader user communities beyond the semiconductor-based research that has formed the basis of the earlier work on the beam line. As an example, an experiment was performed with a new user to study the uptake of metals in cell cultures. The low levels require a fluorescence study; however, the samples are very different from silicon wafers and require very different considerations for quantification and treatment of backgrounds. In another example, collaboration has started with the PI of the NASA Genesis mission which returned samples of solar wind collected at the Lagrangian point for over two years. Unfortunately, due to a parachute malfunction the samples were shattered during the landing. There is optimism that many of the mission goals are still obtainable, but it also is thought that TXRF, due to the ability to distinguish between surface and near-surface contamination, will be an especially effective tool. Flight-spare material as well as one returned sample were studied during the 2005 experimental run.

XAS Studies as a Probe of Electronic Structure / Contribution to Function – X-ray absorption spectroscopy (XAS), at the ligand and metal K- and metal L-edges, is used to determine the electronic and geometric structure of metal-based centers in inorganic and bioinorganic systems. The goal is to understand the involvement of the metal center in catalytic cycles important in industrial and biological catalysis. The experimental approach is complemented by Density Functional Theory (DFT) calculations, photoemission spectroscopy measurements, valence bond simulations and the development of data analysis tools, as well as by other non-synchrotron-based methodologies including MCD, resonance Raman and EPR spectroscopies, where applicable. The combined approach enables significant insight into the geometric and electronic structure and its contributions to reactivity. Currently, studies are focused on systems containing copper, iron, titanium, molybdenum, and tungsten with the anticipation of extending these studies to other transition metal sites.

***Copper*** – A combination of Cu K-edge, EXAFS, and S K-edge studies have been performed on red copper protein, which is the perturbed blue copper-related site in nitrosocyanin. These studies show that there is almost a factor of two decrease in the copper-thiolate covalent interaction relative to the normal blue copper site in plastocyanin (20% in red copper, 38% in plastocyanin), consistent with the elongation of the Cu-S bond from 2.1 Å to 2.3 Å, as observed by EXAFS. Comparison of the S and Cu K-edges of red copper with plastocyanin reveals a stronger ligand field for the red copper site, consistent with MCD studies. These results have been combined with resonance Raman, EPR, MCD, and low temperature absorption

spectroscopies and DFT calculations to evaluate the role of exogenous H<sub>2</sub>O binding to the Cu site and the tuning of the site for inner vs. outer-sphere electron transfer.

Cu K-edge and EXAFS studies have been performed on [(diketiminate)CuO<sub>2</sub>], a mononuclear copper dioxygen complex. These studies show that the copper in this species is in the Cu(III) oxidation state and the molecule can be best described as a Cu(III)-O<sub>2</sub><sup>2-</sup> system. Cu K-edge EXAFS studies have also been performed on [(F8TPP)Fe-O<sub>2</sub><sup>2-</sup>-Cu(TMPA)](ClO<sub>4</sub>), a heme-peroxo-copper complex which mimics the active site for O<sub>2</sub> reduction in cytochrome c oxidase. These studies were coupled with DFT calculations to obtain insight into the electronic and geometric factors which contribute to antiferromagnetic coupling of the Cu and Fe centers. A series of metal-varied blue copper-related model complexes [ML(SC<sub>6</sub>F<sub>5</sub>)] (where L = hydrotris(3,5-diisopropyl-1-pyrazolyl)borate and M = Mn, Fe, Co, Ni, Cu, and Zn) have been studied by S K-edge XAS. These studies combined with MCD, and low temperature absorption and DFT calculations reveal that the metal 3d-thiolate orbital interaction, which contributes to the covalent bonding in these complexes, becomes stronger on going from Mn(II) to Co(II) (the  $\sigma$  contribution) and to Cu(II) (the  $\pi$  contribution). This change in covalency results from the increased effective nuclear charge of the metal atom on going from Mn(II) to Zn(II) and the change in the 3d orbital population (d<sup>5</sup>→d<sup>10</sup>).

**Iron-Sulfur** – Ligand K-edge XAS has been used to obtain a quantitative description of Fe-S bonding in Fe-S model complexes and protein active sites. The results of these studies have been correlated to differences in redox potentials. The pre-edge in ligand K-edge XAS of [Fe<sub>3</sub>S<sub>4</sub>]<sup>0</sup> model complexes and proteins can be resolved into contributions from the  $\mu_2$ S<sub>sulfide</sub>,  $\mu_3$ S<sub>sulfide</sub> and S<sub>thiolate</sub> ligands. The average ligand-metal bond covalencies obtained from these pre-edges are further distributed between Fe<sup>3+</sup> and Fe<sup>2.5+</sup> components, as estimated from DFT calculations. The bridging ligand covalency in the [Fe<sub>2</sub>S<sub>2</sub>]<sup>+</sup> subsite of the [Fe<sub>3</sub>S<sub>4</sub>]<sup>0</sup> cluster is found to be significantly lower than its value in a reduced [Fe<sub>2</sub>S<sub>2</sub>] cluster (38% vs. 61%, respectively). This lowered bridging ligand covalency reduces the superexchange coupling parameter J relative to its value in a reduced [Fe<sub>2</sub>S<sub>2</sub>]<sup>+</sup> site (-146 cm<sup>-1</sup> vs. -360 cm<sup>-1</sup>, respectively). This decrease in J, along with estimates of the double exchange parameter B and vibronic coupling parameter  $\lambda^2/k$ -, leads to an S=2 delocalized ground state in the [Fe<sub>3</sub>S<sub>4</sub>]<sup>0</sup> cluster. The S K-edge XAS of the protein ferredoxin II (Fd II) from *D. gigas* active site shows a decrease in covalency compared to the model complex, for the same oxidation state, which correlates with the number of H-bonding interactions to specific sulfur ligands present in the active site. The changes in ligand-metal bond covalencies upon redox, coupled with DFT calculations, indicate that the redox reaction involves a two-electron change (one electron ionization plus a spin change of a second electron) with significant electronic relaxation. The presence of the redox inactive Fe<sup>3+</sup> center is found to decrease the barrier of the redox process in the [Fe<sub>3</sub>S<sub>4</sub>] cluster due to its strong antiferromagnetic coupling with the redox active Fe<sub>2</sub>S<sub>2</sub> subsite.

To develop a quantitative description of hydrogen bonding in Fe-S systems, a series of P450 model complexes, where the amount of hydrogen bonding was systematically varied, were examined by S K-edge XAS. The S K-edge XAS data show a dramatic decrease in pre-edge intensity with increasing H-bonding to the ligated thiolate. DFT calculations reproduce these effects and show that the observed changes are in fact solely due to H-bonding to the thiolate ligand. The energy of the H-bonding interaction was estimated to be -2.5 kcal/mol in the gas phase. The rather small H-bonding energy appears to be in contrast to the large change in ligand-

metal bond covalency (30%) observed in the data. A bond decomposition analysis of the total energy is developed to correlate the pre-edge intensity change to the change in Fe-S bonding interaction on H-bonding. This analysis shows that the Fe-S interaction energy is greatly reduced due to H-bonding. This effect is greater for the reduced than the oxidized state, leading to a ~350 mV increase in the redox potential. It is also found from a valence bond configuration interaction (VBCI) model that  $E^{\circ}$  should vary linearly with the covalency of the Fe-S bond in the oxidized state, which can be determined directly from S K-edge XAS. The above study was extended to a hydrogen bonded  $[\text{Fe}_4\text{S}_4]^{2+}$  cube, which had an elongated core structure in contrast to the compressed core structures of most  $[\text{Fe}_4\text{S}_4]^{2+}$  cubes. A decrease in pre-edge intensity was observed for the H-bonded cube. DFT calculations indicate that the change in Fe-S covalency observed experimentally had almost equal contributions from the cluster elongation and the H-bonding interaction. These calculations also indicate that the elongation of the  $[\text{Fe}_4\text{S}_4]_{2+}$  cube changes the spin topology of the ground state due to redistribution of the ligand superexchange interactions in the cluster.

### *Non-heme Iron Systems*

*Siderophore* – In order to overcome the immense difference between environmentally and nutritionally available Fe, many microorganisms produce low-molecular-weight iron-chelators called siderophores. Our recently developed L-edge methodology provides a unique way of studying the bonding in these compounds. Fe L-edge data on a small set of compounds,  $\text{K}_3[\text{Fe}(\text{ox})_3]$ ,  $[\text{Fe}(\text{pha})_3]$  and  $\text{K}_3[\text{Fe}(\text{cat})_3]$  have been obtained. Preliminary results show that both the Fe K- and the L- edges shift to lower energy across the series:  $\text{K}_3[\text{Fe}(\text{ox})_3] < [\text{Fe}(\text{pha})_3] < \text{K}_3[\text{Fe}(\text{cat})_3]$ . This shift indicates a decrease in effective nuclear charge and an increase in electron donation by the ligands. The total intensity of the Fe L-edge transitions decreases across the series, implying that  $[\text{Fe}(\text{cat})_3]^{3-}$  is the most covalent of the compounds. By simulating the multiplet structure of the spectra, we are able to calculate the  $\sigma$  and  $\pi$  contributions to bonding in the compounds. Much of the change observed is attributable to increases in  $\pi$ -bonding across the series. The series will be extended to include a broader range of model compounds including those with different H-bonding motifs.

*Cyanides* – Cyanide compounds have played an important role in the development of key concepts in coordination chemistry and are used extensively in new magnetic materials. We are applying our Fe L-edge methodology to two compounds,  $\text{K}_4[\text{Fe}(\text{CN})_6]$  and  $\text{K}_3[\text{Fe}(\text{CN})_6]$  (Fe(II) and Fe(III), respectively). Analysis of the multiplet structure will provide information about the bonding in these systems, which is not available through other methods. We have currently adapted our L-edge methodology to include metal-to-ligand charge transfer and are working to include three configurations in the multiplet simulations.

*Heme vs. Non-Heme Fe* – Fe porphyrin compounds or hemes form the basis for electron transfer in a number of biological systems, with the most well-known being the cytochromes. The delocalization of the Fe d-orbitals into the porphyrin ring and its effect on the redox chemistry of these systems has been difficult to study spectroscopically because of the dominant porphyrin  $\pi$  to  $\pi^*$  transitions. Recently, we have developed a novel methodology that allows for the interpretation of the multiplet structure of Fe L-edges in terms of differential orbital covalency (i.e., differences in delocalization of the different d orbitals) using a valence bond configuration interaction (VBCI) model. Applied to heme systems, this methodology allows experimental

study of the delocalization of the Fe d-orbitals into the porphyrin ring. We have obtained data on two model systems  $[\text{Fe}(\text{tpp})(\text{Him})_2]\text{Cl}$  and  $[\text{Fe}(\text{tpp})\text{py}_2]$  (low spin Fe(III) and Fe(II), respectively) and are comparing their multiplet structure to the two low-spin non-heme compounds  $[\text{Fe}(\text{tacn})_2]\text{Cl}_2$  and  $[\text{Fe}(\text{tacn})_2]\text{Cl}_3$ .

*Lipoxygenases* – Lipoxygenases are non-heme iron dioxygenases that catalyze the hydroperoxidation of 1,4-*Z,Z*-pentadiene-containing polyunsaturated carboxylic acids. Two mechanisms have been proposed for the action of lipoxygenases: one involving an organometallic bond, and the other H-atom abstraction. A mutant of soybean lipoxygenase, N694C, has been produced which would favor the former mechanism, with an  $\text{Fe}^{\text{III}}\text{-S}$  bond providing stabilization of the  $\text{Fe}^{\text{III}}$  species thought to be involved in this mechanism. Studies of enzyme activity show that the N694C mutant is approximately 100 times less active than the native form. Preliminary Fe K-edge X-ray absorption spectroscopy (XAS) pre-edge studies show that the mutant is 5-coordinate. Fe K-edge pre-edge and MCD data will also be obtained on the intermediate form in the anaerobic substitution reaction.

*HPPD* –The  $\alpha$ -ketoglutarate ( $\alpha$ -KG) dependent dioxygenases comprise an extensive class of non-heme iron enzymes which require  $\text{Fe}^{\text{II}}$ ,  $\alpha$ -KG, and dioxygen for catalysis. (4-hydroxyphenyl)pyruvate dioxygenase (HPPD) is an  $\alpha$ -keto acid-dependent dioxygenase involved in the tyrosine catabolism pathway which catalyzes the conversion of (4-hydroxyphenyl)pyruvate (HPP) to homogentisate in a reaction involving decarboxylation, substituent migration, and aromatic oxygenation. From MCD studies, the iron active site appears to have a mixture of 5- and 6-coordination. However, the relative ratios of the 5- and 6-coordinate species could not be established. From XAS pre-edge analysis of Fe K-edge data of this dioxygenase, it has been established that the 6-coordinate species dominates, both in the presence and absence of substrate. EXAFS data will be utilized to obtain more detailed structural information about the enzyme and its interaction with the substrate.

*Titanium Cyclopentadienyl Catalysts* – Ti K- and Cl K-edge XAS studies have been initiated on a series of catalytically relevant Ti-TEMPO complexes ( $\text{TiCl}_3\text{TEMPO}$ ,  $\text{TiCl}_2\text{CpTEMPO}$ ,  $\text{TiClCp}_2\text{TEMPO}$ ). The rate of Ti-O bond homolysis depends sensitively on the ancillary ligation at titanium and indicates that changes in the geometric and electronic structure may be important in understanding catalytic activity. Ti K-edge XAS will be used to determine the oxidation state of the Ti-TEMPO complexes and to provide insight into the contribution of cyclopentadienyl (Cp) to bonding. These data will be complemented by Cl K-edge XAS to determine the effect of the Cp on the spectator ligands. The results of these studies will be coupled with DFT calculations in order to obtain insight into the factors that favor homolytic vs. heterolytic Ti-O bond cleavage.

Organotitanium complexes play important roles as homogeneous polymerization catalysts and have recently received attention as anticancer agents. In order to understand the contribution of Cp ligands to the electronic structure of these complexes, a combination of Ti K-edge and Cl K-edge XAS has been applied to  $\text{TiCl}_4$ ,  $\text{TiCpCl}_3$ , and  $\text{TiCp}_2\text{Cl}_2$ . The results of these studies demonstrate that Cp is a strong donor which decreases the interaction of the titanium with the remaining spectator ligands, resulting in longer, less-covalent Ti-Cl bonds. Using  $\text{TiCl}_4$  as a reference, a configuration interaction based model for 3d-4p mixing has been developed which

demonstrates that pre-edge intensities may be used to define ligand-metal covalency in noncentrosymmetric complexes.

**Molybdenum** – The pterin-dithiolene cofactor is essential to all families of molybdenum oxotransferases. These families of enzymes mediate oxygen atom transfer (OAT) and proton-coupled electron transfer (PCET) to and from a variety of different substrates including DMSO, sulfite, and xanthine. Since the central molybdenum atom and the pterin-dithiolene ligand are both potentially redox active, it is important to evaluate specific contributions to enzymatic function. The electronic structure description for a series of Mo tris(dithiolene) complexes ( $[\text{Mo}(\text{L}_3)]_Z$ ;  $\text{L} = 1,2\text{-Me}_2\text{C}_2\text{S}_2$  and  $Z = 2-, 1-, 0$ ) has been developed based on a combination of S K-edge XAS and DFT. This provides a starting reference for studies of Mo=O dithiolenes related to the mechanism of OAT and PCET in molybdenum oxotransferases.

The methodology developed and applied to molybdenum tris(dithiolenes) (i.e., the correlation of experimentally calibrated density functional theory with S K-edges) is currently being extended to systems of Mo bis(dithiolenes) related to the DMSO reductase and sulfite oxidase families of Mo oxotransferases. Specifically, the wave functions of the model complexes  $[\text{MoO}_n(\text{dithiolene})_2]^{m-}$  ( $n=0, 1, 2$  and  $m=1, 2$ ) are being developed. An understanding of the covalency of Mo-S bonds will provide important insights into the reactivity of the structurally related Mo oxotransferases.

**PES Studies of Electronic Structure Contributions to Function** – The shake-up satellite structure present in core and valence photoemission spectroscopy (PES) data can be used in combination with a valence bond configuration interaction (VBCI) model to experimentally quantify electronic relaxation (i.e., the change in electronic structure of metal complexes upon oxidation) and its contributions to reduction potentials and kinetics of electron transfer (ET). Variable-energy PES (VEPES) experiments provide the tool to maximize the metal while minimizing the ligand contributions to the valence band region through cross section effects (delayed maximum and Cooper minimum) and resonance enhancement. VEPES data on a series of model iron complexes – high spin  $[\text{FeCl}_6]^{4-/3-}$  and low spin  $[\text{Fe}(\text{CN})_6]^{4-/3-}$  and  $[\text{Fe}(\text{tacn})_2]^{2+/3+}$  – have been measured and we will continue measurements on redox heme couples  $[\text{Fe}(\text{tpp})(\text{py})_2]^{1+/0}$ ,  $[\text{Fe}(\text{tpp})(\text{CN})_2]^{1+/0}$ ,  $[\text{Fe}(\text{tpp})(\text{Him})_2]^{1+/0}$ ,  $[\text{Fe}(\text{tpp})]^{1+/0}$ , etc. These redox couples will be analyzed using the methodology (VBCI model and DFT calculations) developed in the studies on  $[\text{FeCl}_4]^{2-/1-}$  and  $[\text{Fe}(\text{SR})_4]^{2/1-}$  ( $\text{R} = \text{Ph}$ ) in FY2003. The effects of increased coordination, high spin vs. low spin, and back bonding will be investigated to define contributions of electron delocalization into the porphyrin (tpp) ligand to electronic relaxation and how this contributes to electron transfer (ET) in the cytochromes.

### Materials Research

Research carried out by SSRL faculty and staff and associated Stanford faculty and students is described in this section which covers a broad set of disciplines: (1) Complex Materials; (2) Magnetic Materials; (3) Scientific and Educational Gateway Program; (4) Nanoscale Ordering in Complex Oxides: Model Systems for Local Probes; (5) Nanoscaled Magnetism in the Vortex State of High- $T_c$  Cuprates; (6) Nano-scale Electronic Self-Organization in Complex Oxides; (7) Nano-Magnetism; (8) Linac Coherent Light Source R&D; (9) Photon Instrumentation for X-ray Experiments at LCLS (PIXEL); and, (10) Ultrafast Science Center. Areas (4) through (7) are

collaborative efforts of the SSRL X-ray Laboratory for Advanced Materials and the Stanford University Geballe Laboratory for Advanced Materials.

### ***1. Complex Materials***

The team has conducted comprehensive experiments using photoemission (Shen), scattering (Greven and Shen), and theoretical investigation (Laughlin and Doniach) on complex materials, and has made substantial progress in this period. There also are synergetic interactions with the nano-science programs of Greven, especially in the area of single crystal growth, and Shen's core program on strongly correlated materials.

A major focus of our program is the electron-doped materials that have presented an important challenge to our systematic understanding of high-temperature superconductors. The Greven group has continued its successful effort on the electron-doped superconductor  $\text{Nd}_{2-x}\text{Ce}_x\text{CuO}_4$  system, built on its early success in growing high quality single crystals [P.K. Mang *et al.*, *Phys. Rev. Lett.* **93**, 027002, 2004]. These data for the spin correlations and ordered moment are in good agreement with recent theory for the Hubbard model, which in turn is based on Shen's earlier ARPES work [Armitage *et al.*, *Phys. Rev. Lett.* **88**, 257001 2002]. These results constitute significant progress toward a full understanding of the normal state of the electron-doped superconductors. Since superconductivity in high- $T_c$  cuprates appears in close proximity to the antiferromagnetic phase, it is essential to understand the nature of nearby magnetic ground states. Through careful X-ray and neutron diffraction work, Greven discovered that the oxygen reduction process, required to render  $\text{Nd}_{2-x}\text{Ce}_x\text{CuO}_4$  superconducting, transforms a fraction of the crystals into cubic  $(\text{Nd,Ce})_2\text{O}_3$ , and that the field effects observed by others and ascribed to a quantum phase transition of NCCO are not intrinsic, but due to this secondary phase [P.K. Mang *et al.*, *Nature* **426**, 139, 2003, and *Phys. Rev. B* **70**, 094507, 2004]. Consequently, the question of genuine magnetic field effects in  $\text{Nd}_{2-x}\text{Ce}_x\text{CuO}_4$  remains an interesting, unresolved research topic. The discovery of spurious magnetism in NCCO is a good example of the benefits of a synergistic growth and scattering effort like that by Greven.

In collaboration with Sette's group at the ESRF, Greven continued the novel use of inelastic X-ray scattering to investigate the collective charge excitations in the model high-temperature superconductor Hg1201, the single-layer material with the highest value of  $T_c$  [Lu *et al.*, preprint]. This latter work, carried out at the APS and made possible by newly available large crystals grown by Greven, led to the discovery of a remarkably rich structure of electron-hole pair excitations in the cuprate superconductors.

Greven's work on the structural phase diagram and charge-order phenomena in the layered manganite [Larochelle *et al.*, *Phys. Rev. Lett.* **87**, 095501, 2001] has been extended to cover a wider range of doping as well as neutron scattering [Larochelle *et al.*, *Phys. Rev. B* **71**, 024435 (2005)]. These results will allow a comprehensive understanding of the structural and magnetic phase diagram.

The angle-resolved photoemission spectroscopy (ARPES) component of the initiative (Shen) has two primary tasks: research, and operation of the beam line 10.0.1 end station at the ALS in support of this research. That activity also benefited a broader community performing ARPES experiments using the end station.

The focus during this period of time is to develop new methodology and apply it to high- $T_c$  superconductors and their related materials. In collaboration with Plummer's group at Oak Ridge National Laboratory, we contributed to the development of a new methodology to extract the bosonic spectral function from ARPES data. Our data with very high signal to noise were essential to extract the Eliashberg function from metal surfaces states as well as deeply underdoped cuprate superconductors [Shi *et al.*, *Phys. Rev. Lett.* **92**, 186401, 2004; Tang *et al.*, *Physica Status Solidi B* **241**, 2345, 2004]. We have also extended this result to the high- $T_c$  superconductors.

Another area of major progress during the period is the new insight on the anisotropy of quasiparticle dynamics between nodes and antinodes [Zhou *et al.*, *Phys. Rev. Lett.* **92**, 187001, 2004]. Such dynamics reveals the nature of microscopic processes involved, and is potentially important both to understand pairing and the connection to other experiments such as STM.

Shen's group also has made important technical progress in applying synchrotron radiation for high resolution spectroscopy experiments. The resolution and flux density at the ALS have been a critical factor for the program in generating a significant database. On the other hand, this also raises the technical problem of space charging. Shen's group has systematically characterized this problem and our finding is generally useful in guiding high resolution photoemission experiments in third generation synchrotron radiation facilities [Zhou *et al.*, *J. Elect. Spectr. Rel. Phenom.*, **142**, 27, 2005].

The Shen group will continue its effort to develop better ways to record and analyze ARPES data from complex oxides. An expected related progress is the experimental finding of fine structures in the abrupt kink in the dispersion that is indicative of collective mode coupling (i.e., the kink is now found to have several substructures). This is the first time such a fine structure is observed in cuprates, due to greatly improved signal-to-noise ratio. This effort benefits greatly from collaboration with the Plummer group and discussions with Laughlin. Shen's ARPES program has also expanded its scope to other transition metal oxides, in particular that of the manganites, cobaltites, and nickelates. We expect these investigations will yield insights on the interplay between spin, charge and orbital degrees of freedoms in these complex oxides.

Greven and Shen have continued their synergistic collaboration on materials and measurements. An important advance in this period is the systematic investigation of the effect of chemical inhomogeneity in the bismuth-based copper oxide superconductors [Eisaki *et al.*, *Phys. Rev. B* **69**, 064512, 2004]. This has enabled many spectroscopic and scattering experiments on materials. This comprehensive approach of materials synthesis, measurement and theory has been the key to enabling higher productivity than the simple sum of the individual efforts. The Complex Materials Initiative also enhances and leverages on other activities in the photoemission study of correlated materials (Shen through SSRL) and advanced crystal growth of novel and model materials (Greven, in collaboration with Beasley, Geballe and Fisher, through SSRL). As these activities are intellectually connected, they have been linked together in this FTP.

Greven has also extended his work on the magnetic field effects in electron-doped superconductors, with particular focus on inelastic neutron scattering, in order to finally unravel the properties of the new ground state that emerges when superconductivity is suppressed by a magnetic field. Greven's neutron scattering work also is being extended to measurements of spin correlation and excitations in reduced, superconducting NCCO, and is expected to lead to a refined understanding of this electron-doped material. Further, Greven is studying the effect of intentionally introduced disorder (Zn and Ni doping) on the magnetic properties of NCCO, and the extent to which Ce (electron) and Zn (dilution) doping effects are additive. Shen's closely related ARPES work, on NCCO crystals grown by Greven, will be extended to as-grown and overdoped samples.

Greven's crystal growth efforts are also being extended to other high-temperature superconductors with the long-term goal of obtaining a deeper understanding of antiferromagnetic and charge/structural degrees of freedom using neutron and X-ray scattering, and to correlate such information with complementary collaborative ARPES and STM work on the same samples. In a major recent breakthrough, Greven [together with Beasley, Geballe, and Fisher] has succeeded in growing samples of the mercury-based superconductor  $\text{HgBa}_2\text{CuO}_{4+\delta}$  (Hg1201) that are two orders of magnitude larger than the previous world record. Hg1201 exhibits the highest superconducting transition temperature of all the single-layer cuprates, and it is the material with the simplest crystal structure. The new samples are large enough to allow the first detailed scattering, ARPES, and, potentially, STM experiments of this model superconductor. Greven's (resonant) inelastic X-ray scattering measurements on Hg1201 will be extended to different doping levels and materials.

The Laughlin group has studied the phase diagram in cuprate high  $T_c$  superconductors. Recent experimental measurements suggest the coexistence of various phases of matter in different regions of the pseudogap regime. Guided by such experiments the group has studied the properties of a spin-density-wave antiferromagnetic mean-field ground state with d-wave superconducting (DSC) correlations. This work concentrates in the case when antiferromagnetic order is turned on weakly on top of the superconductivity, which corresponds to the onset of antiferromagnetism at a critical doping. In such a case a small gap proportional to the weak antiferromagnetic gap opens up for nodal quasiparticles, and the quasiparticle peak would be discernible [Z. Nazario and D.I. Dantiago, *Phys. Rev. B* **70**, 144513, 2004]. Laughlin's group has also done work on metal-insulator transitions. Specifically, the work was motivated by  $\text{V}_2\text{O}_3$  and f-electron systems which have phase diagrams in which a line of first order metal-insulator transition ends at a critical point above which the two phases are indistinguishable. We extended Bob Laughlin's Gossamer technique to show that the gossamer metal in a single-band model will describe a metallic phase that becomes arbitrarily hard to differentiate from an insulator as one turns the Coulomb correlations up. Thus one can go continuously from the metal to the insulator.

The program looked broadly at the many-body problem in condensed matter system, beyond the high- $T_c$  superconductors and transition metal oxides. Work on the superfluid to Mott insulator transition in bosonic systems has been done, where the phase diagram of a single component Bose Einstein Condensate (BEC) in an optical lattice at zero temperature was obtained. In that work, the discontinuous nature of the transition between the superfluid and the Mott insulator (under certain conditions) was elucidated, as well as its independence on commensuration of the



number of bosons with the lattice [Z. Nazario and D.I. Dantiago, *Phys. Lett A* **328**, 207, 2004; *Phys. Rev. B* **70**, 184508, 2004]. Recently measurements which could be interpreted as such a transition have been performed by Mark Kasevich's group of Stanford University. While, being superfluids, BECs share many properties with superfluid helium, they have never been seen to share the existence of roton excitations that are present in helium. Superfluid helium is close to becoming a solid. The roton minimum is a consequence of enhanced density fluctuations at the reciprocal lattice vector of the stillborn solid. Thus rotons have not been observed in BECs in atomic traps since they are not near a solid phase, but if they are tuned near a transition to a Mott insulating phase, a roton minimum will develop at a reciprocal lattice vector of the lattice. Equivalently, a peak in the structure factor will appear at such a wave vector. The smallness of the roton gap or the largeness of the structure factor peak are experimental signatures of the proximity to the Mott transition [Z. Nazario and D.I. Dantiago, *J. Low Temp. Phys.* **137**, 599, 2004].

Doniach has developed a model of “orbital antiferromagnetism in coupled planar systems” to describe pseudogap phenomena in poor metals such as ruthenates [Schroeter and Doniach, *Phys. Rev. B* **69**, 094407, 2004]. In addition, simulations of the molecular dynamics of liquid water have led to the discovery of dynamic defects, or “nanoholes,” with lifetimes on the order of a picosecond. Such transient structures are of interest in connection with the photoionization threshold of water, where they may be responsible for the observed lowering of the threshold by around 1eV. The current focus of the theoretical research is on computations of the expected X-ray scattering from these defects which may be observable using the Subpicosecond Pulse Source.

The Doniach group has also started on a study of correlated electron effects in C<sub>60</sub> lattices. Angle-resolved photoemission studies by the Shen group suggest that the HOMO bands of these crystals have a mass renormalization of around a factor 1.5. There also is a suggestion that quasi-2D layers of this material may have appreciably altered mass renormalization. Studies were initiated into the effects of dimensionality on the electron-phonon mass renormalization effects in these materials. It is anticipated that they may be quite strongly altered by electron correlation effects (following the review by Gunnarson). This could lead to break down of Migdal's theorem.

## **2. Magnetic Materials Research**

Our general program on X-ray studies of magnetic materials concentrated on two areas:

- 1) Exploration of the ultimate speed of magnetic switching.
- 2) Development of resonant soft X-ray methods for lensless imaging of magnetic domains.

(1) This work has shown the existence of a fundamental speed limit in writing the magnetic “0” and “1” bits used for data storage in computer disk drives. This was determined using ultrafast, high-field electron pulses. The study predicts that technology will run into this fundamental speed limit as data storage rates are increased by a factor of about 200 over those in today's computers.

I. Tudosa, H. C. Siegmann and J. Stöhr *et al.*, *Nature* **428**, 831, 2004. For other write-ups see:

[http://www-ssrl.slac.stanford.edu/research/highlights\\_archive/speedlimit.html](http://www-ssrl.slac.stanford.edu/research/highlights_archive/speedlimit.html)

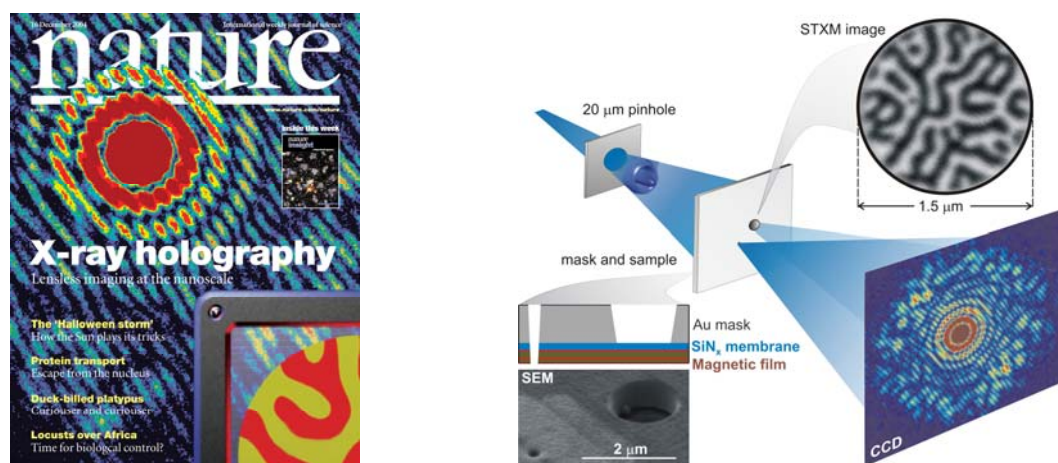
<http://www.slac.stanford.edu/slac/media-info/20040423>

<http://www.stanford.edu/~itudosa/research/research.html>

(2) We have been pursuing a new idea for reconstructing a coherent scattering pattern into a real space image based on Fourier transform X-ray holography. It consists of placing a small reference structure near the sample of interest and recording the holographic interference pattern. Since the inverse Fourier transform of the detected interference pattern is the spatial autocorrelation of reference structure and the sample, this technique should yield an image of the sample with the resolution determined by the size of the reference structure. We have now succeeded in this demonstration which was featured on the cover of *Nature* as shown below on the left. The experimental setup is shown on the right side below and is described in the figure caption.

S. Eisebitt, J. Lüning, W. F. Schlotter, M. Lörngen, O. Hellwig, W. Eberhardt and J. Stöhr  
*Nature* **432**, 885, 2004.

[http://www-ssrl.slac.stanford.edu/research/highlights\\_archive/lensless.html](http://www-ssrl.slac.stanford.edu/research/highlights_archive/lensless.html)



Left: *Nature* cover. Right: Scheme of the experimental setup. Monochromatized and circular polarized X-rays are incident on a mask/sample structure after spatial coherence filtering. The object and reference beam are defined by the mask and the resulting hologram is recorded on a CCD detector. Bottom inset: geometry and scanning electron microscopy image of the mask/sample structure. Top inset: scanning transmission X-ray microscopy image of the magnetic structure illuminated through the sample aperture.

### 3. Scientific and Educational Gateway Program

This continuing, joint effort with the University of Texas at El Paso (UTEP) serves both the Mexican-American and Mexican communities in undergraduate and graduate education by engaging student scholars in science and engineering research programs at all levels. The program provides travel support for Mexican-American and Mexican students and supporting faculty, science and technological support by an SSRL scientific staff member, who also assists participants in beam-line operations and laboratory facilities use, and a scientific staff member at UTEP, who develops and implements computational tools and software for analysis of synchrotron data. These staff members train students in methods of data reduction and analysis

and, jointly with SSRL staff scientists, develop collaborative tools for remote access to instrumentation and data measured at SSRL. This program has been quite effective, as shown by the close to 50 UTEP students participating. These students and staff underwent training and carried out experiments on existing SSRL peer-reviewed proposals coordinated across five separate beam lines during the FY2004 run. The students continue to enhance their training by taking highly successful proposal writing classes at UTEP (Pingitore). SSRL staff work closely with the UTEP faculty and staff to train and support the new students and their research efforts. During the shutdown periods in FY2004 and 2005, the students concentrated on data analysis with the help of SSRL and UTEP staff. Progress during this period was excellent with many students and faculty further developing their proficiency in the use of synchrotron techniques.

The level of synchrotron-related skills increased substantially for both the students and faculty, which will be reflected by refereed publications and meeting presentations of the group. In particular, skills were improved in the areas of SAXS and carbon edge XANES. Progress was made in six core areas: (1) The Chianelli group continued to address structure/function relations in transition metal sulfide (TMS) hydrodesulfurization (HDS) nanocatalysts. The first "Gateway" Ph.D. (Myriam Perez) was graduated; (2) Diffraction studies on Maya Blue demonstrated that the pigment is a surface complex of the indigo dye with palygorskite clay; (3) Data analysis on both the SAXS and WAXS data from asphaltenes, crude oils from Mexico and Venezuela and TMS catalysts was completed; (4) The Gardea group continued to investigate the metal binding properties of the "hyperaccumulators;" (5) The Pingitore group continued to study trace elements in human bone. The incorporation of Sr, Zn, Pb, etc. in human bone is a topic that impacts archaeology, nuclear waste/terrorism, biomedicine, and environmental pollution.

A new project that has arisen is *in situ* studies of fuel cells. This project is in collaboration with Karen Swyder Lyons of the ONR, who will provide an operating fuel cell (*in situ* spectroscopic cell) modified and tested at Brookhaven National Laboratory to the project. This project will combine ONR fuel cell expertise, UTEP fuel cell materials synthesis and characterization expertise with the synchrotron expertise of SSRL and will focus on students training to work in interdisciplinary teams.

Gateway students have achieved in-depth understanding of synchrotron radiation and its application by attending the Stanford-Berkeley summer school. There was a two-day hands-on training session at SSRL in addition to the school for Gateway students.

#### **4. *Nanoscaled Ordering in Complex Oxides: Model Systems for Local Probes***

This program directly addresses scientific questions at the heart of understanding correlated electron behavior in complex materials. Our work explores the conditions of occurrence and mechanisms behind these effects, and examines the consequences for bulk properties and collective phenomena. Our approach is to identify and synthesize model systems that enable us to explore particular interactions in isolation. The essence of the proposed research therefore lies in the design, growth and characterization of novel materials.

#### **Negative-U Impurities**

Over the course of the last two years we have established a multistep synthesis route to produce high-quality single crystals of the unusual superconductor  $(\text{Pb}_{1-x}\text{Tl}_x)\text{Te}$ , with Tl concentrations up to the solubility limit of approximately 1.5%. The Tl impurities appear to act as negative-U

centers in this material, and our research explores the role that these impurities play in both the superconducting and normal state properties. During FY2004 we showed for the first time that a critical concentration of Tl impurities is required to cause superconductivity in PbTe. For Tl concentrations beyond this critical value the Fermi level appears to be pinned, such that the Tl impurities act in a self-compensating manner. It seems that the superconductivity is intimately linked to the presence of a mixed Tl valence, the presence of which also is reflected in the normal state transport of the material. In particular, we have found evidence for a charge Kondo effect associated with degenerate valence states of the Tl impurities. Such an effect supports the notion of an electronic pairing mechanism in superconducting Tl-doped PbTe, perhaps accounting for the unusually high  $T_c$  value. Our ongoing research seeks to further investigate this effect. A manuscript has been submitted to *Phys. Rev. Lett.* (cond-mat/0409174). Through a more detailed exploration of the superconducting properties of Tl-doped PbTe, we found that initial heat-capacity measurements indicate that the superconducting anomaly is rather large, and the material appears to be in a strong-coupling limit. We also have found  $H_{c2}$  to be rather large, up to almost 1 T, with a correspondingly small coherence length. Ongoing experiments through the course of the year will give a clearer picture of the superconducting properties. We also have established collaborations with C. Gough (Birmingham, UK) to measure penetration depth and superfluid density, S. Brown (UCLA) to look for evidence of different Tl sites via NMR, and Z. Schlesinger (UCSC) to explore optical conductivity, especially with regard to elucidating fine details of the electronic structure (relative positions of L and  $\Sigma$  bands). We continue to enjoy theoretical support from J. Schmalian (Ames Laboratory).

### **Charge-Density Waves in Layered Rare Earth Tellurides**

We recently identified the layered rare earth tellurides  $R\text{Te}_3$  and  $R\text{Te}_2$  as model systems to study Fermi surface reconstruction in incommensurate CDW compounds, a topic that has significant bearing on current questions in the field of cuprates and other strongly correlated oxides. These are particularly attractive model systems because (a) the electronic structure is especially simple and the band filling can be tuned by chemical substitution; (b) the CDW gap is large and can be measured by a variety of powerful techniques; (c) we can explore the consequences of the CDW formation on the magnetic properties of the material; and (d) we are able to grow high-quality single crystals, enabling sensitive probes of the Fermi surface including dHvA and ARPES, and real space probes including STM.

We have optimized our synthesis technique and characterized the resulting crystals using TEM and X-ray diffraction, as well as exploring bulk thermodynamic and transport properties. Initial experiments at SSRL confirmed the quality of the crystals and indicated a large CDW correlation length. Angle resolved photoemission experiments in collaboration with Z. X. Shen (SSRL/Stanford) clearly revealed the CDW gap, showing gapped and ungapped regions of the Fermi surface (*Phys. Rev. Lett.* **93**, 126405, 2004). Initial de Haas-van Alphen (dHvA) measurements showed at least three frequencies which vary with angle according to  $1/\cos(\theta)$ , consistent with minimal z-axis dispersion. Comparison with the areas obtained via ARPES implies that a 500 T frequency is likely associated with the ungapped piece of Fermi surface centered around  $(0, \pi/a)$ , while a 1.6 kT frequency arises from reconstructed regions of Fermi surface formed from the other ungapped sections.

Having established the quality of the crystals obtained by our new synthesis route for this material, we have begun a detailed study of the thermodynamic and transport properties. Of

particular note, we find evidence for incoherent transport in the c-axis direction, consistent with minimal z-axis dispersion, and reminiscent of layered oxides. For the heavy rare earth members of the series we also observe that a superzone gap opens at  $T_N$ , *i.e.*, further gapping of the already-gapped Fermi surface (FS). Our ongoing dHvA experiments have begun to reveal the effects of bilayer splitting (due to the twin Te layers), an effect that we are continuing to study through the course of the year both in our own lab and in collaboration with A. Makenzie (St. Andrews, Scotland). Further X-ray diffraction experiments are scheduled for later in the year at SSRL to probe the charge density wave. Results of a collaborative project with S. Dugdale (Bristol, UK) based on positron annihilation as a probe of the ungapped Fermi surface were successful, and a manuscript is currently in press, to be published later in the year. We have also established a collaboration with L. DiGiorgi (ETH Zürich, Switzerland) to measure optical conductivity, potentially giving access to subtle changes in the FS as a function of temperature well below the CDW transition.

### **Electronic Inhomogeneities in Correlated Electron Materials**

One of the goals of this program is to synthesize model systems for the study of nanoscale electronic inhomogeneities that result from the coulomb interactions in correlated electronic materials, and ultimately to study these inhomogeneities using scanning probes. Toward this end, we have been growing thin films of the Mott insulator CuO, in which such nanoscale inhomogeneities have been previously reported. This is perhaps the simplest conceivable copper oxide related to the high temperature cuprate superconductors. Epitaxial thin films of stable monoclinic CuO have been grown on MgO substrates. The composition (and copper valence) has been confirmed using *in situ* XPS. Preliminary attempts to stabilize this material in the rock-salt structure through the use of epitaxy combined with ion-beam-assisted deposition (IBAD), which selects particular orientations and structure of a growing film, have commenced. We have determined that the use of activated oxygen (atomic oxygen) is necessary when using IBAD due to the tendency of the ion beam to reduce the films to Cu<sub>2</sub>O.

In parallel with this effort, we are depositing thin films of ZrO<sub>2</sub> using pulsed laser deposition (PLD) for use as high-K dielectrics for field-effect doping applications. During the past year, we have further optimized the substrate temperature and oxygen pressure during deposition. We have also examined the role of film thickness. Substrate temperature is the most important variable. We now can produce films with dielectric constants around 20 and breakdown fields between 5 and 20 MV/cm. This performance is sufficient to enable field-effect doping densities in the range of  $10^{14}$  charges/cm<sup>2</sup>, which is typical of the cuprate superconductors and other 2D correlated materials. Application of these films for field-effect doping on In-oxide thin films has demonstrated reversible field-effect doping at a level an order of magnitude higher than in previous studies.

Having successfully deposited the stable monoclinic form of CuO, we are now pursuing two lines of activity. First, we are continuing our attempts to grow CuO in the rock-salt structure using epitaxy and IBAD. We will try a number of substrate materials including NiO and SrTiO<sub>3</sub>. We will also continue our use of *in situ* XPS and UPS studies to analyze our synthesis products and to study the effects of charge transfer doping using highly electropositive and electronegative ultra-thin overlayers. Second, we will study the existing monoclinic films using

scanning tunneling potentiometry to see if we can image directly in transport the charge inhomogeneities seen in TEM micrographs of oxygen-deficient crystals of CuO.

We also are now pushing hard the use of our high-K ZrO<sub>2</sub> films for field effect doping of In-oxide. We will first characterize the effects at room temperature using conductance and Hall effect studies and then turn our attention to trying to tune the superconductor/insulator transition being studied in this system by our colleague Aharon Kapitulnik. Time permitting, we may also explore the use of IBAD to better achieve uniformly the tetragonal phase of ZrO<sub>2</sub>, which has a dielectric constant of 40, a factor of 2 higher than our present films.

### **Superconductivity and Magnetism: Pair Density Waves and SrRuO<sub>3</sub>**

Interest has grown recently in the superconductor/ferromagnetic proximity effect because it is proving to be an effective model system for the study of the interaction between superconductivity and magnetism. One of the most striking predictions from theory is the existence of decaying pair density waves in the ferromagnetic side of an SF proximity bilayer due to the exchange field in the F material. Evidence for this effect is mixed. In order to get more detailed information regarding SF proximity structures, we have been doing tunneling density of states studies on the F side of Nb/permalloy SF bilayers as a function of the thickness of the F layer. We find the striking result that the tunneling density of states as a function of thickness (viewed as deviations from the normal density of states) is of constant form with amplitude that scales exponentially over four orders of magnitude as a function of the F layer thickness. This result is in marked contrast with the best available theory, which predicts oscillations related to the expected pair density wave. These results were presented at the recent American Physical Society March meeting and have been submitted for publication.

We also continue to study SrRuO<sub>3</sub> as a rare example of a 4d itinerant ferromagnet. With the group of Lior Klein we have been examining the magnetotransport in SrRuO<sub>3</sub> to test recent theories of the effect of the Berry phase in magnetic systems. We did not confirm the predictions. The results will appear in *Phys. Rev. B* shortly. We have also returned our attention to the thin film synthesis of this material using our new combined PLD/Molecular Beam Synthesis system in order to clarify why the two techniques produce films of markedly different quality as gauged by their residual resistivity values.

Given our present results on the tunneling density of states on Nb/permalloy SF proximity bilayers, it is very important to study other F materials to see if our results are universal or specific to permalloy. In particular, it is important to examine F materials with lower exchange fields, such as the Ni-Cu alloy system studied by many other groups. More careful characterization of possible interface mixing is also important and will be pursued first with RBS studies.

We also plan to use our *in situ* FTIR system to study the optical conductivity of SrRuO<sub>3</sub> at high temperatures. Lower temperature measurements carried out by us with Zack Schlesinger at UCSC showed that a coulomb-like pseudo-gap appears to open at low frequencies as temperature increases. This seems to be part and parcel of the bad metal behavior of this material (*i.e.*, increasing resistivity with increasing temperature beyond the Ioffe-Regal limit). Recent

theories of highly incoherent electrons using dynamical mean-field theory predict such a gap should open. Clearly these predictions need to be tested.

### ***Advanced Superconductors***

The mercury-based materials  $\text{HgBa}_2\text{Ca}_{n-1}\text{O}_{2n+2+\delta}$  are model high-temperature superconductors due to their relatively simple structure, because they appear to be least affected by chemical disorder, and because of their record superconducting transition temperatures (e.g., for  $n = 3$ ,  $T_c = 134$  K at ambient pressure and 164 K at 31 GPa). These materials, therefore, are the most desirable high-temperature superconductors for experimental study. Comparison with results for lower- $T_c$  materials will eventually allow us to separate materials-specific properties from properties shared by all superconducting cuprates. However, the synthesis of this homologous series has remained a serious challenge until recently. Consequently, rather few experiments have been done on the Hg family of superconductors. In a major breakthrough, we succeeded in growing single crystals of Hg1201 ( $n=1$ ) as large as  $30 \text{ mm}^3$ , more than two orders of magnitude larger than the previous world record. Neutron diffraction (at the NIST NCNR) and synchrotron X-ray work (at SSRL) confirmed the single-grain nature of our samples, with a typical mosaic of 0.04 degrees. The new crystals have allowed us to begin systematic transport, magnetometry, and resonant inelastic X-ray scattering (RIXS) experiments (at the APS), and to initiate numerous collaborations, both at Stanford and elsewhere, with scientists using complementary experimental techniques. New optical spectroscopy measurements by Dr. C.C. Homes (BNL) are consistent with a newly discovered scaling law for the superfluid density and were published in *Nature* [C.C. Homes *et al.*, *Nature* **430**, 539, 2004].

We previously investigated the effects of chemical inhomogeneities in the bismuth-based family of copper oxide superconductors,  $\text{Bi}_2\text{Sr}_2\text{Ca}_{n-1}\text{Cu}_n\text{O}_{2n+1+\delta}$  [H. Eisaki *et al.*, *Phys. Rev. B* **69**, 064512, 2004]. The double-layer variant ( $n = 2$ ; “Bi2212”) of this homologous series has been of great interest to the ARPES and STM communities, but systematic neutron scattering work has not been possible due to the lack of sizable crystals. We found that the maximum attainable value of  $T_c$  can be increased to a new record value of 96 K for a small amount of Y doping, *i.e.*, Ca-site disorder, which, in effect, leads to a stoichiometric Bi:Sr ratio of 2:2 and hence zero Sr-site disorder. These results have the important implication that the degree and the type of disorder are very important experimental parameters that can and should be controlled: a new generation of experiments on such optimized samples is clearly called for. Our recent efforts have focused on attempting to grow sizable crystals for inelastic neutron scattering work.

The superconducting properties of our new Hg1201 ( $n=1$ ) crystals are being refined further through a heat treatment in an oxygen atmosphere in order to obtain very underdoped and also overdoped samples. This long-term project is challenging since uniform oxygen control away from optimal doping is a nontrivial task due to the large size of our crystals. Furthermore, we are continuing to explore the growth of the multilayer ( $n>1$ ) members of the Hg family of superconductors. Due to the high Hg partial pressure during the growth, this task is more challenging than the growth of the  $n=1$  system. Our initial RIXS work on Hg1201 [L. Lu *et al.*, submitted to *Phys. Rev. Lett.*] led to the important general discovery of the necessity to employ the incident photon energy dependence of the K-edge RIXS cross section in order to arrive at satisfactory qualitative and quantitative understanding of the charge-transfer excitations in complex oxides. It furthermore led to the surprising observation of a remnant charge-transfer gap

in optimally doped Hg1201. These exciting developments have been very recent, and we expect to be able to refine further the growth conditions to obtain crystals of even larger volume and for  $n > 1$ . This will enable increasingly detailed and valuable experiments on the Hg-based model superconductors, such as X-ray and neutron scattering, optical spectroscopy and Raman scattering, ARPES, STM, as well as thermal and charge transport. Quantitative experimental results for the Hg-based family of materials can be expected to serve as benchmarks for tests of theories of high- $T_c$  superconductivity.

### ***5. Nano-scaled Magnetism in the Vortex State of High- $T_c$ Cuprates***

This work explores fundamental physical processes which give rise to novel collective phenomena and self-assembled nanostructures resulting from high magnetic fields or complex synthesis processes. The complex nanostructures include antiferromagnetism inside the vortex cores and checkerboard charge order of the Cooper pairs in high  $T_c$  superconductors. The research program has recently been broadened to include quantum spintronics, dissipationless quantum spin current and the intrinsic spin Hall effect.

A major accomplishment of our research program has been the theory of the “pair density wave” (PDW), which describes the checkerboard charge order of Cooper pairs in high  $T_c$  superconductors. Due to strong correlations or Fermi surface nesting, electrons can form a self-organized crystal like a Wigner crystal, or a charge-density wave. In these charge-ordered states, the elementary unit cell contains only a single electron. On the other hand, the PDW state is a charge-ordered state of the Cooper pairs, rather than single electrons. We showed that such a state could be favored in underdoped cuprates, where local pairing force is strong, but the kinetic energy of the holes is reduced. We proposed a global phase diagram to describe the competition between the antiferromagnetic state, the d-wave superconducting state and the PDW states. Most remarkably, the PDW state only exists at certain magic, rational doping fractions, e.g. at  $x=1/8$ ,  $1/16$ ,  $3/16$ , where the denominator is a power of 2. At these magic filling fractions, the Cooper pairs form a checkerboard structure.

Some of these theoretical predictions were soon confirmed experimentally. Earlier STM experiments at Stanford and Berkeley have uncovered microscopic charge ordering on the surface of high  $T_c$  cuprates. More recent STM experiments unveiled a more precise  $4 \times 4$  checkerboard charge pattern on the surface of CaNaCuOCl crystals. Close to a doping level  $x=1/8$ , the charge ordering pattern is only consistent with the charge ordering of the hole pairs, in accordance with our theoretical proposal. Another remarkable transport experiment was carried out by Ando’s group, in which they systematically measured the resistivity as a function of doping, and have identified certain “magic doping fractions” at  $x=1/16$ ,  $3/16$ ,  $1/8$  and  $3/8$ , where the resistivity displays a maximum, indicating charge ordering tendencies. This observation is again consistent with our predicted global phase diagram.

Our work on the pair-density-wave and charge ordering received broad attention in the high  $T_c$  community. It was featured in the “News and Views” section of *Science*, in an article entitled “Crystalline Electron Pairs.” The PI was invited to speak at numerous international conferences, including the Gordon Conference and the Aspen winter conference. The two students working on the projects have successfully completed their Ph.Ds, and received prestigious job offers. Handong Chen is going to Caltech as a postdoc, while Congjun Wu is going to KITP/UCSB as a postdoc.



Our work on the theory of the pair-density-wave will concentrate on identifying microscopic interactions which could be responsible for this new state of matter, and study the stability of the PDW state against various perturbations. Through these studies, we can gain insights into the microscopic origin of the pairing interaction.

We also started a new direction of research on quantum spintronics. This work has now become an important focus of our research group. Our theoretical predictions on the dissipationless spin current and the intrinsic spin Hall effect has greatly stimulated the spintronics community. Two experiments have now independently detected the spin Hall effect. One of them, performed by Joerg Wunderlich's group at the Hitachi-Cambridge lab is broadly believed to originate from the intrinsic spin Hall effect we predicted theoretically. The experimental confirmation of the intrinsic spin Hall effect is celebrated as a important highlight of the condensed matter physics community. The news story was covered by the EE Times and *Physics Today*. The PI was an invited speaker at the Symposium on Spin Hall Effect at the APS March meeting and a keynote speaker at Semicon 2005.

Our work on quantum spintronics focuses on developing novel theoretical methods to predict the behavior of spin transport in semiconductor devices. We are working closely with IBM, within the framework of IBM/Stanford spintronics center, to test experimentally the theoretical predictions on the dissipationless spin current. We are also working on a new proposal where the spin Hall effect can become quantized under a strain gradient of the lattice. This would, for the first time, give an example of the quantum Hall effect without the use of an external magnetic field.

### ***6. Nanoscale Electronic Self Organization in Complex Oxides***

Nanoscale ordering in complex oxides, where the valence electrons self organize in ways qualitatively different from those of conventional metals and insulators, is one of the most important outstanding problems in physics today. Our research is inherently multidisciplinary as we show below.

#### *ARPES Program*

The nanoscience funding enabled us to leverage our core program on strongly correlated materials, as the students and postdoctoral associates are taking experimental shifts for each other. In addition to oxide materials, we continue our effort to explore nanoscale science in related materials. We have continued our collaboration with Ian Fisher's group on charge-density wave materials, and have expanded our effort on materials made of carbon nanoclusters.

Electronic Structure of Charge Density Wave State Rare Earth Tellurides – In collaboration with the Fisher group, we have performed extensive ARPES experiments on various rare earth di- and tri- tellurides. These materials manifest many phase instabilities, and can be used as model compounds to study phase and phase competitions among various electronic and lattice instabilities at nanoscale.  $\text{CeTe}_3$  and  $\text{CeTe}_2$  have been the focus of our effort, as the charge-density wave state manifests itself most strongly in these compounds. Through ARPES, the electronic structure, the Fermi surface folding, the coherence factor, the gap anisotropy, are all been investigated. We gained insights about the inner workings of the phase instabilities in these

materials. We have also tested several classical charge density wave concepts using these materials as a platform. A paper was published in 2004 (*Phys. Rev. Lett.* **93**, 126405, 2004)

We have investigated the many-body interactions in tellurides and  $\text{Sr}_2\text{RuO}_4$  with the hope of gaining insights into the microscopic mechanism behind the phase instability and phase competition. These many-body interactions usually manifest themselves in the unusual spectral line shape seen in ARPES experiments. We are developing models to fit the experimental spectra.

Electronic Structure of Solids Made of Carbon Nanoclusters – With much improved momentum resolution, we were able to use ARPES to measure momentum resolved electronic structure of solids made of carbon nano-clusters, exemplified by  $\text{C}_{60}$  and its derivatives. This experimental advance enables us to discover something that has been speculated for a long time but never observed before: a dramatic change in the electronic structure with molecular orientation. This in turn provides possible explanations for many puzzling macroscopic properties. This is an example of how subtle effects at nanoscale can lead to dramatic change in material properties [*Phys. Rev. Lett.* **93**, 197601, 2004].

We studied solids made of carbon nanoclusters such as fullerenes, carbon nanotubes, and diamondoids to study the physics and materials properties of molecular solids, with an eye on the issues of phases and phase competitions, common phenomena in complex oxides. In fullerenes, we have uncovered clear evidence of phase separation near the boundary of metal-to-insulator transition with doping, indicating the importance of screening in these materials. We have also started an investigation of the electronic structure of diamondoids.

#### *Magnetic Imaging Program*

Using novel scanning techniques, we continued our study of several high- $T_c$  systems. In particular we emphasized the study of the interplay between magnetism and superconductivity. Below are some of our advances in the past year:

The Mesoscopic Magnetic Imaging of Very Underdoped Cuprate – We have demonstrated the existence of partial flux quanta, resulting from wandering pancake vortex stacks, in very underdoped YBCO. The possibility of wandering pancake vortices that we invoked in our studies of YBCO complicates the interpretation of penetration depth measurements. Further work on both the YBCO samples and on very underdoped samples of Hg-1201 in collaboration with Martin Greven of the parallel program is needed to sort out the contributing factors to the apparent vortex size.

Nanoscale Ferromagnetism, Antiferromagnetism, and Superconductivity in  $\text{ErNi}_2\text{B}_2\text{C}$  – Hendrik Bluhm from the Moler group in collaboration with Suchitra Sebastian from Ian Fisher's group studied the interplay of ferromagnetism, antiferromagnetism, and superconductivity in  $\text{ErNi}_2\text{B}_2\text{C}$ . The co-existence of these three phases leads to fascinating nanostructured ferromagnetism. We obtained the first high-quality local magnetic images of this nanostructure, reaching two main conclusions. First, the twin boundaries in the antiferromagnetic state strongly pin vortices. This may be a new model for planar pinning structures. Second, a spontaneous vortex lattice has been

theoretically predicted to exist at low temperatures in the ferromagnetic state. We have demonstrated that it does not.

Magnetic Signatures of Time Reversal Symmetry Breaking in  $\text{Sr}_2\text{RuO}_4$  – Per Bjornsson from the Moler group magnetically imaged the ab-plane surface of single crystals of the unconventional superconductor  $\text{Sr}_2\text{RuO}_4$ , including one sample with an array of microholes, using scanning SQUID and Hall probe microscopy in a dilution refrigerator at low applied magnetic fields. The images show dilute trapped vortices, as would be expected in conventional type-II superconductors, and no other magnetic features. We found no direct signs of the spontaneous magnetization that would be expected in a time reversal symmetry breaking (TRSB) superconductor. These measurements set upper limits on the presence of TRSB signatures in this material. A manuscript has been submitted to *Phys. Rev. B*.

### *High Resolution STM Studies*

In order to investigate fully nanoscale ordering phenomena in a variety of materials, our studies seek to uniquely combine both momentum-space and real-space detection techniques for a complete measurement portfolio. In the past year we have continued to extend the capabilities of STM by measuring low-energy vibrational and magnetic excitations, and to couple these new techniques with atomic manipulation. In addition we have developed a new method to apply local stress to materials. The constraints these combined efforts place on the apparatus are extreme, and part of our ongoing work is to integrate these tools with the complex materials that are the focus of this study. This year we operated a low-temperature UHV STM and a custom low-temperature break-junction apparatus in pursuit of proposed goals.

We are extending our STM measurements to new materials synthesized by the Fisher group. In particular, we have learned how to prepare surfaces of PbTe and are exploring the proposed charge-Kondo ground state in these materials via local tunneling spectroscopy. Proposed work will extend these studies synergistically to new magnetic correlated materials. Prime candidates are the colossal magnetoresistive (CMR) manganites. Promising to technology as well, these materials have revealed themselves to be fertile ground for novel correlated electron physics, potentially involving effects such as double-exchange and charge localization via polaron formation. Finally, we are applying our piezo stress measurements to the extreme underdoped region of YBCO, in collaboration with UBC.

Nanoscale Self-Organization in Novel Superconductors – We have concentrated thus far on the most easily cleavable materials to perfect surface preparation in our STM system. We have demonstrated clean surfaces of  $\text{Bi}_2\text{Sr}_2\text{CaCu}_2\text{O}_{8+\delta}$  grown by Greven's group, and are currently performing tunneling measurements on these samples in the presence of a simultaneous current flow. The tunneling measurements are currently taking place in one UHV STM, and are being adapted to our hybrid break junction/STM apparatus. A new method for applying pressure to thin superconducting samples was developed. In this apparatus, a piezo induces either uniaxial or biaxial stress in the plane of conducting layers of the compound under investigation. Strain gauges confirm 70% strain transmission from the piezo to the surface of the samples. This method is currently being applied to BSSCO to distort the unit cell with uniaxial compression and tune across phase boundaries. Currently achievable pressures are estimated at 30 to 90 atm.

Nanoscale Ordering in Correlated Magnetic Materials – Since part of our effort involves the measurement of the two-point propagator or Green's function via a single-point (STM) measurement and employing knowledge of the local scatterers, we previously completed a theoretical analysis of the quantum mirage effect via this formalism. This work, done in collaboration with Heller's group at Harvard, exploited a scattering approach into which Kondo correlations were introduced by the addition of a resonant scattering phase shift. Through the application of this theory, it became clear that our experiment was also a direct measurement of the Kondo phase shift for a single magnetic moment. During this year we have developed this technique into an interferometric procedure in which electrons within a resonator can be used to measure general phase shifts. In collaboration with Greg Fiete, we have analyzed several artificial Kondo lattices and observed a coherence effect in which the Kondo temperature is enhanced in the center of lattices which are resonant with a 2D surface Fermi wavelength. In addition, a correlation hole (the "Kondo hole") in a central vacancy was conclusively observed via experiment and comparison with new theory.

#### *STS of Ordered Structures on High- $T_c$ Materials*

In the past year we concentrated on upgrading our STM-STs system for better stability and noise performance. As a first project to see the impact of the improved system we studied again  $\text{Bi}_2\text{Sr}_2\text{CaCu}_2\text{O}_{8+\delta}$  single crystals cleaved in UHV and measured at low temperatures.

Ordered Structures in the LDOS of BSCCO – One of the greatest virtues of the new system that we constructed is its stability. Indeed we were able for the first time to perform scans of  $128 \times 128$  pixels on a  $500 \text{Å} \times 500 \text{Å}$  samples. This gives us improved k-space sensitivity. However, the greatest value of the improved system has been our ability to measure very slowly at the same atomic point, while at the same time using very small voltage modulation. With this capability we could perform very high-resolution study of the gap structure in real space.  $128 \times 128$  pixels on  $\sim 60$  square samples yielded many interatomic spectroscopic points. Analysis of the coherence peak size which is much more pronounced, suggests that resonances due to bound states near the gap size can contribute to the coherence peak height.

We also continued our study of optimally doped  $\text{Bi}_2\text{Sr}_2\text{CaCu}_2\text{O}_{8+\delta}$  in zero field where we concentrated on the differentiation of dispersive and nondispersive spatial density of states (DOS) modulations as a function of energy in our samples. More evidence was gathered to show that a spatial map of the superconducting coherence peak heights shows the same structure as the low energy DOS. To obtain this result we make a map of the density of states at the gap energy (*i.e.*, the DOS at the peaks of the conductance). Examination of the data shows that while gap inhomogeneity may have some degree of alignment with the superstructure, when the conductance (*i.e.*, LDOS) at the gap energy is plotted, the periodicity of approximately 4-lattice spacing which is 45 degrees to the superstructure is observed. This periodicity is similar to the one most prominent at low energies as discussed in previous sections. The fact that the LDOS at the gap energy ( $\Delta$ ) shows a periodicity similar to the low energy periodicity (*i.e.*,  $G(E)$ ,  $E \ll \Delta$ ) lends support to the fact that the 4-period is a robust feature, independent of dispersive features such as quasiparticle scattering interference.

We have shown that analyzing the location of the defects in the 2-D structure of stripes (checkerboard) reveal that the defects are concentrated in regions of low gap and large coherence

peak. This is the first study of the topology of CDW-like structures in strongly correlated systems.

STS Studies of the CDW State of CeTe<sub>3</sub> – With the improved STM-STs system we have begun a study of CeTe<sub>3</sub> which is a layered compound where an incommensurate Charge Density Wave (CDW) opens a large gap (~400 meV) in optimally nested regions of the Fermi Surface (FS), whereas other sections with poorer nesting remain ungapped. Using STM we succeeded to observe the CDW as well as observe the signal from the ungapped part of the Fermi surface.

### 7. Nanomagnetism

Last year we reported progress toward our goal to directly image and explore the switching of nanoscale structures by injection of a spin polarized current. In particular we reported progress in two areas: (i) development and use of pump-probe techniques to study time-dependent magnetization processes with nanoscale and subnanosecond resolution, and (ii) fabrication and imaging of spin injection structures with scanning transmission X-ray microscopy.

A typical sample is made by optical and e-beam lithography on a SiN coated Si wafer. After building the desired spin injection structure, a 100 x 100 μm<sup>2</sup> picture frame is etched from behind into the Si wafer, leaving the SiN membrane, so that the spin injection structure on front of the SiN membrane can be viewed with a scanning X-ray transmission microscope. A representative image of such a structure is shown in the figure below.

A Cu lead delivers the current to the center of the spin injection structure where the current runs upwards through a small pillar consisting of a Co/Cu/NiFe sandwich structure. The Co layer spin polarizes the current, the Cu layer decouples the Co reference layer from the to-be-switched NiFe layer. The current then exits through another Cu lead.

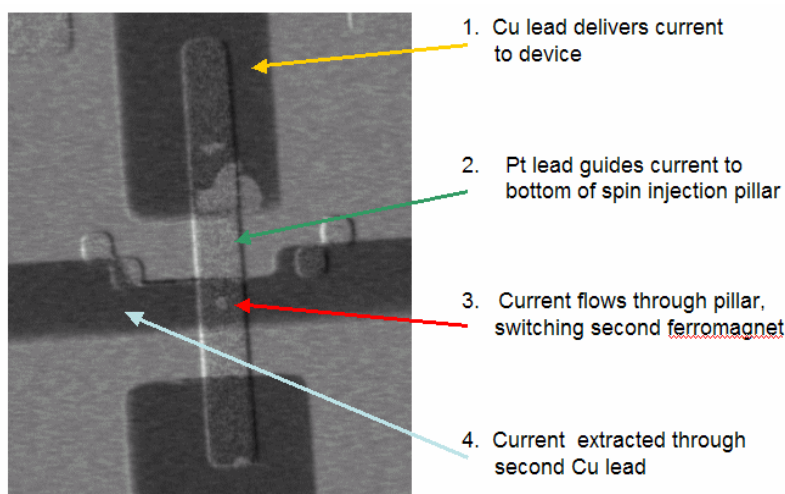
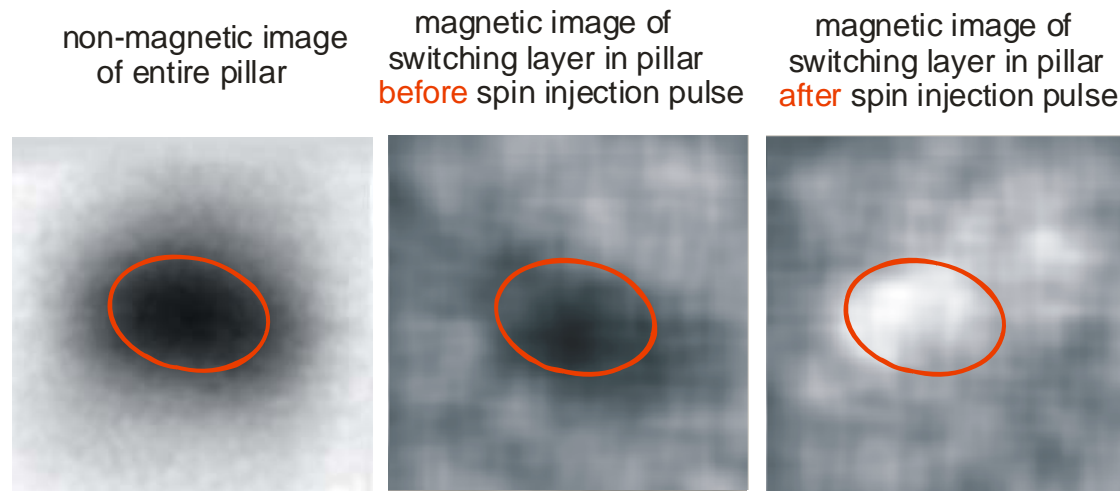


Image of a spin injection structure built lithographically on a SiN coated Si wafer. The image was recorded with a scanning X-ray transmission microscope at the Advanced Light Source. The pillar (seen as a gray dot) in the center has a diameter of about 100 nm.

We have now succeeded in direct imaging of the magnetic switching process by spin injection as shown in the next figure, below. The image has a size of 400 x 400 nm. On the left we show the

oval structure of the pillar revealed by a nonmagnetic image. In the middle, a magnetic image is shown of the switching layer before the spin injection pulse. The magnetization direction can be inferred from the white contrast to point horizontally from left to right. After the pulse the magnetic contrast has reversed and the magnetization now points horizontally from right to left.

Our results are quite exciting. They show for the first time that the switching process is not homogeneous but also contains effects from the Oersted magnetic fields arising from the charge current flowing through the pillar. Both the charge and spin current contribute to the switching process.



Images recorded by scanning transmission X-ray microscopy of the spin injection pillar. The left image is non magnetic and reveals the oval shape of the pillar with dimension  $\sim 300 \times 100$  nm. In the middle we show a magnetic image of the switching layer. Its magnetization points from left to right indicated by the black contrast. On the right we show a magnetic image taken after the spin injection pulse. The layer has now switched its magnetization direction (white contrast).

Now that we have demonstrated our ability to directly image the spin-injection induced switching, we have opened the door to detailed studies of the dependence of the switching processes on the following parameters:

*Pillar Structure* – Any technological application requires the understanding of the most favorable pillar structure such as shape, size and layer thicknesses.

*Magnetic Configurations* – Different relative directions of the magnetizations of the reference and switching layers are expected to lead to very different switching behavior according to theory. Our experiment can distinguish directly between theoretical models.

*Materials* – For manufacturing convenience most experiments have used Co-based magnetic reference and switching layers. From their macroscopic behavior, alloys and multilayers should be more suitable for certain device applications and this will be explored.

*Time Dependence* – We have built improved electronics to measure the detailed time-dependence of the switching process. One of the key questions is how fast spin-injection induced

switching really is. Some theories predict that switching times are limited to the nanosecond scale. We will explore switching as fast as 50 ps.

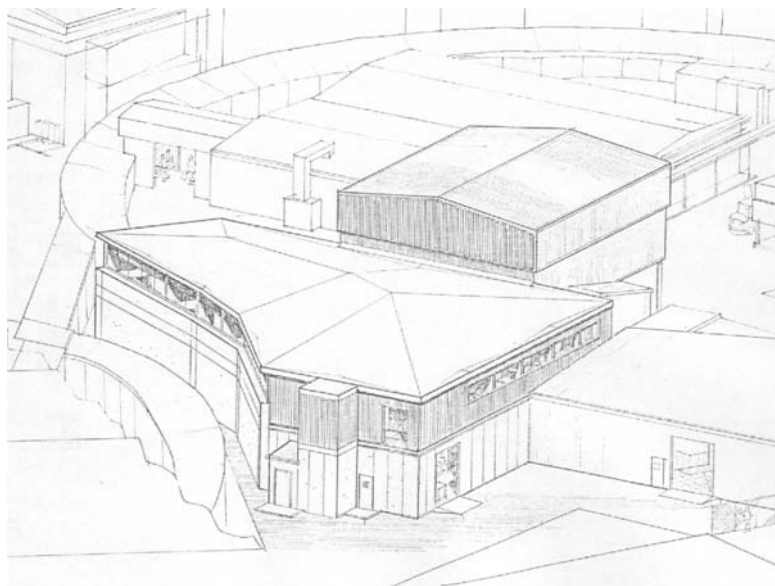
### ***9. Photon Instrumentation for X-ray Experiments at LCLS (PIXEL)***

This project will develop, design, procure, and commission a suite of instruments which will support the use of LCLS for several types of scientific study. The LCLS Science Advisory Committee has identified five major thrust areas for the initial LCLS science program: nanoscale dynamics of condensed matter; atomic, molecular and optical science; high energy density science; single particle and bio-molecule (non-periodic) imaging; and femtosecond dynamics of molecules and clusters. The PIXEL project will develop instrumentation for three of these areas (nanoscale condensed matter dynamics, single particle imaging, and femtosecond molecular dynamics), and possibly for an additional area (soft X-ray coherent imaging).

A comprehensive plan for a phased approach toward the development of these instruments is being developed in collaboration with the scientific community that intends to use them. This plan will result in a statement of mission need that will be used by DOE BES as a basis for establishing PIXEL as a Major Item of Equipment procurement project, through a Critical Decision-0 (CD-0) document. PIXEL will include a development program for an advanced 2-dimensional X-ray detector. This program will require several years of effort, and so in FY2005, based on the advice of the LCLS Detector Advisory Committee (LDAC) we have moved forward on the first stage of research and development aimed at this need.

### ***10. Ultrafast Science Center***

The Ultrafast Science Center (UFC) is in its first full year. Because the ultimate home of the center, the LCLS Central Laboratory and Office Complex (CLOC), will not be available until sometime in 2008, SSRL has decided to use half of the six laboratories of the X-ray Laboratory for Advanced Materials (XLAM) as a temporary home for the UFC laser laboratories. In addition, some of the XLAM office space will be made available for UFC personnel. We are currently building out the second floor of Building 130, shown in the picture below, for this purpose. We expect occupancy of the 6000 sq. ft. office and laboratory space by September of 2005. Below we describe activities in the five funded research areas: Ultrafast AMO Physics; X-ray Studies of Solids; Single Shot Magnetic Imaging; Ultrafast Magnetic Switching with e-Beams; and Toward Single Molecule Imaging with Intense, Short Pulse X-rays.



### 10A – Ultrafast AMO Physics

During the first year of the Ultrafast AMO program, efforts have been divided between establishing an attoscience program, and participating in Subpicosecond Pulse Source (SPPS) research activities. We are building a laboratory on Stanford campus that will house our attosecond laser and vacuum chamber, and we have also been collaborating with A. Lindenberg on experiments of joint interest at SPPS. Senior personnel P. Bucksbaum, R. Falcone, D. Reis, and S. Harris were joined by graduate student D. Fritz and technician M. Glowina. We also are interviewing for a postdoctoral research associate and we have identified our strongest candidate to help lead the attosecond research. D. Reis will spend a research leave at the Ultrafast Science Center in 2006.

A new, amplified, single-cycle stabilized femtosecond laser system will be installed and commissioned, with experiments beginning in FY2006. Major additional purchases will include a vacuum chamber and a Dazzler pulse-shaping system.

Our first experiments will involve creating coherent wave packet states in molecular gases, and probing them by generating high harmonics in the transiently excited medium. This has some advantages of simplicity over the usual method of separating the VUV attosecond pulse with a split multilayer mirror, and then recombining it in a second interaction region.

The transient excitation can be probed by splitting the single-cycle pump laser pulse into two pulses with a variable phase delay, by a new method. We will create a shaped pulse at the entrance to the capillary after the laser amplifier, by means of a Dazzler acoustooptic crystal. Learning algorithms and similar techniques can be used to create the desired pulse shape. To the best of our knowledge, this has never been done before; but the success of Murnane and Kapteyn in preshaping their laser to enhance harmonics gives us great confidence that it is possible. The aim is to gather information about quantum evolution in the earliest stages of these excited systems.

### 10B – Ultrafast X-ray Studies of Solids

We completed data collection on the first femtosecond X-ray experiments at the Subpicosecond Pulse Source (SPPS), probing the ultrafast solid-liquid transition. We confirmed the ultrafast duration of the pulses and the synchronization of optical pump pulses to the linac-based X-ray source. We observed new dynamical effects occurring on short time-scales. We discovered that the first step in the transition is governed by the ballistic motion of atoms on a softened potential energy surface. The transition involves an intermediate state during the first few hundred femtoseconds in which the atoms move a large fraction of an interatomic spacing at their initial room temperature velocity, before the solid has had time to heat up.

We also performed time-resolved X-ray diffraction measurements probing dynamical effects in the structure of water at the Advanced Light Source. We observed ultrafast structural changes (with 100 ps resolution) corresponding to changes in the local structure of the hydrogen-bond



network at constant volume. We showed how time-resolved measurements may be used as an alternative technique to studying isochoric structural changes in hydrogen-bonded liquids.

A postdoctoral research associate, S. Engemann, was hired to support this program. He conducted his thesis research in the group of H. Dosch at the Max Planck Institut in Stuttgart working at the ESRF. He arrived at SSRL in April 2005.

Two papers have been accepted for publication:

1. Atomic-scale visualization of inertial dynamics, *Science* (in press) 2005.
2. Time-resolved measurements of the structure of water at constant density, *J. Chem. Phys.* (in press) 2005.

A primary task is to build up the UFC laboratories and continue development of optical pump-probe experiments leading towards their use on the LCLS, especially focusing on utilization of infrared femtosecond spectroscopy to probe chemical, liquid, and solid-state dynamics. Additionally, a variety of liquid-state experiments at SPPS (in collaboration with K. Gaffney) are planned. Experiments are in preparation in which we hope to probe the delayed onset of liquid-like behavior in InSb through measurement of the liquid structure factor. Experiments probing solution-phase dynamics in both absorption and diffraction geometries also are ongoing.

Preparations are under way (in collaboration with A. Nilsson and J. Lüning) for femtosecond soft X-ray absorption measurements in liquid water. These experiments will probe local structural changes in the hydrogen-bond network following excitation of the OH stretching mode vibration, and should provide direct snapshots of the local hydrogen-bonded structure with 200 fs accuracy. These will be carried out at the ALS femtosecond slicing source.

### 10C – Single Shot Magnetic Imaging

The first year of this program consisted of building up the coherent imaging station on the elliptically polarizing undulator BL5-2 at SSRL. The newly rebuilt beam line is presently undergoing commissioning of a new spherical grating monochromator. The imaging station which was previously used in an experiment at BESSY, has been reassembled and upgraded. In particular, a CCD detector was purchased and new fast X-ray beam shutters were built.

A third-year Applied Physics graduate student, B. Schlotter, is supported under this program. He participated in the experiments at BESSY and already has considerable expertise in many aspects of our program, especially nanoscale mask fabrication techniques.

A postdoctoral research associate, A. Scherz, was hired after completing his Ph.D. at the Freie Universität Berlin in soft X-ray studies of magnetic materials. He also has experience in the fabrication of the ultrathin ferromagnetic films needed for our imaging studies of 2D critical phenomena. These films will be fabricated in a new thin-film deposition system constructed as part of the more general “Magnetic Materials Research” program.

In our first imaging experiments we intend to characterize the properties of the X-ray beam in terms of polarization, intensity and coherence. We then will explore imaging of magnetic nanostructures, lithographically manufactured in a beam defining coherence aperture, by our

previously demonstrated holographic method. Then we will start developing temperature- and time-dependent coherent imaging experiments as discuss below.

#### 10D – Ultrafast Magnetic Switching with e-Beams

We analyzed results obtained during a run in 2003 and a paper was submitted for publication: Dissipation of spin angular momentum in magnetic switching, *Phys. Rev. Lett.* It demonstrates the need to go beyond the Landau-Lifshitz-Gilbert theory of magnetization dynamics in describing magnetic switching at ultrafast time scales. In particular, our experiments expose the opening of a new dissipation channel, which we associate with transfer of energy and angular momentum from the uniform magnetization precession mode to higher spin wave modes. This process surpasses the intrinsic FMR-spin lattice relaxation of Fe by nearly an order of magnitude.

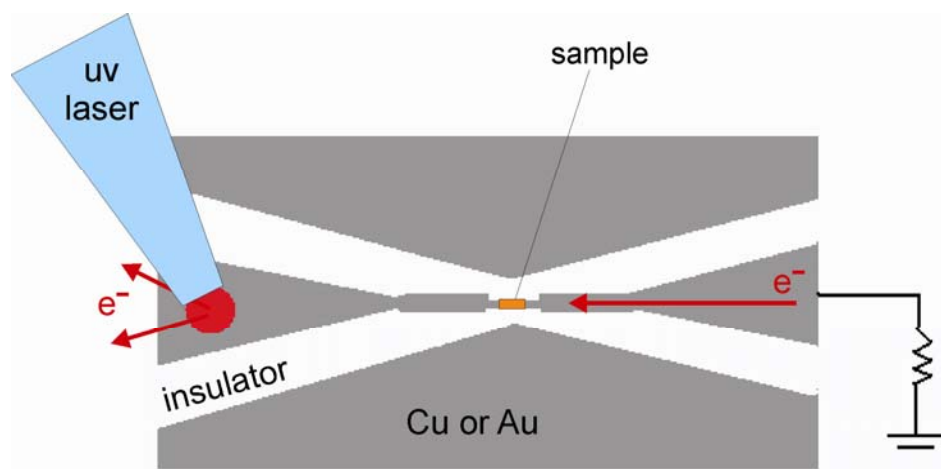
We also prepared for an upcoming experiment in May/June 2005 at the final focus test beam (FFTB) facility.

We have hired a staff scientist, Yves Acremann for our program who has considerable experience in the area of ultrafast magnetism and ultrafast laser techniques. Our previous e-beam experiments at SLAC were supported by I. Tudosa who is finishing his Ph.D. in Applied Physics. A second year Applied Physics graduate student, S. Gamble, has joined our program.

We also have made plans for a new laser-based experiment, described below, that may allow us to study ultrafast magnetization dynamics with electron pulses through ultrathin lithographic wires, so called strip lines. These experiments may possibly substitute for accelerator-based e-beam experiments.

We were scheduled for a run at the FFTB facility in May/June 2005 to explore the time dependence of magnetic switching in the ultrafast regime. During this experiment we had complete control of the linac beam for the first time and could therefore make measurements with electron beams of well-defined cross section and pulse length on the same sample. This detailed pulse-length-dependent series now being analyzed should reveal the exact transition from deterministic to nondeterministic magnetic switching.

As the FFTB facility will be dismantled in 2006 for construction of the LCLS, we will start working on a new laser-based method to create ultrashort strong magnetic field pulses. The scheme is illustrated in the figure below. A lithographically produced sample with a dimension of a few micrometers is positioned on a strip line that is grounded on one side. A UV laser from the SSRL gun test facility will be used to excite photoelectrons from a pad on the other side of the strip line. The laser pulse of variable length and strength may excite up to  $10^{10}$  electrons/pulse and therefore cause a current pulse down the strip line, which in turn will cause a magnetic field pulse at the position of the sample. We will explore just what field strengths and pulse lengths can be achieved with this method. The experiment will be set up in a new laser laboratory in SSRL Building 130. Paul Bolton (SLAC) will be collaborating on these experiments.



Schematic: creating an ultrashort, strong current pulse by photoemission with a 1 ps UV laser. The photoemitted electrons cause a current flow to ground through a stripline on which a sample is positioned.

### 10E – Toward Single Molecule Imaging with Intense, Short Pulse X-rays

This program began near the end of FY2004 with planning as the main focus. This included how the UFC efforts would be coordinated with the other principal collaborating groups at LLNL and Uppsala University (Sweden). The goals of the collaboration were defined to place primary focus on two specific areas: Further evaluation of damage and image reconstruction models by computational approaches (molecular dynamics and hydrodynamics models), and planning for initial experiments using the soft X-ray FEL at DESY for which experimental beam time is expected in FY2005.

Efforts are concentrated on preparing for experimental beam time at the DESY soft X-ray FEL that is scheduled for summer 2005. This includes the assembly of an experimental sample chamber which includes a gas-phase injection system and an in-vacuum CCD detector to record the scattering patterns from the nonperiodic objects. The specific aim of the first set of experiments will be to gain experience with sample injection of simple particles (e.g., nanospheres based on Si compounds) and study their behavior in the intense soft X-ray beam as a function of incident beam fluence. The process will be monitored by small angle scattering and will provide the first direct experimental data against which the theoretical simulations can be benchmarked. In parallel, more detailed simulations will continue, and include the use of the ultrascale high performance computing facility at LLNL (the “Thunder” 4000-processor cluster) to examine how surface-structured water on biomolecules behaves when injected into vacuum. This is an important question that relates to the effect of water acting as a “damper” to slow the radiation damage process.

### **Structural Molecular Biology**

The primary purpose of this work is to develop synchrotron radiation facilities and provide access for the national scientific community through a strong user-support program. Such synchrotron resources are a powerful and versatile tool for research in structural molecular biology, and provide tools relevant to addressing the U.S. Department of Energy mission needs.

The scientific and technological focus of this program includes the applications of synchrotron radiation to macromolecular crystallography, small-angle X-ray scattering (SAXS) and X-ray absorption spectroscopy (XAS). These efforts are led at SSRL by Professors K.O. Hodgson, B. Hedman and W.I. Weis, and Drs. S.M. Soltis and H. Tsuruta.

Key aspects of the program being provided by current and proposed BER funding include:

- Continued availability to, and support of users on, state-of-the-art beam lines and instrumentation on the upgraded 3rd-generation SPEAR3 storage ring for SMB research for a significant fraction of a given year (~9 months or more depending on core operation funding levels).
- Enhanced user support and training for SMB scientists using up to 10 existing stations at SSRL (of which eight are on high-intensity, multipole wiggler beam lines).
- Full operation and user research program on all three stations on the Beam Line 9 facility dedicated to SMB research.
- Continued development and implementation of advanced optics, experimental facilities, detectors, computer resources and software to enable optimal advantage to SMB users of the capabilities of the new 3rd generation SPEAR3 storage ring.
- Continuation of capital improvement projects in areas such as beam-line enhancements, data acquisition systems including detectors, electronics, controls and computer hardware for SMB stations.
- Continued synergistic research and user support in the SMB area with the NIH National Center for Research Resources (NCRR)-funded Biomedical Technology Program (BTP) and the National Institute of General Medical Sciences (NIGMS)-funded macromolecular crystallography operations support and Structure Determination Core of the Joint Center for Structural Genomics.

#### ***BER Funded Staffing and New Opportunities for SMB R&D***

The BER-funded scientific and technical staff at SSRL currently effectively support users of up to ten existing stations, including the three BER-funded Beam Line 9 SMB stations (BL9-1 and BL9-2 for macromolecular crystallography and BL9-3 for X-ray absorption spectroscopy). This is done in coordination with other specialized activities supported by NIH NCRR and NIH NIGMS. Ph.D. level research staff, currently all or in part supported by BER, are R.P. Phizackerley, S.M. Soltis (in crystallography), S. DeBeer George, B. Hedman, K.O. Hodgson (in X-ray absorption spectroscopy), and H. Tsuruta (in small-angle X-ray scattering). Support is also continued for one summer month of salary support for Professor W.I. Weis (a term member of the SSRL faculty with primary appointment in the Department of Structural Biology on Stanford campus; a leading expert in multiple-wavelength anomalous dispersion (MAD) phasing who contributes significantly to continued developments and applications in this important area).

Professor A. Brünger has a joint appointment between SSRL ( $\frac{1}{3}$ ) and the Stanford School of Medicine ( $\frac{2}{3}$ ). His activities focus on computational and methodological macromolecular crystallography, and are having a very positive impact on providing new capabilities for SSRL users and staff. Funding continued in FY2004 and FY2005 for support of a graduate student research assistant (S. Kaiser) to work with Dr. Brünger.

*Five-Year SMB Program Plan for Beam Line and Instrumentation Developments and for User Operations Support* – A competitive five-year renewal proposal for the DOE-BER and NIH NCRR-funded SMB Resource at SSRL was submitted to NIH on June 1, 2004. As per discussion and agreement between the DOE-BER and NIH-NCRR program staff, this renewal formed the basis for a joint evaluation of the synergistically funded and managed SMB program at SSRL. The proposal contained developments directed specifically to the BER-funded program, which focuses mainly on developments and implementation of new instrumentation and beam-line facilities to enable the SMB user community to benefit in the most optimal way from the new capabilities provided by the new SPEAR3 accelerator. The Special Study Section Committee, which performed a site visit at SSRL in November 2004, provided an exceptionally strong endorsement of the SSRL SMB program as a whole, and recommended that the BER funds requested for personnel, travel, materials and supplies and other nonequipment expenses, be provided at the budget level requested in the proposal. For equipment, it was recommended that all proposed items in the BER budget be funded with the one modification: a reduction in scope of a data storage system, from 300 TB to 100 TB. The proposed Operations Funding and Capital Equipment Funding in this FTP are thus beyond the initial plan and guidance, and follow strictly the reviewed proposal modified according the Committee recommendations, as detailed above. NIH-NCRR is presently issuing the formal grant award for its part of the new five-year period of the SSRL SMB program.

### ***Structural Molecular Biology Program at SSRL***

The new SPEAR3 light source continued to demonstrate excellent reliability (95%) and beam quality during its second user run, which began in early February 2005 and ended on August 1, 2005. This is an exceptional achievement for a new ring. As a result of the new ability to perform at-energy injections, the fill times of 20-30 minutes (typical of SPEAR2) were reduced to 2-3 minutes, and excellent lifetimes were reached very early on (30-40 or more hours with currents rarely below 80 mA).

There were early clear indicators of the improved performance of SPEAR3. For example, the fill-to-fill reproducibility of the orbit at the beam position monitors (BPMs) was about 1 micron. With orbit feedback, long-term (many hour) drift was only about 1 micron, again as measured by the BPMs. The rms orbit motion in frequencies between 1 and 100 Hz was about 2 microns, which compares well to other third-generation light sources. There were a number of other observations and measurements that indicate the quality of the SPEAR3 beams, including that the performance of the BL6-2 M0 mirror reflected the much smaller source size of SPEAR3, the horizontal width measuring 860 microns (FWHM), a much smaller value than the SPEAR2 value of 2.3 mm; a standard myoglobin data set taken on BL9-1 gave an anomalous difference map having a superb Fe peak of 17  $\sigma$  at 12 keV, compared to an iron anomalous peak of 13  $\sigma$  in similar myoglobin tests on BL9-1 under SPEAR2; and the focused beam size on BL9-2 is  $\sim \frac{1}{3}$  the area compared to the size of the beam operating under SPEAR2 and there is a commensurate increase of  $\sim 3x$  in intensity. Diffraction images of a small 6- micron crystal of myoglobin only required a short 5-second exposure time and produced an anomalous Fe peak of 20  $\sigma$  at 12 keV.

The strong demand for all SSRL stations continues. Over all the stations at SSRL, the overdemand averaged  $\sim 130\%$  for the 2004 commissioning run and  $\sim 150\%$  for the 2005 run.

Among the most severe in the overdemand category remain the crystallography stations, with a combined overdemand of ~220% for beam lines BL9-1, BL9-2 and BL11-1. The SAXS wiggler station BL4-2 was in overdemand by 214%, whereas BL9-3 (for XAS) was in overdemand by 251%. The fraction of beam time on X-ray stations allocated to structural molecular biology research continues to be ~35-40% while the fraction of SMB users is ~45%. Since the majority of this beam time is awarded on a peer-review competitive basis among all SSRL proposals, SMB proposals continue to compete very well at SSRL.

**User Satisfaction** – As continuing part of user activities at SSRL, each user group is asked at the end of their run to complete an "End-of-run summary form." This form provides an opportunity for pointing out specific problems/issues and offering suggestions as to means of improvement. It also asks several questions to get a reading on overall satisfaction. The information from the forms is analyzed by the SSRL management and by the SSRL Users Organization Executive Committee. The users rate in five categories (Unsatisfactory to Excellent). In the area of "Overall Scientific Experience" 32% overall were very good and 57% were excellent in FY2004. These summaries included all the open SMB beam lines and users and, while subjective, indicate a significant measure of user satisfaction with the operation and service of the facility.

**Beam Line 4 and 7 Upgrade Projects** – The new wiggler insertion devices for BL4 and BL7 were mated with the vacuum chambers and installed in the SPEAR3 ring towards the end of the shutdown in early FY2004. As part of the SPEAR3 commissioning, the wiggler gap was exercised with beam in the ring, and the maximum target fields were achieved. It was established that at maximum field there was no observed effect on the SPEAR3 orbit or beam stability.

As for BL4-2, its final upgrade is delayed until resources have been obtained from DOE BES to perform the associated upgrade of the side stations BL4-1 and 4-3, which is expected to take place in FY2006. Until then, the beam line will be operated with the new wiggler, keeping the existing optical components and operating the wiggler at a reduced magnetic field. BL4 upgrade activities were therefore largely limited to fabricating hardware that share a common design with other similar beam lines. These include the BL4-2 LN<sub>2</sub>-cooled monochromator and the monochromator entrance slits, graphite filters, and Be windows for all three branch lines. BL4 shielding was modified according to current shielding protocols to permit 100 mA operations of BL4-2. Design and fabrication of the key remaining optical components, the M<sub>0</sub> mirrors, began in FY2005, as did the design and fabrication of the remaining masks. In FY2006, design and fabrication of the optics and masks will be continued. During the summer 2006 SPEAR3 shutdown these components will be installed and the beam line, and in particular the dedicated SAXS station BL4-2, will be commissioned.

Beam Line 7 shielding was modified according to current shielding protocols to permit 100 mA operations of BL7-2 during the 2004 run while awaiting final upgrade of all three stations (as the new wiggler at reduced fields does not illuminate the two side stations). Fabrication of the BL7-1 monochromator and of the M<sub>0</sub> mirror systems for all three branch lines were completed in FY2005 as were most of the remaining masks and other components. The upgrade for BL7 started in the FY2005 shutdown and will be completed by the end of the first quarter in FY2006. Following a commissioning period, BL7-1 and BL7-3 will be made available for general user access at 500 mA SPEAR3 performance.

**Beam Line 9 Upgrade Project** –Final assembly of the BL9-2 LN2 monochromator was completed. Most of the remaining slits, masks, filters, and windows for BL9 were completed in FY2005. Installation of the upgraded BL9 components is being done in the summer and fall of 2005, after which commissioning and general user access will follow. All stations on BL9 will then be in their final 500 mA SPEAR3 performance configuration.

**Beam Line 9 Operations** – All three stations for Beam Line 9 saw full user operation starting in FY2004. BL9-1 is a side station for monochromatic macromolecular crystallography, and has become the prime line at SSRL for the performance of single monochromatic experiments, as well as “MAD” in the form of single- (SAD) or double- (DAD) wavelength anomalous dispersion phasing experiments within a limited wavelength range. The end-station BL9-2, also for macromolecular crystallography, is optimized for the collection of multiwavelength data for MAD phasing and high-resolution data. BL9-3 is dedicated for biological X-ray absorption spectroscopy of frozen protein solutions, micro-XAS imaging and tomography, and single-crystal X-ray absorption spectroscopy.

For *macromolecular crystallography* advances in instrumentation and beam line technologies continued. Initially, four MC beam lines were in operation under the new SPEAR3 lattice running at a current of 100 mA (BL9-2, BL9-1, BL11-1 and 50% of the available time on the shared station, BL11-3). The flux was observed to increase by a factor of ~3 for the premier MAD station BL9-2, as expected from the lower emittance of the storage ring. BL1-5 was significantly modified for the SPEAR3 lattice. All beam-line components were moved by up to several inches in order to align the beam line to the new source point. In addition, the beam-line apertures and beam-containment components were upgraded to handle the increased power of the SPEAR3 radiation. Initial commissioning of BL1-5 indicates a factor of ~7 in performance enhancement operating at 100 mA. The MAD capability of BL1-5 will eventually be significantly enhanced during the SPEAR3 era. However, in order to increase the beam intensity by a factor of 50 and realize the full potential of BL1-5 under SPEAR3, the mirror and monochromator will have to be upgraded and relocated for optimal focusing.

Starting in 2004, the robot-based Stanford Auto-Mounting (SAM) crystal screening system was made available as a general user facility on three crystallography beam lines. The SAM system incorporates a robot that can mount 264 samples without any manual intervention and operates in an integrated environment within the Blu-Ice experiment control software that can be used to select and screen samples in a totally automated fashion. The systems were used for 60 experimental user runs which represented 30 unique groups (approximately 30% of all macromolecular crystallography user groups). In total, 5500 samples were screened in a completely automated fashion. A significant increase in efficiency was reported; many groups finished early and commented on how much data they were able to collect using the system. An overall increase in the quality of data was also observed; users were able to screen through all of their crystals before selecting the best quality crystal for data collection.

Other improvements to the macromolecular beam lines and equipment include:

- *Enhanced Tools for the Automatic Crystal Screening System.* A cassette kit was previously developed that assembles the cassettes, sample pins and tools required for

sample loading and cassette transport. The kit includes a sample cassette and 96 Hampton pins, a specialized dewar canister, a teflon ring for canister support, a cassette transfer handle, a magnet tool for testing and mounting pins, a guide tool that allows quick and reliable loading of samples into the SSRL cassette, a styrofoam spacer for stabilizing the cassette when shipping a single cassette, and a styrofoam box for mounting the samples into the cassette under liquid nitrogen. These tools were made available to users, providing valuable feedback on their use. All users who received a kit were able to successfully load samples into cassettes and ship them to SSRL. However, there were some problems related to the Styrofoam loading box. Because this box is large, it requires a large volume of liquid nitrogen to fill (16 L) and therefore prone to ice contamination. To address this issue a new cassette loading Dewar made of blue polyethylene closed-cell foam has been designed, which requires only 4 L of liquid nitrogen to fill; it is extremely durable; and the dark blue color makes it very easy to see any ice in the liquid nitrogen bath. Another suggestion from users was to create tools that would enable transfer of pre-frozen samples stored in cryovials or ALS pucks into the SSRL cassettes. A slotted guide tool was developed as an aid to safely guide sample pins into cassette ports while allowing the sample to remain near liquid-nitrogen temperatures during the transfer. The tool can also be used to remove samples from cassettes for storage into other containers. New web-based directions that describe the use of these tools have been written and posted.

- *Screening System Software Interface Improvements.* The screening tab in the Blu-Ice beam line control system utilizes the Stanford Auto-Mounting (SAM) system for screening large numbers of crystals in an automated fashion. This tab displays information about the crystals contained in a sample cassette, uploaded from a user supplied Excel spread sheet and features a menu of action items to carry out for each sample. Through observation of SAM users during the FY2004 run, SSRL SMB staff found that in some cases the users preferred to have mounted one sample at a time instead of automatically screening all the samples. Taking this into consideration, an additional SAM widget was implemented in the Hutch Tab of the Blu-Ice interface software, which allows mounting and dismounting individual samples in a semi-manual fashion. Normally, users will screen a large number of samples using the Screening Tab interface. After screening is complete, users evaluate the results to determine the best crystals to use for data collection. Several improvements were made to the screening tab to make these experiments more straightforward. In particular, the menus in the screening tab have been streamlined and some operations have been hidden. A ‘tasks list’ has been added to display current and future screening events (analogous to the list of events in the Collect Tab); this allows users that are new to the system to experiment with the screening parameters and review the sequence of events before hitting the “Start” button. New control buttons have been added to provide easy access to the web browser based screening system database for spreadsheet entry. Color coding and status indicators have been improved. The result is a less cluttered and more user-friendly GUI that still retains the full basic functionality of the original version.
- *New Macromolecular Crystallography Web Site.* The MC public Web site has been reorganized in order to make it easier to navigate and maintain. The Web site upgrade took into account users' suggestions to thoroughly document administrative requirements and provide a complete reference to beam line use. Every document in the site can be



accessed directly from at least one of several major menus. These menus, as well as a site search facility, are available from each page in the Web site. The home page also contains beam line information and quick links to the most useful and visited web pages, funding agencies and collaborating research institutions.

BL9-3, dedicated to general user **biological XAS**, provides extremely high intensity over a broad X-ray energy range, and is designed to provide focused beam from  $\sim 4$  keV to  $\sim 23$  keV, and unfocused beam up to  $\sim 30$  keV. The LN<sub>2</sub>-cooled monochromator on BL9-3 has two sets of Si(220) crystal pairs that can be brought in and out of the beam without breaking vacuum, providing a choice of two different azimuthal orientations of the 220 planes with different glitch patterns, allowing a choice for a given element/energy range.

The typical focal spot with SPEAR2 emittance was  $\sim 0.6 \times 4$  mm FWHM, which produced a measured flux of  $\sim 2.5 \times 10^{12}$  ph/s/100 mA at 9000 eV, with no pre- or post-monochromator slit apertures. With a 1x4 mm hutch slit, the flux at the focus (*i.e.*, at the sample) was measured as  $8.1 \times 10^{11}$  ph/s at the same energy/current. With SPEAR3, the focal spot is  $\sim 0.4 \times 3$  mm FWHM, producing a measured flux of  $\sim 2.2 \times 10^{12}$ /100 mA at 9000 eV with 1x4 mm apertures. A factor of five will be gained at 500 mA.

A significant amount of time was devoted to establishing optimized optics configurations, for both crystal sets, for a series of mirror energy cutoffs. As all optical elements are under computer control via the ICS software, these configurations have been stored, resulting in only minor adjustments after they are recalled and the optics set to these values when moving from one cutoff to the other. With the presence of a harmonic rejection M<sub>0</sub> mirror, the monochromator is typically fully tuned during the measurements. The M<sub>0</sub> mirror also reduces the thermal load on the monochromator, the thermal stability of which is further enhanced by having the branch line stoppers located after the monochromator. This, in combination with excellent mechanical stability, has produced a typical observed energy reproducibility of 0.05 eV at 9 keV in 24 hours. With careful adjustment of the collimating mirror, the beam line produces an energy resolution close to the theoretical limit, with the FWHM of the KMnO<sub>4</sub> pre-edge feature at  $< 1.65$  eV with no limiting vertical aperture before the monochromator, attesting to the proper cooling by the LN<sub>2</sub> system.

Beam line 9-3 was the *first* station to see SPEAR3 beam, and produced the first SPEAR3 data set (on an Fe-containing bioinorganic model complex). The tighter focus and higher brightness, coupled with excellent stability, enabled excellent data quality during the SPEAR3 commissioning run. The initial external SPEAR3 user (N. Blackburn, Oregon Health Sciences University) reported excellent Se K-edge data from a 67  $\mu$ M protein solution). R.A. Scott, University of Georgia obtained excellent data from an 86  $\mu$ M Zn protein (below), and also of very small samples of low concentration related to high-throughput technology feasibility tests. These are concentration ranges not reachable under SPEAR2.

During the SPEAR3 commissioning run, detector tests were run on BL9-3 to assess the usefulness of several solid-state detectors including the Canberra X-PIPS, Rontec X-Flash, and Radiant Vortex. All three are Si-based detectors requiring no liquid nitrogen for cooling and are compact, allowing use in crowded experimental environments. The X-PIPS detector was tested

with standard Canberra analog electronics and had very good count rate performance but gave poor energy resolution ( $>500$  eV FWHM at Mn  $K\alpha$ ). The X-Flash detector is a Si drift diode with a  $5\text{ mm}^2$  active area and employed Rontec electronics for signal processing. The X-Flash performed well, but is limited by a very small active area and by electronics with a single preset shaping time. The Vortex detector is also a Si drift diode and uses a repackaged XIA DXP board for signal processing. The Vortex had excellent energy resolution and count rate performance (better than the current fast Ge-detectors) with the same active area as a single element of the Canberra Ge array detectors. In addition, the Radiant preamplifier had exceptionally clean resets and very little peak shift with increasing count rate. Based on these results, a single-element Vortex detector was purchased (using BER funds) to be used as a portable high resolution detector which will be used primarily for imaging experiments.

***Micro-XAS for Imaging and Tomography*** – A commercial Kirkpatrick-Baez (KB) mirror system from Xradia Inc. was commissioned on BL6-2 in a virtual source configuration during the SPEAR3 commissioning run. These mirrors were funded by DOE BES, and additional equipment from the SMB capillary optics-based imaging system was used in a joint development approach. Submicrometer focusing for XAS imaging is obtained using two Rh-coated adjustable KB mirrors in a crossed geometry for vertical and horizontal focusing, each with a self-contained bending mechanism to set the desired surface figure. Before installing this mirror optics in the rear hutch of BL6-2, the bending mechanism of the optics was prealigned using a Long Trace Profiler at the metrology laboratory of the Advanced Light Source. This instrument can measure the shape of an optical surface and allows bending both mirror surfaces into the ideal elliptical shape, as determined by the desired focal and source distances as well as angle of incidence.

By applying two asymmetric bending moments to each end of the mirror, the horizontal focusing mirror was tuned to a 12 cm focal length, while the vertical focusing one was tuned to a 26 cm focal length. With a virtual source distance of about 2 m, this translates into a fixed demagnification ratio of 17.8:1 in the horizontal direction and 7.7:1 in the vertical direction. The angles of incidence have been set to be 4 mrad for HF and VF resulting in an energy cut-off of about 17.5 keV for these Rh-coated mirrors. Deviations from these nominal values will introduce aberrations leading to an increased spot size.

The mirrors were first positioned on an optical bench at the relevant distance from the virtual source slit and focal position using a HeNe laser that was aligned with respect to the X-ray beam. In addition, an adjustable aperture slit was installed upstream of the mirrors allowing limiting the angular acceptance from the virtual source thus improving the focal spot size. Using the X-ray beam at 11 keV photon energy, the effect of translating the mirrors into the X-ray beam, as well as the influence of the angle of incidence on the focal spot size, were carefully studied without modifying the applied bending moments on the optics. The resulting focal spot size was measured for each configuration by scanning a 100-micron-thick tungsten wire through the focus using a high resolution PM500 sample stage. The focal spot obtained ranged from submicron to  $2 \times 2\ \mu\text{m}^2$  for a small virtual source.

***XAS Experiment Control and Data Acquisition Software Developments*** – At present all beam lines utilize the SSRL Instrument Control Software (ICS), which forms the primary interface between control hardware and software. The ICS software provides a consistent, convenient and

flexible interface to a large variety of different types of beam line hardware. In addition, ICS includes a comprehensive set of subroutines for client programs that provide easy-to-use access to all devices in both a synchronous and asynchronous manner. The current production version of ICS is based upon the OpenVMS operating system, and while OpenVMS continues to provide outstanding reliability, the future of this operating system is in some doubt.

In order to address the issue of long-term viability of OpenVMS, an operating system-independent version of the ICS software is under development. Specifically, the new software is being developed for the Linux, Microsoft Windows and OpenVMS operating systems. Support will be maintained for all the existing SSRL instrumentation hardware, and moving to the new software will mean only relatively minor changes to the data acquisition software, such as XAS-Collect.

While the replacement software is in development, it is important that support for the existing ICS software continues. A number of significant improvements have been made, all with a view to the upcoming migration to the new system:

- *Additional Devices under ICS Control.* During the past year several new devices were added to the existing ICS software, including Piezo Jenna Motor controllers, VXI V535 encoder readout, Galil Stepper motors, Galil D.C. Servo, Galil output registers, and National Aperture MPV1 D.C. servos.
- *GUI for Digital Signal Processing Modules.* Over the past year, a graphical user interface, called DXPGUI, was developed for use with X-Ray Instrumentation Associates DXP digital signal processing electronics. DXP electronics are used with one of the SMB 13-element Ge detectors and with Ge detectors on BL11-2. DXPGUI was designed to be more user-friendly than the previous command-line interface and is similar in look-and-feel to the Ge Plus software that is used with the other SMB detectors. Basic features include: displaying fluorescence spectra, setting single channel analyzer (SCA) windows for data collection, measuring total incoming and SCA count rates, and calculating detector energy resolution. Users can also change DXP parameters, save and restore various parameter configurations, and automatically align gains for each DXP channel.
- *Interface to Silicon Drift Detector.* Software is also being developed for use with a Radiant Detector Technologies single-element Vortex detector. Radiant packages its detector with DXP electronics and provides a Microsoft Windows-compatible graphical user interface and dynamic-link library to set up the electronics. Software was developed to communicate between the beam line data collection computer and a PC running the Radiant software. Data was collected with this software during the test run on BL9-3 in July 2004. A graphical user interface for setting up the Vortex detector electronics is being developed for use on the data collection computer. The GUI will be similar in function and appearance to the current Ge Plus software.

**SAXS/D Beam Line 4-2 Operations** – The SSRL small-angle X-ray scattering/diffraction facility on BL4-2 is now dedicated 100% to small angle X-ray scattering studies on biological systems. The expected much improved beam characteristics provided by the combination of the new low-emittance storage ring and the new 20-pole wiggler, both provided by the partnership between NIH and DOE, was established. A number of user/staff research projects took

advantage of these beam characteristics. It is also important to point out that several of new exciting projects, including those in new fields such as lipid structures and biomineralization, were also initiated during this short period, suggesting further growth in beam time demand and continuing need for advanced instrumentation for conducting challenging experiments.

**SAXS/D Hardware Upgrades** – In order to take advantage of the high-brightness SPEAR3 beam, a new instrument has been built to replace the older instrument, which served the community well over 10 years. In line with the submitted DOE-BER/NIH-NCRR grant renewal proposal described above, the main goals of this development are to 1) extend the range of instrument to both large characteristic length as well as to higher structural resolution, and 2) allow multiple instrumental configurations during short beam time by automation. The new instrument incorporates two major innovations: the ability for automatically changing the sample-to-detector distance and a pair of built-in collimator/analyzer crystals in Bonse-Hart geometry for ultra-small-angle X-ray scattering (USAXS) studies. The former feature allows users to select a desired sample-to-detector distance, thereby angular range, among five predesigned distances, 0.5, 0.9, 1.4, 2.0, and 2.5 m. The Bragg spacings,  $d=1/(2\sin\theta/\lambda)$ , in Å covered by these distance ranges are: 4.6-270, 8.7-520, 13-790, 18-1100, 23-1400, respectively, assuming the use of a 9 keV X-ray beam and a 5 mm diameter beam stop. The automated configuration change was achieved by scripting in the SUPER program running under ICS, and many user groups took advantage of this new capability during the FY2004 user run.

Other development projects in FY2005 included:

- *New High-precision Beam Slit and Beam Stop System.* A high-precision in-vacuum slit from JJ X-ray has been implemented, and has shown to improve reliability of operation and accuracy of defining the beam size at the sample. This slit system does not require occasional calibration of the slit openings, in contrast to the system it replaced. The smaller beam size allows the use of a smaller beam stop for almost all experiments. The beam stop design has accordingly been redesigned to incorporate a smaller X-ray photodiode within the narrower footprint of the new beam stop, which is held on a thin piece of machined printed circuit board - an adaptation from the SMB macromolecular crystallography beam stop design.
- *New Remote-Viewing Capabilities.* A long section of Newport/Klinger X95 rail has been mounted above the SAXS instrument near the ceiling for mounting small equipment, such as fiber optic illuminators along the instrument overhead. A 4-channel Axis video image server has been installed on the X95 rail and connected to a video microscope for sample alignment and to two remote-controlled video cameras for remote experiment control. The fourth channel is reserved for viewing of solution samples through one of the windows installed on the in-vacuum sample cell. All real-time images are available on a Blu-Ice software tab window as well as from authorized on-site computers. The sample image from the first channel will be used to automate sample alignment under Blu-Ice in future developments.
- *X-ray Beam Profiler.* The beam profiler has been redesigned to match the smaller beam size available from SPEAR3. Based on a design similar to the previous version, it consists of a high-resolution phosphor screen (CsI crystals columnally grown on a thin carbon fiber plate), a penta prism, a microscope objective lens and a high-sensitivity

CCD video camera. The new profiler gives much higher spatial resolution thanks to the new thinner high-resolution phosphor screen and the microscope optics. A Scion frame grabber for real-time image acquisition and beam intensity profile analysis, implemented with analysis software based on NIH ImageJ, was also added to the setup. The beam profiler will be permanently installed on the detector stage making it possible to greatly reduce the time to record beam intensity profiles (e.g. vertical beam FWHM) at the detector position and optimize beam focus on-the-fly.

### ***New Methodology and Detector Developments***

With all stations on Beam Line 9 in excellent condition for user operation, efforts for the next several years – in addition to providing highest level of user support on a total of 10+ SMB beam lines – will focus on developing novel methodologies – enabled by the new SPEAR3 3<sup>rd</sup>-generation source – and new optics, instrumentation including advanced detectors, computing resources including control, data acquisition and analysis software, and other facilities as driven by the scientific goals of the user community and SSRL SMB faculty and staff. This was described in full detail in the peer-reviewed proposal that was submitted May 2004 and jointly reviewed by DOE-BER and NIH-NCRR in November 2004 (as mentioned above). A representative summary for the five-year joint program, for which activities were initiated in FY2005, is given below for each scientific thrust.

#### **Macromolecular Crystallography:**

The implementation of a new revolutionary X-ray Pixel Array Detector (PAD) that features a large active-area of 400 mm x 400 mm, a dynamic range of 10<sup>7</sup> and an ultimate readout speed of 0.5 ms. The development of precision microdiffractometer and visualization instrumentation for the accurate alignment and manipulation of microcrystals. When coupled with a new high-brightness, in vacuum undulator X-ray beam line currently under construction (BL12), significant advances in pushing the forefront of structural biology on complex systems will be possible.

The development of new data collection features and methodologies that take advantage of innovations in instrumentation, automation and robotics are planned. Integrated together with the implementation of a next-generation of high-performance computational environment, study of more challenging problems and with much more efficiency will result. These developments will be distributed across all the SSRL macromolecular crystallography beam lines.

A series of new instrument and methodology developments, including gas pressurization systems for anomalous phasing and enzyme studies, capabilities for *in situ* spectroscopic UV/Visible and IR monitoring system to study and monitor states, and automated crystal annealing.

Development of Web-Ice – a new browser-based interface tool for operating the beam line instrumentation utilizing integrated robotics and data base management capabilities to carry out crystallography experiments remotely. This builds upon pilot phase developments made during the current program period.

Several upgrades that will significantly increase scientific capability and throughput of existing macromolecular crystallography stations with SPEAR3.

The participation in key scientific collaborations that will capitalize on the new performance of SPEAR3 and drive the proposed technological developments.

***X-ray Absorption Spectroscopy (XAS):***

Implementation of a next generation 100-element monolithic Ge detector array with digital signal processing electronics for the study of ultra-dilute protein solutions, small single crystals, and low-volume/low-concentration samples on BL9-3.

Continued development of microXAS imaging using metal capillary optics (BL9-3) and new Kirkpatrick-Baez (KB) optics (BL6-2) in the hard X-ray energy region – for high-resolution spatial structural and electronic characterization of biological materials.

Development of a new facility for soft X-ray spectroscopy (2-5 keV) for microXAS imaging and for solution studies on BL3-3, developing a unique capability that allows the *in situ* determination of active site structure at low energies.

Continued development of instrumentation and software to perform parallel measurement of polarized single crystal XAS and protein crystallography data. This will enable enhanced electronic and structural information to be obtained and will also allow direct study of radiation damage as coupled to enzyme active sites, in synchrotron-based XAS and crystallography.

Development of advanced high-resolution and site-selective X-ray absorption spectroscopy facilities for biological systems.

Development of high-throughput methodology for XAS data acquisition and data analysis, to be applied to structural genomics applications as well as general user studies.

Development and implementation of a new instrumentation control system (hardware and software) and of enhancement of the XAS data acquisition analysis software, which will enable higher efficiency and reliability for existing approaches and novel methodologies.

Development of further enhancement to XAS data analysis approaches coupled with theoretical developments in collaboration with Prof. John Rehr, University of Washington, in particular the merging of information for the edge and EXAFS regions of the XAS spectrum.

Key scientific collaborations have been developed that push the new developments and will capitalize on the new performance of SPEAR3, higher-performance detectors and software, and that will enable fundamental biological insights.

***Small-Angle X-ray Scattering (SAXS):***

Full optimization of BL4-2 in the new mode of being dedicated 100% as a small-angle X-ray scattering and diffraction facility for SMB will be pursued. This will take advantage of the recently completed hutch rebuild and new SAXS/D camera, and combine with further improvements in software and detector technologies to provide a high-capability, flexible and robust beam line for a range of SAXS/D experiments. When optimized, this beam line will

deliver photon fluxes on typical samples that are comparable with the best available at other beam lines around the world.

Further developments are planned for submillisecond time-resolved studies that will be facilitated by the higher brightness provided by SPEAR3. Improved detectors (CCD or CMOS) are an important aspect of enabling new experiments as is the development of areas like the use of photo-induced reactions using a high-power laser. A next-generation continuous mixer system with mixing dead time of 0.1 ms is planned to complement the existing stopped-flow apparatus. Monitoring capabilities will be provided by a fast (0.1 ms) UV-vis spectrophotometer (fluorescence and absorption measurements).

Higher resolution data collection will be enabled using a new CCD detector optimized for solution scattering, accessing length scales from around 5 Å up to a few microns characteristic lengths. An integral part of the instrument to be implemented will be a channel-cut crystal collimator/analyzer. Automated camera adjustments (length change and alignment) will facilitate adaptability for a range of operating modes of the camera.

Technology developments aimed at enhancing the range of scientific problems that can be studied include implementation of a high throughput solution data collection system, based on an in-vacuum capillary cell interfaced to an automated sample changer/diluter. Complementary information to the SAXS data will be provided by an integrated molecular sizing instrument and built-in real-time aggregation monitor.

Further development and exploitation of anomalous scattering is planned, given the much higher stability and brightness of the SPEAR3 beam, and an optimized BL4-2. A dedicated energy resolving detector for accurate absorption edge determination and rejection of unwanted X-ray fluorescence is one of the technical developments to enable expanding research in this area.

Participation in key scientific collaborations have been developed that push the new developments and will capitalize on the new performance of SPEAR3, helping give rise to one of the best dedicated small angle X-ray scattering stations at any synchrotron facility. These developments will also contribute to an integrated, user-oriented environment which will support the growing community of non-specialists that are expected to make increasing use of SAXS data in their own research.

For all the scientific thrusts, continued dissemination to and training of users in the new capabilities will have high priority, and will take place through presentations at conferences and meetings, and through hands-on instructions and workshops at SSRL and elsewhere.

### **Molecular Environmental and Interface Science**

Synchrotron radiation (SR)-based techniques provide unique capabilities to address scientific issues in molecular environmental and interface science (MEIS) and have emerged as major tools in environmental remediation science, a discipline of MEIS. The high intensity of SR sources and X-ray photon-in/photon-out detection allow noninvasive *in situ* analysis of dilute, hydrated, and radioactive samples. SR techniques allow characterization of the structural chemistry of non-crystalline solids, nanoparticles, complex organic materials, and metal ion complexes dissolved in solution and at environmental interfaces. Further, because of their high

degree of collimation, SR X-rays can be focused to beams of micron dimension, allowing the spatially resolved characterization of chemical species in microstructured samples, chemical microgradients, and microenvironments that often fundamentally control the behavior and release of contaminants in the environment, in waste forms, and in contaminated vessels.

The primary purpose of this work is to increase the access to and utilization of SSRL facilities by BER-funded environmental remediation scientists and collaborators. Major techniques supported in this program include X-ray absorption spectroscopy (XAS), X-ray diffraction (XRD), microbeam X-ray fluorescence ( $\mu$ -Xrf) chemical imaging, and microbeam XAS/XRD. These efforts are led at SSRL by Professor Gordon Brown, Jr. and Dr. John Bargar.

The two major elements of this program are:

- Enhanced user support for BER-funded MEIS research projects at up to nine SSRL beam stations (6 XAS, 3 WAXS), seven of which are on high-intensity multipole wiggler beam lines.
- Development of innovative research techniques, with a present focus on microbeam spectroscopy and diffraction capabilities (2  $\mu$ m spot) optimized for experiments on uranium, neptunium, plutonium, technetium, and other radionuclides that require high-energy X-rays, as well as for nonradioactive contaminants such as chromium, arsenic, selenium, cadmium, mercury, and lead.

### **BER Funded Staffing and New Opportunities for MEIS R&D**

A BER-funded scientific staff member will directly assist first-time and experienced BER MEIS users at SSRL by providing advice for planning experiments, hands-on training and assistance at beam lines, and training and consultation regarding data analysis procedures. These activities will be performed in coordination with other specialized activities supported through the DOE-BER and NIH-NCRR funded Structural Molecular Biology (SMB) program at SSRL. One Ph.D. level research staff, Samuel Webb, is currently supported in full by this BER FWP.

***Instrumentation Development and User Support*** - An FWP proposal was submitted in 2004 to fund the above-described user support program and to develop a microbeam facility optimized for environmental remediation science. Funding for the program started in FY2004 (\$50K) and escalated to \$250K in FY2005. The current FWP award continues through 2008 at a level of \$250K/yr. Engineering, management, and X-ray optics for this project are supported by DOE-BES. Software support for instrumentation control and data acquisition is provided through a parallel effort for biological applications in the SSRL SMB XAS program, with BER-funded personnel.

The microbeam facility is comprised of a Kirkpatrick-Baez (K-B) mirror pair, which focuses incident SR X-rays to a 2-micron spot (this size is specific to SSRL beam line 2-3), and various detectors, video cameras, slits and ion chambers, all of which are mounted on an ambulatory optical bench. Detectors essential for XAS acquisition at this facility are provided by the SSRL SMB XAS support program. The microbeam system is optimized for use at SSRL bending magnet beam line 2-3, with optimal performance between 17 and 23 keV. This energy range includes the important radionuclides U, Np, Pu, Am, and Tc. The planned SSRL facility will



provide significantly enhanced access to microbeam techniques, particularly to national laboratory and academic researchers in the Western US.

### ***Environmental Remediation Science Support Program at SSRL***

The program was initiated and a search for a staff member was conducted. Supplies for the microbeam system including precision X-ray slits, components for sample and beam imaging cameras, and prealignment services for the K-B mirrors were procured.

A dedicated project scientific staff member, Dr. Samuel Webb, was hired to provide user support for BER-funded MEIS researchers, to help commission the microbeam system, and to implement the user support program at the microbeam system. Dr. Webb has 8 years of experience in the field of XAS-based environmental sciences, including three years as a postdoc at SSRL in Dr. Bargar's group, a demonstrated mastery of the experimental techniques required for the position, and a demonstrated strength in user support.

***Instrumentation Development and User Support*** - Support for environmental remediation science programs at SSRL XAS and XRD beam lines will be provided as requested. Current scientific collaborative projects involving Samuel Webb include: S. Fendorf, C. Criddle, and A. Paytan, Stanford University (Speciation of U in reducing aquifers; Speciation of Tc in Hanford sediment;s Mineral dust components in aerosols and their effect on ocean productivity), B. Tebo, Oregon Health and Sciences University, J. Bargar, SSRL, and T. Spiro, Princeton University (Structure of biogenic Mn oxides and oxidative mechanisms of bacteriogenic Mn oxidation), A. Mehta, SSRL, (WAXS investigations of the structure of ions in water), A. Templeton, Scripps Institution of Oceanography (Microbial Fe and Mn oxidation of basaltic glasses), and M. Filella, University of Geneva, Switzerland (Speciation of Sb in acid mine drainage).

Other activities in FY2005 have been dominated by design, implementation and testing of the microbeam system. Initial hardware design, fixture fabrication and assembly have been completed at the date of writing. Orders for major system components, including a high-resolution fast X-Y-Z scanning stage and state-of-the-art digital spectroscopy amplifiers (DXP, Inc.) for Xrf imaging and XAS, have been placed. Initial commissioning tests of the X-ray optics and slit systems have been completed. A focused beam spot size of 2  $\mu\text{m}$  (very close to the theoretical limit) was obtained at 17 keV, far surpassing the first-round commissioning goal of 10  $\mu\text{m}$ . Beam size was found to be stable over long periods of measurement (24 hr). Observed flux was consistent with expectations. Short-term and long-term motions of the focused beam relative to the table were characterized to help assess vibrational stability of the table/optics system, source position/size stability, and thermal stability of the system. Subsequently, table and optics rail designs will be modified to optimize their performance based upon the results of our first commissioning run. Video beam and sample cameras, a table-top optics enclosure, and other components will be assembled and mounted on the optics table. A second commissioning run in June 2005 resulted in improved beam/table stability and the ability to collect EXAFS spectra at 17 keV. Work on data acquisition software was also started.

Another major accomplishment in FY2005 was the creation of a web site for the SSRL-based environmental remediation science community. This site (<http://www-ssrl.slac.stanford.edu/mes/remedi/index.html>) provides key information and links to resources for

these users, including contact information, information on submitting proposals and obtaining beam time, beam line resources at SSRL, science highlights, and a primer on the application of synchrotron techniques to environmental remediation science.

## **16. SCIENCE EDUCATION by Mike Woods**

Education and promoting development of the next generation of scientists and engineers is a key part of SLAC's mission. The primary means for achieving this is by providing research opportunities at SLAC's facilities and centers for experiments in particle physics, particle astrophysics and photon science. A large number of graduate students are supervised by SLAC and Stanford faculty and a much larger number work with faculty at user institutions. In addition, SLAC provides educational opportunities for K-12 students and teachers, community college students and undergraduates. SLAC hosts or participates in several events each year that promote science and science education, such as SLAC Kids' Day, Stanford's Community Day and the DOE Science Bowl. SLAC also continued its successful Public Lecture Series, making the forefront science research carried out at SLAC accessible to the local community.

### **Pre-College (K-12 Students and Teachers, Community College Students)**

SLAC continued participation with the QuarkNet program, completing the final year of a 3-year program to train high school science teachers and provide educational materials for their classrooms. 4 lead teachers had 8-week summer internships during the 1st year, which was followed by a 2-week summer workshop in the 2nd year for 20 teachers. During the academic years and continuing into the 3rd year there were 1-day workshops, with two workshops being hosted at SLAC/Stanford in FY05, each with 10 teacher participants. SLAC continues to support local schools through its surplus equipment donation program and through tours for high school students. In addition, SLAC staff volunteer to assist local schools in a number of ways, including invited presentations and judging at Science Fairs. Three staff scientists judged the Bay area regional science fair held in San Francisco, and one staff member was a judge at the state science fair held in Los Angeles. The Young Particle Physicists (YPP) at SLAC continued their education outreach, mentoring 9 local high school students during the academic year on projects with the BaBar experiment, accelerator physics and astrophysics. Some high school students are hired for specific projects during the summer. SSRL, for example, hired 5 high school students in summer 2005.

### **Undergraduate Students**

In summer 2005, 24 undergraduate students from around the country had summer research internships at SLAC, through DOE's Science Undergraduate Laboratory Internships (SULI) program. These students are housed on Stanford campus and carry out individual projects with SLAC scientists who mentor the students. SLAC's summer science program for undergraduates, now funded through SULI, has operated at SLAC for over 30 years. It has a director and offers a lecture program for the students. SLAC also supported one Pope Fellowship in summer 2005, which is an internship for an undergraduate student at one of the user institutions whose faculty

and students participate in SLAC's research program. In addition to SLAC's programs, a number of user groups bring undergraduate students to SLAC each summer, while a few more students are hired by SLAC staff scientists directly to work on specific tasks. SSRL, for example, had 11 undergraduates as direct hires for the summer and 33 working on synchrotron-based experiments as members of user groups in FY05. SSRL also hosts and guides student tours that are part of the curricula for undergraduate classes at Stanford and other Bay Area universities.

### **Graduate Students**

SLAC is a host for the research of large numbers of graduate students every year. These students work with SLAC and Stanford faculty, or with faculty from other institutions who carry out research at SLAC as users of the facilities, both in the Particle and Particle Astrophysics (PPA) programs and in the Photon Science (PS) programs. PPA currently has 47 Stanford graduate students pursuing Ph.D.s with SLAC faculty and there are an additional 9 1st year graduate students working at SLAC as rotation students for at least one quarter. 30 graduate students are advised by SSRL or Stanford department faculty and work in a field related to photon science as part of their thesis work. SLAC graduate students represent a large range of scientific disciplines and are matriculated in several of the Schools of Stanford University, with home departments including Physics, Applied Physics, Materials Science and Engineering, Electrical Engineering, Chemistry, Structural Biology, Geological and Environmental Sciences, Molecular & Cellular Physiology, Neurology, and Neurological Sciences. Users bring a large number of graduate students to SLAC for their research, in particular for the BaBar experiment at PEP-II and for SSRL. SSRL hosted approximately 300 user graduate students in FY05, and the number was similar for particle physics and accelerator physics experiments at PEP-II and the FFTB and NLCTA facilities. Many of the user groups include non-US students who come to SLAC with faculty from their home institutions, in particular for the BaBar experiment at PEP-II.

### **Postdoctoral Fellows**

SLAC is a major training ground for young post-doctoral scientists either working as SLAC or Stanford University employees or coming here as members of user teams. Postdocs benefit from intense training and immersion in the scientific opportunities provided by SLAC's facilities, working together with SLAC's faculty and staff scientists. Photon Science experiments at the SSRL and the Sub-Picosecond Pulse Source (SPPS) facilities hosted approximately 200 postdocs in FY05. The Babar experiment at PEP-II and accelerator physics and test beam experiments at PEP-II, NLCTA and FFTB also hosted about 200 postdocs in FY05.

### **Affirmative Action Programs for Students**

SLAC has a number of programs designed to enhance diversity in the sciences, including the following programs for students: the Youth Outreach Program (YOP) providing summer employment for local disadvantaged youths between ages 16-22; the National Consortium for

Graduate Degrees for Minorities in Engineering and Science, Inc. (GEM) and the Work Study Program (WSP). 5 students participated in the YOP during FY05; 4 participated in GEM; and 2 participated in WSP. GEM students at SLAC come for summer employment for two or three consecutive summers. WSP students from local high schools and community colleges are provided part-time employment during the academic year and full-time employment during the summer.

### **Summer Schools**

A large number of workshops are held at SLAC each year and provide opportunities for graduate students (and in some cases undergraduate students) to attend and present posters, talks and papers. Three summer schools were held at SLAC in 2005, which are targeted specifically to graduate students and young postdocs. This year, the topic for the 33rd SLAC Summer Institute was "Gravity in the Quantum World and the Cosmos" and attracted 272 participants. The 4th joint Stanford-Berkeley Summer School on "Synchrotron Radiation and Its Applications in Physical Science" attracted 47 participants, and the 5th "SSRL Structural Molecular Biology Summer School" attracted 21 students.

### **Events**

SLAC's 4th Annual Kids at SLAC Day was held in August and attracted 222 children aged 9-16 years old. This fun and informative event provided an opportunity for kids to learn about what is done at SLAC, and to spark interest for potential science-related careers. The event kicked off with a talk by Juana Rudati, a scientist working on the Subpicosecond Pulse Source (SPPS) experiment. Kids then had the option of choosing from among several workshops to attend including Optics, Mechanics, Astrophysics, Waves, Electronics, Catapults, Monster Muscles, Paleontology, GLAST, Radiation, Magnetism, Biology, Electric Motors, and Welding. Activities concluded with a chance to 'Talk Science' with Graham George, former SSRL scientist and now at the University of Saskatchewan in Canada. Kids Day participants received a commemorative shirt which was designed by Jenine Fernandez, a 14-year old participant at the 2004 Kids Day at SLAC.

Twenty-one SLAC staff participated in this year's Community Day at Stanford, providing displays and demonstrations on the "Quantum Universe," cloud chambers, cryogenics and atmospheric pressure. Twenty-five SLAC staff also gave SLAC tours to approximately 400 people for Stanford's commencement day.

SLAC hosted a regional DOE Science Bowl for high school students for the first time and it was a spectacular success. Twenty-three high school teams from 14 schools competed. 60 SLAC staff and faculty participated as organizers, moderators, time keepers, score keepers and team escorts. Awards were presented by Martin Perl, one of SLAC's Nobel Laureates.

## Public Lectures

The SLAC Public Lecture Series opens the doors to the inner workings of SLAC for the local nonscientific community. Lecturers describe what SLAC is all about: the research, the facilities, and the people that make this a world-class research institute. Refreshments are provided after the talks and attendees can chat with staff scientists and faculty, who are on hand to answer questions. Six lectures were offered to the public in FY05 to capacity audiences of over 300 people each. The topics for these lectures spanned dark energy, magnetism, quantum mechanics, protein crystallography for drug design, lasers and neutrinos.

## Tours

Public Tours of SLAC are available to the general public and for school groups, for everyone 12 and older. These are provided free as a public service. Tours include an overview of particle physics research conducted at SLAC, a view of the giant detectors required to observe subatomic particles and a stroll down the Klystron Gallery, the world's longest building. Tours beginning in FY2006 will include parts of SSRL and an introduction to the science at that world-class laboratory.

### **17. FY05 DOE Assessment: Scientific and Technical Information Management by Pat Kreitz**

This year the Technical Publications department (TechPubs) processed a total of 1,224 scientific and technical information (STI) documents and made all appropriate copies publicly accessible. Since FY1998, SLAC has submitted all announcement records to the Department of Energy's Office of Scientific and Technical Information (OSTI) electronically using Form 241.1 in SGML format. In summer 2005, OSTI changed the required format for all submissions to XML. Throughout the year, SLAC worked with OSTI to resolve a reporting issue that was preventing SLAC from participating in XML harvesting. A complete explanation of this problem and SLAC's proposed solution can be found at [http://www-group.slac.stanford.edu/techpubs/reports/SLAC\\_FedSearchProposal.pdf](http://www-group.slac.stanford.edu/techpubs/reports/SLAC_FedSearchProposal.pdf).

Currently we are using an interim solution that allows OSTI to harvest SLAC's full-text announcement for all preprint documents posted in single-PDF format and announcement-only records for all other documents. Based on OSTI's current schedule, SLAC expects to have harvesting implemented in fall 2005. For this year's assessment, one-third of SLAC's total STI was reported in SGML format with the balance expected to be harvested this fall.

SLAC reports its STI publication products as preprints, preprint leaks, and reprints defined below:

Preprint	Original manuscript submitted to SLAC for publication. When we publish preprints, we assign a preprint number and send an electronic report announcement to OSTI along with a link to the electronic version.
Preprint leak	Manuscript submitted to SLAC after publication elsewhere, but the original manuscript is available to SLAC. We assign a preprint number and report it to OSTI along with a link to our electronic version.
Reprint	Manuscript first published elsewhere—typically a journal—and the original manuscript is not available to SLAC. SSRN makes up the bulk of reprints. When we publish reprints, we assign a reprint number and report it to OSTI, but we do not provide a link to the text from the SLAC publications server.

This year there was a 22% decrease from last year's total STI documents processed. For preprint reporting, this decrease is due in part to a loss of staff which impacted TechPubs' ability to perform extended outreach. For reprints, there seems to be a time delay between the actual journal publication date and the hands-on parsing of that metadata into the TechPubs system so these documents can be registered and reported. TechPubs continues to work to streamline this process to ensure numbers better reflect current year reprint activity.

**Table 1. OSTI Preprint Announcements**

	FY01	FY02	FY03	FY04	FY05
Preprints	260	305	299	417	421
Preprint Leaks	69	207	435	438	371
Total submitted to OSTI	329	512	734	855	792*
Leaks as percentage of total:	21%	40%	59%	51%	46%

\*402 preprint records were reported using SGML method. Remaining 380 records will be reported via the XML harvesting method, fall 2005.

**Table 2. OSTI Reprint Announcements**

	FY01	FY02	FY03	FY04	FY05
SSRL Reprints	57	499	176	528	319
SLAC-HEP Reprints	500	145	334	207	103
Total submitted to OSTI	557	644	510	735	422**

\*\* FY05 reprint announcements will be reported via the XML harvesting method, fall 2005.

**Table 3. Total OSTI Announcements Reported**

	FY01	FY02	FY03	FY04	FY05
Total STI reported to OSTI	886	1,156	1,244	1,580	1,224

### FY05 Accomplishments

#### Reduced occurrences of leaked documents

Outreach and process improvement efforts continued to pay off this year with a 9% decrease from last year's totals in the number of leaked documents found and processed.

#### Extended efforts to implement XML harvesting and improve STI accessibility

- Submitted Federated Search Proposal to OSTI
- Implemented automated updating of SPIRES database for XML harvesting
- Developed interim solution for XML harvesting of single vs multi-PDF documents
- Began repository clean up for FY05 and legacy document harvesting

### FY06 Plans

#### Resolve large document reporting issue

We will work with OSTI and the other DOE laboratories to resolve the large, multi-PDF document reporting issue so all STI can be reported properly and accessed. OSTI's current search tool can only index single PDF documents, which is not always an option for large documents. One method SLAC plans to explore further is federated searching, a method OSTI

already uses on their Science.gov site that would allow OSTI to perform full-text searches on multiple PDF documents directly from each laboratory's document server.

### **Prepare for harvesting of SLAC's legacy documents**

SLAC plans to provide OSTI access to their scanned legacy documents, which were previously reported in hardcopy format. Preparation for this harvest includes verifying that PDFs from scanned documents are optimal file sizes, and ensuring that the OSTI ID numbers supplied by OSTI are cross-referenced appropriately in SLAC's databases to ensure a smooth harvest.

### **Continue outreach efforts**

TechPubs will continue to develop and implement methods to educate authors on the processes involved in registering and submitting STI.

- educate authors about the importance of submitting their papers to prevent leaks
- develop automated methods to make registration and submission of documents easier for authors
- and, continue improvements to the internal workflow processes and systems involved in finding and correcting leaks

### **Enhance scientific publishing support for SLAC**

To save time and effort for authors and Technical Publications staff, we plan to continue developing the following enhancements as time and resources allow:

- Automate creation of title pages for newly registered documents
- Automate publication of preprint notifications on web and via e-mail
- Allow electronic file submission at time of paper registration
- Automate collection of keywords at time of paper registration
- Submit author papers to arXiv
- Automate selected internal reporting and tracking tasks

## **18. Fourth Generation Source Development – The Linac Coherent Light Source Project by mark reichanadter**

### **Project Authorization Milestones**

The Project received approval of Critical Decision 3-A, Start of Long-Lead Procurement, in December 2004. A project budget schedule was presented to the Office of Science in November 2004 and accepted as the Project Baseline. The Baseline has been validated by the Office of Engineering & Construction Management. CD-2B (Approval of Project Baseline) was received in April 2005.

### **Environment, Safety and Health**

A review of the Preliminary Fire Hazard Analysis for the new LCLS conventional facilities was carried out in July and August 2005.



The Linac Coherent Light Source Integrated Safety Management System Plan was implemented in July 2005.

A general safety coordinator and an expert construction safety coordinator joined the LCLS organization in December and February 2005, respectively.

### **Management**

At the start of 2005 the LCLS organization was configured to begin construction and long-lead acquisitions. A new procurement organization, 100% dedicated to LCLS but reporting to the SLAC Business Services Division Director, was put in place in January 2005. To best coordinate Project activities, oversight managers have been put in place. The Electron Beam Systems Manager is responsible for oversight of WBS X.2 (Injector), X.3 (Linac) and X.4 (Undulator Systems, in progress at Argonne National Lab). The Photon Beam Systems Manager is responsible for oversight of WBS X.5 (X-Ray Transport, Optics & Diagnostics, in progress at Lawrence Livermore National Lab) and WBS X.6 (End-station Systems). A Laser Group Leader has been hired. Lasers will be an integral part of LCLS operation and experiments; with the creation of a Laser Group, a new core competency will be cultivated at SLAC. A senior physicist has been named head of the group of System Physics Managers. The Project organization has been rounded out with the addition of a Quality Assurance Coordinator, an Information Systems manager, a Deputy WBS Manager for X.9 (Conventional Facilities) and two professional ES&H Coordinators.

The LCLS project reports monthly performance, variances and contingency allocation against an approved baseline. Configuration management is in place which complies with DOE O413.3. Monthly performance status is reported to DOE via the Project Assessment and Reporting System (PARS).

### **Scientific/Technical**

#### **LCLS**

Understanding of the key performance determinants of Self-Amplified Spontaneous Emission Free Electron Lasers (SASE FELs) has improved considerably as knowledge is gained from SASE experiments and FEL design efforts around the world. A discernable pattern of “problem” identification, followed by solution or resolution, emerges from the literature of beam physics as related to SASE; this pattern is easy to see in the bibliography of the LCLS.

The LCLS will begin operation with a gun closely related to the 1.6 cell BNL/SLAC/UCLA design used in successful SASE experiments at the Accelerator Test Facility and Source Development Lab at Brookhaven and the Low Energy Undulator Test Line at Argonne National Lab. Significant modifications of the original design will be incorporated in the LCLS gun. It will have dual power feeds<sup>1</sup>, to eliminate any dipole component in the longitudinal accelerating field. The full-length cell will be racetrack-shaped rather than circular, to eliminate the quadrupole component of the accelerating field. For the same reason, dual-feed power input will be incorporated in the first two S-band accelerating structures in the injector linac. In order to operate at 120 Hz, the gun design has added cooling. To minimize the average power dissipated in the gun, a programmed power pulse will be applied to bring the gun to 120 MV/m as efficiently as possible.

Studies of this design at BNL, ANL and at the Gun Test Facility at SLAC have demonstrated that:

- Projected emittance measurements show the summary influence of thermal emittance, intra-bunch variation of betatron match to the focusing channel, deflecting fields in the gun, and space charge effects. Slice emittance measurements are invaluable in order to characterize the distinct contributions of each influence<sup>ii</sup>.
- In the limit of no space-charge effects, the “thermal” emittance of a copper cathode in an electron gun such as that in the LCLS has proven to be approximately two-fold larger than simple physical models predict. Fortunately, further dilution of the transverse phase space of the beam should be controllable so as to meet LCLS goals.
- Longitudinal space-charge forces, and the dependence of space-charge forces on longitudinal and radial position within the electron bunch, are important contributors to longitudinally correlated energy modulation<sup>iii</sup> and incoherent energy spread<sup>iv</sup>, respectively.

The effects listed above would, if simply preserved in the acceleration process, have negligible effect on the performance of the LCLS. However, space-charge-induced energy modulation of the electrons has detrimental effects on beam quality during the bunch compression process. Space-charge forces cause the head and tail of the bunch to be accelerated and decelerated respectively, relative to the middle. As a result, the compressed bunch has current spikes at the head and tail. These current spikes produce sufficiently intense wake fields to cause significant energy changes within the bunch as it passes down the undulator channel. The wake fields can enhance SASE in one part of the bunch and degrade SASE in another. The use of wake fields to modulate or shorten the x-ray pulse of the LCLS has been proposed by Reiche and Pellegrini<sup>v</sup>. Because of the very short (100-200 femtosecond) electron bunch length and 5-mm undulator beam pipe inner diameter, the frequency dependence of resistivity in the chamber walls must be considered when computing wake fields<sup>vi</sup>. Analysis indicates that, when this AC conductivity effect is taken into account, an aluminum surface produces lower-magnitude wake fields than a copper surface for the LCLS undulator vacuum chamber.

Initial modulation of the electron current as it is produced in the gun will result in a space-charge-induced energy modulation. Such current modulation could be produced by intensity fluctuations in the laser pulse striking the photocathode. It is now understood that these fluctuations can be amplified by coherent synchrotron radiation (CSR) forces during the bunch-compression process. Theory and simulation indicate that relatively small (6%) current modulations can be amplified to unacceptable levels by this phenomenon. Theory and simulation show, however, that imposition of a 40-keV energy spread (actually an energy modulation with period 800 – 1,000 nm) in an inverse free-electron laser will Landau-damp the CSR amplification process, preserving the beam properties desired for SASE<sup>vii, viii</sup>.

The design of the LCLS undulator was recognized as a significant challenge when project R&D began in 1999. A prototype of the 3.4-m LCLS undulator module has been built and thoroughly studied by the Advanced Photon Source at Argonne National Lab. The undulator has a fixed gap.

The very stringent field tolerance (the undulator parameter  $K$  must be maintained within 0.015% of nominal) has been met in the prototype. In order to adjust each undulator to its proper  $K$  value, a weak horizontal variation in  $K$  is designed into the magnet. This allows  $K$  to be adjusted by horizontal translation of the undulator with respect to the electron beam trajectory. It will be possible to make this adjustment remotely, during operations<sup>ix, x</sup>.

The tolerances on electron trajectory straightness and undulator field are very challenging but achievable with beam-based alignment techniques. It has been decided to incorporate quadrupole electromagnets in the undulator channel which can be used to determine precisely the electron beam position with respect to quadrupole centers<sup>xi</sup>. Errors in the undulator  $K$ -parameter that exceed the 0.015% tolerance can be produced by transverse displacement of one or both ends of the undulator, which cannot be detected solely by their effect on the electron beam. Vertical errors have the tightest tolerance, of the order of 50 microns. The LCLS will be equipped with various diagnostic devices such as beam finder wires and magnet alignment systems to permit alignment of the undulators within the desired tolerance. These devices have excellent sensitivity; however their reliability for absolute alignment depends ultimately on high-precision fiducialization and alignment of critical hardware after installation.

Clearly, it would be desirable to have the ability to determine the  $K$  value of an undulator module from observations of the photon beam. Once some SASE gain signal has been detected, it is reasonable to believe that a systematic optimization of FEL power output can be used to direct the alignment of undulators. Since the LCLS undulators have a rather high  $K$  value (3.5), a weak SASE signal will be difficult to distinguish from the copious spontaneous radiation. A lock-in detection technique has been proposed to detect weak gain signals. It is based on modulation of the intrinsic energy spread of the electron bunch without affecting any other characteristic<sup>xii</sup>. In principle, the spontaneous spectrum from an undulator should contain the information necessary to determine the undulator  $K$  value. This aspect of commissioning an X-ray free-electron laser is an area of active study. It has been the subject of workshops organized by UCLA<sup>xiii</sup> and LCLS, and by DESY and LCLS under the auspices of the ICFA Future Light Sources Subpanel<sup>xiv</sup>.

A single-shot spectrometer will be a very powerful diagnostic for the FEL, if sufficient sensitivity and resolution can be achieved. For spontaneous emission, it could be used to verify the correct setting of the undulator  $K$ -value. For the FEL signal, it could be used to infer the pulse duration. A serious challenge to this technique comes from the very small emittance and hence small opening angle of the electron beam. For X-rays of any specific energy, a detectable fraction of a large-emittance beam can be expected to satisfy the Bragg scattering condition. However, in the case of the LCLS the small-emittance beam might simply fail to satisfy the Bragg condition of a spectrometer over part of its intrinsic spectrum. Powder diffraction, bent crystals and other concepts are under consideration for a commissioning spectrometer.

An essential part of many LCLS experiments will be the measurement of duration and timing of the pulse of SASE radiation with respect to a pump or timing laser signal. The LCLS will take advantage of techniques developed at the Subpicosecond Pulse Source (SPPS)<sup>xv, 3</sup> for measuring

---

<sup>3</sup> A.M.Lindenberg, et al., "Atomic-scale visualization of inertial dynamics", Science vol. 308, pp. 392-395, 15 April 2005

the timing and duration of an electron bunch and X-ray pulse. An electro-optic technique has been used to measure the electron bunch length, with resolution of 270 femtoseconds. The duration of the X-ray pulse from the SPPS was directly measured by a laser pump/X-ray probe measurement of nonthermal melting in InSb. -The same laser pulse was used for both measurements. The two measurements of timing (electron bunch with respect to laser, and X-ray pulse with respect to laser) agreed to within 60 femtoseconds. The measurements also show the summary short-term timing jitter of beam delivered from the SLAC damping ring and accelerated to 28 GeV (twice the LCLS energy) is about  $200 \pm 60$  femtoseconds. These results compare favorably to the start-up goals for the LCLS. Furthermore, the LCLS operating configuration can be expected to produce an improvement in timing stability.

#### **FY05 Progress in Linac Coherent Light Source**

The Project has passed the 10% completion point. Long-lead procurements for undulator systems are awarded. Long-lead procurements for the Injector and Linac are on schedule. In particular, the electron gun, gun laser, X-band klystron and “long-lead” bending and focusing magnets have been ordered.

The Architect/Engineer has submitted the Title-II design package to SLAC for review at the “30% of Complete” stage. Construction contracts were awarded for the Magnet Measurement Facility and Injector Annex.

A contract for the Construction Management/General Contractor was prepared in November 2004 and submitted to DOE review in January 2005. Approval to solicit bids was received from DOE in July, and a vendor was selected at the end of the fiscal year.

Detailed information on the Project status and issues may be found in the Monthly Reports, posted at <http://www-ssrl.slac.stanford.edu/lcls/internals/monthlyreports/> .

- 
- <sup>i</sup> L. Xiao, et al., “Dual feed rf gun for the LCLS,” *SLAC-PUB-11213*, May 2005, <http://www.slac.stanford.edu/pubs/slacpubs/11000/slac-pub-11213.html> ; to be published in the proceedings of the *2005 Particle Accelerator Conference*, 16-20 May 2005, Knoxville, TN; also to be published at the Joint Accelerator Conference Website (<http://www.JACOW.org> ).
- <sup>ii</sup> D. H. Dowell, et al., “Slice emittance measurements at the SLAC gun test facility,” *SLAC-PUB-9540*, September 2002, <http://www.slac.stanford.edu/cgi-wrap/pubpage?slac-pub-9540> ; also published in *Nucl. Inst. Meth. A* **507**, pp 327-330, 2003.
- <sup>iii</sup> T. Shaftan, et al., “Experiments with electron beam modulation at the DUVFEL accelerator,” *SLAC-PUB-10858*, 2004, <http://www.slac.stanford.edu/pubs/slacpubs/10000/slac-pub-10858.html> , also published in *Nuc., Inst. Meth. A* **528**, pp. 397-401, 2004.
- <sup>iv</sup> Z. Huang, et al., “Uncorrelated energy spread and longitudinal emittance of a photoinjector beam,” *SLAC-PUB-11240*, May 2005, <http://www.slac.stanford.edu/pubs/slacpubs/11000/slac-pub-11240.html>; contributed to the *2005 Particle Accelerator Conference*, May 2005, Knoxville, TN.
- <sup>v</sup> S. Reiche, et al., “Pulse length control in an X-ray FEL by using wakefields,” published in the proceedings of the *2003 Particle Accelerator Conference*, 12-16 May 2003, Portland, Oregon; published at the Joint Accelerator Conference (<http://www.jacow.org> ) website, <http://accelconf.web.cern.ch/accelconf/p03/PAPERS/TOAC010.PDF>.
- <sup>vi</sup> K. L. F. Bane and G. Stupakov, “Resistive wall wake field in the LCLS undulator,” *SLAC-PUB-11227*, May 2005, <http://www.slac.stanford.edu/pubs/slacpubs/11000/slac-pub-11227.html> , also to be published in the proceedings of the *2005 Particle Accelerator Conference*, 16-20 May 2005, Knoxville, Tennessee; to be published at the Joint Accelerator Conference Website, <http://www.jacow.org>
- <sup>vii</sup> C. Limborg-Deprey, et al., “Computation of the longitudinal space charge effect in photoinjectors,” *SLAC-PUB-11170*, July 2004; <http://www.slac.stanford.edu/pubs/slacpubs/11000/slac-pub-11170.html> ; published in the proceedings of *EPAC 2004*, 5-9 July 2004, Lucerne, Switzerland; also available at the Joint Accelerator Conference Website: <http://accelconf.web.cern.ch/AccelConf/e04/PAPERS/TUPLT162.PDF>
- <sup>viii</sup> L. D. Benton, et al., “Inverse free electron laser heater for the LCLS,” *SLAC-PUB-11170*, July 2004; <http://www.slac.stanford.edu/pubs/slacpubs/11000/slac-pub-11186.html> ; published in the proceedings of *EPAC 2004*, 5-9 July 2004, Lucerne, Switzerland; also available at the Joint Accelerator Conference (<http://www.JACOW.org>) Website: <http://accelconf.web.cern.ch/AccelConf/e04/PAPERS/MOPKF083.PDF>.
- <sup>ix</sup> I. Vasserman, et al., “LCLS undulator design development,” published in the proceedings of the *2004 FEL Conference*, 29 August – 3 September 2004, Trieste, Italy; published at the Joint Accelerator Conference (<http://www.JACOW.org>) Website: <http://accelconf.web.cern.ch/AccelConf/f04/papers/TUBOS04/TUBOS04.PDF>.
- <sup>x</sup> S. Milton, “The Linac Coherent Light Source and undulator system,” these proceedings.
- <sup>xi</sup> P. Emma, et al., “Electro-magnetic quadrupole magnets in the LCLS undulator”, *SLAC-TN-05-016*, <http://www.slac.stanford.edu/pubs/slactns/slac-tn-05-016.html>.
- <sup>xii</sup> P. Emma, et al., “Weak FEL gain detection with a modulated laser-based beam heater,” *SLAC-PUB-11242*, <http://www.slac.stanford.edu/pubs/slacpubs/11000/slac-pub-11242.html> , also to be published in the Proceedings of the *2005 Particle Accelerator Conference*, 16-20 May 2005, Knoxville, TN; to be published at the Joint Accelerator Conference Website (<http://www.JACOW.org> ).
- <sup>xiii</sup> R. Bionta, et al., “Report of the LCLS Diagnostics and Commissioning Workshop, Los Angeles, USA, January 19-20 2004,” *SLAC-R-715*; <http://www.slac.stanford.edu/pubs/slacreports/slac-r-715.html>.
- <sup>xiv</sup> *ICFA (Future Light Sources Sub-Panel) Mini Workshop on Commissioning of X-Ray Free-Electron Lasers*, April 18-22 2005, DESY-Zeuthen; [http://commissioning2005.desy.de/index\\_eng.html](http://commissioning2005.desy.de/index_eng.html) ; a report of the workshop will appear in ICFA newsletter 36 which will appear at <http://www-bd.fnal.gov/icfabd/news.html> .
- <sup>xv</sup> A.L.Cavalieri, et al., “Clocking femtosecond x-rays,” *PRL* **94**, 114801, 4 pages, 2005.